Chair of Materials Science and Testing of Polymers

Doctoral Thesis

Reinforcement of elastomers to obtain anisotropic material properties

Dipl.-Ing. Julia Beter, BSc BSc

February 2021

MONTANUNIVERSITÄT LEOBEN
www.unileoben.ac.at

AFFIDAVIT

I declare on oath that I wrote this thesis independently, did not use other than the specified sources and aids, and did not otherwise use any unauthorized aids.

I declare that I have read, understood, and complied with the guidelines of the senate of the Montanuniversität Leoben for "Good Scientific Practice".

Furthermore, I declare that the electronic and printed version of the submitted thesis are identical, both, formally and with regard to content.

Date 15.02.2021

Signature Author
Julia Beter

„Beim Menschen ist es wie beim Velo. Nur wenn er fährt, kann er bequem die Balance halten.“ (February 5th, 1930)

Albert Einstein
Born: March 14th, 1897
Died: April 18th, 1955

Acknowledgment

I would like to express my deepest gratitude to everyone who advised, supported and encouraged me throughout the preparation and accomplishment of this thesis.

First and foremost, I wish to thank Dipl.-Ing. Dr.mont. Bernd Schrittesser for his continual interest in my research, scientific discussions, valuable ideas and the possibility of using laboratory equipment. Without him and his encouragement, I would not be where I am so this work would have been much more difficult. Especially his personal support and the friendly working atmosphere gave me the decisive support and confidence to have the courage to realize this thesis.

Furthermore, Univ.-Prof. Dipl.-Ing. Dr.mont. Gerald Pinter, Chair of Material Science and Testing of Polymers at the Montanuniversitaet Leoben and my academic advisor of this thesis, for his tremendous confidence, outstanding supervision, scientific assistance in every situation and the chance to write this thesis at his institute.

I would also like to thank Prof. MSc. Dr. tech. Claudia Marano, Department of Chemistry, Materials and Chemical Engineering “Giulio Natta”, at the Politecnico di Milano and mentor of this thesis for her interest in my work, numerous discussions and indefatigable commitment during the realization of my publications and scientific innovations. She guided me especially at the beginning of my doctoral research also in a personal manner. Moreover, I am very grateful to Dipl.-Ing. Dr.mont. Peter Filipp Fuchs for his confidence, support and the chance to write this thesis within his project.

I would like to thank my coworkers MSc. Petra Christöfl, Dipl.-Ing. Dr.mont. Roman Kerschbaumer and MSc. Dr.mont. Winoj Naveen Balasooriya Arachchige for scientific discussions and friendship. Special thanks to Gerald Maier and Bernhard Lechner for the technical support and contagious motivation. Furthermore, I would like to express my appreciation to the members of the PCCL, who always created a warm atmosphere, on and off working hours.

Finally, I want to sincerely thank my parents and my family, who gave me the opportunity to study. In addition, Christoph Apfelknab deserves a mention. He

always had an open ear for my problems and has been a true friend for many years. On a final note, I should mention my partner, for his great understanding, not complaining about some late working hours and lifting me up when it was most necessary during this work.

The research work was performed at the Polymer Competence Center Leoben GmbH (PCCL, Austria) within the framework of the COMET-program of the Federal Ministry for Climate Action, Environment, Energy, Mobility, Innovation and Technology and the Federal Ministry for Digital and Economic Affairs with contributions by the Chair of Material Science and Testing of Polymers of the Montanuniversitaet Leoben, Institute of Lightweight, Design and Structural Biomechanics of the TU Wien and Department of Chemistry, Materials and Chemical Engineering “Giulio Natta” of the Politecnico di Milano. The PCCL is funded by the Austrian Government and the State Governments of Styria, Lower Austria and Upper Austria.

Abstract

The demand of fiber reinforced elastomers representing a new material class with unique capabilities is constantly growing. By constituting hyperelastic elastomers as interesting matrix material, these flexible composites with direction-dependent behavior allows the development of tailored stimuli-responsive properties triggered by load coupling effects like tension-twist or bending-twist mechanisms.

The state of the art regarding the comprehensive material characterization for fiber reinforced elastomers and their load coupling effects showed that current findings for material-specific and suitable test concepts are still barely analyzed. Thus, the objective of this thesis is to provide profound knowledge of the material behavior, reliable testing possibilities and functional solutions concerning fiber reinforced elastomers especially for potential smart composite applications. Therefore, a systematic simplification of a test chain from micro- to macromechanical characterization is realized. A suitable step-by-step principle with conclusive transfer criteria are implemented. Due to the significant influence of the fiber-matrix interaction on the composite performance, the fiber-matrix adhesion and interfacial properties are investigated using fiber debond techniques including further tailored surface treatments to prove the impact on the adhesion. Regarding the material characterization exposed to cyclic loading by dynamic mechanical and step cycle analysis, the investigation of the energy absorption capacity, dynamic properties and force redirecting ability leading to load- and time-dependent behavior is necessary. Another part is the study of load coupling mechanism and the development and verification of a suitable material-related test concept.

Based on the findings from the developed test chain especially for fiber reinforced elastomers, the need of correct transfer criteria for a systematic step-by-step simplification and the importance of precise material data evaluation due to their significant effects on the fiber-matrix interaction was demonstrated. Overall, the fiber bundle pull-out test can be considered as intermediate step representing a link between micro- to macromechanical testing enabling an adequate material study on the fiber-matrix adhesion performance. For the tension-twist load coupling characterization, the verification of the novel test concept offers a promising basis to investigate mechanical triggered load-coupling effects.

Kurzfassung

Die Nachfrage hinsichtlich faserverstärkter Elastomere als neue Materialklasse mit einzigartigen Fähigkeiten, wird deutlich stärker. Durch den Einsatz von hyperelastischen Elastomeren als vielversprechendes Matrixmaterial und die gezielte Ausnutzung der Materialanisotropie ermöglichen diesen flexiblen Verbundwerkstoffen ausgeprägtes richtungsabhängiges Verhalten. Aufgrund der resultierenden Lastkopplungseffekte können durch die Realisierung maßgeschneiderter Eigenschaften, Zug-Torsion oder Biege-Torsion-Mechanismen kontrolliert ausgelöst werden.

Stand der Technik hinsichtlich umfassender Materialcharakterisierung für faserverstärkte Elastomere und deren Lastkopplungseffekte zeigt, dass aktuelle Forschungsergebnisse für materialspezifische und geeignete Prüfkonzepte noch kaum untersucht sind. Ziel dieser Arbeit ist es, grundlegende Kenntnisse über das Materialverhalten, potenzielle Prüfmöglichkeiten und funktionale Lösungen bezüglich faserverstärkter Elastomere im Speziellen für potenzielle Smart-Composite-Anwendungen bereitzustellen. Dazu wird eine systematische Vereinfachung mittels Prüfkette von mikro- bis zur makromechanischen Charakterisierung erarbeitet. Zusätzlich wird ein entsprechendes Stufenprinzip mit nachvollziehbaren Übertragungskriterien implementiert. Aufgrund des maßgeblichen Einflusses der Faser-Matrix-Wechselwirkung auf die Performance im Verbund werden die Faser-Matrix-Adhäsion sowie die Grenzflächeneigenschaften mit Hilfe von Faser-Debond-Techniken untersucht. Zusätzlich wird der Einfluss gezielter Oberflächenbehandlungen auf die Adhäsion demonstriert. In Bezug auf die Materialcharakterisierung unter zyklischer Beanspruchung mittels dynamisch-mechanischer und stufenweiser Zyklusanalyse ist die Untersuchung des Energieaufnahmevermögens, der dynamischen Eigenschaften sowie des Kraftumlenkungsvermögens, welche zu einem last- und zeitabhängigen Verhalten führen, erforderlich. Des Weiteren ist die Betrachtung des Lastkopplungsmechanismus durch die Entwicklung und Verifizierung eines geeigneten werkstoffbezogenen Prüfkonzeptes essenziell.

Anhand der Erkenntnisse basierend auf der entwickelten Prüfkette speziell für faserverstärkte Elastomere konnte die Notwendigkeit geeigneter

Übertragungskriterien für eine systematische, schrittweise Vereinfachung und die Bedeutung einer präzisen Materialdatenauswertung, infolge der entscheidenden Auswirkungen auf die Faser-Matrix-Interaktion, aufgezeigt werden. Somit repräsentiert der Faserbündelauszugstest eine Zwischenstufe, welche ein Bindeglied zwischen mikro- und makromechanischer Prüfung darstellt und eine adäquate Analyse hinsichtlich des Faser-Matrix-Adhäsionsverhaltens ermöglicht. In Bezug auf die Charakterisierung der Zug-Torsion Lastkopplung bietet die Verifizierung des neuentwickelten Testkonzepts eine vielversprechende Grundlage zur Analyse von mechanisch ausgelösten Lastkopplungseffekten.

Table of Content

Acronyms

ASTM	American Society for Testing and Materials
CLT	Classical laminate theory
DIN	German Institute for Standardization
DMA	Dynamic mechanical analysis
EN	European Committee for Standardization
FBPO	Fiber bundle pull-out
GF	Glass fiber
ISO	International Standardization Organization
MDPI	Multidisciplinary Digital Publishing Institute
PDMS	Polydimethylsiloxane
PETF	Polyester fiber
PUR	Polyurethane
SFPO	Single fiber pull-out
TGA	Thermogravimetric analysis
UD	Unidirectional
VARI	Vacuum assisted resin infusion
XPS	X-ray photoelectron spectroscopy

Symbols

Latin notation

A	N/mm	Extensional stiffness matrix
B	N	Coupling stiffness matrix
C	MPa	Stiffness matrix
D	Nmm	Bending stiffness matrix
E_c	MPa	Young's modulus for composite
E_f	MPa	Young's modulus for fiber
E_m	MPa	Young's modulus for matrix
E_{II}	MPa	Young's modulus parallel fiber direction
$E_{\perp}$	MPa	Young's modulus perpendicular fiber direction
E'	MPa	Storage modulus
E''	MPa	Loss modulus
k	–	Number of reinforcement layers
m	MPa	Stress
m_a	g/m²	Fiber weight per area
n	N	Force
t	mm	Thickness
V_f	mm³	Fiber volume
V_{total}	mm³	Composite volume

Greek notation

δ	°	Phase angle
tan(δ)	–	Loss factor
ε	mm/mm	Distortion
κ	1/mm	Curvature
ρ_f	kg/m³	Fiber density
φ_f	%	Fiber volume content

PART I: INTRODUCTION, OBJECTIVES AND BACKGROUND

1 Introduction, objectives and structure of the thesis

Due to the excellent damping, flexibility and absorption properties, the use of elastomers in various applications such as seals, hoses or valves is indispensable. Conventional elastomers are predestined for the significantly lower bearable maximum stresses and thus strongly constrained in their applications, which has resulted in an increased emphasis on multi-material solutions. Fiber reinforced approaches have already shown promising results due their unique material properties with outstanding features in lightweight, highly weight-specific strength and stiffness or an increase in efficiency.

Fiber reinforced elastomers, as a promising new material class in the field of soft matter applications, enable the combined use of elastomers with specifically oriented reinforcement to generate novel flexible composites with distinct direction-dependent properties. Promising approaches of fiber reinforced elastomers with pronounced hyperelasticity implemented in smart material applications demonstrates significant research potential albeit with associated complex challenges that require new scientific approaches. The availability and profound knowledge about such functional materials and the possibility to combine these features with tailored fiber-matrix load coupling effects has significantly influenced the concept and designs of smart structural applications. Especially the development of these composite systems combined with an external stimulus as a trigger (to achieve tailored load coupling effects) can offer promising innovative approaches e.g. aeroelastic wings. In order to find the best solution, the right choice of the elastomer type as well as the suitable combination of these elastomers with the reinforcement structure is a crucial challenge. However, the associated experimental and numerically based approaches in micro- and macromechanical behavior to determine the mechanical properties and material performance regarding the force transmission mechanism have barely been researched.

The analysis of the structure-property relationship is essential, since the reliable determination of characteristic values with corresponding suitable material-related test methods enables accurate and detailed material knowledge. In this context, one main focus of this study is the realization and verification of novel test methods especially for fiber reinforced elastomers in smart composite applications. Another aspect is the comparability and transferability of the measurement concepts developed with proven test methods to enable precise and consistent analysis of the structure-property correlation involved in load coupling effects. Moreover, there are no standardized tests available for this new material class, so there is need for a test chain oriented approach with a specific step principle to scientifically address the complex material behavior starting from model- to component-like topics. Besides the limited scalability between micro- and macromechanical characterizations, the tailoring of material anisotropy especially to maximize the load coupling potential of engineering structures, needs to be exploited.

For the material characterization, basic methods were developed to investigate static and dynamic properties towards the influence of interfacial adhesion performance and anisotropic behavior. In this context, the objective is to understand the fiber-matrix interaction considering the load coupling mechanism, which is strongly affected due to the material combination of the constituents, fiber orientation as well as fiber surface modification. Moreover, the impact on strength, stiffness as well as force redirection and energy absorption are further important findings. Therefore, the objectives of this scientific thesis can basically be structured into four main sections investigating the following fundamental aspects thoroughly in a consistent and constructive approach:

(i) Fiber-matrix interaction:

Characterization of the adhesive interface strength depending on the micro- and macromechanical performance complemented by cause and effect of various specific surface modifications.

(ii) Transferability between micro and macro scale:

Implementation and completion of a suitable test chain from micro to macro level testing with correspondingly defined transfer criteria according to the step-by-step concept.

(iii) Viscoelasticity and energy absorption:

Investigation of dynamic properties, absorption capabilities and force redirecting ability of fiber reinforced elastomers depending on such factors as structure properties, fiber orientation, fiber volume content or viscoelastic performance under load- and time-dependent conditions.

(iv) Load coupling mechanism:

Experimental implementation of tailored load coupling mechanisms in fiber reinforced elastomers including realization and verification of a suitable test device, whilst reproducibility and measurement sensitivity is analyzed by special sensors and accompanying evaluation process.

This thesis is structured basically in two main parts. Towards a comprehensive understanding for this material class and the unique features of fiber reinforced elastomers as flexible composites depending on several influencing factors, a general overview of the research field and background will be given. Within this, part I further implies the introduction, general objectives and structure of the thesis based on six publications and two patents. In this context, part II focuses on the summary and findings, outlook and collection of all six papers and two patents as listed:

Paper 1: Comparison and impact of different fiber debond techniques on fiber reinforced flexible composites (Polymers, MDPI, open access)

Paper 2: Tailored interfaces in fiber reinforced elastomers: A surface treatment study on optimized load coupling via the modified fiber bundle debond technique (Polymers, MDPI, open access)

Paper 3: Investigation of adhesion properties in load coupling applications for flexible composites (Materials Today: Proceedings, Elsevier)

Paper 4: Influence of fiber orientation and adhesion properties on tailored fiber reinforced elastomers (Applied Composite Materials, Springer, open access)

Patent A: Klemmvorrichtung und Verfahren zur Prüfung einer Zugfestigkeit eines Objektes (Österreichisches Patentamt)

Paper 5: Viscoelastic behavior of glass fiber reinforced silicone composites exposed to cyclic loading (Polymers, MDPI open access)

Paper 6: The tension-twist coupling mechanism in flexible composites: A systematic study based on tailored laminate structures using a novel test device (Polymers, MDPI, open access)

Patent B: Prüfvorrichtung zur Messung von Zug-Torsion-Lastkopplungen (Österreichisches Patentamt)

2 Background

In the following, a general outline of smart materials and composites with an additional focus on fiber reinforced elastomers will be given. Furthermore, an overview will be provided of different influencing factors and special features regarding anisotropic material behavior with corresponding characterization approaches for the description of the structure-property performance and fiber-matrix load coupling mechanisms.

2.1 Smart materials

Since the demand for tailor-made materials is already well established and successfully implemented, the unique features of these so-called smart materials have also become interesting. Smart materials and biomimetics are closely linked, as good scientific approaches can be associated with nature. Based on the principle of "learning from nature" e.g. pearlescent mimetic nanostructures [1] or staggered models [2], this method is also followed in the implementation of new intelligent composite structures. Generally, the term biomimetic describes the implementation of nature-based methods, designs or techniques into different fields of science and technology. In this context, smart materials can be generally classified as controllable materials with exceptional properties [3]. The objective to develop such adaptive materials is the tailored stimuli-responsive performance triggered by an external impulse. These materials assume an active role during exposure to an energetic stimulus (in morphology transformation or in generating transformed shape).

Basically, all materials react to external energy, which can be described as the energy transfer which is correlated to the material property versus the change in state [3]. The actual state in a smart material can be individually adjusted by so-called triggers, which use various activation points based on mechanical properties or morphology and take advantage of thermal conductivity, stiffness or deformation behavior. Therefore, typical triggers can basically be structured as follows: (i) pneumatic [4] or fluidic [5], (ii) electric [6,7], (iii) thermal [8,9] or (iv) mechanical stimuli [10,11]. The energy transfer leads to a change in the inner state of the

material, which in turn affects the outer state. For example, in shape memory materials [12,13] or self-folding structures [14,15], the energy input leads to a shift in the molecular structure of the material and thus to a movement [3]. This method of intelligent exploitation primarily uses the geometry of the respective deformation or moving object itself and is also utilized typically for isotropic materials without reinforcement. However, the improvement of fiber polymer composites with smart features is a new approach, since the general direction-dependent performance is complemented by an additional energetic input as stimulus to trigger specific motions related to the reinforcement orientation [16,17]. Related to this, fiber reinforced elastomers as so-called flexible composites further represent a new material class, since the exchange of classic thermoset-based matrices by elastomers as alternative material enables distinct highly motion ranges which cannot be realized with common composite materials such as for aeroelastic wings [18,19] or soft robotic grippers [20,21]. In this thesis, mechanically driven trigger effects will be investigated, since the main emphasis is the load coupling effect and material characterization of fiber reinforced elastomers.

2.2 Composite materials

Composite materials are macroscopically quasi-homogeneous materials consisting of two or more physically different components (phases), interlocked and inseparable, which unite the properties of the individual components favorably and interact in synergy [22]. In general, composite materials are classified into:

(i) particle

(ii) fiber

(iii) layered (laminates)

(iv) interpenetrating composites

Thereby fiber reinforced composites, in particular have become the preferred option for lightweight construction due to their outstanding specific direction-dependent properties [23]. Also from the mechanical perspective, the performance of fiber reinforced composites is strongly influenced by the reinforcement structure due to geometry and design e.g. fiber type, lay-up or orientation combined with the stacking sequence, which is important for the load transfer and further composite

performance. Thus, the production of composite materials aims to achieve properties that cannot be obtained with the respective individual constituents [22,24]. One component is defined as matrix and the other as fiber reinforcement, which are specifically used to improve each other's mechanical properties. Overall, a composite can fulfill its entire potential only through the interaction between fiber reinforcement and the surrounding matrix [23,25]. In this context, the matrix is responsible for (i) the design of the outer shape, (ii) controlled force initiation into the fibers, (iii) force transfer regarding inter- and intralaminar aspects and (iv) fiber protection against external environmental influences, such as mechanical effects or physical and chemical influences [23]. Besides that, the fibers are fixed and supported by the matrix enabling a homogeneous stress distribution in the composite. Subsequently, the main tasks of the fibers as the functional core component are the handling and transmission of the acting stresses and thus contribute significantly to the overall strength [26,27]. This interaction between fibers and the matrix is clearly defined locally via the interface area, since the fiber-matrix adhesion has to ensure homogeneous load transfer and is therefore the decisive third phase [24,27].

Regardless of the type of the applied reinforcing structure, different designs are available depending on the drapability or stacking sequence and are basically structured into: rovings, random nonwoven fabrics, woven fabrics, non-crimp fabrics, braidings or knittings [23,25]. Generally, all semi-finished textile products are characterized according to the area weight with the unit weight per area in g/m². If a specific reinforcement is intended, the application of endless fibers with tailored anisotropic orientation is highly effective. Related to this and taking further economic aspects into account, woven textiles and non-crimp fabrics are often chosen. The two structures differ strongly both in processing and manufacturing as well as in the following mechanical properties in the composite. Therefore, woven fabrics such as textiles are dry semi-finished components containing single rovings (fiber bundles) in a certain sequence (weave type) and direction. The products are plain structures or tubes with a biaxial reinforcing effect and thus bear a load transmission in two directions (warp and weft yarn), since both orientations interact through weave points [22,23]. A main benefit is the enhanced inherent stability and stiffness, especially for high-performance composite structures with defined fiber-matrix load

coupling in the inter- and intralaminar layers [22,28,29]. The drawback of these woven structures are the limited drapability and the fact that at least one direction (referred to the warp yarn) obtains undulations. Hence the undulations lead to incompletely stretched fibers and the resulting mechanical properties are impaired to a certain level [23,29].

In contrast to woven fabrics, non-crimp fabrics are semi-finished components with fibers oriented in parallel without any undulations. This reveals the main advantage that the fiber performance can be exploited completely. However, the inherent stability is significantly reduced. For this reason, mostly stitching threads are used, where several layers (even with different orientations) are fixed together. The influence of the stitching threads on the total composite is negligible. Nevertheless, the mechanical properties are still better than woven fabrics due to the stretched and parallel fibers. Related to this, simulation models for composites focusing on the mechanical performance or damage behavior typically use the well-known laminate theory based on non-crimp fabrics, since, from the numerical standpoint, completely stretched fibers need fewer boundary conditions or simplifications and therefore allows an easier handling [30-32].

For composite manufacturing in particular, a variety of different methods exist, which differ significantly in several aspects such as complexity, degree of automation, number of variations, flexibility, product quality, reproducibility or user influence. Therefore, depending on the requirements and applications, the appropriate as well as the required manufacturing process has to be chosen carefully. Currently available methods can be structured according to the automation level or individual manufacturing flexibility into [25]:

(i) unpressurized method (e.g. fiber spraying or hand lay-up technique)

(ii) high pressure process (such as resin transfer molding, sheet molding compounds or glass mat reinforced thermoplastic)

(iii) low pressure process (like vacuum injection molding or vacuum resin transfer molding)

Especially in the field of research and development, hand lay-up techniques are easily available and therefore an attractive method for the first development steps

in the initial phase, where the main focus is on feasibility and implementation, and the reproducibility or laminate quality are subordinated. Another possibility is the resin infusion process, which is impressive due to its distinct flexibility and fast adaptability, whilst still providing adequate reproducibility and composite quality. This process can be relatively simply equipped with an additional vacuum system to ensure homogeneous compaction and impregnation even in the transversal direction (across the lay-up thickness) related to the impregnation flow or fiber orientation [23,25].

Generally, fiber reinforced composites are distinguished according to the incorporating matrix material and thus can basically be differentiated into thermosets, thermoplastics and elastomers. The majority is thermoset-based composites using epoxy-, vinyl ester or polyurethane resins, which are considered for high performance requirements in lightweight construction with sufficient strength and stiffness or dynamic properties [33–35]. However, due to the highly chemical crosslinking, major disadvantages caused by severe impact loading are the brittle behavior, which tends to lead to break at lower elongations [36]. A promising alternative is the use of composites based on thermoplastic matrices such as polypropylene or polyamides, which offer higher elongation at break and feasible impact resistance compared to thermoset-based composites. Especially in the field of series production with larger batch sizes, these composites have become widely established also for injection molding or forming processes [37–39]. However, owing to their high melt viscosity, the major disadvantages are the associated high process temperatures and consolidation forces to achieve an overall good fiber impregnation quality. Furthermore, also the pronounced creep tendency significantly limits the application range of thermoplastic-based composites [22,23,29]. In this context, fiber reinforced elastomers as so-called flexible composites have a quite extraordinary position, representing a completely new material class with distinct mobility. Elastomers react to chemically crosslinked polymeric networks similar to thermosets, whilst still maintaining high flexibility and impact resistance as well as good damping properties including a low creep tendency along with a broad temperature range regarding the field of application [40]. According to the most recent findings, elastomers as different matrix materials are still considered subordinate, since fiber reinforced polymers are

primarily used to achieve the highest feasible degree of specific stiffness and strength combined with good lightweight potential. But, the latest scientific work on fiber reinforced elastomers has already shown the promising approach to expand into completely new applications. However, the desired distinct flexibility and pronounced higher motion range would hardly be possible with composites considering industrial rubber which are used for automotive tires, high pressure hoses or conveyor belts [36,41,42].

2.3 Properties of anisotropic reinforced polymers

Depending on the requirements of customized composites, the range of different tailored fiber-matrix material combinations becomes almost infinite. Therefore, a comprehensive understanding of material performance and the associated mechanical properties is necessary to consider the application limits as well as failure mechanisms. This is relevant to provide essential material data as input variables for subsequent simulations. Besides the determination of the characteristic parameters, moreover, the focus is on the comparability of different influencing factors, which comprises the following aspects from a material point of view: (i) influence of matrix material e.g. viscoelasticity, thermo-mechanical properties or crosslinking density, (ii) fiber influence such as volume content, orientation, distribution or structure and (iii) effect of different fiber-matrix bonding systems by specific chemical treatment procedures regarding fiber surface sizings [27,41]. Based on this, the reinforcing effect as well as the generation of fiber-matrix load coupled behavior are significantly imparted by the structure-property relationship and the interaction between fibers and matrix [27]. Therefore the mechanical properties of fiber reinforced polymers differ considerably from common homogeneous and isotropic materials [24]. Basically, inhomogeneity refers to the position-dependent properties due to different layers inside the composite. Whereas the anisotropy describes the directional dependence of the properties within the composite [24]. So each layer allows different fiber orientations and may also consist of different materials. Thus, a layer-by-layer approach for the overall analysis is necessary, since the important difference is whether a certain stress occurs parallel or perpendicular to the fibers [25,43].

2.3.1 Young's modulus and fiber volume content

The general term composite structural characterization comprises parameters such as fiber volume content, fiber weight per area, lay-up or density of the constitutes, which have a direct impact on the composite mechanical properties [24,29,30]. The determination of the elasticity parameters depends on the micromechanical analysis, since micromechanics focuses especially on the single layer properties, which result in effective homogeneous parameters from the constituents (fiber, matrix). Thus the definition of a representative volume element as the unit cell constitutes the overall mechanical performance of the composite [30]. Based on this approach, the analytical investigation to determine the direction-dependent behavior (parallel and perpendicular to the fibers) can be described by the well-established mixing rule for composite materials (explained by the Voigt-Reuss model [22,44]), as expressed in Equation (1) for the loading parallel to the fiber direction, studied by Schürmann [30].

$$\mathrm{E_c} = \varphi_\mathrm{f} * \mathrm{E_f} + (1 - \varphi_\mathrm{f}) * \mathrm{E_m} \tag{1}$$

In this context, the representative micromechanical model is simplified due to the acting loads, kinematics and elasticity such as equal Poisson's ratios (fiber and matrix), homogeneous force distribution and fiber-matrix elongation to describe the fiber-matrix load coupling via an analytical approach. Thus, according to the definition of the mixing rule, the Young's modulus E_c of the composite is strongly dependent on the fiber volume content φ_f [31,45]. Where E_f and E_m are defined as the Young's modulus for the fibers *f* and the matrix *m*. Since the stiffness in the fiber direction is dominated by the fibers and thus by the fiber volume content considering the composite cross section area, the approach with the mixing formula still yields a moderate preliminary approximation, despite the specific micromechanical material structure [22,30,44]. This approach regarding Equation (1) is generally valid for composites of exact parallel-directed fibers with brittle (thermoset) matrix systems and due to the strong fiber dominance small deformability is assumed. According to the literature [31,44], further micromechanical concepts supplement these two terms with additional terms, which include the transverse strain restraint and the shear effects from the matrix and the undulation effects when woven textiles are used [28,46]. From an experimental perspective, to determine the

thermo-mechanical parameters, in particular the storage modulus E', the loss modulus E'' and the loss factor tan(δ), as a function of the temperature, the dynamic mechanical analysis (DMA) offers a good method for the basic mechanical characterization of materials [47–49]. For the design and scaling of the respective application scope, a detailed knowledge of the glass transition region (indicating the glass transition temperature) and linked morphology properties within the characteristic main softening range is relevant. The presence of reinforcing fibers leads to a clear increased storage modulus and further to a shifted glass transition region to higher temperatures. This shift is essential for elastomeric matrices due to their main application at the entropy elastic state causing a lower mobility inside the polymer chains which further affects the ability of the elastomeric restoring forces [40,50,51]. Since the elastic properties are mainly described by the Young's modulus, the ideal model according to the analytical approach in the Voigt-Reuss model [22,44] assumes an ideal composite material (without inclusions and perfect interface adhesion), as shown in Figure 2.1.

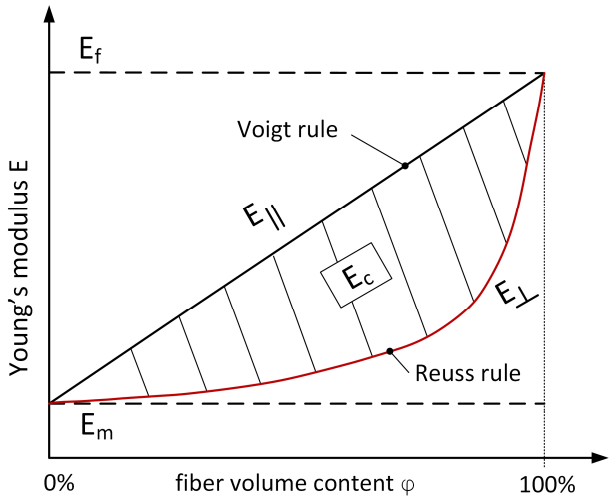

Figure 2.1: Voigt-Reuss mixing rule with the upper $E_{//}$ (parallel fiber direction) and lower limit $E_{\perp}$ (perpendicular fiber direction) on the Young's modulus of a composite material with the actual modulus E_c inbetween [45].

The upper limit $E_{//}$ corresponds to a composite loaded in fiber direction (explained in Equation (1) for the Voigt model), as a parallel configuration, whilst the lower limit $E_{\perp}$ is a composite loaded perpendicularly (equivalent to series configuration). Genuine composites are imperfect due to length distribution, fiber undulations or fiber-matrix clusters related to the statistic distribution in the cross section area,

feasible Young's modulus of common composites are between the two limits [30,45]. Apart from the actual fiber distribution, the determination of the Young's modulus in thermoset-based composites using the analytical or experimental approach is complex. Therefore, the determination of the direction-dependent Young's modulus is even more challenging in fiber reinforced elastomers, since elastomers are known for non-linear deformation and complex mechanical properties due to the high flexibility and entropy elasticity. Because of the distinct high elongations but rather reduced bearable stresses, the behavior is more related to textile-like materials [41,46]. Thus, the fiber volume content and Young's modulus strongly influence the mechanical properties e.g. stiffness or strength, which affects the structure-property relationship and further the load coupling of composite systems.

To determine the fiber volume content φ_f, another concept can be presented due to the volume ratio between pure reinforcement V_f versus total composite V_{total}. Based on this, a general mathematical correlation can be established including the fiber weight per area m_a for one layer as well as the number of layers of the reinforcement k, the composite thickness t (or height of the volume) and the fiber density ρ_f as expressed in Equation (2) [31,45].

$$\varphi_f = \frac{V_f}{V_{total}} = \frac{m_a * k}{t * \rho_f} \tag{2}$$

For the experimental determination of the fiber volume content, besides optical microsection analysis [22,45], thermogravimetric analysis (TGA) provides accurate results and is a reliable standardized method. This test focuses on the determination of a material-related value regardless the used reinforcing structure (layered or woven) [51].

2.3.2 Strength and Young's modulus influenced by fiber orientation

Generally, the tensile strength and Young's modulus are characteristic parameters of the mechanical properties in a fiber reinforced polymer. However, both are especially enhanced in tensile mode compared to the pure polymeric matrix and, beyond that, are significantly affected by the fiber orientation in the composite [52]. Due to the differences in the material properties of the individual constituents (fiber

and matrix), the experimental as well as analytical assessment of tensile strength or Young's Modulus is challenging [29]. Normally, the properties of the composite are lower compared to pure fibers and thus, depending on the fiber volume content, the difference can be considerable. Generally, this aspect can be simplified by comparing respectively the stress-strain curves for pure fiber, matrix and composite in a schematic illustration, as shown in Figure 2.2, using a unidirectional reinforced polymer based on thermoset matrix systems. The behavior of composites with elastomeric matrices will be explained further in a different chapter in more detail.

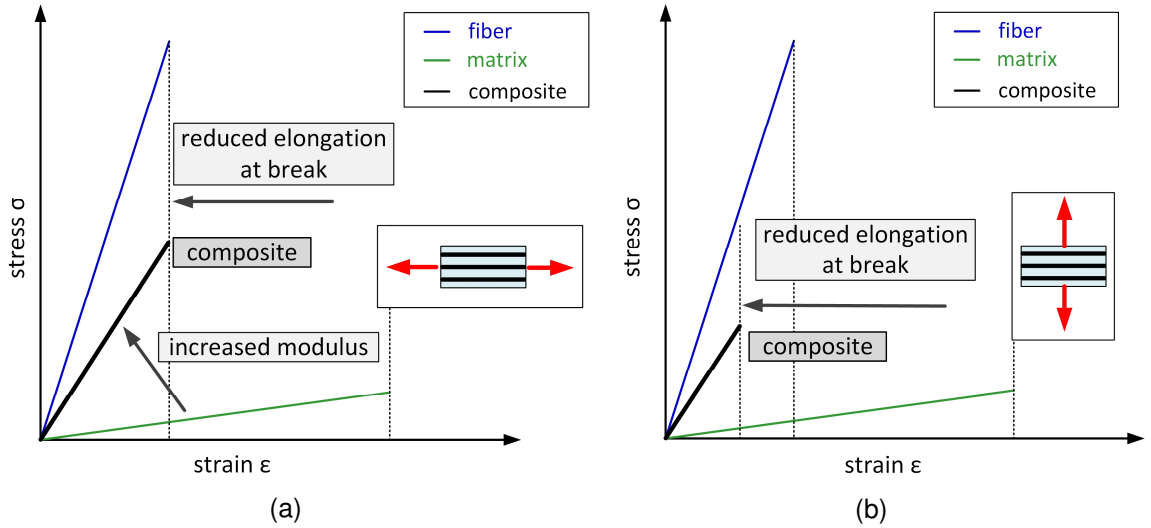

Figure 2.2: Schematic comparison of stress-strain graphs between fiber, matrix and tensile behavior of general composite with brittle matrices with loading parallel (a) and perpendicular (b) to fiber direction [43,45].

Based on this theoretical demonstration, the composite stiffness (parallel to fiber direction) is below the pure fiber stiffness whilst the elongation at break is similar to the pure fibers. Thus, the stress at break increases approximately proportional to the fiber volume content. In contrast to that, the mechanical properties are impaired strongly by loading perpendicular to the fiber orientation and can even lead to a performance lower than the pure matrix especially with a strong decrease in the elongation at break. This can be explained by several factors, such as that the stiff fibers may result in a sort of microscopic notch effect leading to a premature crack formation. Moreover, this stress concentration, especially at the fiber-matrix interface, favors peeling stresses, which cause debonding [29,52].

Another aspect is that the fibers barely deform in transverse direction due to the significantly higher Young's modulus compared to the matrix material, which leads to a pronouncedly decreased elongation at break [23]. Regarding the different Poisson's ratio of fibers versus matrix, the material contraction in perpendicular orientation versus loading direction is hindered [30,53].

According to this concept, the general damage behavior in a fiber reinforced composite (explained by the stress-strain curve in Figure 2.2) can be classified respectively into four theoretical failure regions: (i) fibers and matrix are elastically deformed at initial state, (ii) fibers continue to deform elastically, whilst the matrix starts to deform linear viscoelastically or elastic-plastically, (iii) elastic-plastic deformation of both individual components until the tensile strength of the composite is reached and complete failure occurs (via matrix, interface, fiber or in any combination) [24]. Depending on the composite design and the selected matrix material, as described in chapter 2.2, each of these regions can be rated differently. Thus, a thermoset-based system shows more linear elastic deformation compared to an elastomeric material with a significant, pronounced non-linear elastic behavior [23,52]. Since not all fibers typically fail at the same time, the fiber-matrix adhesion has an essential influence on the load transfer and is necessary for the entire material characterization, especially for complex loading situations.

Besides the detailed knowledge of the composite strength or stiffness related to the respective fiber volume content, also the interfacial shear strength is important. Thus, as shown in Figure 2.3, for random fiber orientations versus corresponding strength and stiffness, the fiber-matrix load transfer mechanism is becoming increasingly affected by the interfacial properties due to the applied load deviating from the fiber orientation [45,52].

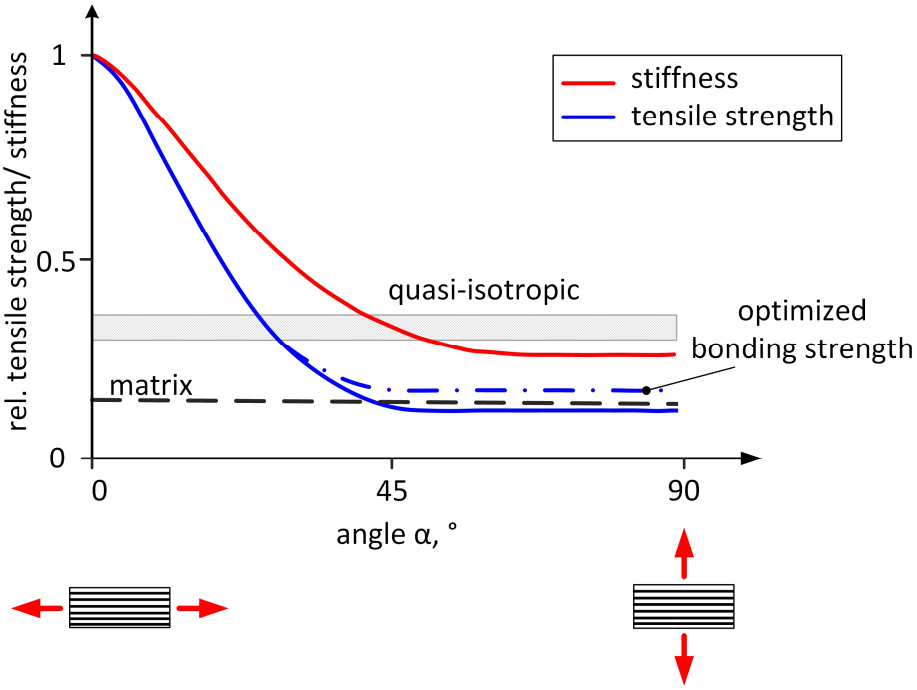

Figure 2.3: Schematic comparison of tensile strength or stiffness depending on the fiber orientation versus quasi-isotropic laminate or pure matrix material [23,29].

For a good understanding and clear explanation, these aspects were discussed based on layered fabrics, which triggers further challenges by using woven fabrics such as textiles. Since textiles have a biaxial reinforcement due to the warp and weft yarn configuration in one layer, additional factors such as fiber undulation, fiber-fiber friction, weave points or affected Poisson's ratio influence the draping properties and thus the composite strength and stiffness [25,45,52].

2.3.3 Composite interface

Typically fibers are specifically coated or sized to improve the bonding and impregnation behavior with the matrix material also during the manufacturing process as well to protect the fibers against environmental influencing factors during storage and transportation [29,39]. The interface in the composite between the reinforcing fibers and the surrounding matrix material is highly relevant for the load transfer or uniform stress distribution [41]. Thus the stability of a composite strongly depends on the bearable adhesive loads in the interface, since the adhesive strength describes the actual microscopic resistance that needs to be overcome for an effective separation [54,55]. This resistance results from the intermolecular interactions between fibers and matrix due to adhesive as well as cohesive forces.

In this context, a further distinction between interface and interphase is necessary, since according to the diffusion theory (theory of mutual diffusion of segments, polymer chains or molecules) no discrete intermediate region is formed by an interface as described in Figure 2.4. Whereas the interphase describes the decreasing/increasing concentration gradient ranging from the pure matrix material to the reinforcing component [54,56].

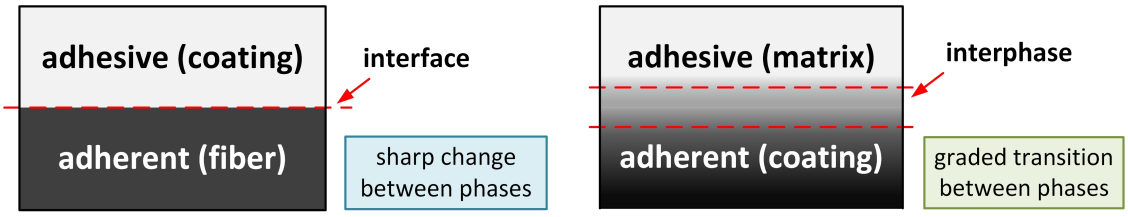

Figure 2.4: Schematic illustration of an interface (a) and interphase (b) between the adhesive and adherent component [54].

Basically, both aspects occur in a fiber reinforced polymer, since there is an interface between the fiber and the surface modification (coating) with a very thin layer and furthermore there is an interphase between the surface modification and the surrounding polymer matrix. However, the term interface in a more general meaning (meso or macro scale research) is typically referred to the entire composite structure, when the fiber-matrix bonding performance is going to be analyzed [57]. Nowadays, the adsorption theory is the most widespread model explaining adhesion phenomena, which can be divided into physical and chemical features. Based on this theory, the adhesive (matrix) bonds with the substrate (coating) due to intermolecular forces along the interface. Chemical primary bonds, such as covalent or ionic bonds, as well as physical secondary bonds e.g. hydrogen- or Van der Waals bonds and dispersion interactions, are formed [54,56,58]. Related to this, the wettability (between substrate and material that needs to be coated) and adhesive bonding are important parameters, since different applied loads have to be transmitted by the matrix onto the fibers via the interface. In order to improve the stiffness and strength corresponding to a good adhesive strength, a high interfacial adhesion is required. Besides the tailored treatment method to achieve specific fiber surfaces, the previous conditioning and cleaning step is important to provide optimized and reproducible fiber surfaces with the desired changed performance

regarding the physical and chemical surface properties [54,59]. Regarding the main focus of this thesis, commercial glass fibers are typically coated with silane-based surface sizings consisting of a mixture of various chemicals adopted for a broad application range for different specifications and mostly for thermoset-based products with a medium adhesion to various resin systems [57]. Therefore, these sizings can also contain filming agents and other components that are responsible for a homogeneous wetting of the fiber surface. Thus, further combined interactions are involved caused by the influence of chemical interactions e.g. covalent bonds as well as physical effects (polar or non-polar effects). For the fiber surfaces in general, these pretreatment procedures can be divided into [54,60]:

(i) mechanical

(ii) chemical

(iii) electrical

(iv) thermal methods

Thereby thermal or mechanical methods are not explained in detail in this thesis due to the lack of a non-destructive bonding method and thus their being unsuitable to use. Chemical processes e.g. wet chemical functionalization, or electrical processes such as low- or atmospheric pressure plasma methods are broad and material-friendly methods and therefore applied in the framework of this thesis.

Since the influence of the fiber-matrix adhesion is essential for the strength and toughness of the composite, local imperfections such as defects or partially bonded fibers lead to a significant reduction in the strength and toughness when subjected to mechanical stresses during loading [27]. Due to the weak or missing adhesion, less energy is required to debond the fibers, which implies subsequently reduced load transfer related to missing adhesive fiber-matrix interactions at the interface [27,61]. In general, the failure process of fiber reinforced polymers is takes place as follows by (i) starting with the damage initiation and continuing with (ii) the damage evolution. Due to the progressively decreasing interface strength (iii) a non-linear softening and reduction of the mechanical performance appear, which further ends in (iv) an uncontrolled complete failure [62]. The differently occurring damage mechanisms in fiber reinforced composites (see Figure 2.5) can be divided

according to the damage initiation into three main categories [62] as matrix, interface and fiber failure. Based on additional findings, also hybrid versions may occur in actual failure conditions coupled with two or more failure types, since in some situations e.g. a matrix and interface failure can be observed simultaneously.

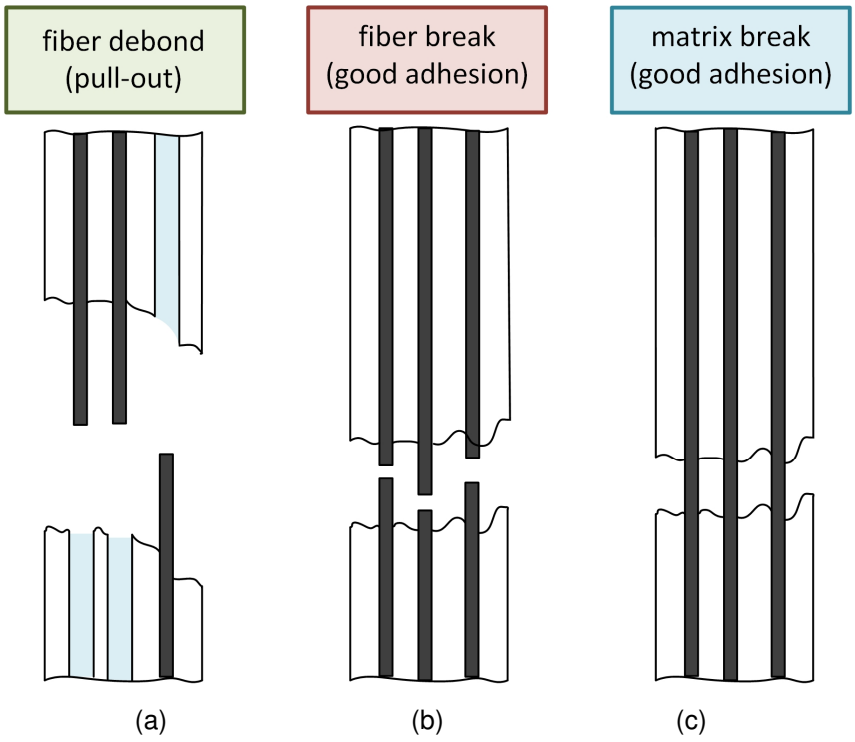

Figure 2.5: Main failure modes in a fiber reinforced composite structured in fiber debond (a), fiber break (b) or matrix break (c) [27,62]

Depending on the properties of the matrix material and the applied load, the separation of adhesive bonds occurs at the fiber interface (usually starting from the fiber end), leading in linear deformable (e.g. thermoset-based) matrices to pull-out or mostly fiber breakage due to the barely detectable matrix deformation. Compared to that, non-linear deformable matrices like elastomers are mainly affected by debonding and pull-out processes or matrix breakage caused by local plasticizing effects including micro-mechanical cavity formation [61,63]. The failure modes are given and described in detail by assuming that pure uniaxial stresses (tensile and compressive stresses) or shear stresses are present, since textiles with distinct bidirectional stress transfer complicate the investigations related to this topic even more. Regarding the material data evaluation, based on the material combination and the selected surface modification in the composite, no material data are typically

openly available. The possible configurations are almost infinite and thus need to be determined usually in a complex and time-consuming manner [64,65]. The influence of the interface behavior and fiber-matrix adhesion strength is crucial for the general tensile strength and toughness properties in composites, which affect the load coupling performance. There is still no standardized test specification with a defined specimen geometry, test parameters, settings or conditioning. Further, the associated structure-property relationship and polymer-related viscoelasticity are also not considered [59]. Related to this, the possibilities of valid existing test methods are basically classified into fiber-loaded and matrix-loaded systems [59,64] as illustrated in Figure 2.6.

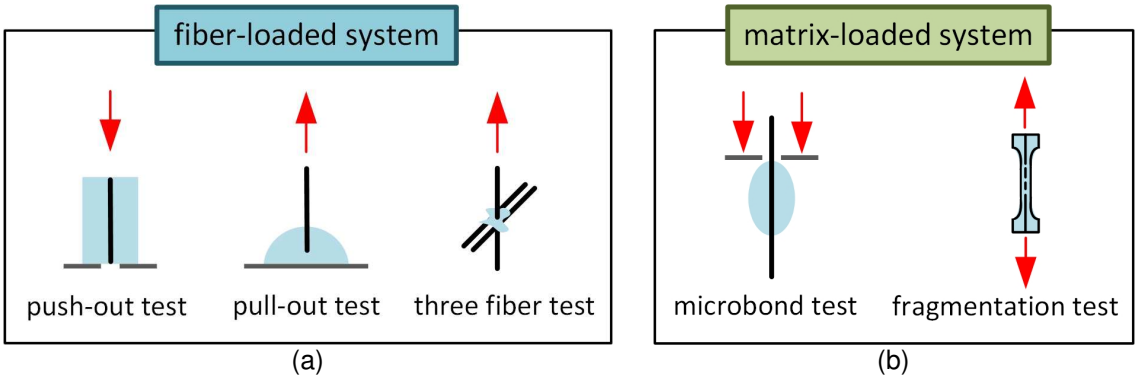

Figure 2.6: Schematic comparison of different configurations on filament tests structured in fiber-loaded system (a) and matrix-loaded system (b) [59].

Most of such tests like the fiber fragmentation test [66,67], microbond test [65,68], single fiber pull-out (SFPO) [69–71] or push-out test [72,73], are designed based on a filament (single fiber) test configuration embedded within a matrix. Within this measuring scale, micromechanical effects can be analyzed quite exactly due to the essential benefit of a defined and verified test situation. In this context, the filament-based tests at micro scale constitute a successively simplified testing model and also loading situation focusing on the central main challenge of interfaces and adhesion strengths between fiber and matrix. Thus, the surface adhesion as well as a clear shear stress distribution, due to the debonding force acting along the embedded fiber surface, can be measured and calculated, since the general unavoidable boundary conditions are reduced to a minimum [74,75]. It should be mentioned, that these test configurations in micro scale, including the simplifications, have significant disadvantages, since the resulting experimental

findings both on the fiber-matrix combination and interfacial adhesion behavior do not reflect the overall composite performance at macro scale [41,76,77]. Based on this, the data obtained from these micro-scale tests are typically implemented directly in simulation models investigating specific macroscopic effects in the composite structure without considering the upscaling effect.

The conclusion of these aspects is that a systematic correlation and transferability of the experimental findings between different test designs is only feasible in a quantitative manner. Due to this limitation of the relative comparability, a methodical simplification via specific test chain (from micro to macro scale) including a suitable step-by-step principle is required for the tailored investigations of fiber reinforced composites in terms of (i) the selection of the single components, (ii) fiber-matrix compatibility and (iii) the subsequent determination of the essential mechanical properties.

Based on the theoretical approach according to the damage equivalence with the further assumption of the damage behavior, suitable transfer criteria need to be determined. Therefore, the results from the model tests at micro scale on simple filaments are essential, since these findings form the basis of the transfer criteria including relevant measurement values for a better validation of the individual single fiber test setups as well as subsequent different test scales. However, the unavoidable size effect due to the upscaling from micro to macro scale and the associated influences have to be taken into account, such as statistical filament distribution (in the fiber bundle and layer), local adhesive imperfections with the matrix or impregnation and consolidation defects [41,78,79]. Furthermore, fiber-fiber and fiber-matrix interactions, e.g. friction effects, local stress concentrations and deformation constraints contribute to the performance of the composite, so that micro scale tests with filaments overestimate the mechanical properties and the accompanying measurement sensitivity. An efficient approach would be measurements on fiber bundles as an intermediate link (meso scale) between model testing and measurements on simple composite lay-ups (with regard to component-like designs) [80].

2.3.4 Laminate theory and load coupling mechanisms

Due to the anisotropic (direction-dependent) material structure, other calculation methods have to be considered for fiber reinforced composites compared to isotropic materials. As explained in detail in chapter 2.3 regarding the influence and effect of direction-dependent stress and fiber compatible force transfer, the analytical calculation (stress- and strength analysis) has to be done layer-by-layer. In addition, the fiber orientation for each layer has to be considered separately [31,81]. Due to the inhomogeneous mechanical properties, fiber reinforced composites in particular tend to undergo interface failure caused by shear stresses, which act in-plane and out-of-plane of the composite layers. These inter- and intralaminar shear-induced damage mechanisms are significantly affected by tensile stresses (reduction of the failure resistance) and thus facilitate failure [24,82].

According to the current state of the art, the classical laminate theory (CLT) represents an important material law as computational method for the stress calculation [32,83] in fiber reinforced composites. This method is based on Kirchhoff's plate theory [84] (assuming UD-single layers as computational unit) and has primarily two objectives: (i) characterization of the mechanical properties of the composite and (ii) determination of the acting distortions and stresses [30]. Concerning the CLT for describing the deformation behavior of composites, an understanding of the performance of multilayer structures is essential, since isotropic materials under normal stresses causing strain or shear stresses only result in shifting. Typically, laminates are subjected to coupled stress behavior, which leads to load coupling mechanisms and depending on the staking sequence, quasi-isotropic (almost direction independent properties), orthotropic (special case of anisotropy with semi-inhibited coupling dimensions equal to the isotropy) or anisotropic (direction-dependent properties) behavior is obtained. In this context, the CLT is conceived so that the homogeneous individual layers are mathematically combined into one complete laminate assuming plane stress conditions, so that homogenized elastic properties can be calculated [29,81]. Moreover, the CLT enables to describe overall deformations through an analytical approach such as bending, twisting or elongation as well as their combinations with each other in a stress coupled manner. According to the mathematical approach, the CLT basically

describes the interaction between internal forces **n** and stresses **m** of the laminate plies versus the associated distortions **ε** and curvatures **κ** of the intermediate surfaces inside the composite, whilst the stiffness matrix C represents the connecting link [31,83] and is expressed in Equation (3) following the purely formal derivation.

$$\begin{Bmatrix} \mathbf{n} \\ \mathbf{m} \end{Bmatrix} = \begin{bmatrix} A & B \\ B & D \end{bmatrix} \begin{Bmatrix} \boldsymbol{\varepsilon} \\ \boldsymbol{\kappa} \end{Bmatrix} \tag{3}$$

Thus, the stiffness matrix (comprises the sub-matrices A, B and D with 9 constants each) is symmetric to the main diagonal, since based on the constitution law and accompanying that each matrix is symmetrical to the main diagonal. This is the basis for the characterization of the load coupled behavior in fiber reinforced composites [32,84].

Due to the fact that different symmetry levels (related to direction-dependent material properties) emerge, depending on the stress-strain interaction related to the material type and the accompanying composite structure (isotropic, orthotropic or anisotropic), the reduction of the number of constraints in the stiffness matrix has to be considered [31,84]. Related to this, the matrix A (in-plane moduli) associates the load transfer with the distortions. Therefore, this part of the stiffness matrix is called the plane quadrant, since in-plane loads are related to in-plane strains. Due to that, the matrix A only comprises strain and shear stiffness (defined as the extensional stiffness matrix). As discussed above, before considering the symmetry effect in the matrix, shear distortions lead to axial forces and elongations result in shear forces [32,84]. Moreover, the matrix D connects the moments with the curvatures and thus this part of the stiffness matrix is referred to as the bending stiffness matrix. According to the symmetry of the matrix D, curvatures result in a twisting moment and torsion leads to bending stiffness. Subsequently, matrix B is the so-called coupling stiffness matrix, combining the curvature of the intermediate surfaces with the axial and shear forces, since the distortions are linked with the intersection moments.

For the stress-strain relation in composites, the three main symmetry cases of the stiffness matrix are represented by anisotropic, orthotropic and isotropic material properties. Thereby the stiffness matrix for anisotropic behavior contains

21 independent constants (red colored) compared to the isotropic behavior with 2 independent constants. Composites with multi-layered structure comprising woven or non-crimp fabrics are typically considered as orthotropic, which reveal 9 independent constants in the stiffness matrix (same positions as isotropic behavior). By using a woven fabric as an example, the coordinate system is placed parallel to the warp and weft yarn as well as perpendicular to the fabric orientation, so that the complete composite system is considered only in the fabric plane. Moreover, specific approaches, such as the layered plate, e.g. contain for the anisotropic case 18 independent constants or for the orthotropic performance only 8 independent constants [81,85]. This can be simplified in a schematic illustration for the stiffness matrix as shown in Figure 2.7 for the stress-strain relation in composites.

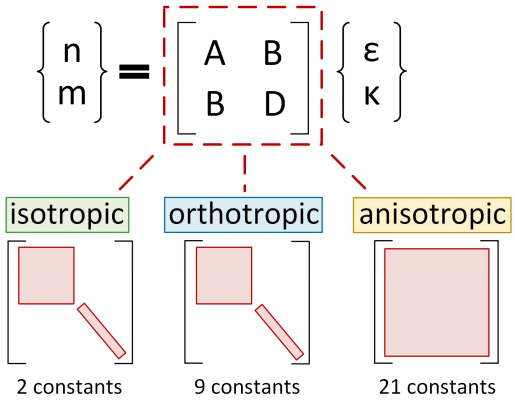

Figure 2.7: Schematic illustration of the independent constant for isotropic, orthotropic and anisotropic material property symmetry cases [81].

In this context, the CLT as an analytical method is a well-established model to analyze load coupled mechanisms in fiber reinforced composites and thus to predict the load transmission in several layers with specific orientations leading to load coupling effects such as bending-twisting, tension-twisting or tension-bending. The schematic explanation in terms of the deformation concept depending on the accompanying distortion possibilities is illustrated in Figure 2.8. However, recent studies investigating load coupled behavior by utilizing the CLT approach highly differ in terms of the research objective. Thus, load coupling has to be eliminated when dealing with certain and unwanted failure mechanisms [11,27], while load coupled effects are intended to create deliberate movements or redirected stresses e.g. modeling unbalanced composites for wind tube blades [86] or aircraft

wings [34,87]. Based on this, the suitable load transmission into the reinforcing fibers is essential to achieve load coupling effects without causing any damage related to the failure criterion [82].

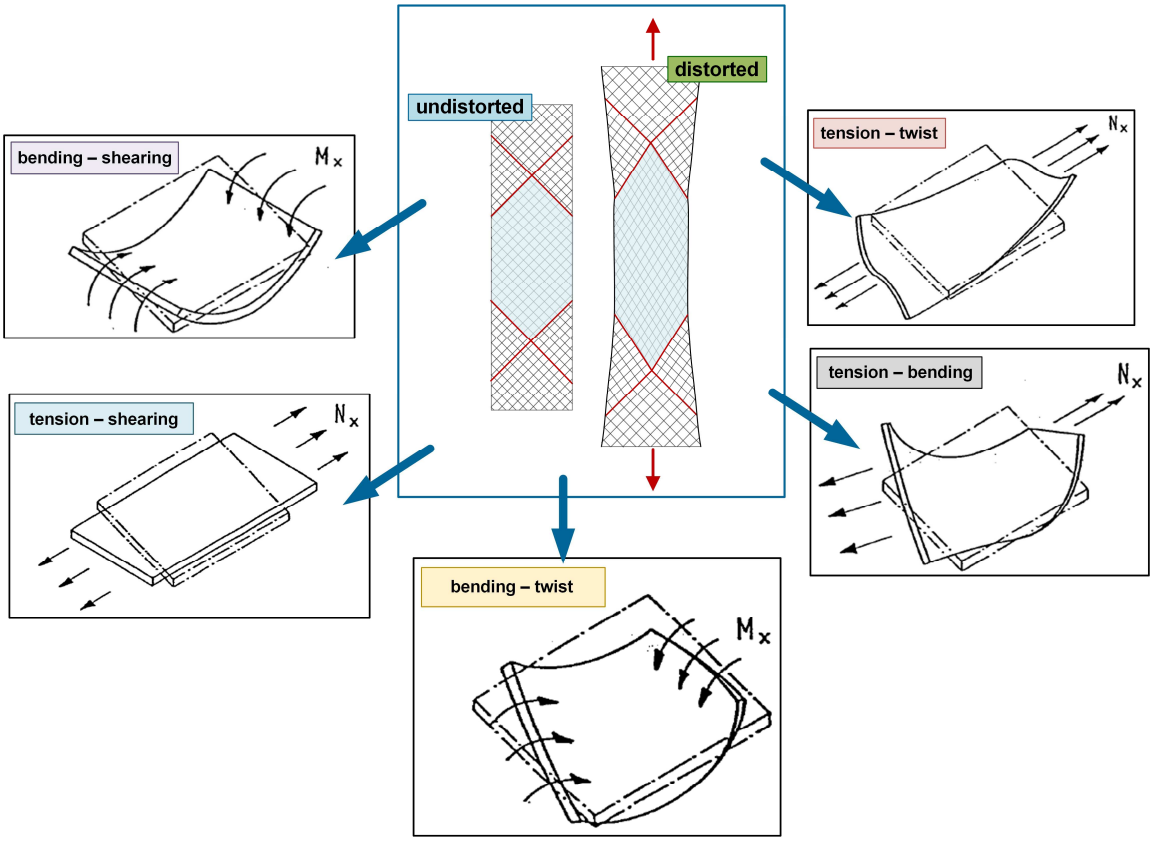

Figure 2.8: Schematic illustration of the deformation process as undistorted and distorted resulting in bending, twisting, shearing and tension related to the load coupling effect according to the material's law for fiber reinforced composites [84].

Nevertheless, for the application of the CLT, boundary conditions have to be assumed, since this approach is only valid under certain restrictions [10,19,83] such as: (i) overall deformation remains small, (ii) all layers are ideally bonded and consequently no relative displacement occurs, (iii) the material behavior is linear as well as ideal elastic and thus linear elastic laws can be applied, (iv) the material is assumed to be homogeneous (cracks, air inclusions are neglected), (v) plane stress conditions are expected, and (vi) all further influences related to the composite thickness such as force distribution, elongations or distortions are considered constant. Extensive studies on the CLT with thermoset-based systems with brittle matrices showing small deformations have been carried out [30,81]. However, for fiber reinforced elastomers as flexible composites, the CLT cannot be transferred

directly, since the matrix material is non-linear elastic with distinct viscoelastic properties [19,83]. Moreover, the assumption of UD-layers and accompanying boundary conditions to simplify the analytical leads to a relatively accurate and fitting solution. Therefore, further terms have to be incorporated in this material law especially by using woven textiles as a reinforcing structure, since the additional fiber undulations result in a significant reduction of the mechanical properties of the overall composite such as specific strength or Young's modulus [24,46]. Therefore it is even more challenging to choose the optimal experimental tests as well as to develop tailored test concepts, which will generate the essential material data values and parameters (also for accompanying customized simulation models). Thus, systematic errors are minimized according to the implemented test chain principle as a promising tool from micro to macromechanical load coupled mechanisms.

2.4 Fiber reinforced elastomers

Due to the strong direction-dependent mechanical properties (as explained in chapter 2.3.2), the potential of elastomeric matrix systems as a promising alternative material leads to completely new possibilities (see chapter 2.2) that cannot be realized with classic composites [41]. Therefore, these flexible composites represent a new material class, which successfully meets today's technology demands e.g. in the aerospace industry such as for satellite components with unfolding and reconfigurable features. This ability to fold is only feasible due to the low bending modulus resulting from utilizing elastomers and high membrane stiffness (by the fiber reinforcement) simultaneously. The stiff fibers are stabilized in the matrix and still have a soft embedding, which permits the fibers to buckle and wrinkle instead of breaking [41,88]. In the context of fiber-matrix load coupling behavior (especially the reconfiguration capabilities), relatively high bending stiffness with simultaneous low shear strength is required to prevent unwanted shear buckling. These unique multifunctional properties are only feasible with elastomeric matrices. Besides this, elastomers are well known and distinguished for their damping, absorbing and flexible performance. The good damping properties absorb vibrations (dynamic loads) that favor damage and simultaneously maintain continuous elastic deformation. Despite the low bearable strength and stiffness of pure elastomers, they can be improved by tailored fiber reinforcement and still retain

high flexibility. Figure 2.9 schematically explains the distinct controversial material properties between linear behavior of the reinforcing fibers and non-linear behavior of the elastomeric matrix. This leads to challenges in the composite (already in a matrix-dominated configuration with ±45° orientation), because both constituents have to be handled simultaneously. However, some recent scientific research projects have ended at the concept phase due to difficult issues of the pronounced non-linear elastic material behavior of elastomers or viscoelasticity related to the fiber-matrix interaction (such as creep or relaxation) causing serious issues during actuation [41]. Based on these approaches, detailed investigations and analysis of the mechanical properties as well as the structural fiber-matrix interactions in flexible composites are necessary [45].

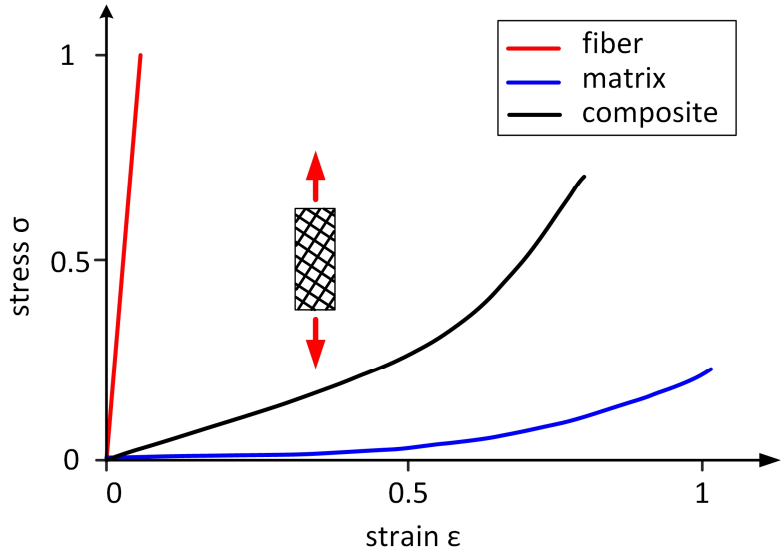

Figure 2.9: Schematic comparison in a stress-stress-strain diagram of fiber, matrix and ±45° oriented flexible composite [45].

Moreover, besides the selection of the constituents (fiber and matrix) a suitable manufacturing process and the determination of the material parameters are basic prerequisites. Although, only a few scientific works deal with flexible composites containing a higher fiber volume content such as Peel [42], Koschmieder [36] or Hoffmann [41]. Thereby the focus has been on the topic of fiber reinforced elastomers more generally, already with promising findings. Furthermore, these offer a good basis for potential material selection, manufacturing possibilities and first analysis related to materials science and testing. Peel [42] clearly focuses his research on prototype designs based on studying the reaction of the matrix to tensile

stresses with accompanying simulation models. The doctoral thesis of Koschmieder [36] on the processing and properties of fiber composites with elastomer matrices includes a comprehensive analysis and classification of elastomers which is limited to winding techniques in manufacturing. The strength of various material combinations was characterized. However, the determined properties are exclusively for wound samples, whereby the fundamental error is the fiber winding angle. Since no specific fiber surface treatment was applied to enhance the interfacial adhesion, the results revealed relatively minor fiber-matrix bonding. The complex topics of surface treatments and adhesion effects among the associated challenges were also addressed and discussed in detail by Hoffmann [41].

Especially for smart material applications, the performance of flexible composites is highly dependent on the manufacturing process. Thus, if compact fibers are combined with high viscosity matrices, a poor impregnation is inevitable. Based on this, all available fiber materials are possible as reinforcement, since the fiber sizing (surface coating) needs to be adapted to ensure an adequate adhesion with the matrix. Hence, the respective composite performance is easily adjustable by selecting the right matrix material. Therefore, the fiber is chosen first, as this primarily dominates the mechanical behavior. For the optimal matrix type, certain requirements have to be fulfilled and thus some factors need to be considered such as viscosity, curing temperature, pot life or bonding to the fibers.

Regarding the manufacturing, infiltration is generally difficult due to the higher viscosity in the mixed state of cast elastomers compared to the considerably lower viscosity of thermosets like epoxy resin. Room temperature-crosslinking silicones in particular possess viscosities of around 3.5-5.0 Pa·s and thus infiltration is only possible in certain conditions. In this context, the vacuum assisted resin infusion (VARI) process represents a promising manufacturing method especially for the laboratory. The VARI process offers good reproducibility also for the composite quality whilst a high degree of flexibility and adaptability according the requirements is simple to achieve [25]. This setup is expendable with appropriate disposable layers such as perforated foils, peel ply or flow help. Moreover, the vacuum unit meets several requirements, like (i) a uniform compact pressure along the thickness

to ensure a homogeneous consolidation, (ii) uniform impregnation with linear flow front distribution and (iii) prevention of air inclusions and porosity in the matrix during the impregnation [25].

2.4.1 Hyperelastic matrices in flexible composites

The handling of elastomers is quite challenging and significantly limits the variety of suitable elastomer materials. Silicones and polyurethanes based on cast systems have become well-established materials as hyperelastic elastomers (material is conservative showing a time- and deformation independent behavior as the applied deformation is fully retained in distortion energy) [50]. The morphology in particular favors elastomers for utilization in flexible composites, as the main application is mostly in entropy elastic regions (above glass transition temperature) so that the wide-meshed crosslinked polymer chains are soft at room temperature with pronounced recovery abilities after deformation. Especially silicone, as an unfilled elastomeric system with few side chain branching, is distinguished due to hyperelastic properties. Furthermore, silicone has no permanent residual deformation, high temperature resistance, creep resistance and hydrophobic properties [23,50]. Based on these previous investigations, silicones and polyurethane as two-component cast systems are chosen for the matrix as well as glass fibers (inorganic and almost isotropic properties) and polyester fibers (organic and representative for thermoplastic fibers) have been studied in this thesis. Moreover, polyurethane elastomers in the context of fiber reinforced elastomers are evaluated due to the good bonding properties, since the use of primer (adhesion agent) is typically omitted [41].

2.4.2 Mechanical properties of fiber reinforced elastomers

The characterization of the mechanical behavior of fiber reinforced elastomers is more complex compared to composites with thermoset matrices. When a load is applied, time- and load-dependent rearrangement processes occur, which lead to relaxation and creep, so that viscoelastic properties (time-, temperature- and frequency dependent elasticity) dominate the behavior, yielding to mobility reduction due to the fiber-matrix interaction [89,90]. These effects in particular are relevant for the mechanical properties of the composite and thus for the fiber-matrix load coupling, since viscoelasticity causes a delayed equilibrium material response

under deformation. Hence, the time-dependent behavior is influenced by the stretching or debonding so that irreversible plasticity due to molecule rearrangements occur depending on the duration and speed of the deformation level. Fiber reinforced elastomers in smart material applications are mostly exposed to semi-cyclic loadings with intermediate holding phases, such as in soft robotics for gripping or position changes of unfoldable satellites, where hysteretic and relaxation mechanisms occur simultaneously [41]. In this context, common carbon black filled elastomers under cyclic loading leads to Payne effect as well as Mullins effect [90,91]. Especially the Mullins effect leads to hysteretical stress softening in the material and to irreversible residual elongations. After a certain number of cycles at constant deformation level, a new equilibrium state (preconditioned material) is reached. Accordingly, the applicability of the “Mullins effect”-like phenomena for fiber reinforced elastomers was also addressed and investigated in the doctoral thesis of Hoffmann [41]. Related to this, similar hysteretic loops can be observed by step cycle tests due to absorbed energy during the loading and unloading phases, caused by the reinforcement and the fiber-matrix interactions. As fiber reinforced elastomers, especially with woven fabrics, show a close performance to textiles, the hyperelastic silicone matrix cannot restore the original position of the fibers subjected to shear stress. The fiber friction as the main effect exceeds the restoring ability of the matrix, which leads to irreversible rearrangements and absorbed energy in the composite. Moreover, additional influences and losses become even stronger due to woven textiles. Hindered deformation related to the fiber undulations occur so that stresses and deformations affect the Poisson’s ratio by interacting with the second perpendicular fiber direction via the surrounding matrix and the weave points [28,46,92–94]. This influences the hysteresis behavior and quantity of absorbed energy. Especially for woven fabrics under tension loading, warp and weft yarns linked by weaving are quasi-inextensible and thus the stretching and reshaping is dominated by in-plane shearing. Thus the shear behavior is an important factor during the deformation of textiles. Moreover, several studies [95,96] have revealed that in-plane and inter-ply shearing is an essential parameter for the micro- and meso scale deformation affecting the deformation of aligned composites. For a particular reinforcement, the in-plane shear is limited depending on the shear angle and is thus strongly affected by the fiber orientation of the woven fabric. As

illustrated in Figure 2.10, the influence of the clamping shows that the material in or near the clamping (region B) is completely hindered in deformation, whilst region C, however, is only partially affected. In contrast to that, in region A the material is completely unaffected by the clamping revealing deformation only due to the fiber-matrix interaction and shearing between the fibers.

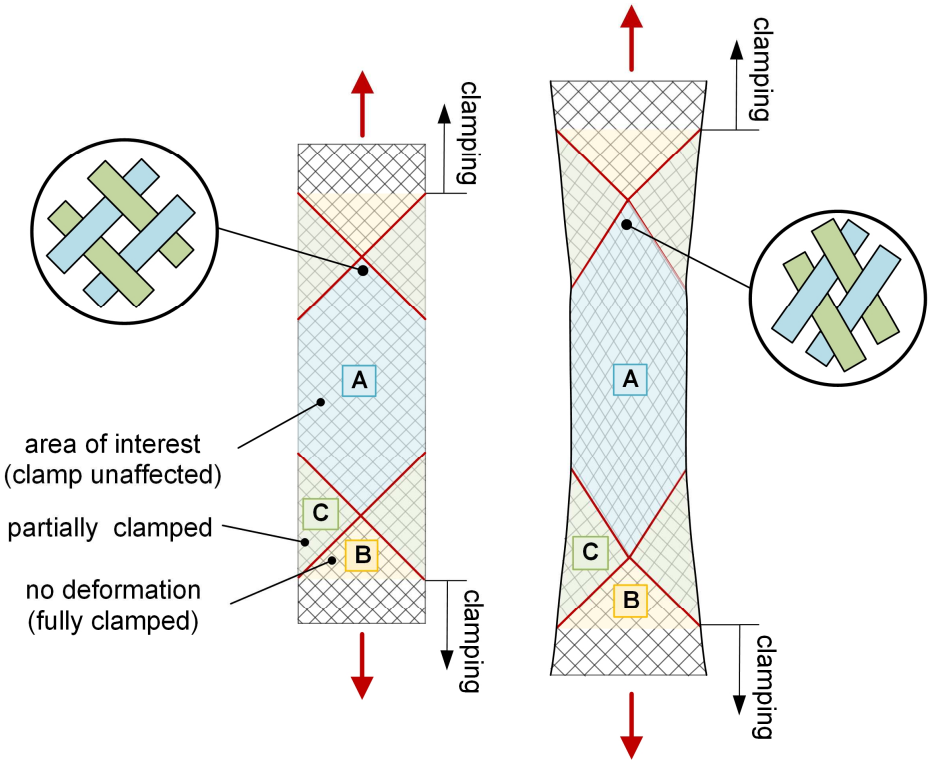

Figure 2.10: Schematic comparison of the general distortion behavior in fiber reinforced elastomers with textile-like performance [28,46,97].

The shearing between warp and weft yarns depend on physical phenomena during in-plane deformation such as fiber friction and this has already been studied in detail by Lindberg et al. [98] and Grosberg et al. [99]. Overall, shearing occurs when the fiber orientation deviates from the loading direction [28]. If a specific threshold value as the so-called locking angle is exceeded, wrinkling will appear resulting in an out-of-plane shearing. In this context, the phenomena of wrinkling is generally dependent on the deformation performance an strength of the woven fabric, since high friction coefficients and inter-ply interactions tend to have a strong impact [88]. Previous research of Gutowski et al. [100] showed that the textile wrinkles, if the required shearing, by accommodating the composite material for a certain geometry, is not feasible. Related to this, Prodromou and Chen [101] demonstrated

that textiles start to wrinkle whenever the critical shear angle is exceeded. This in-plane and out-of-plane deformation behavior of textiles versus the accompanying shear angle is explained schematically in Figure 2.11. At the initial state, warp and weft yarns are aligned orthogonally to each other. Intra-ply shearing becomes dominant when the yarns start to shift (begin to rotate and slide) so that the friction e.g. between weave points or viscous drag contributes to the shearing resistance. When loading is still increased, the yarns start to converge with the loading direction and press against each other (compression stresses) until yarn compaction results and shear stiffness increases. Subsequently, the yarns become locked and out-of-plane shearing as so-called wrinkling or buckling is achieved, correlating with the locking angle. This mechanism is named the trellis effect. At this point, the load increases exponentially to a high value until the tensile strength is exceeded and failure occurs [88].

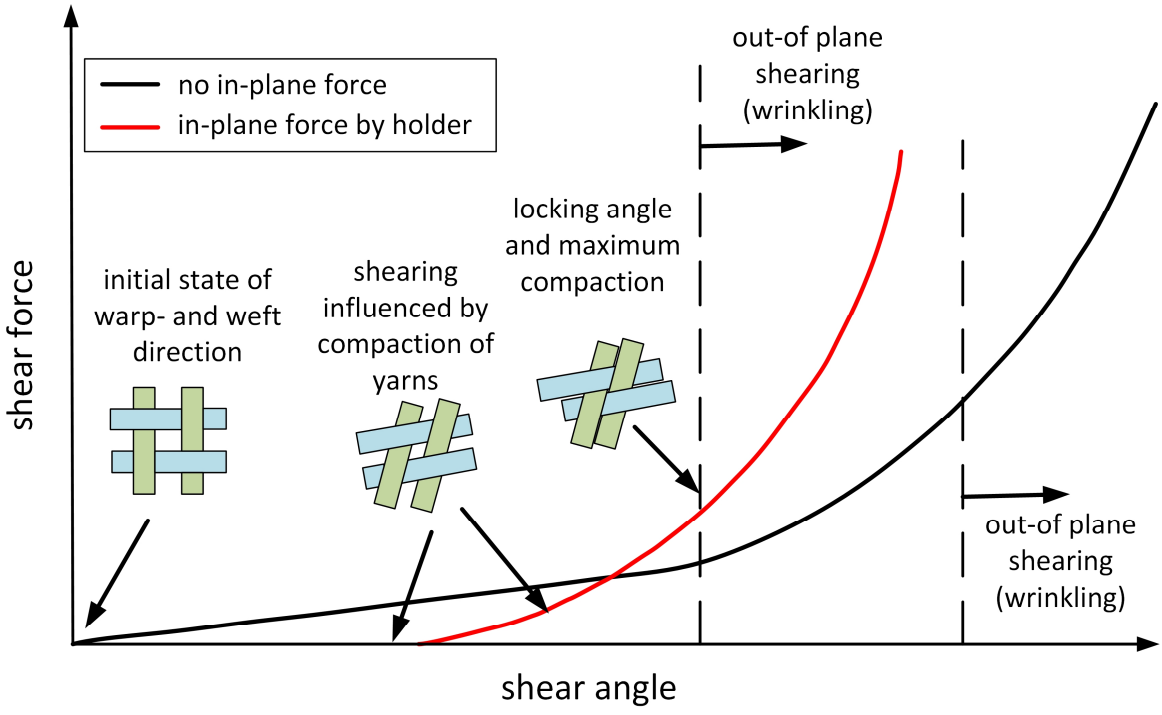

Figure 2.11: Schematic illustration of in-plane shearing versus shear angle showing the trellis effect (locking angle) resulting in an out-of-plane shearing (wrinkling) during progressing loading [88].

2.5 Test concepts

For the comprehensive understanding of the mechanical properties and performance of fiber reinforced elastomers also for accompanying simulations, specific material parameters such as Young's modulus, tensile strength or interlaminar shear strength are important. The literature research focused on recent knowledge on flexible composite testing, revealing a broad range of articles concerning low fiber volume content (approximately 2%) or short fiber reinforcement by injection molding [90,102]. This material composition is easier to handle and thus standardized test procedures with normed sample geometries are mostly used.

Little research has been done on elastomers with endless fiber reinforcements, exceptions are represented by Koschmieder [36] or Hoffmann [41] dealing with significantly higher fiber volume content and further providing interesting approaches for the experimental characterization. Koschmieder determined the stiffnesses and strengths in the fiber direction of various fiber-matrix material combinations tested on standardized ring samples according to ASTM 2290 (ring sample internally loaded in tension by two half cylinders with a horizontal test slot). However, this measuring method is not adequate due to the occurring geometrical discontinuity, especially at the edges near the test slot. Thus, local stress concentrations lead to distorted elongation and inadequate measuring. Therefore the deformation is inhomogeneous throughout the cross-section of the sample so that the sample becomes more stretched on the inside (because of the smaller ring diameter) than on the outside. This test setup shows further clamping issues which cause either slipping or damage due to the hyperelasticity of the silicone. Besides, only wound samples with the essential error indicated by the fiber winding angle were analyzed leading to high scattering in the results and even to invalid measurement values. Koschmieder additionally conducted roving pull-out tests as a promising test setup to study the fiber-matrix strength.

Hoffmann performed experimental characterizations only on pure silicone matrix with modified grips to provide sufficient clamping (to minimize the risk of slippage) without causing damage near the grips due to unavoidable compression stresses. However, the characterization with textile reinforcement is more complex so all tests on fiber reinforced elastomers were performed with UD-non-crimp fabrics

impregnated with a polyurethane matrix (due to the lower viscosity which simplifies the handling). The common approach by using pads as load transfer elements was implemented, although this method did not yield satisfactory results. Thus, the primer substrate was indicated as challenging issue and leading to partial adhesion. However, this finding has to be put into perspective due to the significant deformation behavior of the constituents and the textile-like performance of these flexible composites causing peel stresses between the pads and the specimen. UD-laminates reveal strongly varying characteristic values depending on the test method, sample geometry and layer structure. This effort is increased considerably and thus also the accompanying evaluation of the material parameters becomes challenging. Even the load transfer in UD-laminates is complex without causing any premature failure due to shearing inside the cross section.

Overall, these previous findings [36,41,42,103–106] obtained that the experimental conduction and evaluation of the mechanical material properties of fiber reinforced elastomers is difficult. This can be further explained by the significant orthotropic behavior of brittle fibers with elastomeric matrices. Since the linear elastic fibers and the non-linear elastic matrix are deforming controversially (referred to the change in elongation). In this context, flexible composites with various fiber orientations show distinct deformation inhomogeneities, which cause further issues in the experimental evaluation of the mechanical material properties. For woven fabrics, the orthotropic fiber configuration causes stresses and deformations along the thickness of the laminate and thus the micro-geometry of the fiber bundles in the textile needs to be considered [41].

In the following, proven test concepts with the promising approach according to the test chain (from micro- and meso- to macro scale) described in chapter 2.3.3, including a defined step principle and corresponding transfer criteria, will be presented. The essential mechanical behavior and the structure-property correlation in flexible composites despite the high orthotropy and inhomogeneity can be determined experimentally also for further numerical simulation models.

2.5.1 Fiber pull-out test

As already explained in detail in section 2.3.3, the fiber-matrix adhesion is essential for the mechanical properties of the composite. For the mechanical characterization and evaluation of the interface strength, a special measurement method is required, based on different direct (fiber-loaded) or indirect (matrix-loaded) techniques. In the literature, special test concepts are reported, whereby the fiber pull-out assembly as a direct fiber-loaded configuration is a suitable method for fiber reinforced elastomers with pronounced flexibility. Moreover, single fiber tests are advantageous, due to their reproducibility and high measurement sensitivity, minimizing disturbing influences such as fiber orientation, fiber distribution or impregnation quality, which are unavoidable factors in composites.

Regardless of utilizing filaments or several fibers as a bundle, the basic concept of a fiber pull-out test is that the fibers are torn out of the surrounding matrix under tensile mode. The maximum bearable force or shear stress (related to the embedded fiber surface) is the indicator of the quality of the fiber-matrix strength. The interlaminar shear strength is calculated according to the embedded fiber surface versus the maximum bearable load which is required for the pull-out [58,75,107]. Generally, the force-displacement curve of pull-out tests, schematically illustrated in Figure 2.12 (a), exhibits a characteristic behavior which typically contains four specific regions.

In the initial phase (0-1), the force signal increases almost linearly representing the stable interfacial adhesion. Furthermore, a slight degressive change in the curve (1-2), indicating the initial debond occurs. Sometimes, when a kink or peak close to maximum value appears, the load for debond initialization is high enough and exceeds a certain material related threshold (1') followed by a progressive debonding (1'-2). So the initial debonding performance is associated with the fracture toughness of the fiber-matrix interface properties [64,75,108,109]. For fiber reinforced elastomers, the initial phase can also be affected by the hyperelasticity as well as incompressibility, allows a certain amount of deformation before the fiber-matrix interface starts to get strained. After reaching the maximum, the force level suddenly decreases to a certain level (3-4), which is called load drop.

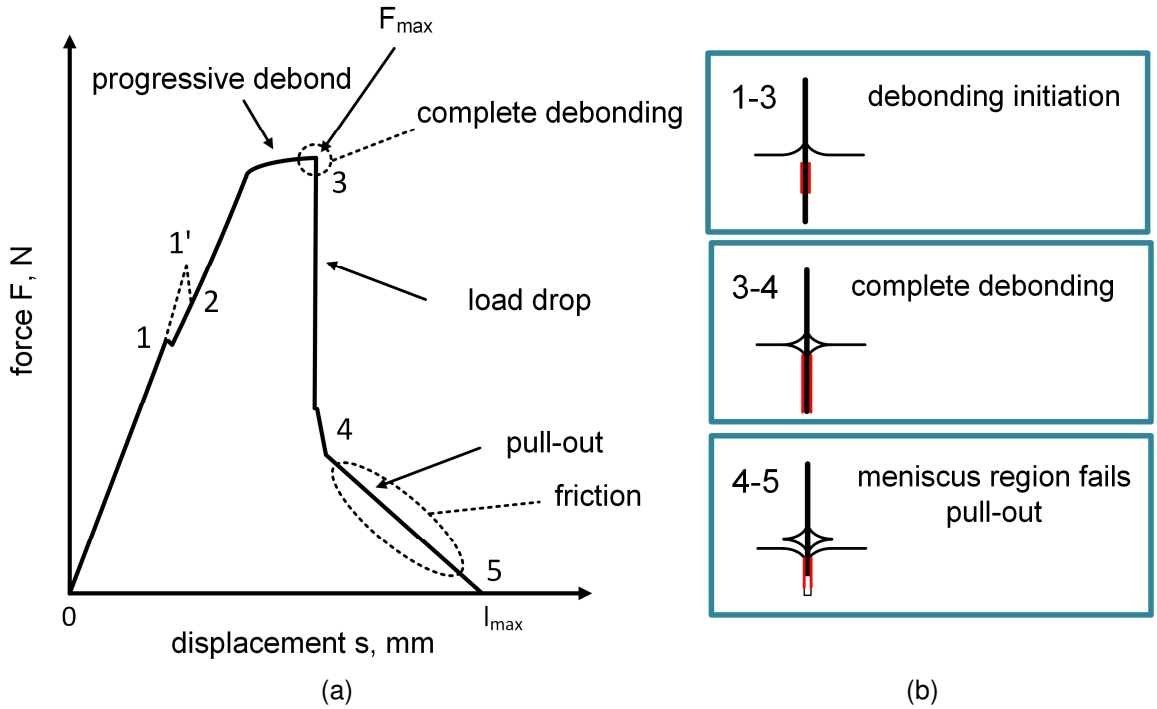

(a) (b)

Figure 2.12: Force-displacement diagram of a fiber pull-out test labelling the main regions (a) including the three principle stages of initiation, debonding and pull-out (b) [64,109].

In Figure 2.12 (b) the debonding process is schematically explained in three main stages (crack initiation, debonding, pull-out). Usually, this process leads to a stable crack propagation throughout the complete embedded fiber length so that the fiber no longer adheres to the matrix [75,108]. Occasionally, the debonding crack tip might reach a sort of stability caused by friction in the fiber-matrix interface and the debonding stops. After applying a certain required incremental force by further pulling, the crack propagation will continue. This phenomenon is indicated as stick-slip in the load-displacement signal. Finally, after complete debonding, the force signal is only transferred in the interface by friction and thus the fiber has to surmount the friction force in the last zone (4-5). The friction decreases proportionally to the remaining contact area in the interface. Subsequently, the maximum displacement value equals the embedded length, whilst the force value converge to zero. In principal, the pull-out tests are limited by two significant parameters: the pull-out speed leading to fiber breakage for high strain ratios and the embedded length itself, since beyond a certain threshold, the interface strength exceeds the fiber tensile strength.

The main advantage of pull-out tests on filaments is that only one fiber-end is partially encapsulated with the matrix enabling a defined wetting depth and thus the interfacial strength can be calculated relatively accurately. However, this concept theoretically assumes two important aspects: (i) the fiber-matrix interface is perfectly intact at the maximum force value and (ii) the shear stresses along the embedded fiber are constant, which premises that the matrix behavior is subjected to ideal plastic deformation near the interface (see Figure 2.13) [64,75]. The stress distribution for real materials such as thermoset-based matrices results in significant local stress concentrations near the transition between fiber entry and matrix surface as well as at the embedded fiber end. This behavior is related to the ideal elastic properties of brittle matrices [110]. According to basic numerical considerations, the calculation of the interface strength would require the highest value at the beginning, which would lead to singularities, e.g. theoretically infinite high stresses due to no embedded fiber surface. Since real stresses only become finite, this approach raises some open points related to the exact maximum shear stress. Besides that, polymeric matrices are typically not ideal plastic or elastic but rather reveal a time-dependent viscoelastic behavior leading to further complex time-dependent stresses or deformations.

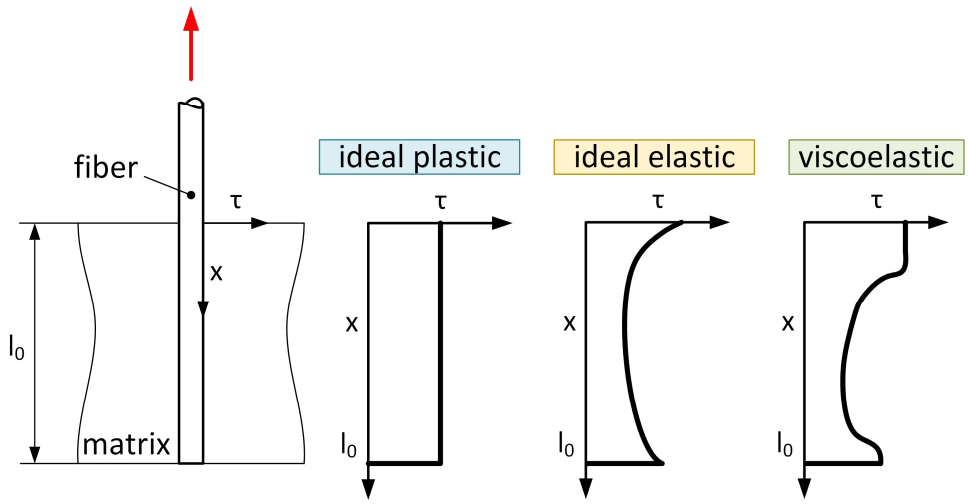

Figure 2.13: Schematic demonstration of shear stress profile in the fiber-matrix interface for different deformation behavior of the matrix material [64,108].

These investigations are challenging and based on current findings, there is still no convincing method or approach. For the failure behavior of fiber-matrix interfaces, the interface toughness corresponds to the crack growth initiation. The assumption

of a singular crack tip with a sharp crack and the local stress concentrations lead to inappropriate characterizations. Therefore cohesive zones are more realistic for the crack initiation and propagation representing a region for the material separation [109]. Related to this, the crack is initiated underneath the matrix surface and a meniscus is formed near the fiber entry, which will also be pulled out [64] and is evident in Figure 2.12 (b).

In this context, the failure performance and interface characterization of elastomeric matrices with stiff fibers by pull-out tests are even more complex, since the distinct hyperelasticity leads to further effects. The crack initiation underneath the matrix surface is additionally affected due to the incompressibility and thus this meniscus can deform favorably according to the pull-out direction and even becomes magnified. Furthermore, most pull-out techniques are based on the concept that the matrix part is clamped in a fixed position, whilst the fiber is pulled out [59,76,77]. This test configuration is not suitable for hyperelastic matrices since the resulting compression stresses are directly transferred to the embedded fiber end. Subsequently, those stresses clamp the fiber and hinder it from being pulled, which leads to fiber breakage. Based on these aspects, there are certain benefits of single fiber debonding methods like the SFPO test or the microbond test. However, such tests also have limited applicability to elastomeric matrices. The single-fiber test requires that the matrix adheres to the substrate (back sheet) better than in the fiber-matrix interface without any evidence of proof. Further, the free fiber end can deform in the loading direction leading to an uncontrolled meniscus during the pull-out [111]. The microbond test reveals a high reproducibility and measurement accuracy, because several matrix droplets are applied onto the ident filament [58,68,108]. Nevertheless, the matrix droplet starts to deform significantly due to the incompressibility before the interface is detached, which influences the results. Since the fiber bundle is considered as the representative unit in composites, there are still no suitable pull-out or debond tests based on bundles [41,76,77]. However, utilizing bundles are affected by several influencing factors that can be excluded by single fiber tests. Since the impact of statistic fiber distribution, impregnation imperfections or fiber friction significantly impair the composite performance, the fiber bundle matrix adhesion leads to a more realistic failure and deformation performance in the interface compared to single fiber tests. Consequently, fiber

bundle pull-out tests reflect the fiber-matrix adhesion more appropriate for composites than single-fiber tests showing a similar measurement sensitivity. In contrast to that, these factors reducing the interfacial strength and thus these findings have to be considered in a relative manner for optimized properties versus a more realistic performance. In conclusion, the complementary knowledge of the micromechanical properties of single fibers and the behavior of bundles at meso level is necessary to investigate the structure properties of simple composites. Hence, the preferred approach constitutes a test chain with suitable transfer criteria by a step-by-step principle.

2.5.2 Composite tension test

Basically, the testing of fiber composites comprising brittle matrix materials is carried out according to standardized methods such as ISO 527, DIN EN 2850 or DIN-EN-ISO 14125. Typically rectangular or cuboid sample geometries are used with additional force introduction elements as so-called cab strips. The cap strips are intended to provide a uniform load introduction and transfer (like tensile or compression stresses) to the entire cross section area of the sample to ensure a homogenous deformation. The performance of these pads can be additionally enhanced by considering a tap angle of about 45° [112]. Due to the adhesive joining with the specimen, typically with an epoxy resin-based agent, the sample surface has to be prepared by carrying out the main steps of roughening, cleaning and degreasing to guarantee sufficient adhesion [60,113]. This method is not applicable for fiber reinforced elastomers due to the structure-property relationship, since these flexible composites are subject to distinct textile-like behavior.

The main challenge for testing flexible composites is the controlled handling of the non-linear or viscoelastic properties related to the elastomeric matrix combined with the anisotropic linear performance of the fibers. Moreover, the fibers have high stress resistance and small elongations controversially to elastomers (with high deformation ability but low maximum stress resistance). This leads to a distinct gap in mechanical properties such as stiffness or strength. Therefore, the use of cap strips is not feasible, since the shear modulus of the brittle agent versus the hyperelastic matrix, e.g. silicone, is significantly higher and subsequently detaching can occur caused by shear stresses in the adhesive surface.

Within the scope of this thesis, the material performance of fiber reinforced elastomers has been investigated primarily according to tensile stresses, since these have been determined to be critical whilst analysis of the compression or bending stresses is not required due to the low inherent stiffness. Concerning the testing procedure, typically the composite samples are clamped by mechanical or pneumatically controlled grips causing compression stresses and leading to shear stresses during the tensile test. Furthermore, common clamping jaws are metallic with a grooved surface to increase the grip and prevent slipping. However, the hyperelastic matrix material in fiber reinforced elastomers such as silicone possess a high notch sensitivity, which leads to local stress concentrations in the clamping area due to the compression. Therefore, clamping jaws with a grooved surface are not suitable. Furthermore, critical stress peaks occur especially at the end of the clamping near the free test length, since no material is clamped and relaxes to the original state. This causes a sharp, notch-like transition in the material leading to a premature failure near the clamps. Related to this, Hoffmann [41] addressed this drawback in his research and presented an interesting approach by implementing additional carbon black filled rubber pads between the clamping jaws and the sample (see Figure 2.14).

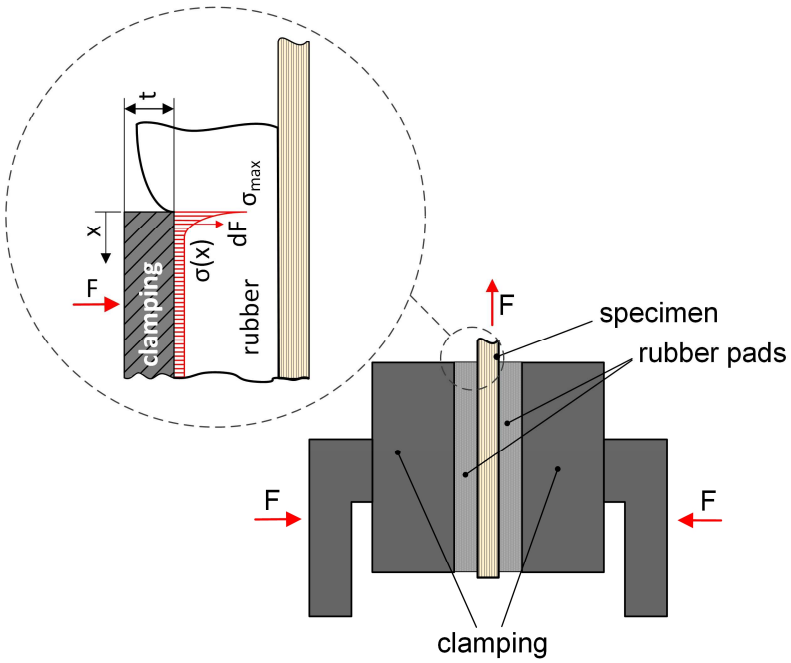

Figure 2.14: Schematic demonstration of the testing concept for fiber reinforced elastomers using rubber pads, including a detail of the local stress concentration in the clamping [80,90].

The concept is based on the assumption that the rubber pads absorb these stress concentrations, so that the sample is unaffected or only minor stresses are acting on them. These findings provide a useful basis, but the conducted tests were limited to the pure matrix material. Furthermore, proven methods focusing on threads or textile-like tapes are already state of the art using circular elements or semi-circular elements instead of clamping jaws [46]. This concept is based on the physical approach according to the Euler-Eytelwein equation (also known as the rope friction equation) by utilizing the effects of static friction related to the wrap angle. For fiber reinforced-elastomers, the test setup for composite tension tests needs to ensure both (i) sufficient clamping for the hyperelastic matrix without causing any local stress concentrations related to compression as well as (ii) successful handling of the reinforcement without slippage. Thus, a combination of the additional rubber pads and the semicircular elements have to be contemplated. In the subsequent part II of this thesis, the concept, implementation and verification of a promising test setup especially for flexible composites will be discussed in detail.

PART II: RESULTS, OUTLOOK AND COLLECTION OF PAPERS

To achieve the above mentioned tasks as discussed in part I, the following chapter part II represents the four main objectives of the thesis based on six papers published in well-known scientific journals and additional two invention disclosures. This section is structured according to the expertise acquired. Generally, some influencing factors such as manufacturing procedure, fiber volume content or fiber-matrix materials are defined as constant and will not be further elaborated in the context of this work and in the listed publications. Nevertheless, these aspects still have a distinct effect on the entire research field of smart composite materials, albeit this will lead to higher complexity and thus are chosen as boundary conditions. Therefore, two different cast elastomers were chosen as matrices. For the tests, polydimethylsiloxane (PDMS), Elastosil RT601 A/B from Wacker Chemie AG (Munich, Germany) and polyurethane (PUR) ClearFlex 50 from SmoothOn Inc. (Lehigh County, USA) were provided. Glass fibers (GF) from CS Interglas AG (Erbach, Germany) and polyester fibers (PETF) from Mates Italiana srl (Milan, Italy) were chosen as reinforcements. For the manufacturing process of all composite samples, the VARI process was chosen with a constant fiber volume content of 50%.

1 Findings of papers

To assume an active role during exposure to an energetic stimulus, an optimized fiber matrix bonding is indispensable to guarantee fiber-matrix load coupling. Besides the efficient load transfer, good adhesive interface moreover reduces the stress concentrations as well as improves the mechanical properties of the entire composite. This requires an in-depth knowledge about the fiber-matrix bonding behavior and the impact on the load coupling performance modified by different fiber surface treatments. Since a fiber bundle, containing several filaments aligned in the same direction, represents almost the smallest representative composite unit, an experimental approach with fiber bundles to study the fiber-matrix interface is

important as an initial performance assessment on composites. However, there is still no existing standardized test method, as discussed above in section 2.5.1, and thus the material characterizations and results from different existing test setups are only comparable in a limited range. Moreover, current well-established testing approaches for interface analysis such as fiber-pull out, fiber push-out or fiber fragmentation test are strongly limited to filaments. However, the literature survey also revealed that these tests focus primarily on the thermoset-based matrices neglecting the clamping challenges associated with hyperelastic materials. In this context, the performance of component-like structures generally includes several influencing factors such as statistic fiber distribution, inhomogeneities or micromechanical material defects, which cannot be evaluated concerning the filament-matrix behavior. Hence, an adequate analysis of the composite behavior involves a large number of bundles with multiple boundary conditions, but a direct correlation between micro- and macromechanical composite properties is not possible.

Therefore, the objective in paper 1, entitled "*Comparison and impact of different fiber debond techniques on fiber reinforced flexible composites*", was the realization of a modified pull-out test especially for fiber bundles. An important focus was the verification of the fiber bundle pull-out test setup to investigate the damage and failure behavior on bundles. This test enables interface measurements on meso scales as an intermediate test level between filament tests (micro scale) and simple composite structures (macro scale). For the interfacial adhesion properties, a manufacturing tool especially for brittle fibers with elastomeric matrices was developed and completed with a special specimen holder to meet the important requirements of a fast and economic handling and causing no further compression effects by clamps. This specimen holder aims to guide the sample by lateral surfaces to provide both, enough space between holder and sample for a free and unaffected deformation as well as prevention from tilting by the low inherent matrix stiffness. In this study, a comparison of two proven filament test methods was carried out. Whilst the single fiber pull-out (SFPO) test represents an ident fiber-loaded condition, the microbond test was conducted for the indispensable statistical comparability. In this context, the influence of the embedded length and pull-out speed as two indicating parameters were analyzed. Due to this, a special

test plan was elaborated to prove the pull-out mechanism within the typical force-displacement curve as discussed in chapter 2.5.1. Moreover, first preliminary tests regarding the fiber surface impact by simple desizing were carried out in addition to demonstrate the measurement sensitivity of the fiber bundle pull-out (FBPO) test. For feasibility and verification, a test plan was elaborated related to different fiber- (GF and PETF) and matrix (PDMS and PUR) material combinations, which were applied on all three debond test setups (FBPO-, SFPO- and microbond test). Subsequently the results were put in relation to each other, since the possibility of the fiber-matrix strength can be proven by obtaining the maximum force as the common characteristic parameter.

For the FBPO tests, all results reveal the load-displacement curve and the accompanying interface failure (due to the debond procedure during the pull-out). The optical damage analysis showed that the separation happened between the bundle and surrounding matrix whilst no fibers were damaged. Further, the indicating meniscus near the surface at the fiber bundle entrance was examined. Moreover, no lateral fiber contraction was visible and thus the fiber bundle begins to peel perpendicular to the fiber orientation due to the compression stresses of the surrounding matrix. Therefore, the separation process starts on top near the meniscus (initiated by the tension stresses in the fiber direction and by the peel forces originating from the compression stresses) and expands along the embedded fiber part in the interface area. As expected, the determination of the pull-out behavior influenced by the embedded length and pull-out speed revealed an increased fiber-matrix strength with a higher embedded length. The chosen displacement speeds led to no clear impact from the hyperelastic behavior of the matrix material so that significantly higher test speeds are required. Furthermore, the removal of the sizing provided from the supplier already enhanced the fiber-matrix adhesion leading to a higher maximum force before debonding. For a comparison among the three debond techniques representing different test scales, a normalization step for the maximum bearable force was carried out, based on the standard material combination (GF-PDMS). This enables the measurement sensitivity to be magnified and better visualized. The results reveal that the same fiber-matrix combination follows the same trend for the relative maximum pull-out force. Moreover, the measurement sensitivity of the microbond test shows the

highest values compared to the FBPO test, which can be explained by several influencing factors such as interactions between the filaments, statistical fiber distribution in the bundle, imperfect adhesion related to defects or inhomogeneous shear stress distribution. Generally, the FPBO test method represents the basis to investigate the interfacial adhesion on bundles as the representative unit in composites. This novel approach aims to quantify the analysis of the composite properties due to the fiber-matrix strength, including more realistic damage behavior.

The findings of paper 1 showed the significant influence of an enhanced adhesive strength via removal of an inappropriate coating and paper 2 with the title "*Tailored interfaces in fiber reinforced elastomers: a surface treatment study on optimized load coupling via modified fiber bundle debond technique*" focuses on the enhanced interface performances for optimized load coupling. This paper addresses two important topics: (i) the crucial effect of different tailored surface treatments on the fiber-matrix interface strength and (ii) the experimental characterization related to the maximum achievable and material-specific reproducibility by implementing the modified FBPO test setup. Due to the gained knowledge that the interface performance in fiber reinforced elastomers is essential for the durability as well as mechanical properties and thus for the tailored load coupling assessment, an optimized fiber surface coating needs to be applied. Therefore, this study aims to prove the feasibility and repeatability of the modified FBPO test to investigate different adhesion performances related to the accompanying chemical surface treatments. Moreover, a further aspect was the qualitative investigation of the reliability and proof of the surface modification procedure. The covalent reaction between the treated fibers and surrounding matrix as well as the bonding of the immobilized silane to the fiber surface was verified by standardized chemical methods (Zeta potential analysis and X-Ray Photoelectron Spectroscopy (XPS)) as well as the structure-property relationship in the FBPO test. Overall, three different silane-based chemical treatments (vinyl-, amino-, and fluoro silane groups) were chosen, whilst GF with a PDMS matrix was set as the constant material combination. Generally, the GF with the coating from the supplier and after desizing by a piranha acid cleaning step were set as reference. Subsequently, the specific modifications were applied on the cleaned and activated fibers. This modified GF possess specific

chemical functionalities depending on different surface energies (unpolar, mid-polar and polar), so that the fiber-matrix bonding and thus interface strength can be affected significantly. As expected, the results for the chemical analysis show that a distinct change in the surface polarity can be observed by the Zeta potential method. These findings were proven by the XPS tests as evidence of the bonding energy versus intensity of several chemical elements. The change in the chemical surface composition could be given by the main indicating functional groups containing the detected elements such as carbon, oxygen, fluoro, nitrogen or silicon. The pull-out behavior was compared for all specific surface treated fiber bundles versus the maximum bearable load. As expected, the results clearly show that the same trend for each different treatment corresponds with the chemical analysis. Therefore, the fluoro silane-based modification gives the lowest adhesion strength, whilst the desized and vinyl silane-based modification leads to the highest interfacial fiber-matrix strength. Nevertheless, a direct correlation between the tailored silane-based fibers and the commercial sized fibers cannot be achieved, since the commercial treatment also contains film-building agents or other influencing components to generate an adequate adhesion. Although these treatments incorporate a mixed surface composition (chemical interactions and physical effects), the results prove that an individual treatment leads to considerably higher reliable interface performance and thus better fiber-matrix load coupling. This approach is also evident in the associated optical damage analysis so that a good adhesive bonding leads to a fully matrix-covered fiber surface where the separation process only occurs in the pure matrix. These results additionally correlate with the pull-out performance and thus has a good agreement with the corresponding mechanical properties achieved by the tailored fiber surface modifications. Overall, these promising findings demonstrate that the modified FBPO test enables reproducible data with a sufficient measurement sensitivity. Moreover, besides the choice of the right constituents (fiber or matrix), a customized surface modification enables an optimized fiber-matrix interface strength which has a significant impact on the load coupling and further on the composite performance.

Since the investigations on filaments and fiber bundles are essential for the fiber-matrix interaction in the interface, the experimental investigation on composites reveal several significant challenges. These include (i) the exclusive

evaluation on single fibers for the composite performance is insufficient, as already shown with the bundle tests. That considerable influence is suboptimal for a perfect performance but necessary to achieve realistic mechanical properties on composites. This in turn demonstrates that (ii) according to the current findings a controlled scalability between filaments and composites incorporating several fabric layers is indispensable. Based on this, paper 3, "*Investigation of adhesion properties in load coupling applications for flexible composites*", focuses on the realization and implementation of a conclusive test chain. To implement this on the scientific approach, a corresponding test chain with suitable transfer criteria based the step-by-step principle needs to be developed. This methodical concept should consider the essential loading conditions even in the micromechanical model at laboratory (micro) scale as well as reflect this by suitable step sizes up to the component-like structure (macro scale). Therefore, the comparability of representative tests was generated starting at micromechanical properties (single fiber tests) up to macromechanical behavior (simple composite tests), within experimental analysis on fiber bundles (modified FBPO test) as the intermediate step at meso scale. For the FBPO test the same test setup was implemented as already used in paper 1. In this context, the step size should be adapted according to the material used, to avoid scaling effects which might influence the interpretation of the mechanical properties. In this paper, the verification of the test chain is based on the identical type of stress (shear stresses in the fiber-matrix interface). Moreover, a test plan was elaborated combining two reinforcements (GF and PETF) with two different matrices (PDMS and PUR). To guarantee shear stresses also for the composites, the fiber orientation was reduced to the ±45° orientation to the loading direction and woven textiles as reinforcement were chosen to ensure in-plane shearing. Furthermore, elastomeric pads were used, to avoid local stress concentrations near the clamps as already discussed in detail in section 2.5.2. For the comparison between the three different test scales, the same normalization was adapted as already discussed for the section of paper 1, where the maximum force value is set as the correlating parameter. Overall, the results show that a relative comparison between the various test scales could be achieved in a quantitative manner. Thus, the study reveals that the measurement sensitivity for the FBPO test is similar to the composite tests with a more realistic failure mode than in

composites. Beyond state of the art, this test is accurate enough to study the performance for macromechanical properties on flexible composites depending on the corresponding fiber-matrix material combination used as the preliminary analysis on bundles at meso scale. In this context, the FBPO test represents a promising link in the test chain since the individual test setups follow the same trend in terms of the accompanying fiber-matrix material combination.

Based on the conducted composite measurements already shown in paper 3 utilizing the prototype-like clamping design, the handling and experimental performance could be improved with additional elastomeric pads. This was because no slippage occurred during the test despite the pronounced deformation of the fiber reinforced elastomers and the local stress concentration could be reduced. Nevertheless, this design was only applied on one fiber orientation so that the research focus in paper 4,"*Influence of fiber orientation and adhesion properties on tailored fiber reinforced elastomers*", deals with the impact of different fiber orientations on the load coupling behavior. As a further main aspect, the distinct effect of shearing (in-plane and out-of-plane) affected by the orientation due to the distinct wrinkling tendency especially in fiber reinforced elastomers was studied. The results show, that depending on the fiber orientation in the textile (0°/90°, 15°/75°, 30°/60° and ±45°) different dispositions and directions of wrinkling occur related to the respective orientation. In this context, especially for small deformations, the stiffness significantly changes depending on the fiber orientation, so that the ±45° oriented composite as a matrix-dominated configuration has the lowest stiffness compared to the 0°/90° oriented composite. Besides that, the ±45°composite still has the highest stress and strain at break compared to the other orientations (with the exception of 0°/90° configuration). This is the reason for the trellis effect caused by the maximum in-plane shearing and locking angle leading to out-of-plane shearing and wrinkling. Although the stiffness increases significantly using a fiber orientation towards the loading direction (reduced deviating angle) whilst the maximum bearable stress is reached faster leading to a preliminary failure.

Due to the performed composite tests focusing on the comparison with different measurement scales and further on the influence of the interface performance related to the shear strength versus different fiber orientations in the composite, the

clamping unit based on the concept of Hoffmann, as discussed in section 2.5.2, has shown considerable improvements. Nevertheless, this design needs to be adapted to the unavoidable clamping force aiming to reach a maximum achievable grip versus minimum required compression force. For this purpose a completely new clamping system was designed and realized, which has also been patented (Patent A). Since fiber reinforced elastomers exhibit a distinctly flexible behavior with almost textile-like performance, the novel clamping system had to fulfill several requirements such as (i) avoiding slippage or failure caused by the grippers, (ii) still maintaining sufficient adhesion and (iii) allowing no damage initiated by the necking of the specimen especially in the transition zone (near end of clamping). Therefore, the design consists of two flat lateral surfaces and an intermediate deflection, so that compression forces (for clamping) and the Euler-Eytelwein approach is combined to achieve an optimal solution. As unique feature, this device enables sufficient clamping without slippage and the required compression stresses in the grips can be minimized to avoid unwanted damage in the material. The additional hinge system allows a permanent autonomous alignment of the sample in the load direction and thus wedging or bending effects can be avoided.

Besides the characterization of quasi-static and monocyclic performance, another important aspect is the investigation of the structure-property relationship due to viscoelasticity under cyclic loading. In this context, the subsequent publication (paper 5) entitled "*Viscoelastic behavior of glass fiber reinforced silicone composites exposed to cyclic loading*" focuses on the influence of different fiber orientations in flexible composites interfering with the mechanical behavior and thus fiber-matrix load coupling. For this, the dynamic mechanical analysis as well as semi-cyclic measurements with step cycle tests under tensile loading were carried out. Especially for the step cycle tests, five different strain levels and specific cycle numbers for the looped behavior were considered, whilst an additional relaxation sequence was interconnected between the loading and unloading to analyse the direct correlation between strain induced stress softening versus amount of relaxation (indicated as stress decrease at constant deformation). Furthermore, this work aimed to study the effects on the reversible energy and irreversible dissipated energy in dependence on the viscoelastic properties exposed to cyclic loading. For this, a special test plan was elaborated to analyze the stiffness and storage modulus

behavior over a defined temperature range for different fiber orientations. Moreover, the test plan for the step cycle tests constitutes, besides differently oriented composites, in addition the impact of different relaxation times and displacement rates especially for the viscoelastic performance. For these tests, the patented clamping device was used for all experiments. All tests clearly revealed a stiffness increase due to the presence of the fiber reinforcement. Furthermore, the dynamic mechanical analysis demonstrated that the storage modulus is significantly influenced by the fiber orientation so that the mechanical properties can be optimized especially in the entropy elastic state as the main application field for elastomers. Thus, the stiffness is controlled and enhanced without affecting the composite properties such as flexibility or structure-property relationship. For the step cycle tests, the results show a distinct impact of the fiber orientation on the maximum achievable stresses which is also directly correlated to the stress softening and intermediate relaxation sequence. This can be attributed to the viscoelastic behavior which is not visible in the pure matrix material for similar loading conditions. In contrast to that, the different relaxation times as well as displacement rates indicate no detectable impact on the strain induced strain softening or relaxation, which can be strongly related to the hyperelasticity of the matrix material. As a new approach, this research reveals a good preliminary study on the cyclic performance of fiber reinforced elastomers and the effect of different composite structures on the load coupling mechanism exposed to dynamic loading. Especially for the material-appropriate development and construction of a novel load coupling test device to investigate tailored fiber-matrix load coupling mechanisms in flexible composites, the profound knowledge of all findings in the studies, which have been carried out, is necessary.

Based on the few findings from suitable tests, which are primarily limited to thermoset-based concepts, this research (paper 6) entitled "*The tension-twist coupling mechanism in flexible composites: a systematic study based on tailored laminate structures using a novel test device*" focuses on the realization of a special test setup with the emphasis on tailored load coupling effects triggered in fiber reinforced elastomers. In this context, several major challenges occur such as structure-property related viscoelasticity, residual strains, fiber matrix interface strength or trellis effects caused by wrinkling due to out of plane shearing. In

particular, this wrinkling effect occurs whenever the twist (caused by fiber-matrix load coupling) is hindered due to two rigid clamping systems resulting in shear stresses out of plane (related to the respective textile plane).This twist can be realized, if one clamping unit is converted into a movable design. Thus, the paper aimed to quantify the effect of tailored tension-twist coupling mechanisms on flexible composites with distinct anisotropy. For the verification, a special test plan was carried out to consider different fiber orientations, whilst all measurements were done on the material configuration GF with PDMS matrix. Especially the distortion process strongly depends on the load coupling behavior related to the material's law for fiber reinforce elastomers, since shear stresses are coupled to the fiber orientation and thus dominated by the in-plane and out-of-plane deformation. Subsequently, the requirement of a new test device has to fulfill several features such as (i) the recording of the torque versus the accompanying twist angle, (ii) a self-aligning mechanism along the machine axis to avoid negative bending or wedging which might falsify the results, as well as (iii) appropriate clamping adapted for fiber reinforced elastomers. This test device offers the opportunity to measure the torque in fixed mode by using a supplementary fixing unit and the twisting angle in movable mode. Related to this, suitable sensors are needed besides to record the general deformation and tension force. All strip-shaped composite samples were stretched until 20% deformation, since an unaffected fiber-matrix bonding can be guaranteed and the pure PDMS matrix shows a linear elasticity until 40% strain so that a reliable load coupling can still be provided. Various orientations (±45° and 30°/60°) and a mixed version (45°//30°/60°) were considered in the test plan, whilst all composite samples had two textile layers as reinforcement in total. Moreover, the gauge length was varied between two states (45 mm and 90 mm) to demonstrate the influence on the inherent stiffness within these highly flexible composites. Overall, the results reveal that, as expected, the 45° oriented composite leads to no twist or torque due to the symmetric structure. In contrast to that the 30°/60° shows the highest achievable twist angle and torque. These findings also agree conclusively with the optical damage analysis. The verification of this load coupling device is validated, whilst this test provides a good basis as a preliminary study on tension-twist coupled behavior in flexible composites. This novel test concept is currently being patented (patent B).

2 Summary and Outlook

For an in-depth knowledge and understanding for tailored fiber reinforcement in elastomers to obtain anisotropic behavior, one main focus was the design, realization and verification of new test methods. Within this, the modified fiber bundle pull-out test with the special sample holder enables the investigation of the interfacial adhesion on bundles as representative unit for composites. By showing similar measurement sensitivity compared to composite structures for the same fiber-matrix material combination, this test setup reveals more realistic damage behavior and represents a novel approach to analyze the fiber-matrix strength correlating with composites. Based on this, the investigations towards the influence of tailored treated fiber surfaces verified the measurement sensitivity of the presented fiber pull-out test on bundles. These essential findings were proven by the impact of specific fiber surfaces on the resulting fiber-matrix strength as well as associated optical damage analysis including a verification of the accompanying chemical surface treatments. Additionally, a systematic transfer based on a suitable developed test chain was realized to describe the micro- to macromechanical behavior. Thereby, reliable transfer criteria were defined according to proven and well-established methods to realize promising tests for enhanced material characterization focusing on the analysis and accurate determination of important material parameters. In this context, a novel clamping system especially for these flexible composites was developed and patented. With the investigation of the viscoelastic behavior under cyclic loading conducted on different fiber orientations, a clear impact on the mechanical behavior and fiber-matrix load coupling was observed. This novel approach offers interesting results for flexible composites exposed to cyclic loading. Regarding the macromechanical characterization of load coupling effects, a new test device was developed and verified to analyze tension-twist coupled behavior. As a promising concept, this new test setup reveals a good basis to analyze mechanical triggered load coupling effects in fiber reinforced elastomers and thus is currently being patented.

Subsequently, this leads to further fundamental and vital research topics, since for the viscoelastic and energy absorption performance exposed to cyclic loading, other fiber-matrix material combinations have to be examined to gain a more detailed assessment, in particular focusing on the mechanical behavior and structure-property relationship. Moreover, these findings have to be complemented by tailored surface modifications similar to those which have already been conducted for the pull-out tests. Another main aspect is the analysis of the strain rate dependence, whilst further tests are targeted to focus on significantly higher displacement rates or impact investigations. In this context, another aspect will be the experimental investigation of fatigue tests including effects such as rubber-bonded phases or hysteretical heating which influences the mechanical properties. Concerning the load coupling test device, the functionality was already successfully demonstrated and thus the subsequent analysis has incorporated further major aspects such as cyclic loading, tailored fiber surface treatment utilizing optimized interface strength as well as the impact of different fiber-matrix material combinations. These findings are required for the improvement of the novel load coupling test and to provide the availability of precise material parameters. The complete interaction of the realized test chain, including the demonstration of the corresponding load coupling mechanism, are required for the built-up of component-like prototypes as demonstrators for smart composite materials. Moreover, this approach offers the potential of a comprehensive study from micro- to macromechanical characterization enabling simulation-based accompanying material models and optimized analysis of the constitutive mechanical properties taking into account load-coupled behavior. In a subsequent step, tension-twist coupling experiments can be implemented as a new test method by using the novel test concept that has been designed and developed in this work. Thereby, the aim is to exploit the obtained material parameters directly in simulations for geometry- and structure-optimized prototypes.

3 Collection of papers and patents

3.1 Paper 1: Comparison and impact of different fiber debond techniques on fiber reinforced flexible composites

Julia Beter[1,*], Bernd Schrittesser[1], Boris Maroh[1], Essi Sarlin[2], Peter Filipp Fuchs[1] and Gerald Pinter[3]

[1] Polymer Competence Center Leoben GmbH, Roseggerstrasse 12, 8700 Leoben, Austria.
[2] Faculty of Engineering and Natural Science, Tampere University, P.O. Box 589, 33014 Tampere, Finland.
[3] Department of Polymer Engineering and Science, Montanuniversitaet Leoben, Otto-Gloeckel- Strasse 2, 8700 Leoben, Austria.

Published in Polymers, 2020, 12(2), 472.

DOI: 10.3390/polym12020472

polymers

MDPI

Article

Comparison and Impact of Different Fiber Debond Techniques on Fiber Reinforced Flexible Composites

Julia Beter [1,*], Bernd Schrittesser [1], Boris Maroh [1], Essi Sarlin [2], Peter Filipp Fuchs [1] and Gerald Pinter [3]

[1] Polymer Competence Center Leoben GmbH, Roseggerstrasse 12, 8700 Leoben, Austria; Bernd.Schrittesser@pccl.at (B.S.); Boris.Maroh@pccl.at (B.M.); PeterFilipp.Fuchs@pccl.at (P.F.F.)

[2] Tampere University, Faculty of Engineering and Natural Science, P. O. Box 589, 33014 Tampere, Finland; essi.sarin@tuni.fi

[3] Department of Polymer Engineering and Science, Montanuniversitaet Leoben, Otto Glöckelstrasse 2, 8700 Leoben, Austria; gerald.pinter@unileoben.ac.at

* Correspondence: Julia.Beter@pccl.at; Tel.: +43-3842-42962-31

Received: 24 January 2020; Accepted: 15 February 2020; Published: 18 February 2020

Abstract: The focus of this paper is the realization and verification of a modified fiber bundle pull-out test setup to estimate the adhesion properties between threads and elastic matrix materials with a more realistic failure mode than single fiber debond techniques. This testing device including a modified specimen holder provides the basis for an adequate estimation of the interlaminar adhesion of fiber bundles including the opportunity of a faster, easier, and more economic handling compared to single fiber tests. The verification was done with the single-fiber and microbond test. Overall, the modified test setup showed the typical pull-out behavior, and the relative comparability between different test scales is given.

Keywords: flexible composite; fiber-matrix adhesion; interface; bundle pull-out test; fiber-matrix debond technique

1. Introduction

Fiber reinforced elastomers (or so-called flexible composites) represent a new class of materials. These composites connect the targeted improvement of the mechanical properties due to the reinforcing fibers used and still retain sufficient flexibility provided by the elastomer matrix. Completely new applications for the technical advances could be found, e.g. in the field of medical engineering to generate artificial muscles [1], exoskeletons for rehabilitation [2], or self-folding structures [3] where flexibility is essential and stability must be guaranteed to provide sufficient mechanical performance. The focus has been on the possibility of load transfer between fibers and their surrounding matrix due to an external input such as a mechanical trigger. Thus, good adhesion properties are important to ensure an efficient load transfer [4], which provides a reduction of the stress concentration as well as an improvement of the general mechanical properties themselves [5]. In-depth knowledge as well as quantitative investigation of the interface properties are essential [6] since an excellent fiber-matrix bonding is important [7]. Currently, the individual approaches regarding the experimental solutions have been limited to the analysis of single fiber-matrix interactions, and, moreover, have usually been reduced to specifically selected material groups like carbon or glass fiber with epoxy thermoset systems. The comparability between various existing test setups is only possible within a limited range. Therefore, an adequate estimation of the material behavior in component-like structures containing a large number of fiber bundles involves numerous boundary conditions. Thus, a direct correlation with the macroscopic composite parts is not feasible [4,6]. Currently, there are several methods to investigate the interface properties in a single fiber and

fiber bundle scale [7–10]. Generally, the single fiber push-out [11] and the pull-out tests [12–14] or the fiber bundle pull-out (FBPO) test [15–18] represent a fiber-loaded system. In these tests, the common measuring tests are carried out for a clamped matrix and therefore less suitable for elastic materials [19]. In contrast to proven test methods at the single fiber scale, the already existing fiber bundle test methods do not show consistent or systematic design. For example, in some systems, the fiber bundle is fully coated with matrix material [4,16], while the matrix block is fixed, which might influence the mechanical behavior [20]. Another setup describes a process in which the fiber bundle sample is extracted from an already produced composite [21]. Existing FBPO tests do not consider a guiding element to eliminate bending [8], which is important for elastomers. In terms of the various test setups, the FBPO test offers the opportunity to perform experiments faster, more easily, and more economically compared to single fiber measuring devices, which need more careful handling [22] and special test equipment [4]. Besides that, the tests are influenced by the following factors: e.g., (i) the complex stress distribution in a fiber bundle [13,23], (ii) fiber-fiber interaction [24] with more real failure modes [23], or (iii) the presence of statistically distributed filaments inside the fiber bundle [25,26]. These points have a significant effect on the interlaminar shear strength due to the variable cross-section areas of the fiber bundle [4]. Nevertheless, single fiber measuring methods have a high experimental outlay [22], and the determination of parameters for the fiber-matrix bonding behavior is only possible when assuming specific material models.

The aim of this research is to present the first development of a modified fiber bundle pull-out test to characterize the adhesion properties of a fiber bundle in elastic matrix. With this test setup, clamping influences or other effects like coated fibers are avoided, which ensures an easy, fast, and economic handling to estimate the fiber-matrix adhesion with more real failure modes. A comparison of the presented test setup with proven test methods based on single fibers was performed [7]. One focus was the verification of the FBPO test with the purpose of a mechanical test standardization as a method to estimate the damage behavior of a fiber bundle when being pulled out of the surrounding matrix. The influence of several parameters was analyzed, namely embedded length, speed, and adhesion properties due to different fiber-matrix combinations. The described modified FBPO test setup aims to provide the basis for an adequate estimation of the properties between a fiber bundle and the surrounding matrix material including more realistic failure modes (e.g., statistical fiber distribution or fiber-fiber interaction). Further, the obtained material data can be used in constitutive approaches for elastic body simulations [27]. In this work, the possibility to obtain the common characteristic parameter maximum force was proven. In addition to that, the adaptation to design a suitable sample manufacturing device including a modified specimen holder was carried out. Additional experiments were performed with proven measuring devices on single fiber scale via microbond and single fiber pull-out (SFPO) tests.

2. Materials and Methods

2.1. Materials

For the experimental investigation of two different fiber types, glass fibers (GF), and polyester fibers (PETF) were chosen as reinforcement. The commercial unidirectional GF reinforcement was provided by CS Interglas AG (Erbach, Germany) as E-type, an area weight of 220 g/m^2 ± 5%, a twine thickness of 68 tex, and a mean fiber diameter of about 10 µm with the standardized warp yarn classification EC9-68x5t0 in the 0° and 90° direction. The PETF reinforcement was provided by Mates Italiana srl (Milan, Italy) from a single batch and with a 2/2 twill weave, an area weight of 200 g/m^2 ± 5%, a twine thickness of 167 tex, and a mean fiber diameter of about 30 µm with an area bundle distribution of 50/50 in the 0° and 90° directions. Extracted from the unidirectional weave, the GF bundles possessed different surface conditions: (a) with commercial silane-based surface treatment, as received from the supplier (finish FK144 treated), and (b) without surface treatment obtained by cleaning the fibers with peroxymonosulfuric acid (untreated). The cleaning procedure was essential to achieve an unmodified status of the GF material. This process was performed at 60 °C for 120 min,

including a thorough washing step with toluol and a drying step at 150 °C for at least 12 h in a convection oven.

Two different cast elastomers, polydimethylsiloxane (PDMS) and polyurethane (PUR) were considered as elastic matrix material. According to the manufacturer, the PDMS (Elastosil RT601 provided from Wacker Chemie AG) is a two-component-system rubber used in the mixing ratio 9:1 (part A: part B), and has a density of 1.02 g/cm³ and a viscosity in the uncured mixed state of 3500 mPas including a pot life up to 90 min at 23 °C. The PUR (ClearFlex 50 provided from Smooth On Inc.) with a mixing ratio of 1:2 (part A: part B) has a density of 1.04 g/cm³. The viscosity of the mixed product in uncured state is 250 m Pas with an indicated pot life limited to around 25 min at 23 °C.

2.2. Preparation and Impregnation Quality of Fiber Bundle Specimens

For the preparation of the FBPO test specimens, a tool (see Figure 1a) was developed. This tool consists of a corpus which contains a defined recess for the matrix including narrow slots occurring at regular intervals for the fiber bundles. In addition, regarding the recess, seals were implemented on both sides to guarantee a definite fiber position without pre-damage and to prevent matrix leakage. The issue was the accurate fiber position in the center of the specimen to avoid negative effects related to tilting or asymmetrical stress distribution. Each specimen, shown in Figure 1b, had the same thickness b of 8 mm as well as width w of 10 mm, and the length l was adjusted according to the desired embedded length l_e.

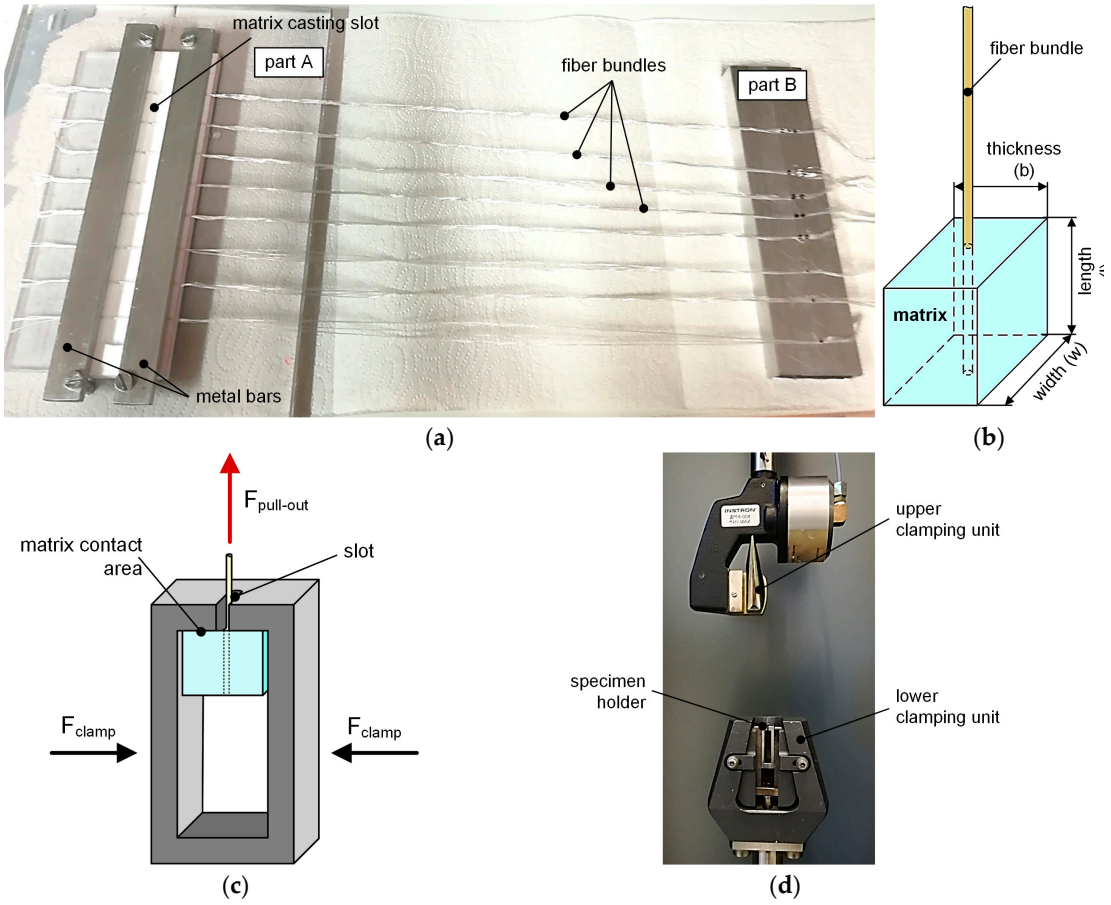

Figure 1. Manufacturing tool including main components (**a**) with specimen (**b**) and schematical test procedure with the modified specimen holder (**c**) with test setup for FBPO test (**d**).

2.3. Specimen Holder

A modified specimen holder was designed to accommodate the cuboid specimen geometry as well as to be able to test the samples with a conventional testing machine. During the test, this holder has to prevent slipping. Also clamping of the surrounding matrix has to be avoided to reduce further stresses induced by the fixing unit, because these stresses were transferred to the elastic matrix and further directly into the embedded fiber bundle, which result in a fiber breakage. A specimen holder [17] originally designed for carbon black filled rubbers was modified for the testing on unfilled elastomer systems. All fiber bundle specimens have to be placed, deformation-free, inside the specimen holder. During the time to reach the preload for equal test conditions, the elastomers were sensitive to small surface imperfections which could lead to tilting or twisting. The specimen holder enables the guidance of the lateral surfaces of the specimen in parallel direction to the lateral inner surfaces of the specimen holder, hereby still providing sufficient space on both sides between the specimen and the holder. This allows the surrounding matrix material to undergo deformation during the loading without causing any additional stresses that might affect the experiment in a negative manner (see Figure 1c).

2.4. FBPO Test

The test setup for the fiber pull-out testing represents a combination of the standardized testing method for pure yarn tension testing, according to the ASTM D2256 enhanced with the specimen holder for the modified FBPO test, shown in Figure 1d. This test setup represents the fiber-loaded measuring device, where the upper clamping device fixes the fiber bundles and represents the movable part [28]. The tests were performed with a constant displacement rate v pull out. Generally, all experiments were carried out with a universal testing machine (5500 Series, Instron GmbH) and performed at standard atmosphere conditions. For the test procedure, a 100 N load cell and a defined gauge length of 50 mm was chosen. In order to have the same initial starting condition, all experiments were carried out with a preload of 1 N. As the upper clamping device for the fiber bundles, the mandrel-shaped clamping system was used and the specimen holder was inserted in the lower clamping device. As can be observed from Figure 1c, the matrix part was centered between the inner lateral surfaces and was only in contact with the upper surface area during the testing to avoid lateral clamping forces.

To evaluate the influence of the test parameters, one material combination (represented by silane-based treated GF with PDMS matrix) was employed representatively. Due to the influence of the pull-out speed v pull out, and embedded length of the fibers mentioned in the literature [13,19], a methodically validated testing plan was developed (see Table 1). The embedded length as well as the pull-out speed were tested at three different levels, including all possible combinations in each case. As the reference setting 5 was chosen.

Table 1. Methodical testing plan for FBPO tests.

Setting	**1**	**2**	**3**	**4**	**5**	**6**	**7**	**8**	**9**
embedded length l_e, mm		8			10			12	
pull-out speed $v_{pull\text{-}out}$, mm/min	0.5	1.0	2.0	0.5	1.0	2.0	0.5	1.0	2.0

In order to determine the maximum force for the obtained interface properties, the average value for at least five specimens for each setting was calculated. Besides the influence of the test parameters (i.e., embedded length, pull-out speed), the impact of different fiber-matrix combinations using the same test setup was analyzed in a subsequent step. Therefore, the GF and PETF were combined for each setting with both matrix materials and measured with the same reference setting 5 similar to the first testing plan with an embedded area of 10 mm as well as a pull-out speed of 1 mm/min.

2.5. Single Fiber Pull-Out Test

The experiments to investigate the adhesion behavior of one single filament was carried out with the SFPO tester [14] at the Federal Institute for Materials Research and Testing (BAM, Berlin, Germany). These tests were performed to verify the modified test setup used for the FBPO tests as well as to prove

the reproducibility for identical fiber-matrix combinations. The SFPO test emphasized a similar loading situation compared to the FBPO test. This test set-up was designed so that the specimen holder containing the matrix droplet was placed in the rigid test device with a fiber orientation perpendicular to the matrix surface. One fiber end was impregnated with the matrix droplet, which also allowed defining the corresponding embedded length individually, as shown in Figure 2a. The fixed end of the single fiber is loaded until a fiber detachment from the surrounding matrix in the interface occurs and is then pulled out completely. The load displacement signal of each specimen was measured to determine the required maximum force until the initiation of the debonding with the indicated load-drop (see Figure 2b). The tests were performed with a 50 N load cell, and a defined pull-out speed of 1 µm/s. All samples were manufactured with an embedded length of about 186 µm using the same specimen preparation conditions as for the FBPO tests.

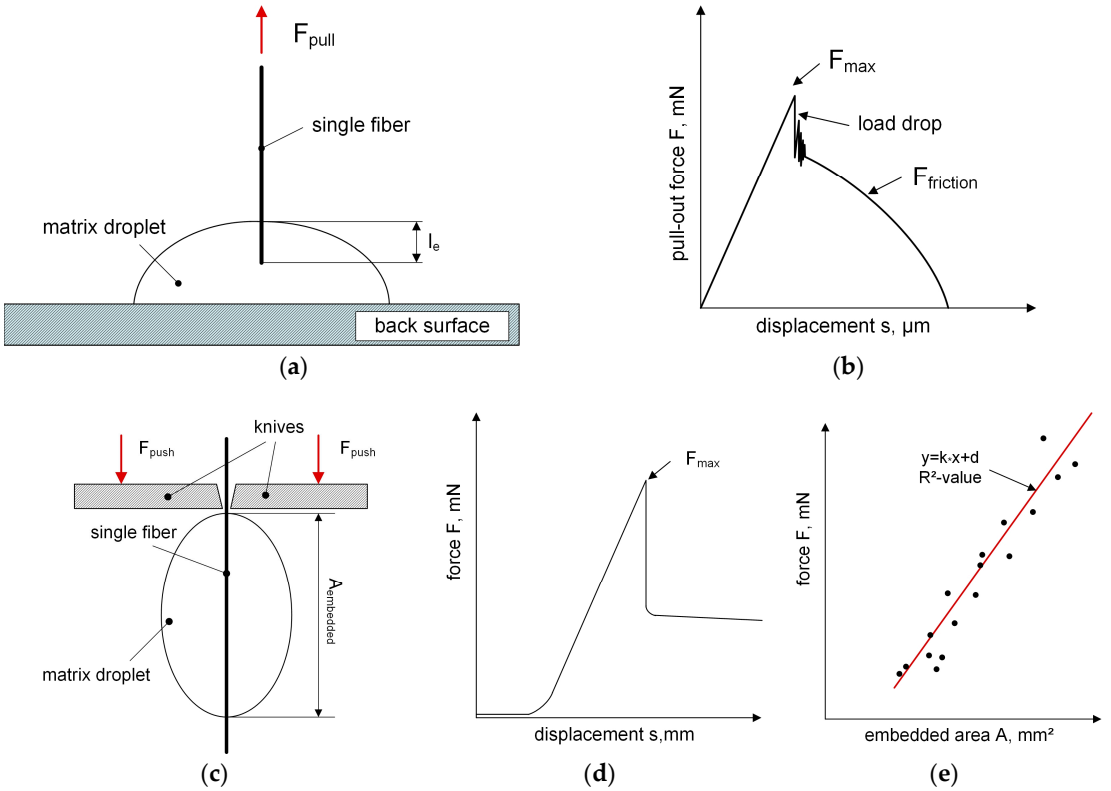

Figure 2. Schematic test procedure (**a**) and a typical force-displacement graph (**b**) of the SFPO test [13,22] with schematical test setup (**c**) and typical test graphs (**d**,**e**) of a microbond test [29,30].

2.6. Microbond Test

The investigation of the fiber-matrix interface properties was carried out with the FIBRObond micro-droplet tester [29,30] at the Tampere University (Tampere, Finland). The reason for using this test setup was to assess the fiber-matrix adhesion properties in different loading conditions, i.e., matrix loading in the microbond test versus fiber loading in the SFPO test, as well as to determine their comparability. With the test procedure shown in Figure 2c, the force that is needed to detach the matrix droplet from the attached filament area is determined. Several matrix droplets with different sizes were applied on the surface of one single fiber. In order to determine the necessary debonding and maximum force, each individual matrix droplet is loaded until the debonding takes place at a constant displacement rate of 0.5 mm/min (see Figure 2d). The maximum debonding force and the corresponding embedded area are reported as one data point in the maximum force-embedded area diagram, as shown in Figure 2e. Due to different matrix droplet sizes, several data points resulted due to the different debonding forces required, and a curve with a linear correlation was evaluated in conclusion. Generally, for each setting, about 15 droplets were tested to ensure sufficient accuracy and

determined with the R^2-value. Hence, the evaluated parameter k represents the slope, and thus, the adhesion property, so that a higher k-value indicates a stronger interlaminar bonding. All tests were carried out with a 1 N load cell at standard atmosphere conditions.

2.7. Optical Observation of Fracture Surfaces

To enhance the characterization as well as the comparability of the tested single and fiber bundle tests, optical damage analysis was performed using an optical microscope (BX51, Olympus Austria GesmbH, Vienna, Austria), and the scanning electron microscopy (SEM) (Tescan Vega II, Tescan Brno, s.r.o., Dortmund, Germany). Regarding all FPBO tests, a camera system (Prosilica GT 6600, Allied Vision Technologies GmbH, Stadtroda, Germany) was operated additionally to follow the material behavior during the debonding process more accurately.

3. Results and Discussion

3.1. Fiber Bundle Pull-Out Test

Concerning the FBPO tests, all experiments show the typical shape of the load-displacement curve for the type of failure occurring at the interface area [14,19,26] and is represented in Figure 3a for three measurements with the reference setting, respectively. A reason for this deviation for the same setting could be differences in the adhesive connection to the fiber, which might be influenced by inhomogeneities of the commercial silane-based surface treatment from the supplier. Other influences could be the presence of interface defects or deviations of fiber bundle orientation due to the placing process. These influences can be reduced by optimizing the manufacturing process of the samples. The load-displacement curve illustrates the increased force during the test until it reaches the maximum force F_{max}, and then to the clearly discernible load drop shown in Figure 3a, at which point the fibers separated from the surrounding matrix. After complete debonding, the fiber bundle is pulled-out with $F_{pull\text{-}out}$, which contains several different parts including the friction force. Some tests exhibited a stepwise crack growth that led to an oscillation in the load signal, which was optically recorded as a crack initiation perpendicular to the pull-out direction. A reason for this behavior could be several mechanisms for fiber-matrix bonding, such as mechanical interlocking, adsorption interaction, or the enabling of elastic deformation due to oversized free clamping distance of the fiber bundle between both clamping units. Therefore the fiber bundles could probably bear elastic deformation energy, which would be released during the debonding procedure and could probably cause compression stresses which would lead to a vertical stress reduction and crack initiation [6,10,31]. More experiments varying the free clamping distance and other upper fixing devices for the fiber bundles should be carried out in further investigations to optimize the pull-out behavior. During the loading procedure, a cone at the end of the fiber bundle inside the sample is visible, where the elastic matrix is deformed, and drawn in the direction parallel to the fiber bundle (see Figure 3b). In the meantime, the adhesive bonding of the surrounding matrix is undamaged. The separation process can be recognized by the shift of the light refraction. The crack initiation starts on top of the embedded area, where only the matrix surface is in contact with the bottom area of the specimen holder. The reason for this could be the stress concentration of the already deformed elastomer [11]. Due to the elasticity of the matrix, a slight deformation in the pull-out direction was observed since a small gab between the fiber bundle and the lateral surface of the slot has to be considered to avoid friction. Further, no lateral contraction of the fiber bundle during the stretching was depicted. Because of this compression of the elastic matrix, the local matrix surrounding the fiber bundle starts to peel perpendicular to the fiber orientation, and therefore, tension stresses to the fiber bundle, which leads to the separation effect [7,10,13]. Figure 3c represents the optical microscopic images of the embedded area of one GF bundle with the PDMS matrix after the FBPO test. It is visible that the complete GF bundle was pulled out without fiber breakage. The initiation of debonding at the fiber entrance area is shown in more detail in Figure 3d in the SEM picture. The separation happened at the interface area and was initiated by the stress concentration occurring on top of the fiber entrance area into the matrix as well as at the fiber end [6,11].

SEM images were taken from the cross-section area to ensure a complete impregnation of the fiber bundle, which is exemplary shown for GF with PDMS matrix (see Figure 3e).

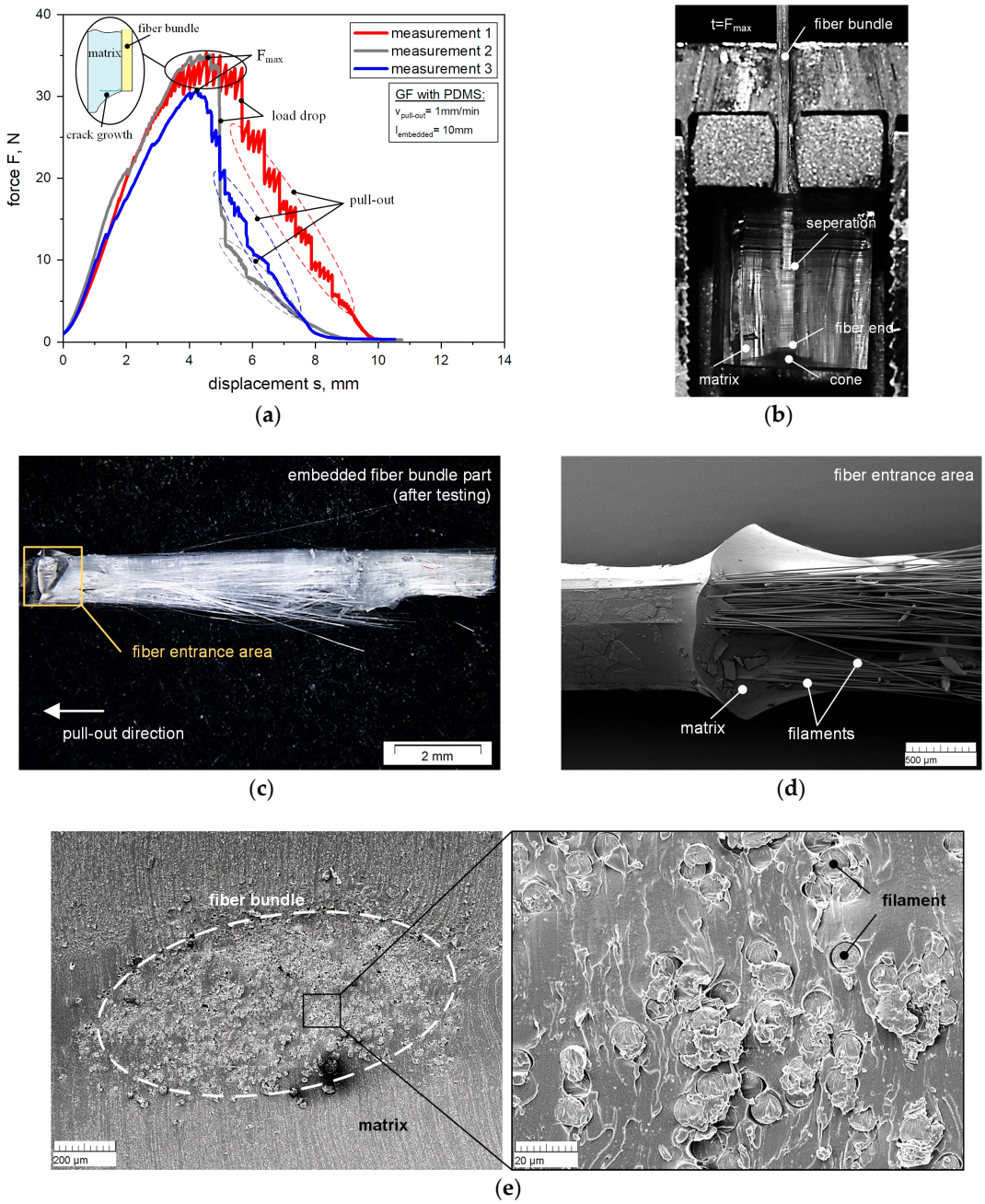

Figure 3. Force-displacement curves obtained from FBPO test on GF with PDMS matrix (**a**) with the separation process (**b**) during pull-out and microscopic images of a FBPO specimen (GF with PDMS) after the test: part of embedded area of GF- bundle (**c**) and SEM of GF- bundle (**d**) and image of cross-section area of embedded GF bundle (**e**).

For the determination of the pull-out behavior due to the influence on the test parameters (i.e., embedded length, pull out speed) themselves versus the maximum force F_{max}, the results of GF with PDMS matrix are shown in Figure 4a. As expected from previous researches [19,32] focusing on the investigation and impact on the interface behavior as well as debond mechanism influenced by different embedded lengths, the maximum pull-out force increases with higher embedded length. A reason for this is the fact that there is more adhesive bonding due to the increased embedded length (more fiber

bundle surface). There is no clear effect on the influence of the pull-out speed regarding the viscoelastic behavior of the matrix material to relate to higher force values. This could be due to the fact that the range of 0.5 to 2 mm/min was too small to achieve sufficient influence on the elastic material. However, the standard deviation tends to increase with higher pull-out speed, such as for setting 1 compared with setting 3. For the investigation to verify the sensitivity of the measuring by the modified test setup for FBPO testing, the results concerning the material influence due to different fiber-matrix combinations is presented in Figure 4b. Generally, the results reveal that the GF-bundles for both matrix materials (PDMS and PUR) lead to a higher maximum force, which may be related to the higher number of single fibers in the fiber bundle and the larger effective surface area between fibers and matrix resulting thereof. The highest pull-out force was obtained with GF(a)- PUR matrix. Moreover, the pull-out force required for PETF with a PUR matrix was higher, with about 21.3 N, than PETF with a PDMS matrix with approximately 8.7 N. However, in terms of the GF bundles, the results show that the removal of the silane-based surface treatment of the GF increased the pull-out force to about 45.6 N. A possible reason for this could be (i) the incompatible sizing provided by the supplier or (ii) the presence of rougher surface conditions [11,25] induced by the piranha acid treaded GF bundles, which was applied to remove the silane-based treatment from the manufacturer. Moreover, all reported measurements for GF show generally higher deviations in contrast to the results with PETF.

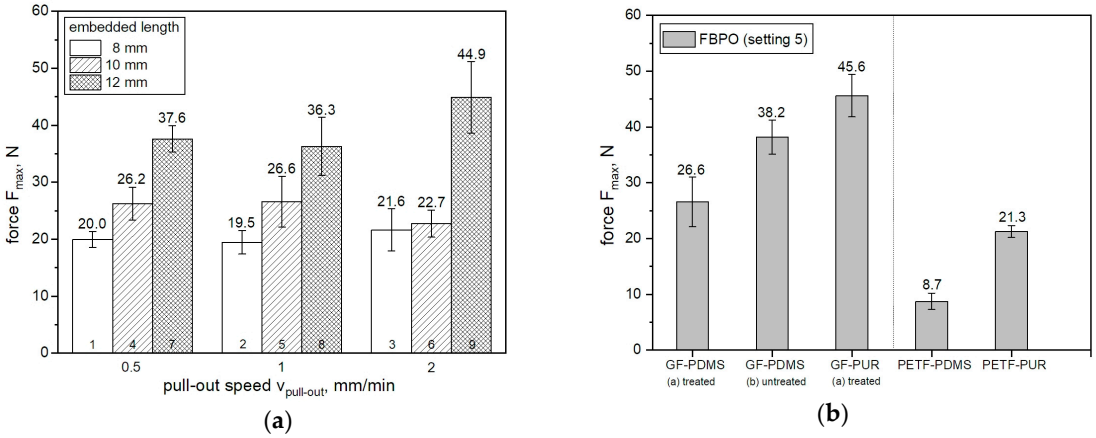

Figure 4. Influence of the parameters on the pull-out force for GF and PDMS matrix (**a**) and on different reinforcement-matrix material combinations tested on reference setting (**b**).

As an overview, the results of each fiber-matrix combination for all the different test methods (FBPO, SFPO-, and microbond test) have been summarized in Table 2.

Table 2. Results for FBPO-SPFO and microbond test for different fiber-matrix combinations.

Fiber-Matrix	FBPO	SFPO	Microbond	
	av. max. Force Fmax, (± std. dev.), N	av. max. Force Fmax, (± std. dev.), mN	Slope (k), mN/mm²	R^2 -
GF (a)-PDMS	26.6 ± 4.5	11.6 ± 1.4	0.01	0.8
GF (b)-PDMS	38.2 ± 3.0	25.7 ± 1.8	0.1	0.7
GF (a)-PUR	45.6 ± 3.8	48.8 ± 15.0	1.4	0.8
PETF-PDMS	8.7 ± 1.5	19.5 ± 10.5	0.2	0.8
PETF-PUR	21.3 ± 1.1	65.3 ± 15.0	1.4	0.9

3.2. Comparison Between Different Test Scales

For a suitable comparison of the FBPO test with other test methods (SFPO- and microbond test), a normalization was carried out on the basis of the two reinforcement fiber types (GF as well as PETF) in combination with the PDMS matrix regarding the maximum force needed to debond the fiber bundles from the matrix, as shown in Figure 5a,b.

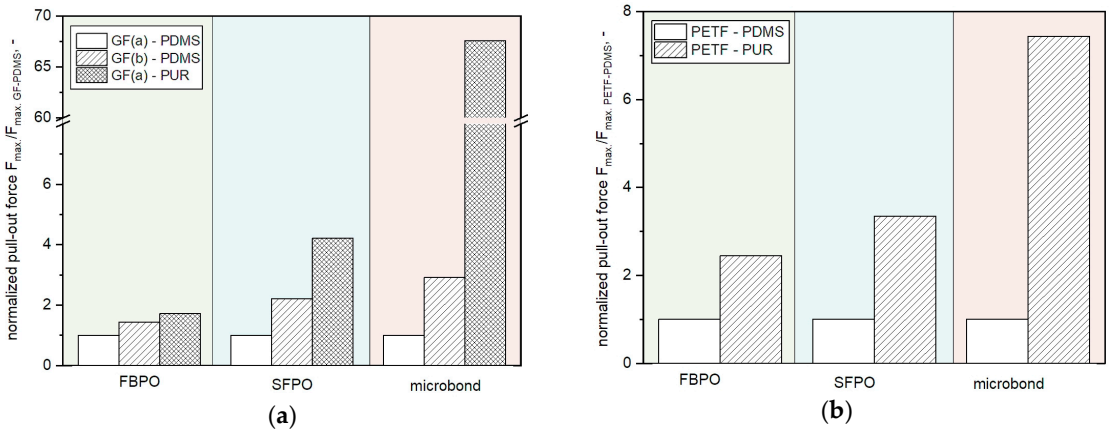

Figure 5. Comparison of the relative pull-out force for FBPO, SFPO and microbond tests performed with different fiber-matrix combinations with GF (**a**) and PETF (**b**).

Reasons for this are as follows: (i) both fiber types have different properties such as surface quality or fiber diameter, (ii) comparability is needed for tests at different measurement scales (micro-meso level), and (iii) the sensitivity of the measurements should be better visualized. For the normalization of the microbond tests, one pre-defined embedded area was chosen with the corresponding force value.

Generally, the results reveal that for the individual test setups, the same fiber-matrix combinations follow the same trend regarding the corresponding relative pull-out force $F_{max,\ normalized}$. In terms of measurement sensitivity, it can be seen that the difference for all tests of the FBPO test setup with GF is smaller than in comparison to the measurement methods on single fibers. Thus, the combination GF(a) with the PUR matrix has four times higher $F_{max,\ normalized}$ than GF(a) with the PDMS matrix, which is the normalized reference setting. The comparatively low measurement sensitivity of FBPO tests can be related to several factors, such as (i) interaction effects between single fibers in the fiber bundle by fiber friction, (ii) the statistical distribution of single fibers and the matrix in the bundle, and (iii) different shear stress distribution upon pull-out.

4. Conclusions

The modified FBPO test setup here described is intended to provide the basis for an adequate estimation of interlaminar properties between a fiber bundle and the surrounding matrix material including more realistic failure modes (e.g., statistical fiber distribution or fiber-fiber interaction) with the aim of a mechanical test standardization. The obtained material data can be used in constitutive approaches for elastic body simulations. With the FBPO test, it is feasible to perform the experiments in a faster, easier, and more economical way compared to the single fiber debond technique devices which require a more careful handling.

The results of the FBPO tests reveal that the separation procedure occurred at the interface area. Additional studies for the various fiber surfaces to influence the adhesion with tailored chemical fiber surface modifications as well as matrix material combinations are currently being carried out to prove the measurement sensitivity and to study the interfacial surface interactions. Further researches are already in progress to investigate the other important failure phenomena, e.g., load drop, friction force, and debonding initiation to get a deeper knowledge of the physical phenomena behind the presented test. Another aspect is the analysis of the specimen geometry focusing on the lateral surface dimensions and their effect on the cone during testing. Overall, the results reveal that the modified FBPO test setup with both measurement methods on a single fiber (SFPO- and microbond test) is relatively comparable, including the fact that these test setups belong to different measuring scales. Knowing this, verification of the modified FBPO test is validated, which allows sufficient accuracy of the material pre-analysis for adhesion properties in a faster and easier way. Moreover, additional studies should be carried out regarding the comparability to macro scales for composite structures, and that the presented modified

FBPO test method provides a base model as well as a possible link in the test chain between micro scale- (single fiber) and macro scale (composite components) testing.

Author Contributions: Literature research, investigation, visualization, writing—original draft preparation, J.B.; conceptualization, test conduction J.B. and B.M.; validation, methodology writing—review and editing, J.B., B.S.; supervision, validation B.S., E.S. and G.P.; project administration, funding acquisition P.F.F. and G.P. All authors have read and agreed to the published version of the manuscript.

Funding: This research was funded by the Federal Ministry for Transport, Innovation and Technology and Federal Ministry for Economy, Family and Youth, grant number 854178.

Acknowledgments: The assistance of Gerhard Kalinka (Federal Institute for Materials Research and Testing (BAM) in Berlin, Germany) for single fiber pull-out testing and Pekka Laurikainen (Tampere University in Finland) for the microbond testing are gratefully acknowledged. This research work was performed at the Polymer Competence Center Leoben GmbH (PCCL, Austria) and within the COMET-modul "Polymers4Hydrogen" within the framework of the COMET-program of the Federal Ministry for Transport, Innovation and Technology and Federal Ministry for Economy, Family and Youth, with contributions by the Department of Polymer Engineering and Science (Montanuniversitaet Leoben). The PCCL is funded by the Austrian Government and the State Governments of Styria, Lower Austria and Upper Austria.

Conflicts of Interest: The authors declare no conflict of interest. The funders had no role in the design of the study; in the collection, analyses, or interpretation of data; in the writing of the manuscript, or in the decision to publish the results.

References

1. Connolly, F.; Walsh, C.J.; Bertoldi, K. Automatic design of fiber-reinforced soft actuators for trajectory matching. *Proc. Natl. Acad. Sci. USA* **2017**, *114*, 51–56, doi:10.1073/pnas.1615140114.
2. Lu, T.; Shi, Z.; Shi, Q.; Wang, T.J. Bioinspired bicipital muscle with fiber-constrained dielectric elastomer actuator. *Extreme Mech. Lett.* **2016**, *6*, 75–81, doi:10.1016/j.eml.2015.12.008.
3. Zhang, Q.; Wommer, J.; O'Rourke, C.; Teitelman, J.; Tang, Y.; Robison, J.; Lin, G.; Yin, J. Origami and kirigami inspired self-folding for programming three-dimensional shape shifting of polymer sheets with light. *Extreme Mech. Lett*. **2017**, *11*, 111–120, doi:10.1016/j.eml.2016.08.004.
4. Koschmieder, M. Verarbeitung und Eigenschaften von Faserverbundkunststoffen mit Elastomermatrix, Ph.D. Theses, Rheinisch-Westfälischen Technischen Hochschule Aachen, Aachen, Germany, 2000.
5. Zhang, X.; Fan, X.; Yan, C.; Li, H.; Zhu, Y.; Li, X.; Yu, L. Interfacial microstructure and properties of carbon fiber composites modified with graphene oxide. *ACS Appl. Mater. Interfaces* **2012**, *4*, 1543–1552, doi:10.1021/am201757v.
6. Kalinka, G.; Neumann, B. Bestimmung von Interface-Festigkeit oder Trennarbeit mit dem Pull-out-Versuch: Kassel, Germany, 2005. Available online: https://opus4.kobv.de/opus4-bam/frontdoor/index/index/docId/6085 (accessed on 17 February 2020).
7. Kim, J.-K.; Mai, Y.-W. *Engineered Interfaces in Fiber Reinforced Composites*, 1st ed.; Elesvier Science Ltd: Oxford, UK, 1998; pp. 43–93, ISBN 0-08-042695-6.
8. Zhou, J.; Li, Y.; Li, N.; Hao, X.; Liu, C. Interfacial shear strength of microwave processed carbon fiber/epoxy composites characterized by an improved fiber-bundle pull-out test. Compos. *Sci. Technol.* **2016**, *133*, 173–183, doi:10.1016/j.compscitech.2016.07.033.
9. Piggott, M.R. Why interface testing by single-fibre methods can be misleading. *Compos. Sci. Technol*. **1997**, *57*, 965–974, doi:10.1016/S0266-3538(97)00036-5.
10. Zhandarov, S. Characterization of fiber/matrix interface strength: Applicability of different tests, approaches and parameters. *Compos. Sci. Technol*. **2005**, *65*, 149–160, doi:10.1016/j.compscitech.2004.07.003.
11. Kerans, R.J.; Parthasarathy, T.A. Theoretical Analysis of the Fiber Pullout and Pushout Tests. *J. Am. Ceram. Soc*. **1991**, *74*, 1585–1596, doi:10.1111/j.1151-2916.1991.tb07144.x.
12. Penn, L.S.; Bowler, E.R. A new approach to surface energy characterization for adhesive performance prediction. *Surf. Interface Anal*. **1981**, *3*, 161–164, doi:10.1002/sia.740030405.
13. Desarmot, G.; Favre, J. Advances in pull-out testing and data analysis. *Compos. Sci. Technol*. **1991**, *42*, 151–187, doi:10.1016/0266-3538(91)90016-I.
14. Hampe, A.; Kalinka, G.; Meretz, S.; Schulz, E. An advanced equipment for single-fibre pull-out test designed to monitor the fracture process. *Composites* **1995**, *26*, 40–46, doi:10.1016/0010-4361(94)P3628-E.

15. Yue, C.Y.; Padmanabhan, K. Interfacial studies on surface modified Kevlar fibre/epoxy matrix composites. *Compos. Part B* **1999**, *30*, 205–217, doi:10.1016/S1359-8368(98)00053-5.
16. Zhamu, A.; Zhong, W.H.; Stone, J.J. Experimental study on adhesion property of UHMWPE fiber/nano-epoxy by fiber bundle pull-out tests. *Compos. Sci. Technol*. **2006**, *66*, 2736–2742, doi:10.1016/j.compscitech.2006.03.005.
17. Palola, S.; Sarlin, E.; Kolahgar Azari, S.; Koutsos, V.; Vuorinen, J. Microwave induced hierarchical nanostructures on aramid fibers and their influence on adhesion properties in a rubber matrix. *Appl. Surf. Sci*. **2017**, *410*, 145–153, doi:10.1016/j.apsusc.2017.03.070.
18. Niroomand, M.; Hejazi, S.M.; Sheikhzadeh, M.; Alirezazadeh, A. Pull-out analysis of laser modified polyamide tire cords through rubber matrix. *Eng. Fail. Anal.* **2017**, *80*, 431–443, doi:10.1016/j.engfailanal.2017.07.013.
19. Sørensen, B.F.; Lilholt, H. Fiber pull-out test and single fiber fragmentation test—Analysis and modelling. *IOP Conf. Ser. Mater. Sci. Eng*. **2016**, *139*, doi:10.1088/1757-899X/139/1/012009.
20. Hatamleh, M.M.; Watts, D.C. Effects of bond primers on bending strength and bonding of glass fibers in fiber-embedded maxillofacial silicone prostheses. *J. Prosthodont*. **2011**, *20*, 113–119, doi:10.1111/j.1532-849X.2010.00653.x.
21. Brandstetter, J.; Peterlik, H.; Kromp, K.; Weiss, R. A new fibre-bundle pull-out test to determine interface properties of a 2D-woven carbon/carbon composite. *Compos. Sci. Technol*. **2003**, *63*, 653–660, doi:10.1016/S0266-3538(02)00250-6.
22. Schulz, E.; Kalinka, G.; Auersch, W. Effect of transcrystallization in carbon fiber reinforced poly(p -phenylene sulfide) composites on the interfacial shear strength investigated with the single fiber pull-out test. *J. Macromol. Sci. Part B* **2006**, *35*, 527–546, doi:10.1080/00222349608220393.
23. Domnanovich, A.; Peterlik, H.; Kromp, K. Determination of interface parameters for carbon/carbon composites by the fibre-bundle pull-out test. *Compos. Sci. Technol*. **1996**, *56*, 1017–1029, doi:10.1016/0266-3538(96)00060-7.
24. Kalinka, G.; Leistner, A.; Hampe, A. Characterisation of the fibre/matrix interface in reinforced polymers by the push-in technique. *Compos. Sci. Technol*. **1997**, *57*, 845–851, doi:10.1016/S0266-3538(96)00159-5.
25. Zarges, J.-C.; Kaufhold, C.; Feldmann, M.; Heim, H.-P. Single fiber pull-out test of regenerated cellulose fibers in polypropylene: An energetic evaluation. *Compos. Part A* **2018**, *105*, 19–27, doi:10.1016/j.compositesa.2017.10.030.
26. Viel, Q.; Esposito, A.; Saiter, J.-M.; Santulli, C.; Turner, J. Interfacial Characterization by Pull-Out Test of Bamboo Fibers Embedded in Poly(Lactic Acid). *Fibers* **2018**, doi:10.3390/fib6010007.
27. Muliana, A.; Rajagopal, K.R.; Tscharnuter, D.; Schrittesser, B.; Saccomandi, G. Determining material properties of natural rubber using fewer material moduli in virtue ofa novel constitutive approach for elastic bodies. *Rubber Chem. Technol*. **2018**, *91*, 375–389, doi:10.5254/RCT.18.81675.
28. Beter, J.; Schrittesser, B.; Fuchs, P.F. Investigation of adhesion properties in load coupling applications for flexible composites. *Mater. Today-Proc.* **2020**, doi:10.1016/j.matpr.2020.01.181.
29. von Essen, M.; Sarlin, E.; Tanhuanpää, O.; Kakkonen, M.; Laurikainen, P.; Hoikkanen, M. Automated high-throughput microbond tester for interfacial shear strength studies. In Proceedings of the SAMPE Europe Conference, Stuttgart, Germany, 13–16 November 2017; pp. 14–16, ISBN 978-90-821727-7-5.
30. Thomason, J.L.; Yang, L. Temperature dependence of the interfacial shear strength in glass–fibre polypropylene composites. *Compos. Sci. Technol.* **2011**, *71*, 1600–1605, doi:10.1016/j.compscitech.2011.07.006.
31. Zhandarov, S.; Mäder, E. Analysis of a pull-out test with real specimen geometry. Part I: Matrix droplet in the shape of a spherical segment. *J. Adhes. Sci. Technol*. **2013**, *27*, 430–465, doi:10.1080/01694243.2012.715730.
32. Bartoš, P. Analysis of pull-out tests on fibres embedded in brittle matrices. *J. Mater. Sci*. **1980**, *15*, 3122–3128, doi:10.1007/BF00550385.

3.2 Paper 2: Tailored interfaces in fiber reinforced elastomers: A surface treatment study on optimized load coupling via the modified fiber bundle debond technique

Julia Beter[1,*], Boris Maroh[1], Bernd Schrittesser[1], Inge Mühlbacher[1], Thomas Griesser[2], Sandra Schlögl[1] and Gerald Pinter[3]

[1] Polymer Competence Center Leoben GmbH, Roseggerstrasse 12, 8700 Leoben, Austria.

[2] Chair of Chemistry of Polymeric Materials, Montanuniversitaet Leoben, Otto-Gloeckel Strasse 2, 8700 Leoben, Austria

[3] Department of Polymer Engineering and Science, Montanuniversitaet Leoben, Otto Gloeckel- Strasse 2, 8700 Leoben, Austria.

Published in Polymers, 2020, 13(1), 36.

DOI: 10.3390/polym13010036

polymers

MDPI

Article

Tailored Interfaces in Fiber-Reinforced Elastomers: A Surface Treatment Study on Optimized Load Coupling via the Modified Fiber Bundle Debond Technique

Julia Beter [1,*], Boris Maroh [1], Bernd Schrittesser [1], Inge Mühlbacher [1], Thomas Griesser [2], Sandra Schlögl [1], Peter Filipp Fuchs [1] and Gerald Pinter [3]

[1] Polymer Competence Center Leoben GmbH, Roseggerstrasse 12, 8700 Leoben, Austria; Boris.Maroh@pccl.at (B.M.); Bernd.Schrittesser@pccl.at (B.S.); Inge.Muehlbacher@pccl.at (I.M.); Sandra.Schloegl@pccl.at (S.S.); PeterFilipp.Fuchs@pccl.at (P.F.F.)

[2] Chair of Chemistry of Polymeric Materials, Montanuniversitaet Leoben, Otto-Gloeckel Strasse 2, 8700 Leoben, Austria; Thomas.Griesser@unileoben.ac.at

[3] Department of Polymer Engineering and Science, Montanuniversitaet Leoben, Otto-Gloeckel Strasse 2, 8700 Leoben, Austria; Gerald.Pinter@unileoben.ac.at

* Correspondence: Julia.Beter@pccl.at; Tel.: +43-3842-42962-31

Abstract: The interface between the reinforcement and surrounding matrix in a fibrous composite is decisive and critical for maintaining component performance, durability, and mechanical structure properties for load coupling assessment, especially for highly flexible composite materials. The clear trend towards tailored solutions reveals that an in-depth knowledge on surface treating methods to enhance the fiber–matrix interfacial interaction and adhesion properties for an optimized load transfer needs to be ensured. This research aims to quantify the effect of several surface treatments for glass fibers applied in endless fiber-reinforced elastomers with pronounced high deformations. Due to this, the glass fiber surface is directly modified with selected sizings, using a wet chemical treatment, and characterized according to chemical and mechanical aspects. For this purpose, the interfacial adhesion performance between fibers and the surrounding matrix material is investigated by a modified fiber pull-out device. The results clearly show that an optimized surface treatment improves the interface strength and chemical bonding significantly. The fiber pull-out test confirms that an optimized fiber–matrix interface can be enhanced up to 85% compared to standard surface modifications, which distinctly provides the basis of enhanced performances on the component level. These findings were validated by chemical analysis methods and corresponding optical damage analysis.

Keywords: fiber-reinforced elastomers; fiber–matrix interface; surface modification; chemical sizing; fiber bundle pull-out test

Citation: Beter, J.; Maroh, B.; Schrittesser, B.; Mühlbacher, I.; Griesser, T.; Schlögl, S.; Fuchs, P.F.; Pinter, G. Tailored Interfaces in Fiber-Reinforced Elastomers: A Surface Treatment Study on Optimized Load Coupling via the Modified Fiber Bundle Debond Technique. *Polymers* **2021**, *13*, 36. https://dx.doi.org/10.3390/polym13010036

Received: 3 December 2020
Accepted: 22 December 2020
Published: 24 December 2020

1. Introduction

Flexible composites combine reinforcing fibers with elastomeric matrix resulting in good mechanical properties and stability but still maintain a flexible structure. Completely new applications for those advanced composite material classes considering supplementary biomimetic approaches [1] could be found, e.g., in the field of medical engineering to generate artificial muscles [2], exoskeletons for rehabilitation [3] or aeroelastic skin-like wings [4,5]. To ensure sufficient mechanical performance for these materials and to avoid unwanted stress concentrations [6,7], efficient load transfer between fibers and the matrix [8] as well as excellent fiber–matrix adhesion are required [9,10]. Thus, in-depth knowledge and quantitative investigations of the interface properties [11,12] are essential, which are resulting from the decisive impact due to targeted surface modifications [10] but also from the characteristics of the combined individual components themselves [13,14]. Test methods to study the fiber–matrix interface have been designed for the single fiber (micro scale), fiber

bundle (meso scale) and laminate level (macro scale). The single-fiber- and fiber-bundle-level tests provide data that are well related to the interfacial properties [10–12,15,16], whereas the data obtained from the laminate level testing are sensitive, e.g., to fiber directions [17] and other laminate processing-related factors [8,18]. To ensure sufficient performance at component level, which is known to consist of a large number of threads and therefore includes numerous boundary conditions [19], it is important to investigate the material behavior at bundle level as a representative volume unit and to define the global structural behavior accordingly [20,21]. In relation to this, a direct correlation between the micro and meso scale tests with the macroscopic composite parts is not feasible [8,22]. The considered methods to investigate the interface properties for composites are mainly carried out with single fiber or fiber bundle tests like the well-known single-fiber push-out test [23,24], single-fiber pull-out test [25,26] and fiber bundle pull-out (FBPO) test [15,27]. Nevertheless, there is still no consistent design or standardization for the interface characterization, and, therefore, comparability between various test setups is only possible within a limited range. Hence, the essential material data obtained from these tests need to be validated [10,14].

Regarding the different test devices, FBPO testing generally provides the potential to conduct measurements faster, easier and with less complexity to estimate the fiber–matrix adhesion with more realistic failure modes (e.g., statistical fiber distribution or fiber–fiber interaction) than the single fiber tests, which, however, require more sensitive handling [8,14] as well as expensive special test equipment [28,29]. In addition, the FBPO tests are significantly influenced by several factors such as (i) the complex stress distribution in a fiber bundle [21,30], (ii) fiber–fiber interaction [29] with more real failure modes [14,31] or (iii) the presence of statistically distributed filaments inside the fiber bundle [32,33]. Due to the variable cross-section areas inside a fiber bundle, these aspects influence the interlaminar shear strength [19,34], and, therefore, the results can be considered more reliable for performance predictions on laminate lay-ups [19]. Previous research was conducted focusing on the verification of a modified FBPO test device for a more precise interface characterization so that even fiber-reinforced elastomers can be handled adequately due to their distinct flexible performance [35]. Moreover, this study revealed that, besides the right choice of the fiber–matrix combination, the sizing on the fibers has a strong impact on the bearable load coupling and further on the composite performance [15,19]. Apart from the common function of stabilization of the pure fibers due to storage, processing or environmental influences [36], the sizing poses the unique possibility to chemically bond materials with completely different properties and can therefore act as a link to achieve an optimum adhesion at the fiber–matrix interface area [13,37–39]. This knowledge provides the opportunity to combine controversial materials. In this context, other researchers already have reported problems with an inadequate fiber–elastomer adhesion and demonstrated that the understanding of fiber sizing and fiber–rubber adhesion is essential to produce high-quality specimens and reliable results for further technical applications [40–42]. For example, conventional glass fibers (GF) are typically coated with a silane-based sizing mixture, which is chosen mostly due to economic aspects to generate a widespread usage in industry for several thermoset applications [37]. Subsequently, this treatment obtained a good adhesion, e.g., to polyurethane matrix but compared to that offering a negative effect on the adhesion with silicone rubber, which confirms the use of an appropriate primer [43]. Sufficient wetting of the fibers by the matrix material as well as good adhesion between the surface sizing and polymer-based matrix are required to ensure good mechanical performance in terms of load bearing in composite materials [44–46]. Several studies report on the essential influence of the fiber surface treatment, since a tailored adhesive fiber–matrix bonding emphasizes significant differences in the static and dynamic mechanical properties of a composite [47,48]. As such, this strongly influences the force transmission and load coupling between reinforcing structures and their surrounding matrix material [49]. Based on this knowledge, a custom-made surface modification is crucial to achieve an optimized performance of the composite depending on the requirements and material combination. Established surface modification methods for glass fibers

include plasma techniques [50] and chemical approaches such as coating or covalent attachment of selected functional coupling agents [51]. In particular, silanization reactions proved to be an ideal method for tailoring surfaces of glass fibers [52]. Previous studies conducted on FBPO tests have already demonstrated that the removal of the fiber treatment that originated from the supplier (more specialized for thermoset application) leads to a distinct improvement in adhesive strength [35]. This research was carried out with the aim of understanding the effect of different sizing and their impact on the fiber–elastomer adhesion as well as on the specific setting of the mechanical properties demonstrated by a fiber pull-out method. In this context, a modified FBPO test setup is presented to enable the characterization of the adhesion behavior in the interface in a fiber-reinforced elastomer. Moreover, the data recording reveals similar measurement sensitivity compared to tests on composite samples, which was proven in previous conducted studies focusing on the influence of fiber orientation and adhesion properties on tailored fiber-reinforced elastomers [34]. Based on this knowledge, it is obvious that pull-out tests on single fibers are indispensable especially for the detailed analysis in the microstructure. Hence, the interface characterization is focused primarily on the main research problem at model scale, and, therefore, unnecessary disruptive factors can be successfully eliminated. However, to predict the interface performance for composite components [48], single fiber tests show an overly high measurement sensitivity, and, thus, experiments on fiber bundles reveal more realistic results [14]. Regarding the advice of a customized fiber surface treatment for optimized fiber matrix adhesion, various silane-based coatings were applied to the same fiber–matrix material combination to demonstrate this impact on the mechanical properties as well as on the further composite performance. Accordingly, different chemical and optical analysis were carried out additionally to prove the modified surface quality. Moreover, an optimized surface modification for flexible composite materials is presented for a tailored load transferability between fiber and elastomeric matrix, which is further important for the load coupling mechanism in flexible composites [19,20].

Thus, the main focus of this study is the feasibility and repeatability of the modified FBPO test to detect the specific bonding properties of fiber–matrix interfaces related to the chemical surface treatments and to provide a qualitative investigation method with an appropriate measurement sensitivity. Therefore, the reliability and proof of the surface modification procedure is determined by the bonding of the immobilized silane groups to the fiber surface and by the covalent reaction with corresponding verification tests, such as zeta potential analysis and X-ray photoelectron spectroscopy (XPS). For a complete survey, a standard industrial surface coating and the pure fiber surface (cleaned and decoated) are analyzed in addition. Subsequently, the interfacial bonding strength, an important parameter, is investigated, where the maximum required force for debonding combined with the pull-out behavior represents the basic performance of the mechanical proprieties. Therefore, the adhesion between the fiber bundles with tailored surface conditions and the elastomeric matrix was investigated with the FBPO test setup as a corresponding verification test. Accompanying optical damage analysis provides a visual confirmation of the failure mode. Overall, this study provides a successful evaluation of reliable material data regarding the fiber–matrix interface performance for subsequent simulations [53] and enables customized data for numerical models on elastic bodies with specific reinforcement structures [19,54]. Furthermore, this can be exploited for several other material clusters based on the requirements of the individual components in the composite. In adaption to this aspect combined with a systematic scaling from micro- to macro-mechanical properties, the profound findings regarding the adhesive fiber–matrix strength resulting in an optimized load coupling in the composite yield the basis for promising approaches, such as tension-twist coupling in fiber-reinforced elastomers [55] for novel smart composite material applications, such as aeroelastic spoilers, flaps or aileron in the aircraft and automotive sectors.

2. Materials and Methods

2.1. Materials and Chemicals

For the experiments, commercial E-type GF reinforcement provided by CS Interglas AG (Erbach, Germany) with the standardized warp yarn classification EC9-68 × 5 t0 from a single batch and with a 2/2 twill weave was used. The reinforcing structure with an area weight of 220 g/m^2 ± 5% and an area bundle distribution of 50/50 in the 0°/90° direction was coated with a standard industrial silane-based surface treatment FK144 with a twine thickness of about 68 tex, respectively. The mean diameter of the filament is indicated with approximately 10 µm. Regarding the mechanical properties of the pure reinforcing structure, tensile tests according to the ASTM D2256 [56] were already conducted in detail in previous research focusing on the influence of fiber orientation and adhesion properties of tailored fiber-reinforced elastomers [57]. Pneumatically driven grips with a mandrel shape were considered to ensure good clamping without causing clamp-induced damages among the fixed fiber parts considering a preload of 1 N to ensure identical initial test conditions.

As matrix material, Elastosil RT601 A/B as a polydimethylsiloxane (PDMS) obtained from Wacker Chemie AG (Munich, Germany) was chosen for preparing the bundle pull-out specimens. This PDMS is a vinyl-terminated hyperelastic two-component cast system (the prepolymer, part A and crosslinking system, part B) to analyze the impact on the pull-out behavior due to hyperelasticity (highly flexible elastomers). The polyaddition reaction of PDMS via platinum catalyst involves a hydrosilylation reaction between vinyl-terminated difunctional Si–O groups (part A) and the methylhydrosilane-dimethylsiloxane crosslinker (part B). This hydrosilylation process involves the addition of a silane group to the double bond of the difunctional Si–O group to result in a hyperelastic crosslinked polymer network [58].

Due to the typical inorganic structure as well as organic groups comprising siloxane units, PDMS represents a suitable intermediate position between inorganic and organic compounds. Apart from the high heat, weathering, ozone resistance or good low-temperature flexibility, unfilled PDMS reveals further essential properties due to its low side-chain branching and high free volume within the polymer chains. In this context, by exploiting these structure properties, the higher bonding energy of PDMS in combination with GF can lead to beneficial interface adhesion, which subsequently influences the flexible composite properties, especially for load coupling effects in a specific manner. Hence, these promising findings can be further enhanced by optimized chemical modifications of the fiber surface to investigate the influence and its effects on the fiber–matrix bonding by a tailored fiber surface treatment in more detail. Regarding the technical datasheet, the PDMS with a mixing ration 9:1 (part A: part B) has a density of 1.02 g/cm^3 and a viscosity of the mixed product (uncured) of 3500 mPas (at room temperature). The pot lifetime was indicated with about 90 min at 23 °C and a hardness of 35 Shore A. Based on the manufacturer's recommendations, the elastomeric matrix was produced following the respective mixing ratio, including an intermediate pre-degassing vacuum step to avoid air bubbles, followed by a final curing step at 70 °C for 60 min in an air-circulating drying oven. For the experimental study on the mechanical performance of these hyperelastic matrices, tests according to the ISO 37 [59] with type 2 specimens were carried out in previous research [57].

Overall, three different chemical silane-based treatments were considered for tailored GF surface modifications and implemented in the specially developed treatment procedure. The used chemicals for this procedure were anhydrous toluene, anhydrous ethanol and 30 wt.% hydrogen peroxide purchased from VWR International LLC (Radnor, PA, USA), including 96 wt.% sulfuric acid and 30 wt.% ammonium hydroxide solution, which were obtained from Carl Roth GmbH + Co. KG (Karlsruhe, Germany). In terms of the three different silanes, 3-aminopropyltriethoxysilane (APTES), (1H,1H,2H,2H-perfluoro-1-octyl)triethoxysilane (FOTES) and vinyltriethoxysilane (VTES) were provided by Sigma-Aldrich, Inc. (Missouri, MO, USA). All chemicals were applied without any further

purifications. For the intermediate washing sequences, deionized water was used over the entire treatment procedure. All of the different fiber surface conditions are listed in Table 1, including a clear labelling also adapted in the further sections.

Table 1. Different surface modifications of glass fibers prior to and after desizing, and attached organo-silane treatments with respective labels.

Surface Modification	Feature	Label
1	commercial sizing FK144	sized
2	piranha treatment	desized
3	vinyltriethoxysilane	VTES
4	3-aminopropyltriethoxysilane	APTES
5	1H,1H,2H,2H-perfluoro-1-octyl)triethoxysilane	FOTES

2.2. Desizing Procedure of the Glass Fibers

The treated commercial GF from the supplier contained an organic-based sizing, which was removed by a three-step cleaning method comprising two separate cleaning phases, desizing and activation. In the first step, a part of the coating was removed by placing the extracted GF bundles in the acidic peroxymonosulfuric acid (colloquially also called as piranha solution) consisting of four equivalents of 96 wt.% sulfuric acid (H_2SO_4) and one equivalent of 30 wt.% aqueous hydrogen peroxide (H_2O_2), in which the fiber bundles were leached and treated for 30 min. After this treatment, the fibers were taken from the acidic piranha solution and repeatedly rinsed with deionized water straight afterwards. In the second step, the cleaned GF were exposed to basic piranha solution comprising one equivalent of 30 wt.% ammonium hydroxide solution (NH_4OH) and one equivalent of 30 wt.% aqueous H_2O_2, where the fibers were treated for 20 min at 60 °C. Once again, the fibers were repeatedly rinsed with deionized water. For the activation, the purified fiber bundles were wetted with anhydrous ethanol (C_2H_5OH) and finally dried for 60 min at 120 °C in an air-circulating drying oven. All processing steps were carried out at standard atmosphere conditions according to DIN EN ISO 291 (20 °C, 50% r.h.) [60].

2.3. Fiber Surface Modification

For the tailored surface modification step, several cleaned and activated fiber bundles were leached and treated with three different silane-based solutions separately. The solutions consisted either of 1 wt.% solution of FOTES or VTES in anhydrous toluene or 1 wt.% solution of APTES in anhydrous ethanol. Each fiber bundle was treated for 240 min at 60 °C in the respective silane solution followed by the washing step with the corresponding anhydrous solvent (used at the treatment procedure) for three times repeatedly. In the final step, the surface modified fibers were dried for 60 min at 120 °C in an air-circulating drying oven.

2.4. Sample Preparation

In this work, FBPO specimens were prepared for the analysis on tailored fiber–matrix bonding. The modified FBPO test benefits from a fast, easy and economic test condition with a more realistic failure mechanism e.g., statistical filament–matrix distribution, fiber–fiber friction or a more realistic interfacial shear strength distribution. The verification of this presented test setup was described and investigated in detail in another study focusing on a modified FBPO method for the characterization of fiber-reinforced hyperelastic elastomers [35]. For this purpose, a novel specimen manufacturing tool [35] was designed, which had to fulfill the main requirements of (i) an exact fiber bundle positioning in the center of the surrounding matrix material to avoid negative effects caused by tilting or asymmetrical stress distributions along the specimen thickness; (ii) fixing of the fiber bundles, avoiding any pre-damage; (iii) straight placing of the fiber bundle without generating tensile stresses; and (iv) good sealing, especially in the transition region between

the embedded and non-embedded fiber bundle due to creep and adhesion forces in fiber bundle direction causing impaired data recording and errors in the results. The handling and assembly design with the main components are schematically illustrated in Figure 1a. Generally, the tool consists of two parts, where part A contains a corpus with narrow slots for the bundles with a defined recess for the cast matrix system. Subsequently, seals have to be implemented on both sides next to the recess to ensure an exact fiber positioning as well as leakage prevention due to the impregnation process. Part B is designed in a movable way with the purpose of aligning the placed fiber bundles in a straight manner. Regarding the surrounding matrix part, all specimens have the exact same geometry with a width w of 10 mm, a thickness b of 8 mm and a length l of 10 mm, where l is equal with the embedded length l_e for the impregnated fiber bundle part (see Figure 1b). Regarding the sample preparation of the FBPO samples, after the casting step of the non-crosslinked prepolymer, the same manufacturing concept was implemented as before, producing the pure elastomeric matrix materials.

2.5. Test Setup and Measurement Procedure

The FBPO tests were performed on a universal testing machine (5500 Series, Instron GmbH, Darmstadt, Germany) using a 100 N load cell, a gauge length of 50 mm and a constant pull-out speed of 1 mm/min. Five reproducible tests per setting within the test plan were conducted to obtain sufficient data for a reasonable statistical evaluation. Moreover, a combination of the ASTM D2256 [56] standard for the fiber bundle (using the same mandrel shaped grips for the pure fiber bundle) with a modified specimen holder (for the surrounding matrix) was implemented, which is depicted in Figure 2a. This holder [35] was specially designed to accommodate the possibility to test with a conventional testing machine (see Figure 2b).

Due to the pronounced flexible behavior of the FBPO specimens with the hyperelastic matrix, further challenges in the test procedure emerged: (i) Clamping of the surrounding matrix has to be avoided to prevent further stresses caused by the grips from resulting in fiber breakage. These stresses would be transmitted through the elastomeric matrix and onward into the embedded fiber bundle. Despite this, (ii) no slippage is permitted to occur, as this could seriously impair the data recording. Since the hyperelastic matrix material is prone to micro surface defects that could cause tilting or twisting, (iii) lateral surfaces have to be considered for the specimen holder. These additional surfaces provide guidance regarding the specimen front surfaces parallel aligned to the inner sides of the modified holder. However, this support is only required at the initial state (until the preload is reached) of each experiment, whilst no contact between the sample and the holder is present, and, thus, sufficient space is available. Hence, the elastic matrix can deform without any additional stresses that could negatively influence the experiment. The FBPO specimens were placed deformation-free inside the specimen holder. To ensure the same testing conditions at initial state and to minimize negative effects e.g., fiber stretch or tilting, a preload of 1 N applied at 1 mm/min was considered. According to the results and the data interpretation, the fiber–matrix adhesion at the interface was determined by recording the load–displacement value, where the maximum occurred load F_{max} was set as the significant value for the required pull-out force $F_{max,pull}$. For the crucial debonding (indicated by the followed load drop signal), the fiber bundle was loaded until detachment from the surrounding matrix in the interface area emerged, and it was then pulled out completely (followed by the friction-induced pull-out phase).

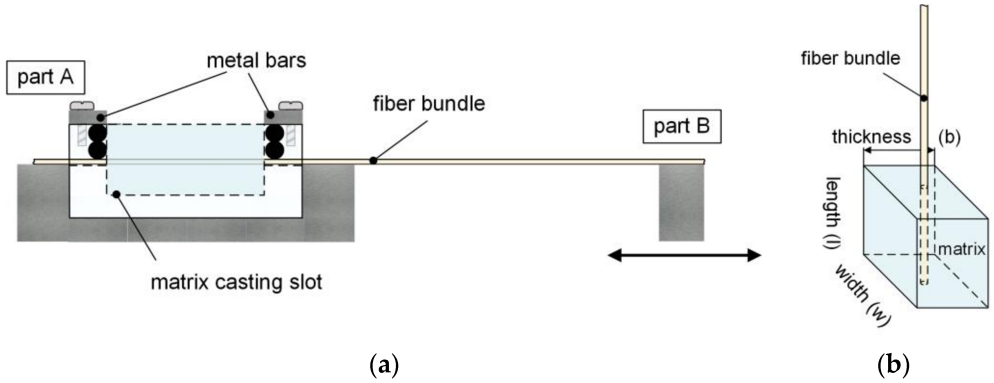

Figure 1. Schematic illustration of the working principle of the manufacturing tool with the main components (**a**) and fiber bundle pull-out (FBPO) specimen (**b**) [35].

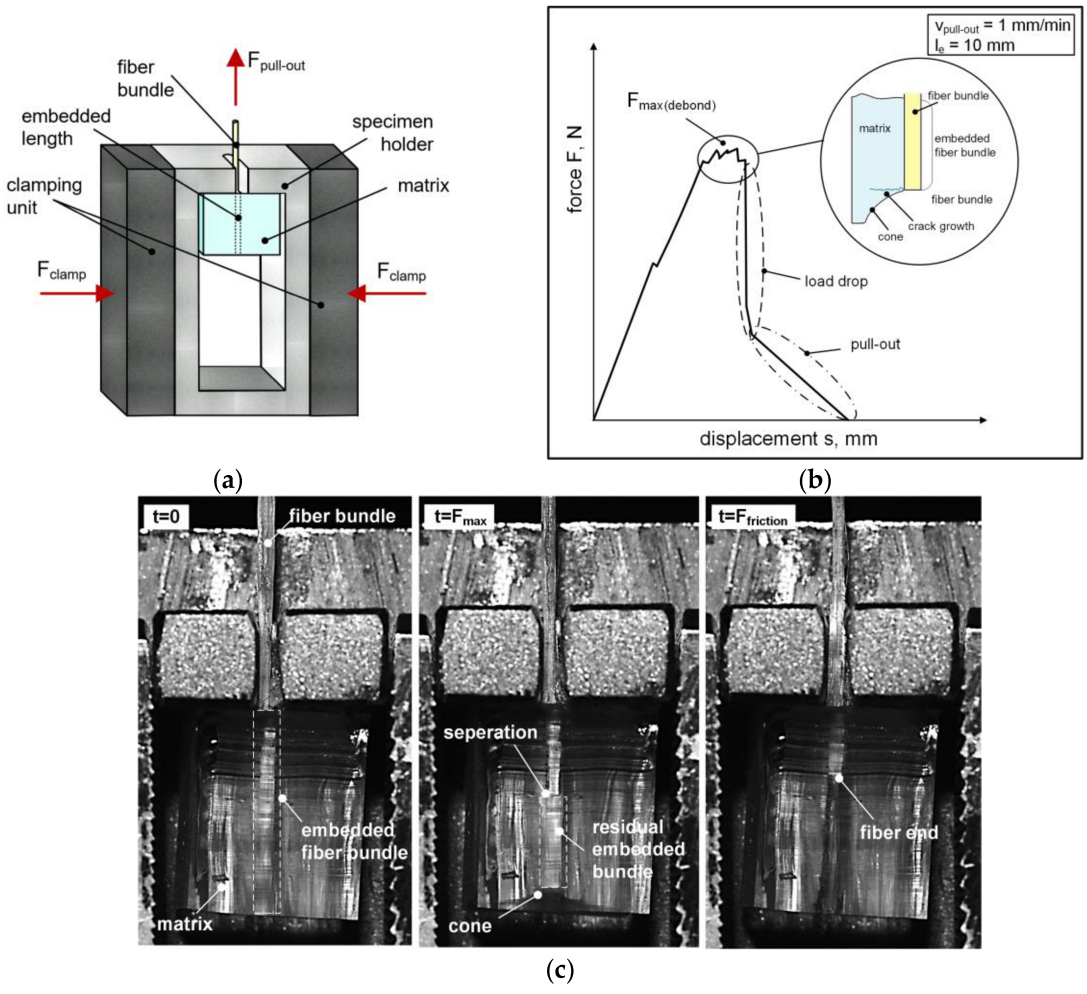

Figure 2. Schematic illustration of the test procedure considering the modified specimen holder (**a**), typical force–displacement graph including the principal performance steps (**b**) and timeline of an FBPO test representing the separation procedure (**c**).

The FBPO test emphasizes a fiber-loaded configuration resulting in a fiber orientation perpendicular to the matrix surface so that only shear stresses in the fiber–matrix interface is achieved. As discussed in some studies, the elastic deformation energy that is probably released can lead to an initiated step-wise crack growth perpendicular to the longitudinal

loading direction (in fiber orientation), which emits during the debonding process [9,12,61] and is schematically explained in Figure 2b. Due to the high elastic behavior especially for PDMS, a cone (see Figure 2c) at the end of the embedded fiber bundle within the sample is clearly observable, whilst the adhesive fiber–matrix bonding to the surrounding matrix is still maintained. Figure 2c shows that the separation mechanism is indicated by the refraction of the light. As expected, the crack initiation begins at the top of the embedded area, whilst only the matrix surface is in contact with the sample holder.

2.6. Surface Characterization

Zeta potential analysis was carried out with the "SurPASS" electrokinetic analyzer (Anton Paar GmbH, Graz, Austria). In general, the streaming potential method was chosen to measure the zeta potential of modified GF in 1mM KCl, whereby the analysis started from the natural pH level to lower acidic values by increasing the titration media up to 50 mM HCl or to higher pH values by increasing it up to 50 mM NaOH with an autotitration unit (RTU, Anton Paar KG, Graz, Austria). The chemical surface analysis of glass fibers was carried out by XPS with a K-Alpha X-ray Photoelectron Spectrometer (Thermo Fisher Scientific Inc., Erlangen, Germany) equipped with a Al-Kα X-ray source (hν = 1486.6 eV). The survey scan was performed with a pass energy of 200 eV and an energy resolution of 1.0 eV. The pass energy amounted to 10 eV (for narrow resolution spectra) with an energy step size of 0.1. The peaks were fitted according to the Gaussian–Lorentzian mixed function considering a Shirley background correction with the provided software of the supplier (Data Analysis Software—Thermo Avantage v5.906, Thermo Scientific, Vienna, Austria).

2.7. Optical Damage Analysis

Supplementary optical damage analysis was carried out via light microscope (Axioscope 7, Carl Zeiss GmbH, Graz, Austria) to support the comparability and interpretation of the performed FBPO tests. Due to the high elasticity of the elastomeric matrix material and the above-mentioned crack growth process, a camera system (Prosilica GT 6600, Allied Vision Technologies GmbH, Stadtroda, Germany) was additionally employed for all FPBO tests to improve the correlation of the recorded data of the material behavior during the pull-out with the optical-supported debonding failure process. Subsequently, the following calculation and interpretation of the results were conducted more accurately, which enabled a reliable performance prediction of the adhesive fiber–matrix bonding influenced by different interface modifications.

3. Results and Discussion

In previous work, promising and reliable results were achieved using the modified FBPO test setup method for the investigation of different fiber–matrix material combinations [35]. Based on these findings, the emphasis in the following study is on the measurement sensitivity of the modified FBPO test setup towards surface sizings. Therefore, fiber surfaces with varying chemical surface composition were created whilst a constant fiber (GF) matrix (PDMS) combination was applied. With this approach, the influence of controlled surface modifications on the pull-out behavior could be studied in detail. To achieve a tailored adhesion between the glass fibers and the surrounding elastomeric matrix, functional organo-silanes comprising vinyl-, amino- or perfluoro-groups were attached to the fiber surface. Modified GF were obtained with varying surface polarity and chemical functionality, which are expected to distinctively affect the bond strength at the fiber–matrix interface. The applicability of the FBPO test setup was assessed to determine the adhesion strength as a function of the attached silane and to gain a deeper insight into the mechanical properties of fiber–matrix interfaces.

3.1. Surface Characterization

Zeta potential measurements were carried out to investigate the change in the surface charges of GF prior to and after the modification procedure (see Figure 3). Commercially

available fibers were used with a proprietary sizing, which was removed by a treatment with acidic and basic piranha solution. The results reveal an isoelectric point (IEP) of the GF with the treatment from supplier (prior the desizing step) of about 3.8, indicating the presence of weak basic groups [62]. After the desizing and activation of GF with acidic and basic piranha solution, the IEP shifts to a lower value of about 2.4 [37]. This can be explained by the presence of a high number of acidic silanol moieties of the inorganic GF, which become dominant after the successful removal of the organic sizing during the acidic and basic piranha treatment. Along with the removal of the sizing, the silanol groups were activated on the surface for the subsequent immobilization of the organo-silanes [63]. Figure 3 shows negative zeta potential values, which are characteristic for GF surfaces, since the acidic groups on the surface are fully separated in the basic pH range, resulting in negative potential surface charges [64,65].

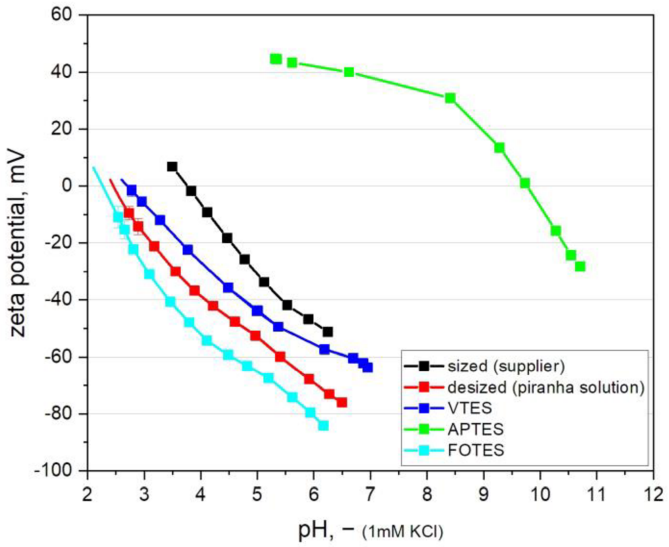

Figure 3. Zeta potential as a function of the pH value of glass fibers prior and after desizing (acidic and basic piranha treatment) and subsequent modification with functional organo-silanes.

Regarding the zeta potential of the modified fibers, the results reveal that the attachment of the perfluorinated silane (FOTES) slightly shifts the IEP to a lower pH value of about 2.2 compared to the IEP of 2.4 of the desized fibers [66]. This result indicates the change in the surface chemistry of GF since FOTES shifts the IEP values towards the acidic region and can lead to a superhydrophobic surface with a significantly low surface energy [67,68]. For the surface modification with the vinyl-functional silane (VTES) a higher IEP of about 2.8 is observed, which is explained by the conversion of acidic silanol groups and the attachment of non-charged and neutral vinyl groups [69]. In contrast to that, the immobilization of organo-silanes with basic amino groups (APTES) significantly increases the pH value of the surface with an indicated IEP of about 9.9 [70]. At low pH values, the amino groups become protonated, whilst an increase in pH causes deprotonation and adsorption of OH^- ions, which leads to a negative surface charge in the high pH range [64]. Generally, for all zeta potential results, it should be noted that specimens from fibers possess a higher measurement sensitivity due to their larger surfaces compared to planar samples [71]. Consequently, the small difference between the zeta potential measurements of FOTES, VTES modified fibers and desized fibers in particular was considered as significant.

Moreover, the changes in the chemical surface composition of the modified glass fibers were evidenced by XPS analysis. The detected elements are summarized in Table 2, where all results are referred to the surface composition with the unit in atom-%.

Table 2. Chemical surface composition of glass fibers prior to and after desizing and attachment of functional organo-silanes in atom-%.

	Sized	Desized	VTES	APTES	FOTES
Si	9.4	20.3	11.9	21.4	14.2
C	58.0	33.2	61.8	40.2	25.4
O	32.6	46.5	26.3	35.2	32.3
F	-	-	-	-	28.1
N	-	-	-	3.2	-

On the surface of the desized GF, C signals corresponding to various carbon species (e.g., C–C, C–O and C=O) are still detectable in the XPS spectrum (Figure 4). The results suggest that the desizing process was not able to fully remove the organic sizing. However, the desizing of the GF leads to a significant increase in the Si and O content compared to the commercially available sized GF, and the formed silanol groups can be exploited as reactive anchor groups for the subsequent coupling of functional organo-silanes. In particular, the attachment of APTES is confirmed by the appearance of the N signal at about 401.6 eV [72], whilst the coupling of FOTES is related to the appearance of the F signal in the characteristic bonding energy region at about 689.7 eV [73]. The comparison of the high resolution C 1s spectra for GF with different surface modifications is given in Figure 4.

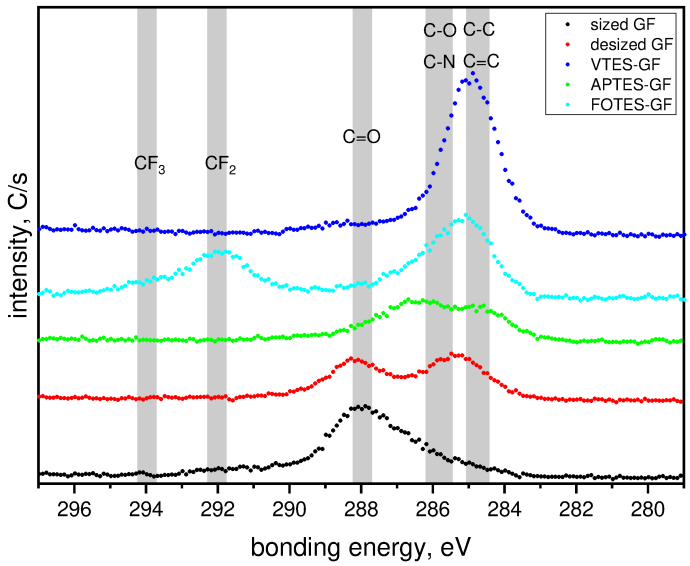

Figure 4. High resolution C 1s spectra of the glass fiber surface prior to and after desizing (acidic and basic piranha treatment) and subsequent modification with functional organo-silanes.

The GF sized by the supplier shows two components of the C 1s spectrum related to C–O at 286.2 eV and C=O at 288.0 eV. After the acidic and basic piranha treatment, both characteristic signals for CO_2 impurities could be observed at 285.5 and 288.1 eV (C–O to C=O ratio of 1 to 0.9). The results confirm that the carbon signal detected in the desized GF is indeed from physisorbed CO_2 and not related to residues of the organic sizing. The attachment of VTES is associated with an increase in the carbon content on the surface as reported in Table 2, which can be explained by the C–C and C=C bonds (285.0 eV) present in the structure of the organo-silane. In contrast, the APTES-modified GF comprise some CO_2 impurities and additional signals for C–C bond at 284.6 eV and C–N bond, which was overlapping with the signal for the C–O bond at 286.4 eV [72,74]. For the FOTES modified GF, the results revealed two characteristic signals for the CF_2 group at 292.0 eV and the CF_3 group at 294.1 eV [73].

3.2. Characterization of Fiber–Matrix Interaction

Concerning the pull-out behavior of modified fiber–matrix interfaces versus the maximum bearable load $F_{max,pull}$, the results of GF incorporated within a PDMS matrix are graphically compared in Figure 5. As expected, the attached functional groups of FOTES gave the lowest adhesion strength with a maximum force of about 2.5 N due to the hydrophobic nature of perfluorinated surfaces and absence of any chemical interactions (e.g., covalent bonds, H-bonds or ionic interactions). Thus, fiber–matrix interactions were successfully impaired and further physical or other chemical bonding reactions were considerably hindered [67]. The treatment with APTES reveals a clearly lower maximum pull-out forces of about 6.7 N compared to the commercially sized fibers from the supplier with a $F_{max,pull}$ of about 14.5 N. This can be explained by the weaker bonding energy of amino groups with the PDMS matrix, and, therefore, this leads to less compatibility, especially in the fiber–matrix interaction [70], which can be clearly observed in Figure 5. However, it can be seen that the removal of the commercial sizing with piranha solution improves the fiber–matrix interface performance significantly, and the maximum pull-out force $F_{max,pull}$ amounts to 20.5 N (approximately 40%) compared to commercial sized fibers. We assume that this improved adhesion performance is related to the presence of ketone groups from the oxidized sizing residues, which are known to undergo catalyzed hydrosilylation with Si-H bonds [75]. Thus, a direct coupling of the oxidized residues of the sizing with the PDMS matrix (which is a two-component system containing activated Si–H) is obtained, leading to an enhanced pull-out force. In relation to this, the results for VTES-treated GF reveal the highest adhesion strength between the fiber bundles and the surrounding matrix, indicated by the high required maximum pull-out force of about 27.1 N (approximately 85%) compared to commercially available sized fibers from the supplier. During the hydrosilylation process of the PDMS with the vinyl-terminated silanes, the modified glass fiber surface via VTES additionally reacts with the methylhydrosilane groups of the crosslinker, which leads to good covalent bonding between the GF and the PDMS matrix [58]. This effect can be enhanced by using higher processing temperatures during the sample manufacturing process of about 70 °C, where the bonding of the vinyl groups during the curing steps via platinum catalyst co-reacts and can be proceed more easily. It is evident that results of the FBPO test with the commercial sizing from the supplier reveal an intermediate position compared with all other treated GF-PDMS samples. A reason for this is that those sizings are usually a mixture of various chemicals typically for a broader range of composite application with emphasis on different specifications, such as the economical aspect for large production units, mostly thermoset-based products and medium adhesion to different resin systems [37]. In general, a direct correlation between the tailored silane-treated fibers and the fibers with a commercial sizing should be considered carefully, since the commercial fibers may also contain film-building agents and other components that are responsible for a homogeneous wetting of the fiber surface. Therefore, additional mixed interactions occur, since the influence of chemical interactions due to covalent bonds as well as physical effects, such as polar or non-polar effects or adhesive interactions, are involved.

As an overview, the results of the FBPO tests versus influence of different surface-treated GF are summarized in Table 3 to examine the measurement sensitivity and corresponding pull-out behavior related to the maximum bearable force $F_{max,pull}$.

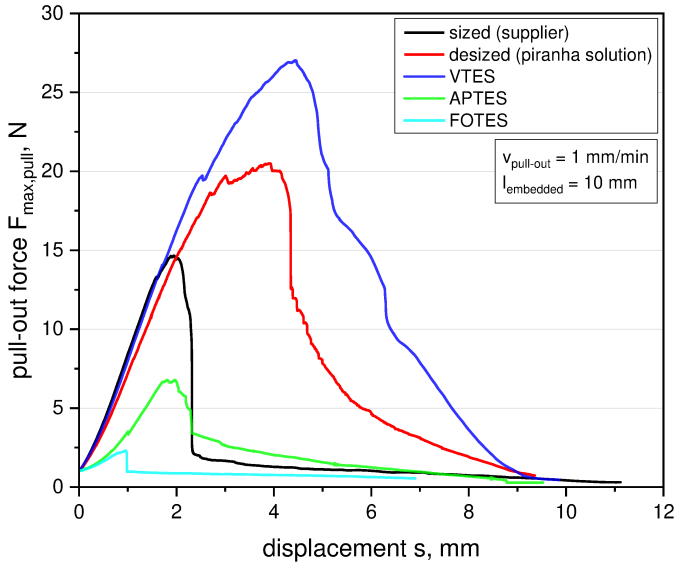

Figure 5. Force–displacement curve determined from the FBPO test on glass fiber (GF) bundles with the polydimethylsiloxane (PDMS) matrix for different fiber surface modifications.

Table 3. Maximum pull-out force $F_{max,pull}$ from FBPO tests for different surface-treated GF bundles combined with the PDMS matrix.

Surface Treatment	Sized (Supplier)	Desized (Piranha Solution)	VTES	APTES	FOTES
max. pull-out force $F_{max,pull}$, N	14.5 ± 1.8	20.5 ± 2.4	27.1 ± 2.9	6.7 ± 1.1	2.5 ± 0.5

In this context, the FBPO test setup proved to be concise, and significant results with an indicated reasonable standard deviation were obtained. Thus, a reliable data interpretation can be carried out, which is listed in Table 3. Despite various influencing factors, such as the statistical fiber distribution inside the bundle or occurring fiber–fiber friction during the pull-out process, a more realistic failure behavior, especially with an accompanying preliminary analysis of suitable surface modifications depending on the application, can be achieved. Furthermore, it is proven that even with a lower interface adhesion, e.g., with FOTES or APTES modifications, a clear difference in pull-out performance can be observed, which confirms the valid assessment of the FBPO test setup.

Besides the results obtained from the FBPO test, the accompanying optical damage analysis provides further information about the pull-out performance and fracture surfaces, which show good agreement with both analysis methods, the zeta potential and FBPO tests. As illustrated in Figure 6a, the optimized interface adhesion of VTES-modified fibers corresponds to the resulting damage surface. It is evident that the complete GF bundle is encapsulated with PDMS, which indicates that the adhesive fiber–matrix bonding is higher than the strength of the matrix. The resulting fracture surface is located near the interface inside the pure PDMS, where the stress concentration of the already deformed elastomer is maximized. Moreover, this effect can be further obtained for desized GF, revealing an adequate fiber–matrix adhesion due to the formed covalent bonds between GF and siloxane monomers of PDMS, which is visible in Figure 6b. In contrast to this, PDMS residues can be barely depicted on the fracture surface of APTES modified GF. This can be explained by the high surface polarity of the amino groups compared to hydrophobic PDMS matrix leading to lower chemical interactions between the treated GF with PDMS (see Figure 6c). Figure 6d shows an example of an original GF bundle (before PDMS wetting) and with the corresponding surface sizing from the supplier.

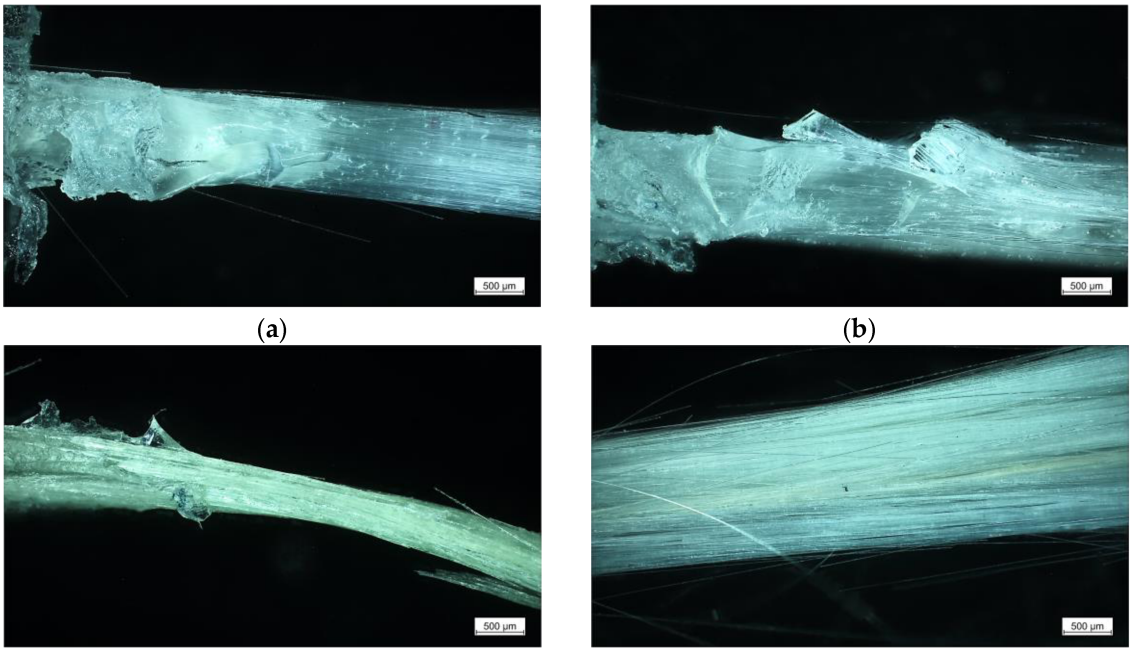

(**a**) (**b**)

(**c**) (**d**)

Figure 6. Light micrographs after the fiber bundle pull-out test of VTES-modified GF (**a**), GF desized with acidic and basic piranha solution (**b**), APTES-modified GF (**c**), GF sized from the supplier (**d**).

4. Conclusions

In this study, the surface of glass fibers was modified by immobilizing selected organo-silanes to investigate the influence of the chemical surface composition on the fiber–matrix interface and further on the load coupling. Since the research interest in "smart materials" is permanently growing, elastomeric matrix materials with high flexibility and reinforced with stiff glass fibers (GF), in particular with silicone as matrix material, were studied exclusively in this work. Moreover, the emphasis was placed on the assessment and validation of the measurement sensitivity of the modified fiber bundle pull-out device induced by different fiber surface conditions. Three organo-silanes were specifically chosen to create different fiber surface energies, whilst the fiber–matrix material combination was kept constant for all experiments. The modification and desizing of GF were confirmed by zeta potential tests, indicating a clear shift of the corresponding isoelectric point (IEP) from 3.8 to 2.4 at the desized state in the first step and an IEP of about 9.9, 2.2 or 2.8 with the specific surface modifications in the following step. XPS measurements confirmed the changes of the chemical surface composition by the appearance of characteristic signals for N and F and the associated changes in the C 1s spectra. Through zeta potential and XPS measurements, the FBPO test and optical damage analysis, the results reveal that the fiber–matrix interface performance was significantly improved using a vinylsilane-based surface modification, since the maximum bearable load was enhanced from about 14.5 to 27.1 N (85% higher values) compared to the commercially treated fibers from the supplier. This study on FBPO tests achieved that for the same fiber–elastomer material combination including different surface coatings, significant changes in the adhesion and fiber matrix bonding were observed. In this context, the modified FBPO test proved a clear intended difference between the results of the fluoro- and aminosilane-based modifications, which emphasizes the verification of measurement sensitivity and sufficient reproducibility. The attached functionalities were additionally compared with optical damage analysis, which correlates with the results of the pull-out performance, and they were in good agreement with the corresponding mechanical behavior caused by the tailored surface treatments. Thus, an optimized interface adhesion of vinylsilane-modified fibers corre-

sponds to the resulting damage surface, demonstrating an unaffected fiber–matrix interface during debonding and failure Overall, the results demonstrated that the fiber–matrix adhesion was adequately achieved and controlled by a suitable surface modification of the glass fibers. Therefore, besides the choice of single material components (matrix or reinforcing material), an optimized fiber–matrix interface significantly contributes to the load coupling between fibers and the surrounding matrix and further in the performance of composite applications. Based on this research, the important findings concerning tailored fiber surfaces for optimized fiber–matrix interfaces is a crucial part in ongoing studies focusing on load coupling mechanisms triggered in flexible composites. Further studies are in progress to investigate the dependence of optimized interfacial adhesion properties and their impact on the cyclic behavior related to the structure–property interactions. Moreover, these findings provide more precise material parameters which are implemented in accompanying ongoing simulation models for fiber-reinforced elastomers to generate accurate material behavior of composites with distinct flexibility.

Author Contributions: Literature research, investigation, formal analysis, writing—original draft preparation, J.B.; conceptualization, methodology, J.B., B.M.; visualization J.B., B.M., T.G. and B.S.; test conduction J.B., B.M., I.M. and T.G; validation, writing—review and editing, J.B., B.M., I.M., S.S. and B.S.; supervision, project administration B.S., S.S., P.F.F. and G.P. All authors have read and agreed to the published version of the manuscript.

Funding: This research was funded by the Federal Ministry for Climate Action, Environment, Energy, Mobility, Innovation and Technology and the Federal Ministry for Digital and Economic Affairs under grant numbers of 854178 and 21647053.

Acknowledgments: This research work was performed at the Polymer Competence Center Leoben GmbH (PCCL, Austria) and within the COMET-modul "Polymers4Hydrogen" within the framework of the COMET-program of the Federal Ministry for Climate Action, Environment, Energy, Mobility, Innovation and Technology and the Federal Ministry for Digital and Economic Affairs, with contributions by the Department of Polymer Engineering and Science (Montanuniversitaet Leoben). The PCCL is funded by the Austrian Government and the State Government of Styria.

Conflicts of Interest: The authors declare no conflict of interest.

References

1. Kim, S.; Laschi, C.; Trimmer, B. Soft robotics: A bioinspired evolution in robotics. *Trends Biotechnol.* **2013**, *31*, 287–294. [CrossRef]
2. Connolly, F.; Walsh, C.J.; Bertoldi, K. Automatic design of fiber-reinforced soft actuators for trajectory matching. *Proc. Natl. Acad. Sci. USA* **2017**, *114*, 51–56. [CrossRef] [PubMed]
3. Lu, T.; Shi, Z.; Shi, Q.; Wang, T.J. Bioinspired bicipital muscle with fiber-constrained dielectric elastomer actuator. *Extrem. Mech. Lett.* **2016**, *6*, 75–81. [CrossRef]
4. Peel, L.D.; Mejia, J.; Narvaez, B.; Thompson, K.; Lingala, M. Development of a Simple Morphing Wing Using Elastomeric Composites as Skins and Actuators. *J. Mech. Des.* **2009**, *131*, 91003. [CrossRef]
5. Debiasi, M.T.; Chan, W.L.; Jadhav, S. Measurements of a Symmetric Wing Morphed by Macro Fiber Composite Actuators. In Proceedings of the 54th Aerospace Science Meeting, San Diego, CA, USA, 4–8 January 2016. [CrossRef]
6. Zhang, X.; Fan, X.; Yan, C.; Li, H.; Zhu, Y.; Li, X.; Yu, L. Interfacial microstructure and properties of carbon fiber composites modified with graphene oxide. *ACS Appl. Mater. Interfaces* **2012**, *4*, 1543–1552. [CrossRef] [PubMed]
7. Gohs, U.; Mueller, M.T.; Zschech, C.; Zhandarov, S. Enhanced Interfacial Shear Strength and Critical Energy Release Rate in Single Glass Fiber-Crosslinked Polypropylene Model Microcomposites. *Materials* **2018**, *11*, 2552. [CrossRef] [PubMed]
8. Koschmieder, M. Verarbeitung und Eigenschaften von Faserverbundkunststoffen mit Elastomermatrix. Ph.D. Thesis, Rheinisch-Westfälischen Technischen Hochschule Aachen, Aachen, Germany, 2000.
9. Kalinka, G.; Neumann, B. Bestimmung von Interface-Festigkeit oder Trennarbeit mit dem Pull-out-Versuch: Kassel, Germany. 2005. Available online: https://opus4.kobv.de/opus4-bam/frontdoor/index/index/docId/6085 (accessed on 2 December 2020).
10. Kim, J.-K.; Mai, Y.-W. *Engineered Interfaces in Fiber Reinforced Composites*, 1st ed.; Elesvier Science Ltd.: Oxford, UK, 1998; ISBN 0-08-042695-6.
11. Piggott, M.R. Why interface testing by single-fibre methods can be misleading. *Compos. Sci. Technol.* **1997**, *57*, 965–974. [CrossRef]
12. Zhandarov, S. Characterization of fiber/matrix interface strength: Applicability of different tests, approaches and parameters. *Compos. Sci. Technol.* **2005**, *65*, 149–160. [CrossRef]
13. Shakun, A.; Sarlin, E.; Vuorinen, J. Material-related losses of natural rubber composites with surface-modified nanodiamonds. *J. Appl. Polym. Sci.* **2019**, *137*, 48629. [CrossRef]

14. Hoffmann, J. Characterization of Fibre Reinforced Elastomers for Shape Morphing Structural Surfaces. Ph.D. Thesis, Technical University of Munich, Munich, Germany, 2012.
15. Zhou, J.; Li, Y.; Li, N.; Hao, X.; Liu, C. Interfacial shear strength of microwave processed carbon fiber/epoxy composites characterized by an improved fiber-bundle pull-out test. *Compos. Sci. Technol.* **2016**, *133*, 173–183. [CrossRef]
16. Kim, B.W.; Nairn, J.A. Observations of Fiber Fracture and Interfacial Debonding Phenomena Using the Fragmentation Test in Single Fiber Composites. *J. Compos. Mater.* **2016**, *36*, 1825–1858. [CrossRef]
17. Cordin, M.; Bechtold, T.; Pham, T. Effect of fibre orientation on the mechanical properties of polypropylene–lyocell composites. *Cellulose* **2018**, *25*, 7197–7210. [CrossRef]
18. Berthold, U. Beitrag zur Thermoformung Gewebeverstärkter Thermoplaste Mittels Elastischer Stempel. Ph.D. Thesis, Technische Universität Chemnitz, Chemnitz, Germany, 2001.
19. Cherif, C. *Textile Werkstoffe für den Leichtbau. Techniken-Verfahren-Materialien-Eigenschaften*; Springer: Berlin, Germany, 2011; ISBN 978-3-642-17992-1.
20. Mansouri, M.R.; Fuchs, P.F.; Criscione, J.C.; Schrittesser, B.; Beter, J. The contribution of mechanical interactions to the constitutive modeling of fiber-reinforced elastomers. *Eur. J. Mech. A Solid* **2020**, 104081. [CrossRef]
21. Domnanovich, A.; Peterlik, H.; Kromp, K. Determination of interface parameters for carbon/carbon composites by the fibre-bundle pull-out test. *Compos. Sci. Technol.* **1996**, *56*, 1017–1029. [CrossRef]
22. Schulz, E.; Kalinka, G.; Auersch, W. Effect of transcrystallization in carbon fiber reinforced poly(p-phenylene sulfide) composites on the interfacial shear strength investigated with the single fiber pull-out test. *J. Macromol. Sci. Part B* **2006**, *35*, 527–546. [CrossRef]
23. Kerans, R.J.; Parthasarathy, T.A. Theoretical Analysis of the Fiber Pullout and Pushout Tests. *J. Am. Ceram. Soc.* **1991**, *74*, 1585–1596. [CrossRef]
24. Kalinka, G.; Leistner, A.; Hampe, A. Characterisation of the fibre/matrix interface in reinforced polymers by the push-in technique. *Compos. Sci. Technol.* **1997**, *57*, 845–851. [CrossRef]
25. Sørensen, B.F.; Lilholt, H. Fiber pull-out test and single fiber fragmentation test—Analysis and modelling. *IOP Conf. Ser. Mater. Sci. Eng.* **2016**, *139*, 012009. [CrossRef]
26. DiFrancia, C.; Ward, T.C.; Claus, R.O. The single-fibre pull-out test: Review and Interpretation. *Compos. Part A* **1996**, *27*, 597–612. [CrossRef]
27. Brandstetter, J.; Peterlik, H.; Kromp, K.; Weiss, R. A new fibre-bundle pull-out test to determine interface properties of a 2D-woven carbon/carbon composite. *Compos. Sci. Technol.* **2003**, *63*, 653–660. [CrossRef]
28. von Essen, M.; Sarlin, E.; Tanhuanpää, O.; Kakkonen, M.; Laurikainen, P.; Hoikkanen, M.; Haakana, R.; Vuorinen, J.; Kallio, P. Automated high-throughput microbond tester for interfacial shear strength studies. In Proceedings of the SAMPE Europe Conference, Stuttgart, Germany, 13–16 November 2017; ISBN 978-90-821727-7-5.
29. Hampe, A.; Kalinka, G.; Meretz, S.; Schulz, E. An advanced equipment for single-fibre pull-out test designed to monitor the fracture process. *Composites* **1995**, *26*, 40–46. [CrossRef]
30. Desarmot, G.; Favre, J. Advances in pull-out testing and data analysis. *Compos. Sci. Technol.* **1991**, *42*, 151–187. [CrossRef]
31. Palola, S.; Sarlin, E.; Kolahgar Azari, S.; Koutsos, V.; Vuorinen, J. Microwave induced hierarchical nanostructures on aramid fibers and their influence on adhesion properties in a rubber matrix. *Appl. Surf. Sci.* **2017**, *410*, 145–153. [CrossRef]
32. Viel, Q.; Esposito, A.; Saiter, J.-M.; Santulli, C.; Turner, J. Interfacial Characterization by Pull-Out Test of Bamboo Fibers Embedded in Poly(Lactic Acid). *Fibers* **2018**, *6*, 7. [CrossRef]
33. Zarges, J.-C.; Kaufhold, C.; Feldmann, M.; Heim, H.-P. Single fiber pull-out test of regenerated cellulose fibers in polypropylene: An energetic evaluation. *Compos. Part A* **2018**, *105*, 19–27. [CrossRef]
34. Beter, J.; Schrittesser, B.; Meier, G.; Fuchs, P.F.; Pinter, G. Influence of Fiber Orientation and Adhesion Properties on Tailored Fiber-reinforced Elastomers. *Appl. Compos. Mater.* **2020**, 149–164. [CrossRef]
35. Beter, J.; Schrittesser, B.; Maroh, B.; Sarlin, E.; Fuchs, P.F.; Pinter, G. Comparison and Impact of Different Fiber Debond Techniques on Fiber Reinforced Flexible Composites. *Polymers* **2020**, *12*, 472. [CrossRef]
36. Neitzel, M.; Mitschang, P.; Breuer, U. *Handbuch Verbundwerkstoffe: Werkstoffe, Verarbeitung, Anwendung*, 2nd ed.; Carl Hanser Verlag: Munich, Germany, 2014; ISBN 978-3-446-43696-1.
37. Sahin, M.; Schlögl, S.; Kalinka, G.; Wang, J.; Kaynak, B.; Mühlbacher, I.; Ziegler, W.; Kern, W.; Grützmacher, H. Tailoring the interfaces in glass fiber-reinforced photopolymer composites. *Polymer* **2018**, *141*, 221–231. [CrossRef]
38. Kanerva, M.; Korkiakoski, S.; Lahtonen, K.; Jokinen, J.; Sarlin, E.; Palola, S.; Iyer, A.; Laurikainen, P.; Liu, X.W.; Raappana, M.; et al. DLC-treated aramid-fibre composites: Tailoring nanoscale-coating for macroscale performance. *Compos. Sci. Technol.* **2019**, *171*, 62–69. [CrossRef]
39. Zhang, D.; He, M.; Qin, S.; Yu, J. Effect of fiber length and dispersion on properties of long glass fiber reinforced thermoplastic composites based on poly(butylene terephthalate). *RSC Adv.* **2017**, *7*, 15439–15454. [CrossRef]
40. Zhamu, A.; Zhong, W.H.; Stone, J.J. Experimental study on adhesion property of UHMWPE fiber/nano-epoxy by fiber bundle pull-out tests. *Compos. Sci. Technol.* **2006**, *66*, 2736–2742. [CrossRef]
41. Liu, M.H.; Li, R.; Wang, G.; Hou, Z.Y.; Huang, B. Morphology and dynamic mechanical properties of long glass fiber-reinforced polyamide 6 composites. *J. Therm. Anal. Calorim.* **2016**, *126*, 1281–1288. [CrossRef]

42. Vleugels, N. Short Fibre-Reinforced Elastomeric Composites: Fundamental Routes towards Improvement of the Interfacial Interaction of Short-Cut Aramid Fibres in a SBR Compound, to Improve Friction and Wear Properties. Ph.D. Thesis, University of Twente, Enschede, The Netherlands, 2017.
43. Peel, L. Fabrication and Mechanics of Fiber-Reinforced Elastomers. Doctoral Thesis, Brigham Young University, Brigham, UT, USA, 1998.
44. Sideridou, I.D.; Karabela, M.M. Effect of the structure of silane-coupling agent on dynamic mechanical properties of dental resin-nanocomposites. *J. Appl. Polym. Sci.* **2008**, *110*, 507–516. [CrossRef]
45. Wilson, K.S.; Allen, A.J.; Washburn, N.R.; Antonucci, J.M. Interphase effects in dental nanocomposites investigated by small-angle neutron scattering. *J. Biomed. Mater. Res. A* **2007**, *81*, 113–123. [CrossRef] [PubMed]
46. Wilson, K.S.; Antonucci, J.M. Interphase structure-property relationships in thermoset dimethacrylate nanocomposites. *Dent. Mater.* **2006**, *22*, 995–1001. [CrossRef] [PubMed]
47. Lung, C.Y.K.; Matinlinna, J.P. Aspects of silane coupling agents and surface conditioning in dentistry: An overview. *Dent. Mater.* **2012**, *28*, 467–477. [CrossRef]
48. Liao, M.; Yang, Y.; Hamada, H. Mechanical performance of glass woven fabric composite: Effect of different surface treatment agents. *Compos. Part B* **2016**, *86*, 17–26. [CrossRef]
49. Calabrò, R. Mechanical characterization of elastomers under quasi-static and dynamic biaxial loading conditions. Ph.D. Thesis, Politecnico di Milano, Milan, Italy, 2013.
50. Lim, K.-B.; Lee, D.-C. Surface modification of glass and glass fibres by plasma surface treatment. *Surf. Interface Anal.* **2004**, *36*, 254–258. [CrossRef]
51. Liu, Z.; Zhang, L.; Yu, E.; Ying, Z.; Zhang, Y.; Liu, X.; Eli, W. Modification of Glass Fiber Surface and Glass Fiber Reinforced Polymer Composites Challenges and Opportunities: From Organic Chemistry Perspective. *Curr. Org. Chem.* **2015**, *19*, 991–1010. [CrossRef]
52. Plueddemann, E.P. *Silane Coupling Agents*, 2nd ed.; Springer: Boston, MA, USA, 1991; ISBN 978-1-4899-2070-6.
53. Mansouri, M.; Fuchs, P.F.; Schuecker, C. Hyperelastic modeling of woven structures undergoing large deformations. In Proceedings of the 18th European Conference on Composite Materials ECCM18, Athen, Greece, 24–28 June 2018.
54. Muliana, A.; Rajagopal, K.R.; Tscharnuter, D.; Schrittesser, B.; Saccomandi, G. Determining material properties of natural rubber using fewer material moduli in virtue ofa novel constitutive approach for elastic bodies. *Rubber Chem. Technol.* **2018**, *91*, 375–389. [CrossRef]
55. Beter, J.; Schrittesser, B.; Meier, G.; Lechner, B.; Mansouri, M.; Fuchs, P.F.; Pinter, G. The Tension-Twist Coupling Mechanism in Flexible Composites: A Systematic Study Based on Tailored Laminate Structures Using a Novel Test Device. *Polymers* **2020**, *12*, 2780. [CrossRef] [PubMed]
56. American Society for Testing and Materials. *ASTM D2256-02: 2015: Test Method for Tensile Properties of Yarns by the Single-Strand Method*; American Society for Testing and Materials: West Conshohocken, PA, USA, 2015.
57. Beter, J.; Schrittesser, B.; Fuchs, P.F. Investigation of adhesion properties in load coupling applications for flexible composites. *Mater. Today Proc.* **2020**. [CrossRef]
58. Roth, L.E.; Vallés, E.M.; Villar, M.A. Bulk hydrosilylation reaction of poly(dimethylsiloxane) chains catalyzed by a platinum salt: Effect of the initial concentration of reactive groups on the final extent of reaction. *J. Polym. Sci. A Polym. Chem.* **2003**, *41*, 1099–1106. [CrossRef]
59. International Organization for Standardization. *ISO 37: 2011-12: Rubber, Vulcanized or Thermoplastic—Determination of Tensile Stress-Strain Properties*; International Organization for Standardization: Geneva, Switzerland, 2011.
60. International Organization for Standardization. *ISO 291:2008-08: Plastics—Standard Atmospheres for Conditioning and Testing*; International Organization for Standardization: Berlin, Germany, 2008.
61. Zhandarov, S.; Mäder, E. Analysis of a pull-out test with real specimen geometry. Part I: Matrix droplet in the shape of a spherical segment. *J. Adhes. Sci. Technol.* **2013**, *27*, 430–465. [CrossRef]
62. Jacobasch, H.-J. Surface phenomena at polymers. *Makromol. Chem. Macromol. Symp.* **1993**, *75*, 99–113. [CrossRef]
63. Cras, J.J.; Rowe-Taitt, C.A.; Nivens, D.A.; Ligler, F.S. Comparison of chemical cleaning methods of glass in preparation for silanization. *Biosens. Bioelectron.* **1999**, *14*, 683–688. [CrossRef]
64. Bismarck, A.; Boccaccini, A.R.; Egia-Ajuriagojeaskoa, E.; Hülsenberg, D.; Leutbecher, T. Surface characterization of glass fibers made from silicate waste: Zeta-potential and contact angle measurements. *J. Mater. Sci.* **2004**, *39*, 401–412. [CrossRef]
65. Mittal, K.L. *Silanes and Other Coupling Agents*, 4th ed.; CRC Press: Boca Raton, FL, USA, 2007; ISBN 978-9-04-742001-9.
66. Wang, D.; Goel, V.; Oleschuk, R.D.; Horton, J.H. Surface modification of poly(dimethylsiloxane) with a perfluorinated alkoxysilane for selectivity toward fluorous tagged peptides. *Langmuir* **2008**, *24*, 1080–1086. [CrossRef]
67. Sedai, B.R.; Khatiwada, B.K.; Mortazavian, H.; Blum, F.D. Development of superhydrophobicity in fluorosilane-treated diatomaceous earth polymer coatings. *Appl. Surf. Sci.* **2016**, *386*, 178–186. [CrossRef]
68. Pazokifard, S.; Mirabedini, S.M.; Esfandeh, M.; Farrokhpay, S. Fluoroalkylsilane treatment of TiO_2 nanoparticles in difference pH values: Characterization and mechanism. *Adv. Powder Technol.* **2012**, *23*, 428–436. [CrossRef]
69. Liu, J.; Wu, S.; Zou, M.; Zheng, X.; Cai, Z. Surface modification of silica and its compounding with polydimethylsiloxane matrix: Interaction of modified silica filler with PDMS. *Iran. Polym. J.* **2012**, *21*, 583–589. [CrossRef]

70. Goscianska, J.; Olejnik, A.; Nowak, I. APTES-functionalized mesoporous silica as a vehicle for antipyrine—Adsorption and release studies. *Colloids Surf. A Physicochem. Eng. Asp.* **2017**, *533*, 187–196. [CrossRef]
71. Stamm, M. Polymer Surfaces and Interfaces. In *Characterization, Modification and Applications*, 1st ed.; Springer: Berlin/Heidelberg, Germany, 2008; ISBN 978-3-540-73864-0.
72. Jakša, G.; Štefane, B.; Kovač, J. XPS and AFM characterization of aminosilanes with different numbers of bonding sites on a silicon wafer. *Surf. Interface Anal.* **2013**, *45*, 1709–1713. [CrossRef]
73. Kaynak, B.; Alpan, C.; Kratzer, M.; Ganser, C.; Teichert, C.; Kern, W. Anti-adhesive layers on stainless steel using thermally stable dipodal perfluoroalkyl silanes. *Appl. Surf. Sci.* **2017**, *416*, 824–833. [CrossRef]
74. Flink, S.; van Veggel, F.C.J.M.; Reinhoudt, D.N. Functionalization of self-assembled monolayers on glass and oxidized silicon wafers by surface reactions. *J. Phys. Org. Chem.* **2001**, *14*, 407–415. [CrossRef]
75. Lipke, M.C.; Liberman-Martin, A.L.; Tilley, T.D. Elektrophile Aktivierung von Silicium-Wasserstoff—Bindungen in katalytischen Hydrosilierungen. *Angew. Chem.* **2017**, *129*, 2298–2335. [CrossRef]

3.3 Paper 3: Investigation of adhesion properties in load coupling applications for flexible composites

Julia Beter[1,*], Bernd Schrittesser[1] and Peter Filipp Fuchs[1]

1 Polymer Competence Center Leoben GmbH, Roseggerstrasse 12, 8700 Leoben, Austria.

Published in Materials Today: Proceedings, 2020, 2214-7853.

DOI: 10.1016/j.matpr.2020.01.181

Materials Today: Proceedings xxx (xxxx) xxx

Contents lists available at ScienceDirect

Materials Today: Proceedings

journal homepage: www.elsevier.com/locate/matpr

Investigation of adhesion properties in load coupling applications for flexible composites

Julia Beter *, Bernd Schrittesser, Peter Filipp Fuchs

Polymer Competence Center Leoben GmbH, Roseggerstrasse 12, 8700 Leoben, Austria

ARTICLE INFO

Article history:
Received 28 August 2019
Received in revised form 18 December 2019
Accepted 8 January 2020
Available online xxxx

Keywords:
Flexible composite
Fiber-reinforced elastomers
Fiber bundle pull-out (FBPO) test
Fiber-matrix adhesion
Hyperelastic elastomers

ABSTRACT

The focus of this study is the investigation of the adhesion properties of hyperelastic fiber-matrix composites as well as the comparability of tests conducted at micro-, meso- and macro-scale. A modified fiber bundle pull-out (FBPO) test was performed to estimate the adhesion properties between fiber bundles and a hyperelastic matrix material with more realistic failure modes. This FBPO test setup provides the basis for a sufficient estimation of the interlaminar adhesion of fiber bundles along with the benefit of a faster, easier and more economic handling compared to single fiber pull-out (SFPO) tests. Two reinforcing fiber types (GF and PETF) and two hyperelastic matrix materials (PDMS and PUR) were analyzed in all combinations. Characteristic load-displacement curves were obtained during FBPO tests, showing debonding at the fiber-matrix interface. The maximum pull-out force of each fiber-matrix combination was determined to assess the adhesion properties of the flexible composites. The study reveals that a good comparability between different testing levels is given for all fiber-matrix combinations.

1. Introduction

The use of new material composites is necessary in order to fulfill certain requirements that cannot be achieved by using the pure components. Flexible materials such as elastomers are distinguished for their excellent damping and absorption properties, whilst their mechanical performance is highly affected by media and temperature ageing mechanisms [1]. Fiber-reinforced elastomers or so-called flexible composites represent a special new composite material class, which is employed especially to improve the mechanical properties whilst still retaining sufficient flexibility provided by the hyperelastic elastomer matrix [2]. This broadens the range of possible applications, e.g. exoskeletons for rehabilitation or military usage [3,4], in the field of medical engineering to generate artificial muscles [5,6] or shape memory benefits of self-folding structures [2,7,8] where stability must be guaranteed to provide sufficient mechanical performance in combination with sufficient flexibility. The focus is put on the ability of load transfer between the fibers and the matrix upon an external input (like mechanical trigger). Subsequently, an appropriate fiber-matrix bonding is indispensable to ensure good adhesion between the reinforcement and the surrounding matrix in order to enable efficient load transfer [9]. Good adhesion provides a reduction of stress concentrations in the interface-region as well as an improvement of the mechanical properties [2,10]. As stiffness and strength of fibers and elastomers differ significantly, the determination of mechanical values of the composites is much more difficult than it is for classical composites comprising thermosetting resins. Subsequently, the microgeometry of the fiber bundles (e.g. distribution and alignment) has to be considered. For these reasons, profound knowledge and an adequate quantitative investigation regarding the interface properties fiber-matrix bonding is necessary [11]. Most of the existing measurement devices for interface tests are limited to the single-fiber level [12–14] at micro-scale. These tests require a good measurement sensitivity along with a clearly defined load situation and an exact specimen geometry to analyze the interfacial shear strength along the filament and the matrix. The fiber bundle pull-out (FBPO) test represents a more convenient measuring device due to the faster, easier and more economic handling [9] compared to common single fiber test setups [15].

In this study, a test setup suitable for FBPO tests of aramid fiber-reinforced elastomers filled with carbon black [16] was modified to conduct FBPO tests on fiber-reinforced hyperelastic elastomers

* Corresponding author.
E-mail address: julia.beter@pccl.at (J. Beter).

https://doi.org/10.1016/j.matpr.2020.01.181
2214-7853/

without additional filler, which exhibit a significantly lower dimensional stability. The interlaminar shear strength determined by FBPO tests is influenced by the complex stress distribution inside a fiber bundle [17,18], fiber-fiber interactions [19] with complex failure modes [20] and the presence of statistically distributed filaments inside a fiber bundle [18,21]. Therefore, the determination of material parameters that describe the fiber-matrix bonding behavior is only possible when specific material models are assumed. Although a direct correlation between different testing scales is not feasible, the material behavior of component-like structures can be qualitatively estimated by using FBPO tests under the assumption of certain boundary conditions [9,11]. The aim of this research was the study of the adhesion behavior of flexible composites with hyperelastic elastomer matrix, and the correlation of the test results obtained from different test levels ranging from meso- to micro- and macro-scale. Single fiber pull-out (SFPO) test were performed for the transferability in the test chain due to different measuring scales in a relative manner. The results from FBPO tests show a good correlation with the results from single-fiber pull-out (SFPO) tests. The study reveals that the FBPO test enables an adequate quantitative estimation of the interlaminar properties between a fiber bundle and the elastomer matrix. It represents a link in the test chain between single fiber tests at micro-scale and composite tests at macro-scale.

2. Experimental

2.1. Materials

For the experiments, two reinforcing fiber types were considered. The glass fibers (GF) provided by CS Interglas AG (Erbach, Germany) are E-type fibers with the finish FK144 and the classification EC9-68x5t0, an area weight of 220 g/m^2 ± 5%, and a mean fiber diameter of about 10 μm. The polyester fibers (PETF) are supplied by Mates Italiana srl (Milan, Italy) with a 2/2 twill weave, an area weight of 200 g/m^2 ± 5%, a twine thickness of 167 tex and a mean fiber diameter of about 30 μm with an area bundle distribution of 50/50 in the 0° and 90° directions. With regard to the matrix material, two different hyperelastic elastomers, polydimethylsiloxane (PDMS) from Wacker AG, and polyurethane (PUR) from SmoothOn Inc., were considered. Both elastomers are addition-curing two-component systems. According to the technical datasheet, the PDMS has a hardness of 35 Shore A, a density of 1.02 g/cm^3 and a viscosity in uncured, mixed state of 3500 mPas with a pot life of about 90 min at 23 °C. The PUR reveals has a hardness of 50 Shore A, a density of 1.04 g/cm^3, a viscosity in uncured, mixed state of 250 mPas with a pot life of about 25 min at 23 °C. Elastomers with different mechanical properties were selected to evaluate the effect of the flexibility of the hyperelastic matrix on the pull-out behavior of the fibers. The tensile properties of the selected elastomers were previously determined in corresponding tests according to ISO 37 [22] with type 2 specimens. The elastomers were cured using the mixing ratio recommended by the suppliers and a curing time of 60 min at 70 °C in an air-circulating oven. A pre-degassing step in a vacuum chamber was implemented to avoid air bubbles formed during the stirring process.

2.2. Test setups and measurement procedures

The experimental investigation of the pull-out of single fibers at micro-scale testing was performed with the SFPO tester [13] at the BAM (Berlin, Germany). The tests were carried out with a similar loading situation compared to the FBPO test to enable a sufficient comparability. A fiber is oriented perpendicular to the surface of the matrix droplet that is placed on a specimen holder in a testing device. One end of the fiber is embedded in the droplet with a defined length. The other end of the fiber is mounted in a clamping unit and subjected to the pull-out testing. The fiber-matrix adhesion is characterized by the apparent shear strength so that the applied load is given as the function of the displacement of the fiber end. Load-displacement curves at standard atmosphere conditions (23 °C, 50% humidity) are recorded to determine the maximum force F_{max} until debonding in the fiber-matrix interface occurs, which is followed by a load-drop. The schematic test setup of the SFPO tester is given in Fig. 1(a), where the test procedure is explained in Fig. 1(b). All tests were carried out with a pull-out speed of 1 μm/s and an embedded length of about 186 μm. The maximum force of each test was indicated as the critical value for the mandatory debonding at the interface area as the supposed interfacial shear strength. For each fiber-matrix material combination, at least five tests were considered for the statistical evaluation.

Regarding the specimen preparation for the FBPO test, the elastomeric matrix has a cuboid dimension (thickness b of 8 mm, a width w of 10 mm and an embedded length l_e of 10 mm). The fiber bundle is placed in the center of the uncured matrix in stretched state. After curing for 60 min at 70 °C, the specimens were tested with a test setup modified for FBPO tests [23] using a universal testing machine (5500 Series, Instron GmbH, 100 N load cell) at standardized testing conditions. This test is a combination of the standardized testing method for pure yarn testing according to the ASTM D2256 [24] with a modified specimen holder [23]. This specimen holder is designed based on the test setup of pull-out

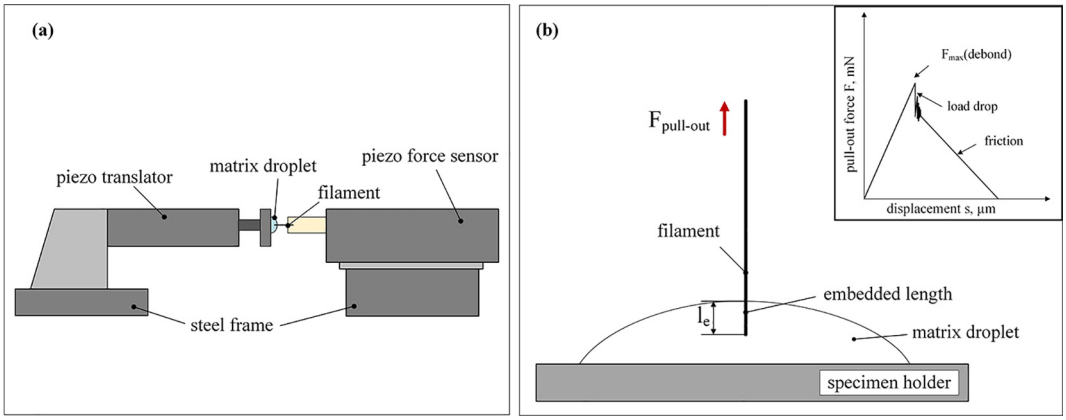

Fig. 1. Schematic test setup (a), test procedure and a force-displacement graph (b) of a single-fiber pull-out (SFPO) test [15,17].

Please cite this article as: J. Beter, B. Schrittesser and P. F. Fuchs, Investigation of adhesion properties in load coupling applications for flexible composites, Materials Today: Proceedings, https://doi.org/10.1016/j.matpr.2020.01.181

tests of aramid fibers from elastomers that were additionally reinforced with carbon black [16]. The tilting of hyperelastic elastomers (without black or white fillers) is avoided by a compression-free loading situation without any additional stress imparted by the clamping unit, which is illustrated schematically in Fig. 2(a). An exemplary load-displacement curve is given in Fig. 2(b), which shows the displacement of the embedded fiber bundle as a function of the applied load. As in the SFPO test, the load-displacement signal during the FBPO tests is measured to detect the debonding at the fiber-matrix interface that occurs at the maximum force (F_{max}). F_{max} is considered as the critical value for the comparison of the different fiber-matrix material combinations. All tests were performed at standard atmosphere conditions with a constant displacement rate $v_{pull-out}$ of 1 mm/min by using a 100 N load cell, a pre-load of 1 N and a gauge length of 50 mm. Five tests of each fiber-matrix combination were performed due to a sufficient statistical evaluation.

To prepare the specimens for the flexible composite tension tests, a vacuum resin infusion (VARI) process [26], visible in Fig. 3(a), was chosen, as it allows the economic manufacturing of high-quality composite components. For this purpose, a glass plate was selected as mold due to its smooth surface condition, and pretreated with a mold release agent (Mono-Coat 1625 W, Chem-Trend GmbH). After placing a dry fiber layer in the mold, the inlet tube (resin side) and outlet tube (vacuum pump side) were positioned in such a way to ensure an optimum impregnation quality and a good consolidation of the flexible composite. Disposable materials like the peel ply, a flow medium and a perforated foil were used. The vacuum bag represented the outer encapsulation layer of the assembly. A permeable line was installed under the vacuum bag to guarantee a linear flow front during the impregnation process in order to ensure a good manufacturing quality. The impregnation in the presence of vacuum yields additional benefits, such as (i) the existence of a compaction pressure due to the pres-

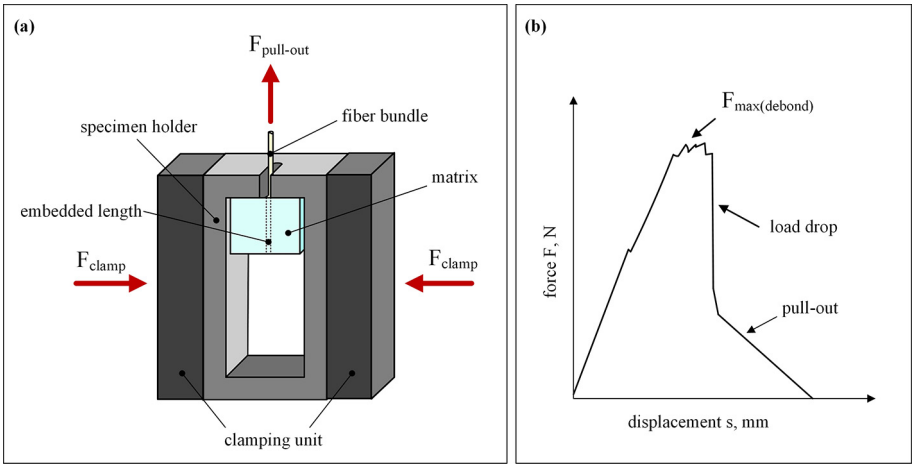

Fig. 2. Schematic test setup [23] (a) and force-displacement curve (b) of fiber-bundle pull-out (FBPO) tests [18,25].

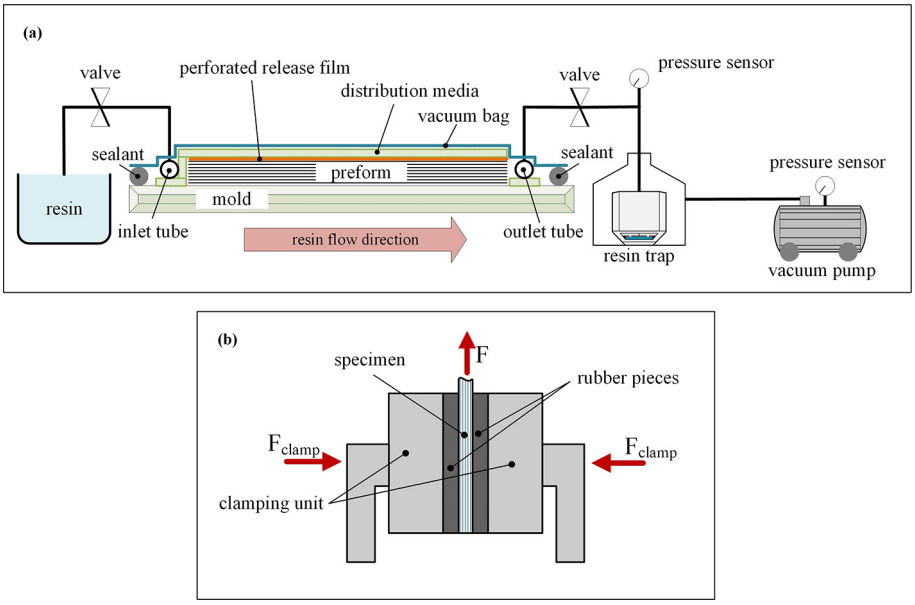

Fig. 3. Schematic build-up of the vacuum resin infusion (VARI) process [26] (a) and test setup of the composite tests [2] (b).

Please cite this article as: J. Beter, B. Schrittesser and P. F. Fuchs, Investigation of adhesion properties in load coupling applications for flexible composites, Materials Today: Proceedings, https://doi.org/10.1016/j.matpr.2020.01.181

sure gradient (difference between outer atmospheric pressure- and inner pressure), (ii) the formation of a composite sheet with homogeneous thickness, and (iii) and adequate consolidation to ensure the generation of a high-quality laminate with excellent impregnation for several fiber-matrix combinations. Basically, the elastomer matrix was mixed using a pre-degassing step in a vacuum chamber to avoid air bubbles generated upon mixing. After the completion of the infiltration process with the VARI technique, the complete assembly was sealed on both sides (inlet tube and outlet tube) to guarantee the persistence of the vacuum during the consolidation period. The impregnated composite was cured in an air-circulating oven at 70 °C for 60 min. Subsequently, the crosslinked elastomer composite sheets were demolded, and tensile testing specimens were prepared according to the testing method ISO 527-4 [27], specimen type 2. All composite samples have a fiber orientation of ±45° to the loading direction containing one fiber layer as woven reinforcement. The tests were performed with a universal testing machine (Z250, Zwick Roell GmbH & Co. KG) with a 10 kN load cell and a crosshead speed of 50 mm/min at standard atmosphere conditions. The gauge length was set to 50 mm and a measurement length of 20 mm was used. The clamping unit is displayed in Fig. 3(b). It is noted that rubber pieces were used on both sides of the specimens to aid in the clamping and to avoid slippage. As flexible composites show a higher deformation behavior during the loading process than composites based on thermosets, a higher clamping force (F_{clamp}) has to be used, which causes an additional stress concentration at the edges of the clamping device. As the samples undergo relaxation after being clamped, the stress concentration generates a notch-shaped like area causing failure of the specimens near or in the clamping units [2].

2.3. Optical observation of fracture surfaces

To enhance the characterization of the impregnation quality regarding the VARI-process for flexible composites, optical damage analysis using the scanning electron microscopy (SEM) (Tescan Vega II, Tescan Brno, s.r.o.) were performed. Regarding the optical analysis of the cross section area for each fiber-matrix material combination, a razor blade was used for the sample preparation.

2.4. Comparison between different test scales

To enable a qualitative comparison between the different test setups, a normalization step was carried out. This normalization, regarding the maximum force, was done separately for GF and PETF due to the significant differences between the two fiber types in combination with both matrices (PDMS and PUR). Reasons for this are that: (i) both fiber types have different properties such as surface quality or fiber diameter, (ii) the established comparability for testing at different measurement scales (micro-meso level) and (iii) the sensitivity of the measurements can be better visualized. Moreover, the warp- and weft yarn orientation of the textile had to be set to ±45 in terms of the loading direction. The main reasons for this are (i) to guarantee the characterization of the fiber-matrix adhesion in the interface between both perpendicular to each other aligned yarns, (ii) to ensure that no fibers are influenced by the clamps and (iii) only shearing is transmitted in the middle of the flexible composite specimen to realize a load-equivalent testing regarding the systematic simplification for the test chain in terms of the pull-out tests [28].

3. Results and discussion

To evaluate the quality of the flexible composites, the cross-section area for each fiber-matrix combination was examined with a scanning electron microscope. All SEM-pictures were selected in that way to represent the laminate quality of the entire sample and depicted in Fig. 4. The images allow only a qualitative analysis of the fiber distribution and the occurrence of defects. The SEM images reveal that a good impregnation quality and an appropriate interlaminar bonding is obtained with the GF fibers in combination with both elastomer matrix materials, PDMS (see Fig. 4(a)) and PUR (see Fig. 4(b)). The single fibers are evenly distributed in the fiber bundles after impregnation. The fibers in the fiber bundle are more compact and more closely aligned in GF-PDMS composites and in GF-PUR composites that influences a good consolidation. Especially for the GF-PDMS composite, a sufficient quality of the intralaminar impregnation is still given, although the viscosity of the used PDMS elastomer compared to the PUR is about 10 times higher [9]. Regarding PETF-reinforced elastomer composites, a low fiber content and a higher number of defects is observed in combination with PDMS (see Fig. 4(c)). A reason for this could be the insufficient adhesive bonding at the interface area due to the limited adhesion of the PMDS matrix to the PETF which is assumed to be related to the polarity differences. A partial separation between fibers and the elastomer matrix is visible. This is related to the sample preparation process, as shear force was transmitted into the sample by the used razor blade. The SEM images clearly show that a good impregnation and consolidation quality is given for GF-PUR and PETF-PUR composites, which is related to the low viscosity of the PUR, which facilitates the impregnation process.

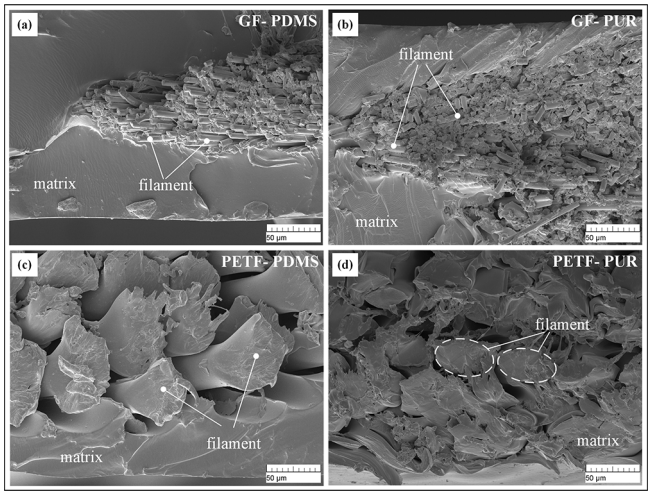

Fig. 4. SEM images of cross-section areas of flexible composite samples, GF-PDMS (a), GF-PUR (b), PETF-PDMS (c), and PETF-PUR (d).

For the investigation of the FBPO specimens and the influence of different fiber-matrix combinations on the adhesive properties, the maximum pull-out force values of each material combination are summarized in Table 1.

The results reveal that a higher maximum pull-out force is obtained with GF reinforcement for both matrix materials (PDMS and PUR). Moreover, it is visible that the GF-bundles have a slightly higher scattering compared to the PETF for both hyperelastic matrix materials. GF-PUR shows the highest pull-out force of 45.6 N, whilst a pull-out force 26.6 N is obtained with GF-PDMS. In contrast, with PETF-PDMS and PETF-PUR, a lower pull-out force is obtained (8.7 N and 21.3 N, respectively). A reason for the lower pull-out force values could be the weaker fiber-matrix adhesion with PETF. Further, the reported measurements for PETF show generally lower deviations in contrast to the results with GF. The maximum pull-out force for each different material combination is given in Fig. 5(a).

Please cite this article as: J. Beter, B. Schrittesser and P. F. Fuchs, Investigation of adhesion properties in load coupling applications for flexible composites, Materials Today: Proceedings, https://doi.org/10.1016/j.matpr.2020.01.181

Table 1
Maximum pull-out force obtained from fiber bundle pull-out (FBPO) tests of different fiber-matrix material combinations.

Fiber-Matrix	GF-PDMS	GF-PUR	PETF-PDMS	PETF-PUR
max. pull-out force F_{max}, N	26.6 ± 4.5	45.6 ± 3.8	8.7 ± 1.5	21.3 ± 1.1

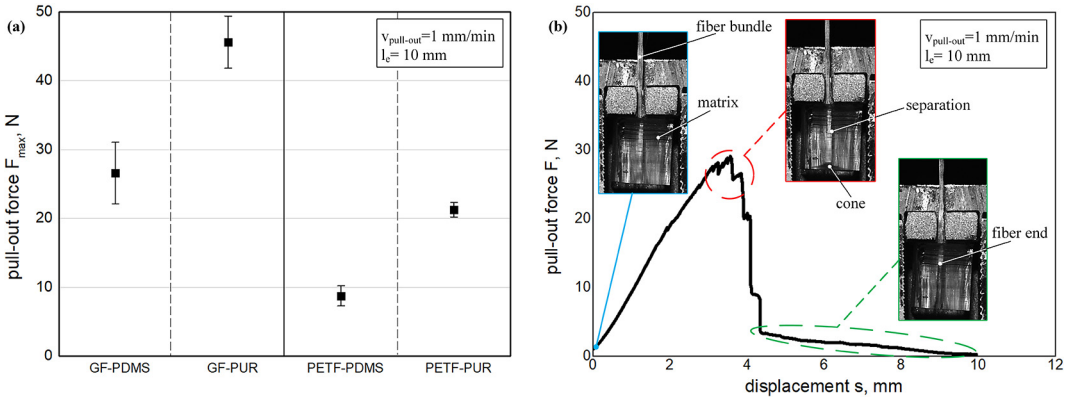

Fig. 5. Maximum pull-out force of different fiber-matrix combinations obtained from FBPO tests (a), and exemplary load-displacement curve during fiber pull-out.

Table 2
Maximum pull-out force obtained from FBPO, SPFO and composite tension tests for different fiber-matrix combinations.

Test method	SFPO test	FBPO test	Composite tension test
Fiber-Matrix	max. pull-out force F_{max}, mN	max. pull-out force F_{max}, N	max. force F_{max}, N
GF-PDMS	11.6 ± 1.4	26.6 ± 4.5	48.4 ± 2.1
GF-PUR	48.8 ± 15	45.6 ± 3.8	79.2 ± 0.9
PETF-PDMS	19.5 ± 10.5	8.7 ± 1.5	18.3 ± 1.8
PETF-PUR	65.3 ± 15.0	21.3 ± 1.1	42.8 ± 2.1

In all FBPO tests, the hyperelastic matrix is able to deform free during the entire test without any additional clamping stress imparted by the clamping unit (shown in Fig. 2(a) and Fig. 5(b)). A typical load-displacement curve obtained during the fiber pull-out process is shown in Fig. 5(b). The force increases until the maximum pull-out force F_{max} is reached, which is followed by a load drop where the debonding at the interface occurs. Finally, the detached fiber is pulled out from the matrix completely, showing a decrease of the force with increasing pull-out length until completion of the pull-out process (when the displacement becomes equal to the initial embedded length).

The maximum pull-out force of the different test methods (SFPO tests, and FBPO tests) and the force at break as the maximum force of the uniaxial tension tests performed on composites of all fiber-matrix combinations are presented in Table 2. For each measuring device, all results are reported with the average maximum force of five tests including the corresponding deviation.

The correlation for the different test setups versus the corresponding normalized maximum pull-out force $F_{max,normalized}$ of each fiber-matrix combination obtained from SFPO, FBPO and normalized maximum force of composite tension tests are shown in Fig. 6(a) and (b) for GF and PETF, respectively.

For the individual test setups, the same fiber-matrix combinations follow the same trend regarding the corresponding force $F_{max,normalized}$. The normalized results reveal that GF-PUR exhibits a higher relative maximum pull-out force $F_{max,normalized}$ compared to GF-PDMS. Similarly, PETF-PUR shows better adhesion properties and thus a higher force $F_{max,normalized}$ than PETF-PDMS. Regarding the SFPO tests, it can be seen that these measurement device shows the highest sensitivity, i.e. the highest difference between the different fiber-matrix material combinations, and thus the highest resolution, is obtained with SFPO tests. In contrast to that, a similar measurement sensitivity is obtained with both FBPO and composite tensile tests regarding the relative maximum pull-out force. The pull-out force $F_{max,normalized}$ for the GF-PUR material combination is about 1.8 times higher compared to the GF with PDMS matrix. The same trend is visible for the material combination of PETF-PUR (about 2.5 times higher force $F_{max,normalized}$) com-

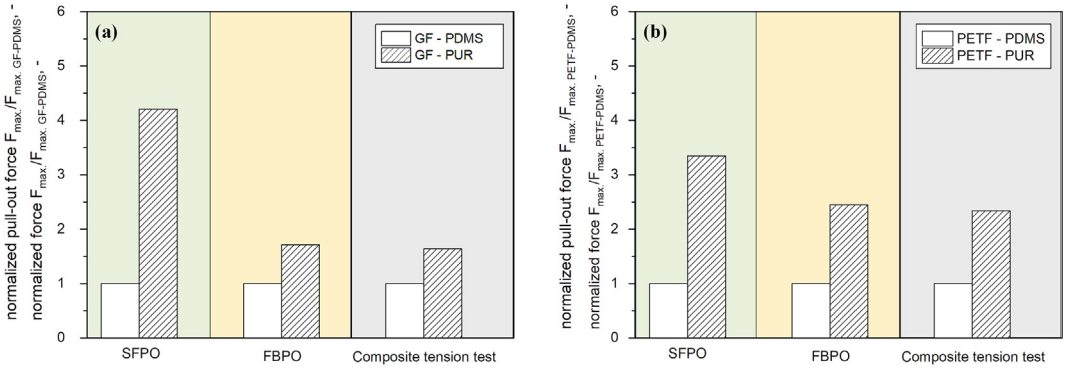

Fig. 6. Comparison of the relative maximum pull-out force obtained from SFPO, FBPO and composite tension tests of different GF-elastomer (a) and PETF-elastomer (b) combinations.

Please cite this article as: J. Beter, B. Schrittesser and P. F. Fuchs, Investigation of adhesion properties in load coupling applications for flexible composites, Materials Today: Proceedings, https://doi.org/10.1016/j.matpr.2020.01.181

pared to PETF-PDMS. In contrast to that, the measurement sensitivity of FBPO tests are similar to the composite tension tests. This can be explained by several reasons due to the more real failure modes, such as (i) interaction effects between single fibers in the fiber bundle (i.e. fiber friction), (ii) the statistical distribution of single fibers and the matrix in the fiber bundle and (iii) different shear stress distributions in dependence on the used materials upon pull-out. Hence, the FBPO test represents a link in the test chain between micro- and macro-scale tests, enabling an adequate material study regarding the adhesive performance by different fiber-matrix combinations and a preliminary estimation on flexible composite can be done.

4. Summary and conclusion

The aim of this research was to investigate the adhesion properties of flexible fiber-reinforced composites with hyperelastic matrix materials as well as the comparability between different test levels from micro- over meso- to macro-scale. The modified FBPO test setup provides the basis for an adequate estimation of the interlaminar properties between a fiber bundle and the surrounding matrix with more realistic failure modes, such as the statistical fiber distribution or fiber-fiber interactions. Additionally, a modified specimen holder was implemented, which enables to use the FBPO test method for hyperelastic elastomer matrix materials that undergo significant deformation upon fiber pull-out. Due to the differences in measurement sensitivity between the different test methods for the characterization of the fiber-matrix adhesion properties, i.e. SFPO test (micro-scale), FPBO test (meso-scale) and composite tension test (macro-scale), a relative comparison regarding the various test methods was performed in a quantitative manner.

The study clearly shows the relative comparability between the FBPO-, the SFPO- and the composite tension test although the experiments were conducted on different measurement scales. Thus, the modified FBPO test was proven to be accurate enough to enable the analysis of adhesion properties of a fiber bundle and the surrounding matrix with more realistic failure modes, whilst still enabling a fast and easy handling. It was shown that an adequate material study on fiber-matrix composites can be performed using the FBPO test, and that this testing method represents a link in the test chain between micro- and macro-scale tests.

CRediT authorship contribution statement

Julia Beter: Conceptualization, Methodology, Data curation, Writing - original draft. **Bernd Schrittesser:** Writing - review & editing, Supervision. **Peter Filipp Fuchs:** Supervision, Project administration.

Declaration of Competing Interest

The authors declare that they have no known competing financial interests or personal relationships that could have appeared to influence the work reported in this paper.

Acknowledgements

The author would like to thank Dr. Gerald Kalinka from the Federal Institute for Materials Research and Testing (BAM) in Berlin, Germany, for the support of the experimental work of this project. The research work was performed at the Polymer Competence Center Leoben GmbH (PCCL, Austria) within the framework of the COMET-program of the Federal Ministry for Transport, Innovation and Technology and Federal Ministry for Economy, Family, and Youth, with contributions by the Department of Polymer Engineering and Science (Montanuniversitaet Leoben). The PCCL is funded by the Austrian Government and the State Governments of Styria, Lower Austria, and Upper Austria.

References

[1] W. Balasooriya, B. Schrittesser, G. Pinter, T. Schwarz, Induced material degradation of elastomers in harsh environments, Polym. Test. 69 (2018) 107–115.
[2] J. Hoffmann, Characterization of fibre reinforced elastomers for shape morphing structural surfaces, Dissertation, 2012.
[3] M. Cianchetti, C. Laschi, A. Menciassi, P. Dario, Biomedical applications of soft robotics, Nat. Rev. Mater. 3 (2018) 143–153.
[4] T. Lu, Z. Shi, Q. Shi, T.J. Wang, Bioinspired bicipital muscle with fiber-constrained dielectric elastomer actuator, Extreme Mech. Lett. 6 (2016) 75–81.
[5] F. Connolly, C.J. Walsh, K. Bertoldi, Automatic design of fiber-reinforced soft actuators for trajectory matching, Proc. Natl. Acad. Sci. U.S.A. 114 (2017) 51–56.
[6] E.T. Roche, R. Wohlfarth, J.T.B. Overvelde, N.V. Vasilyev, F.A. Pigula, D.J. Mooney, et al., A bioinspired soft actuated material, Adv. Mater. Weinheim 26 (2014) 1200–1206.
[7] Q. Zhang, J. Wommer, C. O'Rourke, J. Teitelman, Y. Tang, J. Robison, et al., Origami and kirigami inspired self-folding for programming three-dimensional shape shifting of polymer sheets with light, Extreme Mech. Lett. 11 (2017) 111–120.
[8] R.V. Martinez, C.R. Fish, X. Chen, G.M. Whitesides, Elastomeric origami: programmable paper-elastomer composites as pneumatic actuators, Adv. Funct. Mater. 22 (2012) 1376–1384.
[9] M. Koschmieder, Verarbeitung und Eigenschaften von Faserverbundkunststoffen mit Elastomermatrix, Dissertation, Aachen, Germany, 2000.
[10] X. Zhang, X. Fan, C. Yan, H. Li, Y. Zhu, X. Li, et al., Interfacial microstructure and properties of carbon fiber composites modified with graphene oxide, ACS Appl. Mater. Interfaces 4 (2012) 1543–1552.
[11] G. Kalinka, B. Neumann, Bestimmung von Interface-Festigkeit oder Trennarbeit mit dem Pull-out-Versuch (2005).
[12] M. Essen, E. Sarlin, O. Tanhuanpää, M. Kakkonen, P. Laurikainen, M. Hoikkanen, et al., Automated high-throughput microbond tester for interfacial shear strength studies, The SAMPE Europe Conference, November 2017, (2017), pp. 14–16.
[13] A. Hampe, G. Kalinka, S. Meretz, E. Schulz, An advanced equipment for single-fibre pull-out test designed to monitor the fracture process, Compos. 26 (1995) 40–46.
[14] M. Kanerva, S. Korkiakoski, K. Lahtonen, J. Jokinen, E. Sarlin, S. Palola, et al., DLC-treated aramid-fibre composites: Tailoring nanoscale-coating for macroscale performance, Compos. Sci. Technol. 171 (2019) 62–69.
[15] E. Schulz, G. Kalinka, W. Auersch, Effect of transcrystallization in carbon fiber reinforced poly(p-phenylene sulfide) composites on the interfacial shear strength investigated with the single fiber pull-out test, J. Macromol. Sci. Part B 35 (2006) 527–546.
[16] S. Palola, E. Sarlin, S. Kolahgar Azari, V. Koutsos, J. Vuorinen, Microwave induced hierarchical nanostructures on aramid fibers and their influence on adhesion properties in a rubber matrix, Appl. Surf. Sci. 410 (2017) 145–153.
[17] F.J. Desarmot, Advances in pull-out testing and data analysis, Compos. Sci. Technol. 42 (1991) 151–187.
[18] Q. Viel, A. Esposito, J.-M. Saiter, C. Santulli, J. Turner, Interfacial characterization by pull-out test of bamboo fibers embedded in poly(lactic acid), Fibers (2018).
[19] G. Kalinka, A. Leistner, A. Hampe, Characterisation of the fibre/matrix interface in reinforced polymers by the push-in technique, Compos. Sci. Technol. 57 (1997) 845–851.
[20] A. Domnanovich, H. Peterlik, K. Kromp, Determination of interface parameters for carbon/carbon composites by the fibre-bundle pull-out test, Compos. Sci. Technol. 56 (1996) 1017–1029.
[21] J.-C. Zarges, C. Kaufhold, M. Feldmann, H.-P. Heim, Single fiber pull-out test of regenerated cellulose fibers in polypropylene: an energetic evaluation, Compos. Part A 105 (2018) 19–27.
[22] ISO 37, Rubber, Vulcanized or Thermoplastic – Determination of Tensile Stress-Strain Properties, International Organization of Standardization. Technical Committee ISO/TC 45, Geneva, CH, 2011.
[23] J. Beter, B. Schrittesser, B. Maroh, E. Sarlin, P.F. Fuchs, G. Pinter, Comparison and impact of different fiber debond techniques on fiber reinforced flexible composites, Polymers (2020), under review.
[24] ASTM 2256, Test Method for Tensile Properties of Yarns by the Single-Strand Method, ASTM International. D13 Committee, West Conshohocken, PA, 2015.
[25] B.F. Sørensen, H. Lilholt, Fiber pull-out test and single fiber fragmentation test – analysis and modelling, IOP Conf, Ser.: Mater. Sci. Eng. 139 (2016).
[26] M. Neitzel, P. Mitschang, U. Breuer, Handbuch Verbundwerkstoffe, first ed., Carl Hanser Verlag GmbH & Co. KG, München, 2014.
[27] Plastics, Determination of Tensile Properties, BSI British Standards. Eurpean Commitee for Standardization, London, 1997.
[28] C. Cherif, Textile Werkstoffe für den Leichtbau: Techniken – Verfahren – Materialien – Eigenschaften, Springer-Verlag, Berlin Heidelberg, Berlin, Heidelberg, 2011.

Please cite this article as: J. Beter, B. Schrittesser and P. F. Fuchs, Investigation of adhesion properties in load coupling applications for flexible composites, Materials Today: Proceedings, https://doi.org/10.1016/j.matpr.2020.01.181

3.4 Paper 4: Influence of fiber orientation and adhesion properties on tailored fiber reinforced elastomers

Julia Beter[1],*, Bernd Schrittesser[1], Gerald Meier[1], Peter Filipp Fuchs[1] and Gerald Pinter[2]

[1] Polymer Competence Center Leoben GmbH, Roseggerstrasse 12, 8700 Leoben, Austria.

[2] Department of Polymer Engineering and Science, Montanuniversitaet Leoben, Otto- Gloeckel- Strasse 2, 8700 Leoben, Austria.

Published in Applied Composite Materials, 2020, 27(3), 149-164.

DOI: 10.1007/s10443-020-09802-w

Applied Composite Materials (2020) 27:149–164
https://doi.org/10.1007/s10443-020-09802-w

Influence of Fiber Orientation and Adhesion Properties On Tailored Fiber-reinforced Elastomers

Julia Beter[1] · Bernd Schrittesser[1] · Gerald Meier[1] · Peter Filipp Fuchs[1] · Gerald Pinter[2]

Received: 28 January 2020 / Revised: 28 January 2020 / Accepted: 1 April 2020 /
Published online: 4 May 2020

Abstract
This research focuses on the investigation of endless fiber-reinforced elastomeric materials with special tailoring by different fiber orientations in the composite structure. Therefore, a modified testing device including a suitable specimen production was carried out and the comparability of tests conducted at different test scales (micro- to macro testing level) was proven. Two elastic matrix materials (silicone and polyurethane) and reinforcing fiber types (glass- and polyester fibers) were investigated in all combinations. Due to the important effect on the shear behavior during the deformation of textiles significantly influenced by the fiber orientations of the warp- and weft-yarns, a testing plan was established by using one material combination as a reference setting. Generally, the results reveal a good comparability between different testing levels for the same fiber-matrix combinations and the modified composite testing device has been proven. Furthermore, the significant influence of different fiber orientations on the shear stiffness was investigated.

Keywords Flexible composite · Fiber-reinforced elastomers · Fiber-matrix adhesion · Fiber orientation · Infusion process · Shear strength

1 Introduction

Fiber-reinforced elastomers as potential novel flexible composite materials enable interesting new applications to extend the use of common elastomers and improve the mechanical performance besides the established good damping, absorbing and flexible properties. However, these requirements are difficult to achieve with classical thermoset-based composites,

✉ Julia Beter
julia.beter@pccl.at

[1] Polymer Competence Center Leoben GmbH, Roseggerstrasse 12, 8700 Leoben, Austria

[2] Department of Polymer Engineering and Science, Montanuniversitaet Leoben, Otto Glöckeltrasse 2, 8700 Leoben, Austria

which are widely used as proven materials for lightweight applications. Nevertheless, pure elastomers are limited because of their low strength compared to other material classes and can no longer comply with the requirements in terms of the demanded bearable loads nowadays. Further their mechanical behavior is significantly influenced due to media and temperature ageing mechanisms [1]. With a specific reinforcement, the performance of elastomers as alternative matrix material can be enhanced, whilst the right choice of the elastomer type as well as the suitable combination of these elastomers with the reinforcement structure is necessary to find the best solution. The challenge for these fiber-reinforced elastomers is to combine stiff fibers with elastic matrix material to increase the mechanical properties but still retaining sufficient flexibility [2]. Due to that, the fiber-matrix adhesion at the interface plays an important role especially for load transmission and further for the load coupling [3]. This enhances the range of potential applications, like in the field of medical engineering to generate artificial muscles [4, 5], shape memory benefits of self-folding structures [2, 6, 7] or exoskeletons for rehabilitation or physical support [8, 9] where stability and long-time performance must be ensured to maintain sufficient mechanical behavior combined with enough flexibility. An appropriate fiber-matrix bonding is indispensable, since an optimized adhesion provides a reduction of stress concentrations in the interface and an improvement of the mechanical properties [2, 10]. Since the stiffness and strength of fibers versus elastomer matrices differ distinctly, the mechanical values of the composites are much more complex to determine compared to classical composites with thermoset resins. Subsequently, it is important to distinguish between the respective level of observation in the micro (single fiber), the meso (yarn) or the macro scale (textile structure), whereby appropriate transfer criteria have to be defined in order to ensure a transferability within the test chain [11]. For these reasons, in-depth knowledge and an adequate quantitative investigation with respect to the interface properties are necessary [12]. Based on this, there are several methods to study the interface properties at single fiber and fiber bundle scale [13–16]. The different methods regarding the experimental approaches are mainly applied to investigate the single fiber-matrix interactions, since the inhomogeneous composite structure are described by the locally varying material properties. Nevertheless, these single fiber tests are distinguished by a high measurement sensitivity with a well-defined loading situation and a precise specimen geometry. For the characterization of the globally varying material properties, tests based on fiber bundles [17, 18] at meso scale are more suitable, due to the faster, easier and more economic handling [3] compared to single fiber tests [19]. Additionally, fiber bundle tests show a more realistic failure mode influenced by the complex stress distribution inside a fiber bundle [20, 21], fiber-fiber interactions [22] with complex failure modes [23] and the presence of statistically distributed filaments inside a fiber bundle [21, 24]. In order to measure the anisotropic global material properties caused by the orientation of the reinforcement structure, appropriate tests on reinforced structures (textiles) are necessary [11]. The key issue is a suitable testing device that fulfill the experimental requirements of these fiber-reinforced elastomers due to their pronounced deformation ability. Typically, tabs as load transfer elements are considered for the clamping area (tab region), which usually indicate a shaft with a certain angle (tab taper angle) but are not expedient regarding the high necking and therefore lead to a release in the interface between the composite sample and the tab [11]. Moreover, the significant flexibility causes slippage out of the clamping, which requires a higher clamping pressure. Subsequently, this induces stress concentrations or fiber damage causing a pre-damage in the composite sample [2]. Further, detailed knowledge of the composite material properties for tensile-, bending- and shear strength is essential in order to investigate the maximum deformation as well as the

complex load coupling behavior due to the anisotropy and thus direction- dependent complex material properties [11]. Shearing is an important factor during the deformation of textiles and mainly influenced by the fiber orientation of the woven textile, that occurs whenever the direction of the force on the textile deviates from the direction of the fibers [25].

This work has been conducted with the purpose of designing and implementing a modified testing device, which is able to perform tests on flexible composites consisting stiff fibers with elastomer matrix. A sufficient clamping without clamping damage has to be achieved regardless of the distinct high deformation. Therefore, a test setup [2] for pure elastomers was combined with a further test method for pure (unimpregnated) textiles, to avoid the friction and fiber redirection in the clamping [26, 27]. The aim of this study is the analysis of the adhesion behavior of flexible composites with elastic matrix, and the correlation of the test results obtained from different test levels (from micro to macro-scale). However, a direct correlation between different test scales is not possible, the material performance of component-like structures can be assessed by implementing fiber bundle pull-out (FBPO) tests assuming defined boundary conditions [3, 12]. Consequently, the determination of material parameters characterizing the fiber-matrix bonding is only possible by assuming certain material models based on an adequate quantitative investigation at different test scales and further to verify potential transfer criteria within a completed test chain. Subsequently, the FPBO test setup represents a link in the test chain between single fiber pull-out (SFPO) tests at micro-scale and composite tests at macro-scale [18]. The results from composite tension tests show a good correlation with the results from SFPO- and FBPO tests. In addition to that, the effect of shearing depending on different fiber orientations and their impact on wrinkling, stress concentrations or orientation-depended inhomogeneous stretch performance was investigated in detail using the modified testing device for flexible composites. Overall, this experimental approach and the obtained material data can be implemented in constitutive models for elastic body simulations [28] and further the possibility of modelling and simulation of textile reinforcement structures based on multi-scale approaches for the determination of load couplings [11, 29].

2 Experimental

2.1 Materials

2.1.1 Fiber Materials

Two different fiber types were selected as the reinforcing structure and were available as woven fabric. The glass fibers (GF) were obtained from CS Interglas AG (Erbach, Germany) as E-type fibers with a standard industrial finish (FK144) and the classification EC9-69 × 5t0 with a twine thickness of about 68tex. The mean fiber diameter of a single filament was determined with about 10 µm and an area weight of 220 g/m² ± 5%. The polyester fibers (PETF) as second fiber type were purchased from Mates Italiana srl (Milan, Italy) with a fiber diameter of approx. 30 µm, an area weight of 200 g/m² ± 5% with a twine thickness of about 167 tex. The reinforcement is a 2/2 twill weave textile with an area bundle distribution of 50/50 in the 0° and 90° fiber direction. To investigate the mechanical properties of both reinforcement types, tensile tests according to ASTM D2256 were performed with a universal testing machine (5500 Series, Instron) using a 1

kN load cell, a crosshead speed of 300 mm/min with a gauge length of 250 mm including a pneumatically controlled mandrel-shaped clamping system to fix the fibers.

2.1.2 Matrix Materials

For the matrix material two different cast elastomers with different mechanical properties were considered to study the effect of the elastic materials on the pull-out behavior of the fibers as well as the deformation characteristics on composite built-ups. Polydimethylsiloxan (PDMS), supplied by Wacker AG, was chosen due to its siloxane moieties and the resulting chemical adhesion properties, especially in combination with glass fibers. The PDMS has a hardness of 35 Shore A with a density of 1.02 g/cm³ and a viscosity (uncured, mixed state) of 3500 mPas with a pot lifetime of approx. 90 min at room temperature. Furthermore, cast polyurethane (PUR) provided from SmoothOn Inc. was considered due to its high resilience, good damping performance and high mechanical strength. According to the technical datasheet, PUR reveals a hardness of 50 Shore A with a density of 1.04 g/cm³ and a viscosity (uncured, mixed state) of 250 mPas with a corresponding pot lifetime of about 25 min at room temperature. For both elastomeric matrix materials, the single components were stirred according to the manufacturer's specifications with the suggested mixing ratio, where an intermediate pre-degassing vacuum step was implemented to avoid air bubbles. The elastomers were cured in an air-circulating oven at 70 °C for 60 min recommended by the supplier. The mechanical properties of the pure elastomers were determined in corresponding uniaxial tensile tests according to ISO 37 [30] with type 2 specimens. For the tests, a universal testing machine (Z010, Zwick Roell GmbH & Co. KG) was chosen with a 500 N load cell and a crosshead speed of 10 mm/min. The gauge length was set to 50 mm including a pneumatically controlled clamping unit and a measuring length of 20 mm. Due to the high elasticity of the matrix material, the local strain ratio was measured with an optical camera system (Prosilica GT 6600, Allied Vision Technologies GmbH) and a spray pattern was applied on the specimen surface.

2.2 Sample Preparation

In this study, the vacuum assisted resin infusion (VARI) process [25] was chosen for manufacturing the elastomeric composite specimens, due to the economical production at low costs and high-quality of the composite parts (see Fig. 1a). This process consists of one-sided rigid mold and a vacuum bag, which represents the flexible upper mold half. For this purpose, a glass plate was selected for the lower mold half due to its smooth surface properties. The mold release agent (Mono-Coat 1625W) was provided by Chem-Trend GmbH. According to the placing order of the lay-up as well as the fiber orientation of the woven textile, the required dry fabrics for both reinforcing structures were cut with a cutter (G3 M-1600, Zünd Systemtechnik AG). Further, the inlet tube (resin side) and outlet tube (vacuum pump side) were positioned regarding to the composite parts as well as size of the manufacturing process to ensure an optimum inter- and intralaminar impregnation and a sufficient consolidation since the maximum pressure difference is limited with ≤ 1 bar [25]. The high viscosity of the uncured elastomeric matrix caused several challenges like (i) the necessary implemention of a suitable flow medium, (ii) reduced impregnation speed, which is additionally infected by the pressure gradient and described in the law of D'Arcy in one-dimensional form [25] as well as (iii) incomplete cavity filling and higher risk of porosity. Besides the used disposable materials like the peel ply, the flow medium and the perforated foil, the vacuum bag was the outer

encapsulation layer of the complete assembly. Additionally, a permeable line was inserted right next to the tubes under the vacuum bag to ensure a fast distribution and a linear flow front during the impregnation process. The impregnation in the presence of vacuum had additional benefits, such as (i) the homogeneous thickness of a composite sheet, (ii) the presence of a compaction pressure due to the pressure difference (difference between outer atmospheric pressure- and inner pressure), and (iii) a sufficient consolidation to ensure a high-quality laminate with good impregnation for several fiber-matrix combinations. The matrix material was produced according to the recommended specifications by the supplier with an included degassing as intermediate step before infiltration. In the next step, both tube ends (inlet and outlet) had to be completely clamped in order to ensure a permanent vacuum for the impregnated lay-up during the consolidation period and further for the curing. The impregnated composite was cured in an air-circulating oven at 70 °C for 60 min like for the pure elastomer matrix. The crosslinked elastomeric composite plates were demolded carefully due to its distinct flexibility and samples similar to type 2 specimen geometry were prepared for uniaxial tensile tests according to the testing method in ISO 527-4 [31]. All specimens had a width to length ratio of w:l = 1:3 (see Fig. 1b) in the testing area (without considering the clamping area of the sample) to guarantee experiments, where the data recording of the measurement area was unaffected by clamped fibers [11, 29].

2.3 Test Setups and Measurement Procedures

Due to the pronounced flexible behavior of these special composite materials, clamping entails new complexities such as (i) significant necking at the clamping area so that tabs are useless, (ii) higher risk of the specimen slipping out ("clamp slippage"), thus the clamping force has to be increased, and (iii) subsequently, the local stress concentration in the clamping unit increased which could lead to a fiber damage [11]. Besides the choice of the clamping type and –force, the clamping surface as well as its used material for the pads are important, since particularly corrugated or rough profiles are common even though smooth profiles are rarely used [11]. Therefore, a specimen holder [2] originally designed for pure elastic materials was modified for the use on endless fiber-reinforced elastomers to fulfill these critical points and additional rubber pieces were considered (see Fig. 2a). Besides the slipping prevention, the purpose of these rubber pieces is to reduce the occurring local compression stresses especially at the edges, which are schematically explained in Fig. 2b. The main reason for this is the sudden transition in the material between clamping and testing area, where the composite

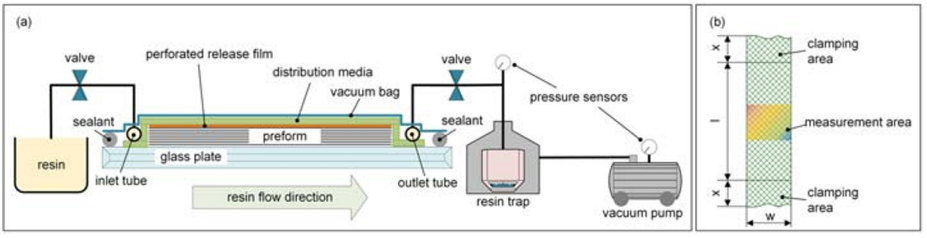

Fig. 1 Schematic build-up of the vacuum resin infusion (VARI) process [25] (**a**) and the specimen of a composite tensile test (**b**)

specimens undergo relaxation after being clamped and the stress concentration generates a “notch-shaped like area” causing failure near or in the clamping due to the occurred multi-axial stresses in the edges.

The composite tension tests were performed according to the testing method ISO 527-4 [31] with the universal testing machine (Z250, Zwick Roell GmbH & Co. KG) with a 10 kN load cell and a constant crosshead speed of 50 mm/min at standard atmosphere conditions. The gauge length l was set to 90 mm and a measurement length l_m of 30 mm was used. Due to strong deformations and the use of elastomer matrices, the strain measurement was carried out contactless by the ident optical image correlation system used for the pure matrix tests, whereby a fine spray pattern was applied on the specimen surface. The presented test setup for flexible composites was already implemented in previous research, whereby the transferability between experiments with single fibers (micro scale) and tests with composite parts (macro scale) was investigated [18]. Hence, an intermediate step at meso scale was inserted for fiber bundle tests, because this represents the smallest unit in a woven textile for composites but with a more realistic testing performance (like fiber friction or statistic fiber-matrix distribution) than single fiber tests [2, 18]. To confirm this assumption, the same fiber types and matrix materials were selected for all test methods to achieve an accurate comparability and minimized negative batch influence. For the investigation of fiber-matrix adhesion properties in flexible composites at different test scales, suitable transfer criteria for a proper comparability were considered and therefore composite specimens with ± 45° textile orientation were chosen for the composite tension tests respectively (see Fig. 2c). Based on this knowledge, it was possible to determine the fiber-matrix adhesion properties, because the fibers in the measurement area were not affected by the clamps and only influenced by ondulations at the weave points and adhesive bonding with the matrix [11, 27].

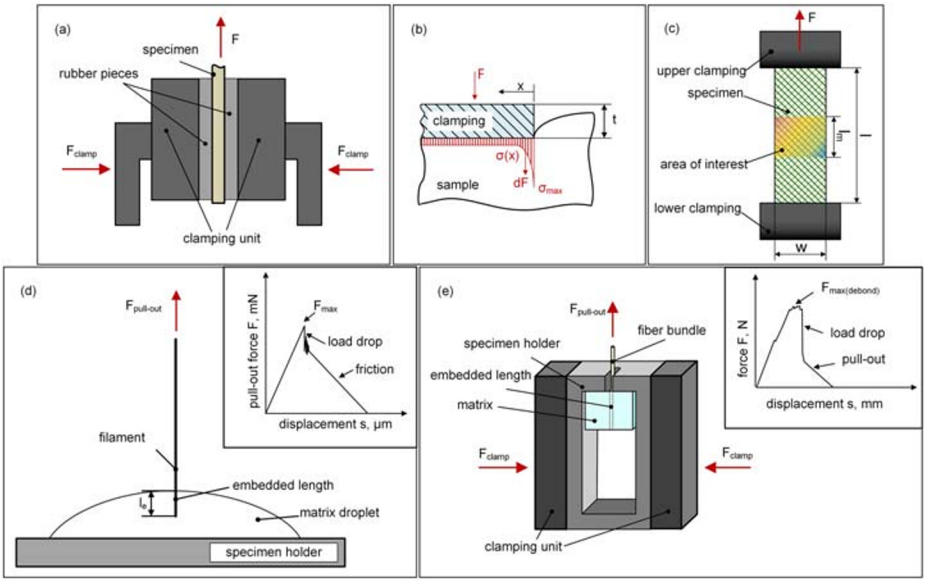

Fig. 2 Schematic illustration of composite clamping [18] (**a**), with the stress concentration situation [2] (**b**), and composite tension test setup (**c**) with the according test method for SFPO test [32] (**d**), and FBPO test [18] (**e**)

The testing at micro scale was performed with the SFPO test [32] at the BAM (Berlin, Germany) due to the similar loading situation (fiber loaded system) [22] compared to the FBPO test [18] to ensure an accurate comparability. Generally, the method based on a fixed single fiber, which is perpendicular aligned to a matrix droplet, where one fiber-end is embedded with a specific length in the matrix droplet and the other fiber-end is mounted in a clamping unit (see Fig. 2d). During the pull-out procedure, the fiber-matrix adhesion is analyzed by the apparent shear stress and the load-displacement signal is recorded. The actual load value is a function of the displacement of the defined fiber-end, whilst the debonding in the interface between fiber and matrix is determined as the maximum occurred force value F_{max} and clearly indicated by a significant load drop [18, 32]. The tests were performed with an embedded length l_e of about 186 μm, a pull-out speed $v_{pull-out}$ of 1 μm/s at standard atmosphere conditions. The intermediate step for the FBPO tests at meso scale was achieved with a specially modified test setup. This FBPO test setup provides the basis for a sufficient estimation of the interlaminar adhesion of fiber bundles along with the benefit of a faster, easier and more economic handling compared to the SFPO test [2, 18]. The elastomer matrix material had a cuboid dimension (thickness b of 8 mm, width w of 10 mm, embedded length l_e with 10 mm). Regarding the specimen preparation, the fiber bundle was placed straight in the center of the uncured matrix and after the curing (60 min at 70 °C) in an air-circulating oven, the specimens were tested with the modified test setup [18] and inserted in a universal testing machine (5500 Series, Instron GmbH). The experiments were carried out with a 100 N load cell, a constant speed of $v_{pull-out}$ of 1 mm/min and with a gauge length of 50 mm including a defined pre-load of 1 N to minimize the effect of fiber stretch and ensuring that all tests were done at the same initial conditions. According to the tilting, which is a critical issue for elastic materials, a compression-free loading situation without any additional stresses imparted by the clamping unit is important and has to be avoided. This is illustrated schematically in Fig. 2e. Due to that, a special modified specimen holder [18] had to be designed based on the test setup of a pull-out test for aramid fibers with elastomers that were additionally reinforced with carbon black [17]. Regarding the measurement method, this test is a combination of the standardized testing method for pure yarn testing according to ASTM D2256 [33] with a modified specimen holder [18] and is exemplary shown in Fig. 2e. The adhesion between the fiber bundle and surrounding matrix in the interface area was investigated by measuring the load-displacement signal during the pull-out, while the maximum occurred load value F_{max} was defined for the fiber-matrix debonding. Regarding the data evaluation, the displacement of the embedded fiber bundle was monitored as function of the applied load. Due to comparison of the different fiber-matrix material combinations, F_{max} was considered as the critical value for FBPO as well as for SFPO tests. All further settings and detailed investigations for this SFPO test as well as for the FBPO test were described and analyzed in previous research focusing on the fiber-matrix adhesion properties in flexible composites [18]. In general, for all different presented testing methods, five reproducible tests were performed for each individual setting of the test plan at standard testing conditions to achieve sufficient data for the statistical evaluation.

2.4 Effect of Fiber Orientation On Shear

Shearing is an important factor during the deformation of textiles and mainly influenced by the fiber orientation of the woven textile occurring whenever the direction of the force on the textile deviates from the direction of the fibers. According to the set width to

length ratio of the specimens, three main zones are defined in the textile due to an applied tension loading, which undergo different deformations and are schematically illustrated in Fig. 3a and b. The area of zone A obtains no deformation due to the clamping. Whilst zone B has partly fixed and free fiber areas and thus constitutes a mixed form of shear elongation. However, the area of interest is represented by zone C, since the fibers (warp- and weft yarns) are no longer influenced by the clamping and only fixed by adhesion to the surrounding matrix and their insertion into the textile (such as ondulations or stitching). Thus, this area was defined as stress free and only shear is present. For the evaluation of the influence on different fiber orientations in an elastomeric fiber-reinforced composite and their impact on the mechanical properties [11], one material combination was employed representatively, which is represented by the GF with PDMS matrix. Different tailored reinforced composites were investigated by a methodically validated test plan to study the stress-strain behavior, which is influenced by different orientations of the reinforcement structures and their changing fiber angles related to the loading direction [11]. Based on this, the test plan was defined with four different settings (0°/90°, 15°/75°, 30°/60° and ±45°) in total. In general, this test method leads to strong boundary effects in the clamping, since the transverse contraction of the textile is inhibited and therefore only the intermediate region (zone C) was observed in the tests. Based on this, composite specimens containing one fiber layer as woven reinforcement were considered as representative smallest lay-up design.

2.5 Optical Observation of Impregnation Quality

2Due to the high viscosity of elastomers and to improve the impregnation quality in terms of the VARI-process for fiber reinforced elastomers as well as for the FBPO test, optical damage analysis using the scanning electron microscopy (SEM) (Tescan Vega II, Tescan Brno, s.r.o.) were performed. For the specimen preparation, a razor blade was used for the visual inspection of the cross-sectional area of all fiber-matrix material combinations.

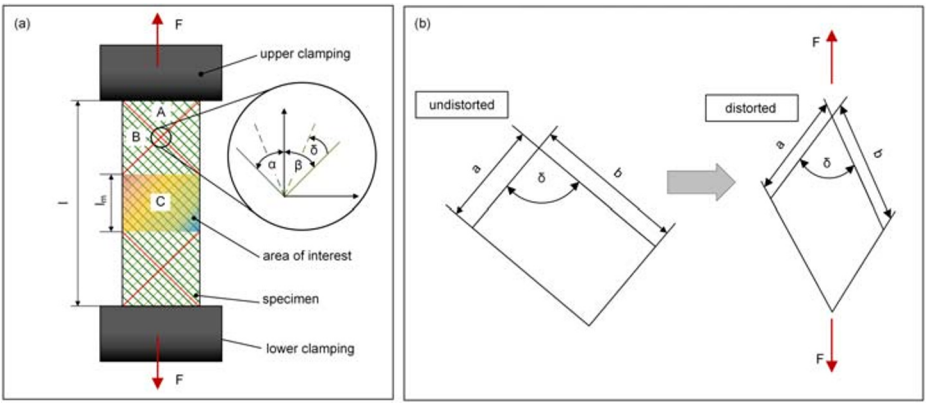

Fig. 3 Schematic illustration of the three main shear zones (A,B,C) according to the fiber orientation in a composite tension test [11] (**a**) with the graphical explanation of the effect on shearing due to undistorted and distorted [26] (**b**)

3 Results and Discussion

3.1 Fiber and Matrix Material

For the investigation of the tensile behavior of both different reinforcement fiber types, the results for GF as well as PETF are compared in a force-strain graph (see Fig. 4a). Further, the reported values for breaking force, tensile strength and elongation at break are given, whilst the average values with an accuracy of ± 2% are represented. The results show, that the experimentally determined tensile strength for GF bundles is significantly higher with a lower elongation at break of approximately 2.3% compared to the PETF that reveals an elongation at break of about 15.2%. As expected, both reinforcing materials differ in their shape of the curve: GF shows the typical linear deformation behavior, whereas a pronounced non-linear deformation of the PETF can be observed. This can be related to the differences in the chemical structure of the inorganic glass material compared to the PETF, which shows a typical behavior like thermoplastic material. The results of the uniaxial tension tests on the pure elastic matrix material are plotted in the technical stress-strain graph (see Fig. 4b) and confirm that the PDMS has a slightly higher elongation at break with about 108.5% compared to the PUR with about 100.2%. It is shown, that PDMS has significantly higher stress at break of about 5.0 MPa whereat PUR reveals approximately 1.6 MPa. This may be due to the difference in the morphology of both materials that influences the structure-property relationship regarding the cross-linking density and chemical structure (more mobility). Generally, both materials differ in their shape of the stress-strain curve, whilst PUR has a steeper modulus at the beginning and with increased elongation a nearly linear behavior until the specimen fails. In contrast to that, PDMS reveals a lower increase first, whereas the slope rises significantly towards a higher deformation and leads into complete failure with a comparatively exponential behavior, which can be explained by the increased mobility and reorientation of the polymer chains in loading direction [34]. It should be noted, that the deviation for all measurements of the PDMS material tends to a higher deviation observed for the stress at break value with approximately ± 1 MPa (PUR with about ± 0.1 MPa) as well as the strain at break value with approximately ± 8% compared to PUR with about ± 2%.

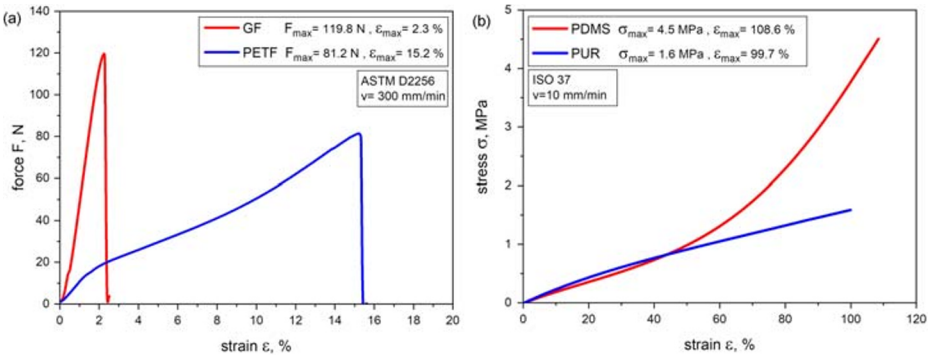

Fig. 4 Force-strain curves of GF and PETF-bundles (**a**) and stress-strain curves of PDMS and PUR (**b**) obtained from tensile tests

3.2 Impregnation Quality

To ensure a complete impregnation of the fiber bundle, SEM images were taken from the cross-section area. Regarding the microscopic analysis, the single filaments within one fiber bundle-matrix specimen were unevenly distributed with an irregular cross-section area for both reinforcing materials. Representatively, the graphical comparison between the encapsulated GF in a PDMS matrix is given in Fig. 5a, where the SEM-picture illustrates the overview of the cross-section area with a good impregnation quality. It can be observed, that a partial separation had been occurred between some fibers and the matrix. This can be explained due to the sample preparation since shear forces were transmitted by the used razor blade. For the quality of the flexible composites, the SEM-pictures for each fiber-matrix combination constitute the laminate quality of the entire sample (crosssection area), hence GF with PDMS and PUR matrix were representatively chosen and depicted in Fig. 5c and d. The images allow only a qualitative analysis of the fiber distribution and the occurrence of defects. Generally, GF with both elastomeric matrices reveals a good interlaminar bonding and a sufficient impregnation quality was proven. According to that, the single fibers are compact aligned, which correlates with a good consolidation. Moreover, the material combination GF with PDMS matrix leads to an adequate impregnation despite the high viscosity of the PDMS, which is significantly higher compared to the PUR. All further material combinations like PETF with PDMS or PUR matrix were already investigated in detail in previous research [18].

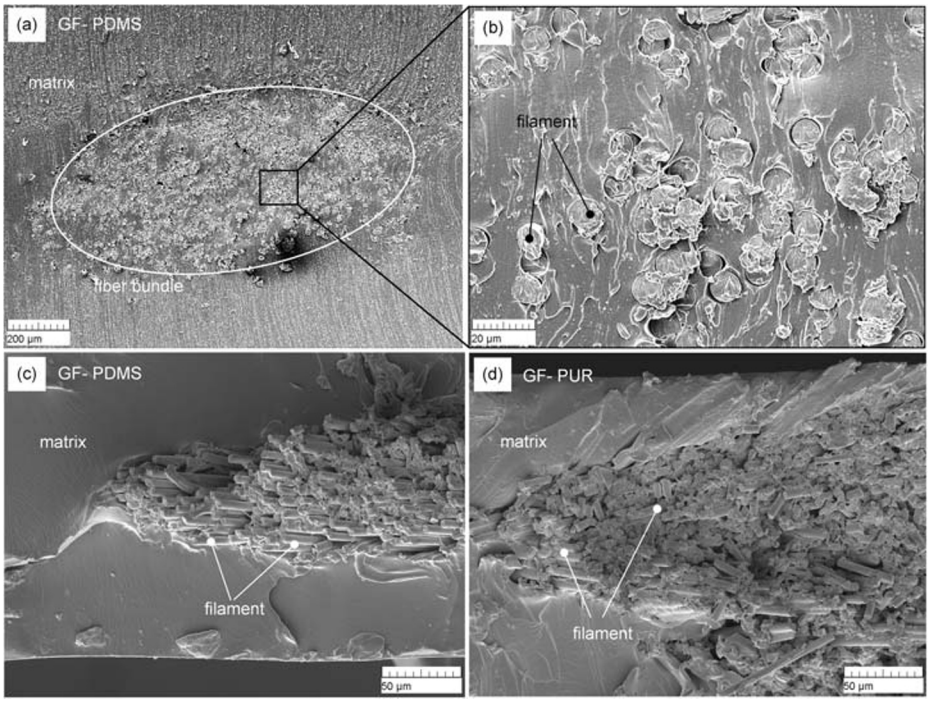

Fig. 5 SEM images of cross-section areas of FBPO sample (GF-PDMS) respectively (**a,b**), and composite sample of GF-PDMS (**c**), and GF-PUR (**d**)

3.3 Fiber-reinforced Elastomeric Composite Tension Test

Regarding the presented uniaxial tension tests on fiber-reinforced elastomeric composites, the maximum force F_{max} was obtained in a stress- strain graph for each different fiber-matrix material combination and is visually compared in a corresponding graph (see Fig. 6a). It is visible, that a higher F_{max} can be achieved with the material combination GF for both elastomeric matrix materials (PDMS and PUR). A reason for this can be the significant higher stiffness of GF compared to PETF. Moreover, it can be observed that GF with PUR matrix shows the highest force of approximately 79.2 N, whilst the F_{max} of about 48.4 N is obtained with GF-PDMS. This can be explained due to the higher stiffness of PUR as well as the different chemical crosslinking kinetics between both elastomer matrices. Regarding the FBPO tests for the same fiber-matrix material combination, the results reveal that GF is supposed to have the highest maximum pull-out force for both elastomer matrix materials. Furthermore, the material combination GF-PUR reveals the highest pull-out force of about 45.6 N compared to the pull-out force of about 26.6 N for GF-PDMS. In contrast to that, a significant lower maximum pull-out force is depicted for the material combinations PETF-PDMS with about 8.7 N and PETF-PUR with approximately 21.3 N. A possible explanation for this lower pull-out force values could be the weaker fiber-matrix adhesion with PETF. In addition, all recorded measurement data for PETF bundles reveal lower deviations compared to the results with GF bundles for both elastomer matrices (PDMS and PUR), which are shown in Fig. 6b. The typical load-displacement graph of a fiber bundle pull-out test regarding the distinctive values like load drop, maximum bearable force or interface debonding was proven in previous researches focusing on the fiber-matrix adhesion properties according to the pull-out behavior on stiff fiber bundles with elastic matrix materials [18].

Due to the expected identical trend of the maximum force values for the same fiber-matrix material combinations and to enable a qualitative correlation between the different test setups at different test levels (from micro to macro scale), a normalization step regarding the maximum force for SFPO-, FBPO- and composite tension test were carried out. This implemented normalization, in terms of the maximum force, was tested separately for GF and PETF due to the significant differences between the two fiber types in combination with both matrices (PDMS and PUR) [18]. Reasons for this are: (i) more suitable visualization of the measurement sensitivity, (ii) different properties like surface quality or fiber diameter for both fiber types and (iii) the established comparability for experiments at different test scales (micro-meso level). The comparison for the corresponding normalized maximum pull-out force and normalized maximum force of each fiber-matrix combination versus the different test setups was obtained from SFPO-, FBPO- and composite tension tests, which is illustrated in Fig. 6c for GF and d for PETF, respectively [18].

In terms of the individual test setups, the transferability between experiments with single fibers (at micro scale) and tests with composite parts (at macro scale) had been investigated and proven in detail in previous researches, whereby the same fiber-matrix combinations follow the same trend regarding the corresponding force $F_{max,normalized\ pull-out}$ for SFPO and FBPO as well as $F_{max,normalized}$ for composite tests [18]. Overall, the normalized results for all test setups reveal that the material combination GF-PUR leads to a higher relative maximum force and thus better adhesion properties than GF with PDMS matrix. Moreover, PETF with PDMS exhibits a reduced normalized force in contrast to PETF-PUR that indicates a better adhesion at the fiber-matrix interface. Based on this, the SFPO test leads to a similar trend for all material combinations but additionally obtains the highest sensitivity of the presented test

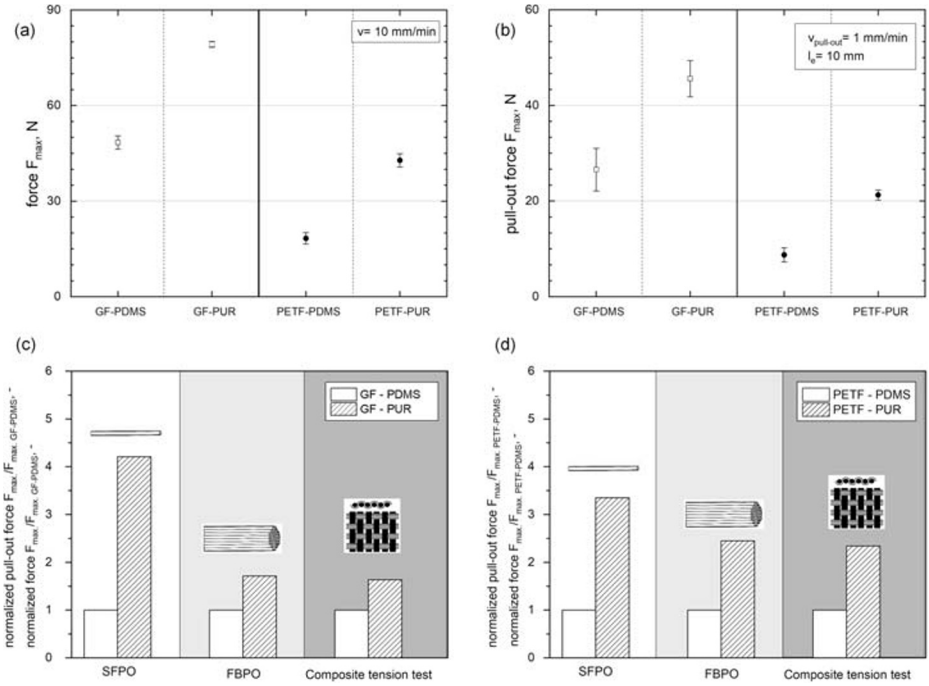

Fig. 6 Comparison of different fiber-matrix combinations obtained from composite tension tests (**a**) and FBPO tests [18] (**b**), and comparison of the relative maximum pull-out force obtained from SFPO, FBPO and composite tension tests for GF (**c**) and PETF (**d**) with both elastomer matrices [18]

methods, which can be depicted with the biggest difference between the certain material combinations. This effect can be explained because the SFPO test performs at micro level and thus the test setup as well as the associated possible influencing factors at model level can be reduced to a minimum. In contrast to that, the relative maximum force for the FBPO and composite tension test show similar measurement sensitivity, hence the relative maximum force for GF with PUR matrix is approximately 1.8 times higher versus GF-PDMS. Further, this trend can be obtained for both material combinations of PETF-PUR compared with PETF-PMDS, where the difference in the relative maximum force is about 2.5 times. It is evident, that the measurement sensitivity between the FBPO test and the composite tension test is similar, which was studied in detail in previous investigations on these various test methods at different testing scales [18]. That can be explained by several reasons due to the more real failure modes, such as (i) the statistical distribution of single fibers and the matrix in the fiber bundle, (ii) different shear stress distributions in dependence on the used materials upon tension loading and (iii) interaction effects between single fibers in the fiber bundle (i.e. fiber friction). Therefore, the transferability between micro to macro test scale in a test chain was observed, where a preliminary estimation on the mechanical performance for different fiber-matrix material combinations could be achieved. This enables a tailored material study regarding the adhesive performance on flexible composite parts [18].

In addition, the maximum pull-out force of the test methods SFPO- and FBPO tests as well as the maximum force of the uniaxial tension test (performed on composites) for all fiber-matrix combinations are listed in Table 1. In terms of each testing method, the results are reported with the average maximum force of five tests including the corresponding deviation.

3.4 Effect of Different Fiber Orientations On Shearing

As an overview, the results of the composite tension tests have been summarized in Table 2 to study the shear deformation and the influence of different orientations for warp- and weft yarn on the mechanical properties.

For the influence of different fiber orientations on the mechanical performance and thus on the shearing, the results for GF with PDMS matrix are compared in a stress-strain graph (see Fig. 7) respectively.

Generally the results reveal, that with a decreasing fiber angle from ± 45° to 0°/90° the bearable strain at break and the according stress at break is significantly lower. Due to the expected behavior, the ± 45° fiber orientated composite reveals more matrix dominated performance compared to the configuration of 0°/90° composite (fiber dominated) [35]. Furthermore, it is visible that the stiffness increases especially at small strain ratios (from 0% up to approximately 10%). Hence, the configuration (besides the 0°/90°orientation) with ± 45° fiber orientation leads to the highest stress at break of about 30 MPa with a strain at break of about 40%. Compared to this, the configuration with 15°/75° fiber orientation exhibits a significant lower stress at break with about 12 MPa and about 10% strain at break that can be depicted in Fig. 7. A reason for this might be clamped fibers from lower and upper clamp. This can be explained by several reasons due to effect of shearing during the deformation, which is mainly influenced by the fiber orientation of textiles [11]. Depending on how strongly the orientation of the fibers deviates from the loading direction, shearing becomes more and more dominant [26]. These can be induced because (i) warp and weft threads (with a certain angle to each other at the beginning) start to shift, which goes on until the fibers converge with the direction of force, or become deformed and compressed until they obstruct each other. Subsequently, (ii) the shear force starts to increase significantly since the displacement of the fibers relative to each other reach a maximum angle known as the "locking angle" [11, 26]. As a result, (iii) no further in-plane deformation is possible, which leads to wrinkling (deformation perpendicular to the textile plane) or fiber break [11]. This shearing process is commonly termed as the "trellis effect" [11, 26]. Moreover, this critical point is additionally affected by the friction conditions between warp- and weft yarns as well as the pre-tension of the textile in the direction of the fibers [26]. Another possible influence can be for example the use of elastomers as matrix material instead of a traditional thermoset like epoxide resin. Based on this, more experiments by varying the free clamping distance or different ratios of the specimen geometry as well as multi-layer built-ups to study the influence of the fiber volume content should be carried out in further investigations for an optimization with a detailed investigation on the performance of fiber-reinforced composites with elastomeric matrix

Table 1 Maximum pull-out force obtained from SPFO, FBPO and composite tension tests for different fiber-matrix combinations [18]

Material combination		GF-PDMS	GF-PUR	PETF-PDMS	PETF-PUR
SFPO test	max. pull-out force $F_{max,pull-out}$ mN	11.6 ± 1.4	48.8 ± 15	19.5 ± 10.5	65.3 ± 15.0
FBPO test	max. pull-out force $F_{max,pull-out}$ N	26.6 ± 4.5	45.6 ± 3.8	8.7 ± 1.5	21.3 ± 1.1
Composite tension test	max. force F_{max} N	48.4 ± 2.1	79.2 ± 0.9	18.3 ± 1.8	42.8 ± 2.1

Table 2 Maximum stresses obtained from composite tension tests for different warp- and weft yarn orientations

Orientation	0°/90°	15°/75°	30°/60°	±45°
stress σ_{max} MPa	63.79 ± 0.9	9.82 ± 0.2	19.50 ± 2.8	34.30 ± 2.9

materials. Moreover, the cause and mechanism of the "trellis effect" will be studied in further scheduled research to identify and influence shear deformation in a specific manner.

4 Summary and Conclusion

The aim of this study is the validation of a modified testing device for fiber-reinforced elastomers with elastic matrices as well as the analysis of the fiber-matrix adhesion in flexible composites and further the influence of different fiber orientations on the mechanical properties. Therefore, a modified testing device was designed, which enables the characterization of endless fiber-reinforced elastomers that undergo significant deformations compared to classical thermoset-based composites without clamp slippage or clamp induced stress concentrations. Based on this, suitable transfer criteria for the comparability of tests conducted at different test scales (micro- to macro testing level) were established. According to the different measurement sensitivities between the individual test methods in terms of the investigation of the fiber-matrix adhesion, such as SFPO test (micro-scale), FPBO test (meso-scale) and composite tension test (macro-scale), a relative comparison for the various test methods was carried out quantitatively. In addition, the significant influence of specific deviating fiber orientations versus the shear strength were analyzed by a designed test plan. The results obtained, that the accuracy of the modified composite testing device is given and the relative comparability

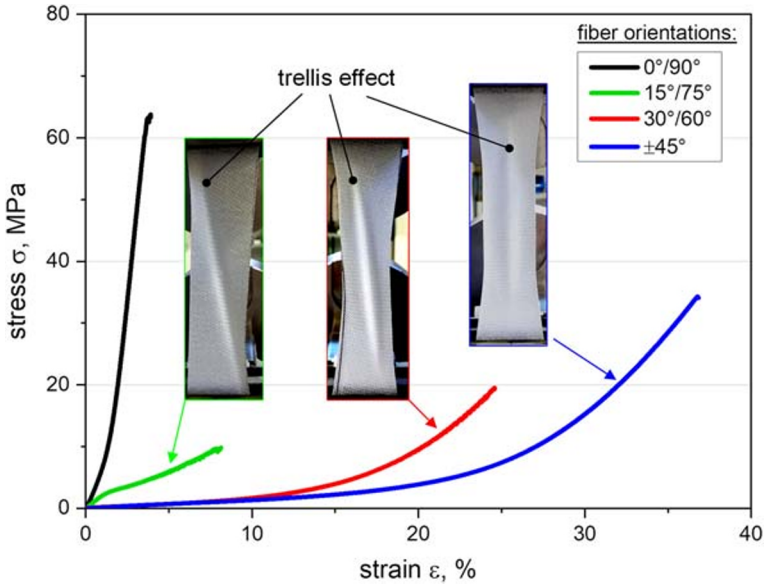

Fig. 7 Comparison of the different warp- and weft yarn orientations for the GF-PDMS composite obtained from stress- strain curves of composite tension tests

between different measurement scales regarding the fiber-matrix adhesion could be proven. Furthermore, the significant influence of different fiber orientations on the shear stiffness was demonstrated.

Acknowledgements The author would like to thank Dr. Gerald Kalinka from the Federal Institute for Materials Research and Testing (BAM) in Berlin, Germany, for the support of the experimental work of this project. The research work was performed at the Polymer Competence Center Leoben GmbH (PCCL, Austria) within the framework of the COMET-program of the Federal Ministry for Transport, Innovation and Technology and Federal Ministry for Economy, Family, and Youth, with contributions by the Department of Polymer Engineering and Science (Montanuniversitaet Leoben). The PCCL is funded by the Austrian Government and the State Governments of Styria, Lower Austria, and Upper Austria.

References

1. Balasooriya, W., Schrittesser, B., Pinter, G., Schwarz, T.: Induced material degradation of elastomers in harsh environments. Polym. Test. **69**, 107–115 (2018). https://doi.org/10.1016/j.polymertesting.2018.05.016
2. Hoffmann, J.: Characterization of fibre reinforced elastomers for shape morphing structural surfaces. Dissertation, Technical University of Munich (2012)
3. Koschmieder, M.: Verarbeitung und Eigenschaften von Faserverbundkunststoffen mit Elastomermatrix. Dissertation, Rheinisch-Westfälischen Technischen Hochschule Aachen: (2000)
4. Connolly, F., Walsh, C.J., Bertoldi, K.: Automatic design of fiber-reinforced soft actuators for trajectory matching. Proc. Natl. Acad. Sci. U.S.A. **114**, 51–56 (2017). https://doi.org/10.1073/pnas.1615140114
5. Roche, E.T., Wohlfarth, R., Overvelde, J.T.B., Vasilyev, N.V., et al.: A bioinspired soft actuated material. Adv. Mater. Weinheim **26**, 1200–1206 (2014). https://doi.org/10.1002/adma.201304018
6. Zhang, Q., Wommer, J., O'Rourke, C., Teitelman, J., et al.: Origami and kirigami inspired self-folding for programming three-dimensional shape shifting of polymer sheets with light. Extreme Mech. Lett. **11**, 111–120 (2017). https://doi.org/10.1016/j.eml.2016.08.004
7. Martinez, R.V., Fish, C.R., Chen, X., Whitesides, G.M.: Elastomeric Origami. Programmable Paper-Elastomer Composites as Pneumatic Actuators. Adv. Funct. Mater. **22**, 1376–1384 (2012). https://doi.org/10.1002/adfm.201102978
8. Cianchetti, M., Laschi, C., Menciassi, A., Dario, P.: Biomedical applications of soft robotics. Nat. Rev. Mater. **3**, 143–153 (2018). https://doi.org/10.1038/s41578-018-0022-y
9. Lu, T., Shi, Z., Shi, Q., Wang, T.J.: Bioinspired bicipital muscle with fiber-constrained dielectric elastomer actuator. Extreme Mech. Lett. **6**, 75–81 (2016). https://doi.org/10.1016/j.eml.2015.12.008
10. Zhang, X., Fan, X., Yan, C., Li, H., et al.: Interfacial microstructure and properties of carbon fiber composites modified with graphene oxide. ACS Appl. Mater. Interfaces **4**, 1543–1552 (2012). https://doi.org/10.1021/am201757v
11. Cherif, C.: Textile Werkstoffe für den Leichtbau. Techniken - Verfahren - Materialien - Eigenschaften. Springer-Verlag Berlin Heidelberg, Berlin (2011)
12. Kalinka, G., Neumann, B.: Bestimmung von Interface-Festigkeit oder Trennarbeit mit dem Pull-out-Versuch (2005)
13. Zhou, J., Li, Y., Li, N., Hao, X., et al.: Interfacial shear strength of microwave processed carbon fiber/epoxy composites characterized by an improved fiber-bundle pull-out test. Compos. Sci. Technol. **133**, 173–183 (2016). https://doi.org/10.1016/j.compscitech.2016.07.033
14. Piggott, M.R.: Why interface testing by single-fibre methods can be misleading. Compos. Sci. Technol. **57**, 965–974 (1997). https://doi.org/10.1016/S0266-3538(97)00036-5
15. Zhandarov, S.: Characterization of fiber/matrix interface strength. Applicability of different tests, approaches and parameters. Compos. Sci. Technol. **65**, 149–160 (2005). https://doi.org/10.1016/j.compscitech.2004.07.003
16. Kim, J.-K., Mai, Y.-W.: Engineered interfaces in fiber reinforced composites, 1st edn. Elesvier Science Ltd, Oxford (1998)
17. Palola, S., Sarlin, E., Kolahgar Azari, S., Koutsos, V., et al.: Microwave induced hierarchical nanostructures on aramid fibers and their influence on adhesion properties in a rubber matrix. Appl. Surf. Sci. **410**, 145–153 (2017). https://doi.org/10.1016/j.apsusc.2017.03.070

18. Beter, J., Schrittesser, B., Fuchs, P.: Investigation of adhesion properties in load coupling applications for flexible composites. Mater. Today-Proc. (2020). https://doi.org/10.1016/j.matpr.2020.01.181
19. Schulz, E., Kalinka, G., Auersch, W.: Effect of transcrystallization in carbon fiber reinforced poly(p - phenylene sulfide) composites on the interfacial shear strength investigated with the single fiber pull-out test. J. Macromol. Sci. Part B. **35**, 527–546 (2006). https://doi.org/10.1080/00222349608220393
20. Desarmot, G., Favre, J.: Advances in pull-out testing and data analysis. Compos. Sci. Technol. **42**, 151–187 (1991). https://doi.org/10.1016/0266-3538(91)90016-I
21. Viel, Q., Esposito, A., Saiter, J.-M., Santulli, C., et al.: Interfacial Characterization by Pull-Out Test of Bamboo Fibers Embedded in Poly(Lactic Acid). Fibers (2018). https://doi.org/10.3390/fib6010007
22. Kalinka, G., Leistner, A., Hampe, A.: Characterisation of the fibre/matrix interface in reinforced polymers by the push-in technique. Compos. Sci. Technol. **57**, 845–851 (1997). https://doi.org/10.1016/S0266-3538(96)00159-5
23. Domnanovich, A., Peterlik, H., Kromp, K.: Determination of interface parameters for carbon/carbon composites by the fibre-bundle pull-out test. Compos. Sci. Technol. **56**, 1017–1029 (1996). https://doi.org/10.1016/0266-3538(96)00060-7
24. Zarges, J.-C., Kaufhold, C., Feldmann, M., Heim, H.-P.: Single fiber pull-out test of regenerated cellulose fibers in polypropylene. An energetic evaluation. Compos. Part A **105**, 19–27 (2018). https://doi.org/10.1016/j.compositesa.2017.10.030
25. Neitzel, M., Mitschang, P., Breuer, U.: Handbuch Verbundwerkstoffe. Werkstoffe, Verarbeitung, Anwendung. Carl Hanser Fachbuchverlag, Munich (2014)
26. Berthold, U.: Beitrag zur Thermoformung gewebeverstärkter Thermoplaste mittels elastischer Stempel. Dissertation, Technische Universität Chemnitz: (2001)
27. Keilig, Th, Arendts, F.J.: Ermittlung und Modellierung des Umformverhaltens von thermoplastischen Gewebeprepregs unter besonderer Berücksichtigung der Atlas-1/7-Bindung. In: Verbundwerkstoffe und Werkstoffverbund. Verbundwerkstoffe und Werkstoffverbund, Kaiserslautern, Germany, September: (1997)
28. Muliana, A., Rajagopal, K.R., Tscharnuter, D., Schrittesser, B., et al.: Determining material properties of natural rubber using fewer material moduli in virtue ofa novel constitutive approach for elastic bodies. Rubber Chem. Technol. **91**, 375–389 (2018). https://doi.org/10.5254/RCT.18.81675
29. Mansouri, M., Fuchs, P.F., Schuecker, C.: Hyperelastic modeling of woven structures undergoing large deformations. In: 18th European Conference on Composite Materials ECCM18, Athen, 2018 (2018)
30. Technical Committee ISO/TC 45: Rubber, vulcanized or thermoplastic - Determination of tensile stress-strain properties. International Organization of Standardization, Geneva (2011) CH(ISO 37)
31. Eurpean Commitee for Standardization: Plastics. Determination of tensile properties. BSI British Standards, London ICS 83.120 (1997)
32. Hampe, A., Kalinka, G., Meretz, S., Schulz, E.: An advanced equipment for single-fibre pull-out test designed to monitor the fracture process. Compos. **26**, 40–46 (1995). https://doi.org/10.1016/0010-4361(94)P3628-E
33. D13 Committee: Test Method for Tensile Properties of Yarns by the Single-Strand Method. ASTM International, Conshohocken, W., PA(ASTM 2256) (2015)
34. Abts, G.: Einführung in die Kautschuktechnologie. Hanser, München (2019)
35. Lang, R.W., Stutz, H., Heym, M., Nissen, D.: Polymere hochleistungs-faserverbundwerkstoffe. Angew. Makromol. Chemie **145**, 267–321 (1986). https://doi.org/10.1002/apmc.1986.051450115

3.5 Patent A: Klemmvorrichtung und Verfahren zur Prüfung einer Zugfestigkeit eines Objektes

Julia Beter[1,*], Bernd Schrittesser[1] and Franz Grassegger[2]

[1] Polymer Competence Center Leoben GmbH, Roseggerstrasse 12, 8700 Leoben, Austria.

[2] Department of Polymer Engineering and Science, Montanuniversitaet Leoben, Otto- Gloeckel- Strasse 2, 8700 Leoben, Austria.

Published in Österreichisches Patentamt, 2020, A 50009/2020.

This patent entitled “Clamping device and method for testing a tensile strength of an object” comprises a clamping system to measure preferably continuous fiber-reinforced elastomers. In particular, there are two clamping elements, which are movable relative to each other so that the specimen can be fixed between the clamping elements, thus enabling tests without bending moment. Furthermore, the tensile strength of a fiber-reinforced elastomer can be obtained due to the special geometry ensuring sufficient grip without clamping-induced material damage as well as no slippage.

Polymer Competence Center Leoben

An
Frau DI Julia Beter
Schlachthofgasse 6
8700 Leoben

Leoben, am 25. Jänner 2021

Bestätigung der Mitwirkung an einer Diensterfindung

Es ist uns eine Freude zu bestätigen, dass Frau DI Julia Beter, geboren am 19. Mai 1992, während ihrer Forschungstätigkeit als Mitarbeiterin der Polymer Competence Center Leoben GmbH im Rahmen eines Projektes des COMET-K1-Zentrums PCCL maßgeblich als Erfinderin an folgender Diensterfindung bzw. folgendem Patent beteiligt war:

> Titel des Patents: *„Klemmvorrichtung und Verfahren zur Prüfung einer Zugfestigkeit eines Objektes“*

Für die zugrundeliegende Diensterfindung haben wir ein nationales Patent unter der Anmeldenummer A 50009/2020 beim Österreichischen Patentamt eingereicht; im Verfahren wurde bereits die Erteilung des Patents verfügt; es ist nur noch die Rechtskraft des Beschlusses ausständig.

Mit freundlichen Grüßen

DI Dr. Elisabeth Ladstätter
(Geschäftsführerin)

Polymer Competence Center Leoben GmbH
Roseggerstraße 12, A-8700 Leoben
www.pccl.at

Tel: +43 3842 42962-0
Fax: +43 3842 42962-6
office@pccl.at

Firmenbuch: LG Leoben
FN 223698v
UID-Nr. ATU 54829208

Steiermärkische Sparkasse
IBAN AT41 2081 5000 4032 7439
BIC STSPAT2GXXX

3.6 Paper 5: Viscoelastic behavior of glass fiber reinforced silicone composites exposed to cyclic loading

Julia Beter[1,*], Bernd Schrittesser[1], Bernhard Lechner[1], Mohammad Reza Mansouri[1], Claudia Marano[2], Peter Filipp Fuchs[1] and Gerald Pinter[3]

[1] Polymer Competence Center Leoben GmbH, Roseggerstrasse 12, 8700 Leoben, Austria.

[2] Department of Chemistry, Materials and Chemical Engineering “Giulio Natta”, Politecnico di Milano, Piazza Leonardo da Vinci 32, 20133 Milan, Italy

[3] Department of Polymer Engineering and Science, Montanuniversitaet Leoben, Otto- Gloeckel- Strasse 2, 8700 Leoben, Austria.

Published in Polymers, 2020, 12(9), 1862.

DOI: 10.3390/polym12091862

polymers

MDPI

Article

Viscoelastic Behavior of Glass-Fiber-Reinforced Silicone Composites Exposed to Cyclic Loading

Julia Beter [1,*], Bernd Schrittesser [1], Bernhard Lechner [1], Mohammad Reza Mansouri [1], Claudia Marano [2], Peter Filipp Fuchs [1] and Gerald Pinter [3]

1 Polymer Competence Center Leoben GmbH, Roseggerstrasse 12, 8700 Leoben, Austria; Bernd.Schrittesser@pccl.at (B.S.); Bernhard.Lechner@pccl.at (B.L.); Mohammad.Mansouri@pccl.at (M.R.M.); PeterFilipp.Fuchs@pccl.at (P.F.F.)

2 Department of Chemistry, Materials and Chemical Engineering "Giulio Natta", Politecnico di Milano, Piazza Leonardo da Vinci 32, 20133 Milan, Italy; claudia.marano@polimi.it

3 Department of Polymer Engineering and Science, Montanuniversitaet Leoben, Otto Gloeckelstrasse 2, 8700 Leoben, Austria; Gerald.Pinter@unileoben.ac.at

* Correspondence: Julia.Beter@pccl.at; Tel.: +43-3842-42962-31

Received: 29 July 2020; Accepted: 17 August 2020; Published: 19 August 2020

Abstract: The aim of this work was to analyze the influence of fibers on the mechanical behavior of fiber-reinforced elastomers under cyclic loading. Thus, the focus was on the characterization of structure–property interactions, in particular the dynamic mechanical and viscoelastic behavior. Endless twill-woven glass fibers were chosen as the reinforcement, along with silicone as the matrix material. For the characterization of the flexible composites, a novel testing device was developed. Apart from the conventional dynamic mechanical analysis, in which the effect of the fiber orientation was also considered, modified step cycle tests were conducted under tensile loading. The material viscoelastic behavior was studied, evaluating both the stress relaxation response and the capability of the material to dissipate energy under straining. The effects of the displacement rate of the strain level, the amplitude of the strain applied in the loading–unloading step cycle test, and the number of the applied cycles were evaluated. The results revealed that an optimized fiber orientation leads to 30-fold enhanced stiffness, along with 10 times higher bearable stress. The findings demonstrated that tailored reinforced elastomers with endless fibers have a strong influence on the mechanical performance, affecting the structural properties significantly.

Keywords: flexible composite; dynamic mechanical analysis; cyclic loading; step cycle test; viscoelasticity; fiber-reinforced elastomer

1. Introduction

Fiber-reinforced composites offer a synergetic combination of properties consisting of two or more individual components. Due to their beneficial interactions, completely new mechanical behavior can be generated, which cannot be achieved using the individual components [1]. This approach has been already applied very successfully to elastomers, where a specific improvement of mechanical properties is achieved via the use of fibrous reinforcement while still maintaining the high flexibility of the elastomeric matrix [2]. This enables higher bearable loadings while the good damping and absorption behavior are retained. In the industry, typical fiber-reinforced rubber products are used for several applications, such as automotive tires [3], dampers [4,5], conveyor belts [6], and seismic-fiber-reinforced elastomer isolators (FREI) [7], where sufficient strength and flexibility have to be ensured. Hence, the requirement to improve the mechanical performance in specific directions cannot be accomplished by using non-reinforced elastomers [8,9]. Recent studies have revealed that this knowledge is also

considered in so-called smart materials with distinct high (or hyper-) elasticity [10,11]. Such flexible composites are a completely new material class, which evolved due to the increasing demand for improved functionality inspired by certain biomimetic approaches [12], as well as the stronger interest in sustainability and decarbonization [13]. The primary advantage of these flexible composites is the ability to tailor physical properties such as deformation, stiffness, and non-linearity over a much wider range than conventional fiber-reinforced rubbers [10,14]. These concepts can be found in some recent developments, such as artificial muscles [15], exoskeletons, or artificial fingers [16], as well as aeroelastic wings [17,18] with significantly large deformations. Generally, it is evident that these applications of fiber-reinforced elastomers are mostly subjected to cyclic loading. According to the current scientific research activities, industrial fiber-reinforced rubber products or other composite material clusters in the field of civil engineering, e.g., FREI or cement-based composite materials, are investigated regarding fracture mechanics aspects [19,20]. Therefore, important composite material properties in terms of toughness or fracture-mechanics-induced damage are crucial for fatigue lifetime assessments [21,22]. In contrast, recent studies confirm that the applications for smart materials with distinct high elasticity mainly involve exposure to semicyclic loading conditions within a quasistatic range, combined with significantly lower numbers of cycles [12,16]. Therefore, the viscoelastic focus is particularly important in this field. Studies focusing on numerical simulation approaches have addressed this problem, especially for hyperelastic elastomers in combination with stiff reinforcing fibers and their interactions (e.g., fiber–fiber interactions and fiber–matrix interactions), which cause several challenges [23,24]. Therefore, the assessment of dynamic properties and the viscoelastic behavior of those composite materials are essential, as these parameters are decisive when generating specifications for subsequent component designs and lifetime estimations [8]. In order to understand and describe the dynamic and viscoelastic behavior of flexible composites, an extensive characterization can be performed by means of dynamic tests of the temperature, frequency, time, or strain level. Using these characterization methods, dynamic mechanical analysis (DMA) [25,26], and step cycle tests [27,28], the composite structure and performance [8] can be efficiently and quickly investigated.

Many publications have focused on DMA tests, including for fiber-reinforced polymers, which have mainly analyzed short fibers combined with natural rubber or thermoplastic matrices [8,29,30]. The use of short fibers has advantages, such as increased material stiffness and strength, but also has considerable limitations caused by the fiber orientation, which cannot be directed in a specific load-optimized manner. The fibers are rather predominantly aligned in the flow direction during the injection molding process [31–33] and the bearable load transfer is limited. It has already been proven in previous studies [34] that reinforced fabrics are more beneficial and economical when enhancing the mechanical properties of composite materials comprising fully unidirectional materials or short fibers. For this reason, some studies have been carried out related to the experimental analysis of composites with continuous fibers or textiles under cyclic loading [2,35–37]. Nevertheless, these investigations have focused on natural fibers such as hemp, jute, or cellulose, revealing the disadvantage of moisture absorption [36,38]. The step cycle test represents a promising test method for determining the viscoelasticity and entropic elasticity, which are important parameters in the characterization of the mechanical performance of elastomers and fiber-reinforced composites. Under cyclic loading, rubbers are known to exhibit pronounced viscoelastic behavior [39], including stress softening and hysteresis [28,40]. Significant softening is observed after the first cycles, which can be explained due to the fact that the stress values at reloading are significantly lower than the stress obtained in the first cycle at a similar strain [41]. Consequently, if the deformation is not increased stepwise to higher strain levels, an approximately stationary cycle is achieved after repeated loading, which is characterized by an equilibrium state with preconditioned behavior (stationary hysteresis). Some research has been done in this field, focusing on fiber-reinforced elastomers [33,42,43]. Thus, this approach reveals promising potential for the investigation of the viscoelastic behavior of flexible composites, which was already studied extensively by Peel [10], who provided the basis for the fabrication and mechanics of fiber-reinforced elastomers designed for smart material usage. Moreover, flexible composites have large

differences in the stiffness and flexibility between the fibers and elastomeric matrix, causing a textile-like performance [44]. In this context, conventional test setups are not appropriate, and therefore special test devices need to be designed, particularly for these materials [45]. In this context, the fiber–matrix connection is crucial, since the interface is essential for the load transmission [46], and thus for the load coupling (as investigated in previous studies [47]).

The aim of this work is to investigate the mechanical properties of tailored fiber-reinforced elastomers under cyclic loading. The focus includes the dynamic mechanical and viscoelastic behavior, combined with the influence on relaxation, in order to provide information about the near-application performance. Since the presence of fibers makes the characterization of materials even more complex, the influence of the fiber orientation was analyzed, together with parameters such as displacement rate, frequency, and temperature. Regarding the step cycle test, a novel clamping device [48] was implemented for flexible composites, providing sufficient clamping at high deformation and guaranteeing that no material damage was caused by the grips and that no slippage occured. In order to investigate the effects of the large difference in mechanical properties between stiff fibers and flexible matrices, glass fibers (GF) combined with polydimethylsiloxane (PDMS) were chosen as the materials for the flexible composites. The knowledge obtained in these tests provides a better understanding of the performance and application of dynamically loaded flexible composites by considering fiber–matrix load coupling effects. This study aims to obtain customized material parameters for subsequent implementation in numerical simulation models, thus enabling the generation of tailored simulations for elastomeric composites with pronounced textile behavior and high flexibility, followed by the establishment of realistic prediction models of viscoelastic behavior [24,49]. Based on the findings of this study, further applications can be realized by considering other composite material clusters for subsequent fatigue and fracture mechanics life assessments, which can be dealt with using Weibull models [50].

2. Materials and Methods

2.1. Materials

A commercial E-type GF-fabric supplied by CS Interglas AG (Erbach, Germany) was chosen as reinforcement from a single batch, with a 2/2 twill weave and an area weight of 220 g/m^2 ± 5%. The standardized yarn classification of the GF was EC9-68xt0, with an indicated twine thickness of 68 tex (grams per kilometer), a mean fiber diameter of approximately 10 µm, and an area bundle distribution of 50/50 in the 0°/90° direction, respectively. The PDMS matrix material, which is available as a cast elastomer (Elastosil RT601 A/B), was chosen for the flexible composite laminates and was provided by Wacker Chemie AG (Munich, Germany). This elastomer is a two-component system (the prepolymer as part A and the crosslinking system as part B) with a density of 1.02 g/cm^3, a viscosity (in uncured mixed state) of 3500 mPas (at room temperature), and a pot life of about 90 min at room temperature, which was prepared according to the supplier's specifications at a mixing ratio of 9:1 (part A/part B). As recommended by the manufacturer, the matrix material was then cured in an air circulating drying oven at 70 °C for 60 min. Regarding the mechanical properties of the individual components (i.e., fibers and matrix) and the flexible composite, corresponding tensile tests were carried out as in previous studies [51]. The mechanical properties of the fibers were tested in tensile tests according to ASTM D2256 [52], the elastomeric matrix with ISO 37 [53], while the composite material was investigated based on ISO 527-4 [54]. Thus, an elongation at break value of about 108.6% was determined for the silicone, with a corresponding stress at break value of about 4.5 MPa. Compared to this, the pure fiber material showed an elongation at break value of approximately 2.3%, with a force at break value of about 119.8 N. Subsequently, the mechanical properties of the tailor-made fiber-reinforced elastomers were analyzed regarding the influence of the fiber orientation and adhesion properties. Representative for the flexible composite, the ±45° orientation revealed a determined elongation at break value of about 38.2%, with a corresponding stress at break value of approximately 34.3 MPa [51].

2.2. Preparation of Specimens

For the manufacturing step, the commercial vacuum resin infusion (VARI) process [1] was chosen to prepare the flexible composite specimens, which is schematically illustrated in Figure 1. The VARI process offers advantages in terms of economical production and high individuality, especially at the laboratory scale or for the production of prototypes. Basically, the infusion process comprised two mold halves: a rigid mold on the lower side and a flexible upper mold half, which is the vacuum bag itself. In this investigation, a glass plate was chosen as the rigid lower mold due to its smooth surface and chemically advantageous properties during the infusion. The applied mold release agent (Mono-Coat 1625W) was provided by Chem-Trend GmbH (Maisach, Germany). In order to achieve a linear flow front and considering the size of the manufacturing process, the inlet tube (related to the resin side) and the outlet tube (connected with the vacuum part) were placed at opposite each other on the glass plate. Furthermore, this arrangement enabled optimized inter- and intralaminar impregnation, as well as adequate consolidation quality due to the limited maximum feasible pressure difference of about 10^5 Pa (atmospheric pressure) [1,55]. For the placing order of the layer structure and the fiber orientation of the woven fabric, the dry textile was cut with a professional cutter G3 M-1600 by Zuend Systemtechnik AG (Altstaetten, Switzerland). This cutter is equipped with a vacuum table to avoid drape defects or unwanted fiber undulations during the cutting procedure. Among the applied disposable materials, such as the flow help, distribution foil, perforated release film, and peel ply, the last layer of the total assembly was constituted by the vacuum bag (outer encapsulation). Moreover, permeable lines were added under the vacuum bag next to both tubes (inlet and outlet) to provide relatively fast media distribution at the beginning of the infiltration, while maintaining a linear progression of the flow front. In this context, a complete impregnation with the prepolymer-based mixture matrix cannot be obtained without the presence of a vacuum. Additionally, further advantages were achieved by using a vacuum, such as (i) the active compacting pressure resulting from the pressure gradient between the vacuum and atmosphere, (ii) uniform layer thickness, and (iii) good consolidation. These aspects are essential to ensure optimized laminate quality.

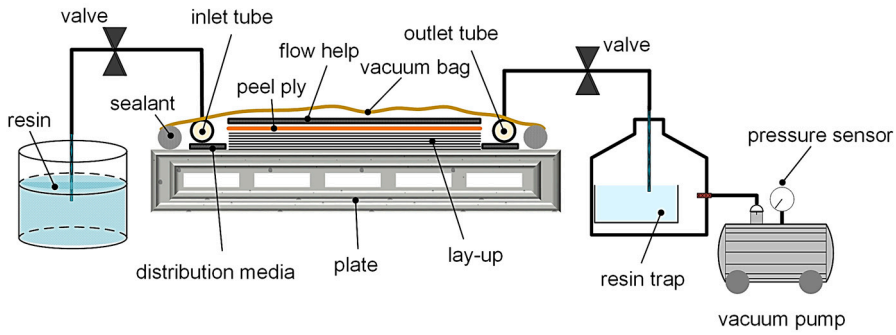

Figure 1. Schematic build-up of the applied vacuum resin infusion (VARI) process for the production of flexible composite plates [1].

In terms of the infusion procedure, the prepolymer and crosslinking systems were first mixed and subjected to a degassing step prior to the infiltration. The higher viscosity of the prepolymer compared to classical thermosets at processing temperature in an uncured state raises serious problems, such as causing more complex and challenging impregnation (causing a higher flow resistance and a lower flow rate) because of the pressure gradient (described in D'Arcy's law for one-dimensional flow form [1]). For this reason, the pot life or infusion time window is negatively affected, which implies the need for a suitable flow to help minimize the risk of incomplete cavity filling or potential porosity. After the infusion, the inlet and outlet vents were clamped to maintain a stable vacuum during the curing step, which was carried out under the same conditions suggested for the curing of the pure elastomeric matrix (60 min at 70 °C in an air circulating drying oven). After the careful demolding of the crosslinked PDMS reinforced with GF (GF-PDMS) composite plates, strip-shaped

specimens were produced with the cutter. DMA tests were carried out in tensile loading conditions with the corresponding sample preparation according to ISO 6721-1 [56]. The step cycle tests were also performed under tensile loading, using rectangular samples with a defined length/width ratio of 90:30 (l is the specimen gauge length, between the clamping fixture), ensuring smooth data recording without any effects caused by the clamping area due to affected deformation or hindered fiber reorientation. This sample geometry was already applied in a previous study [51], where the influence of the sample geometry on structural properties, the effects of fiber orientation on shear stresses, and the tensile properties of flexible composites were investigated. For all tests, a defined fiber volume content of about 50% was set, which was verified through thermogravimetric analysis (TGA). Furthermore, to exclude batch variations, only measurements of the same batch were chosen for the DMA and step cycle tests.

2.3. Dynamic Mechanical Analysis

In this study, dynamic mechanical tests were performed to determine the viscoelastic behavior of fiber-reinforced elastomers. Therefore, the influence of different fiber orientations on the stiffness and entropic elasticity, as well as the impact of frequency variation on the mechanical properties, were investigated in detail. The effects of different fiber orientations of the reinforcement structure and changes of fiber angles related to the load direction were analyzed in previous studies using a methodically validated test plan [44]. In this context, composite samples with a defined warp and weft yarn configuration of ±45°, 30°/60°, and 0°/90° (versus the loading direction) were considered. Figure 2a schematically illustrates how they were obtained from the composite plate. The samples considered in this work were set with a length l of 30 mm, a width w of 4 mm, and a thickness of about 0.35 mm, (see Figure 2b), according to S2 tensile specimens in the ISO 4664 standard [57]. The tests were performed on a Perkin Elmer DMA 8000 (Perkin Elmer VertriebsgmbH, Brunn am Gebirge, Austria). The evaluation and calculation steps were carried out with the corresponding software package Pyris Instrument Managing Software (Perkin Elmer VertriebsgmbH, Brunn am Gebirge, Austria). The storage and loss moduli, as well as the loss factor, were calculated according to ISO 4664. All measurements were carried out in tension mode using a frequency of 1 Hz at a clamping distance of 10 mm. The tests were carried out in temperature ramp mode in the range of −80 °C to +100 °C, with a heating rate of 3 K/min. A static force of 0.3 N was applied and a displacement oscillation amplitude of 5 µm was set. At least five specimens were used for each setting to ensure sufficient repeatability. As reference values for the following data interpretation, the mean value of each setting was determined, along with the corresponding standard deviation.

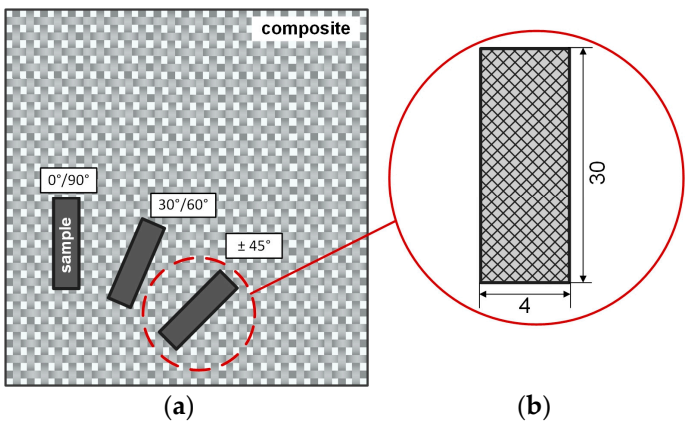

Figure 2. Schematic illustration of the specimen preparations with different fiber orientations (**a**) and the specimen used in the dynamic mechanical analysis in tension mode (**b**).

2.4. Step Cycle Test

The tests were carried out according ISO 527-4 [54] at standard atmosphere conditions according to ISO 291 (20 °C, 50% r. h.) [58] with a universal testing machine Z010 (Zwick Roell GmbH and Co. KG, Ulm, Germany) equipped with a 10 kN load cell. A gauge length l of 90 mm was selected, along with a defined displacement rate v (10 mm/min, 100 mm/min, and 1000 mm/min) to investigate the influence of the strain rate dependency within a wide range according to ISO 37 standard for elastomers, as well as ISO 527-4 standard for composites. The measurement length l m was set to 30 mm. Due to the high flexibility of the composites, the measurement lengths were recorded with an optical image correlation system Prosilica GT 6600 (Allied Vision Technologies GmbH, Stadtroda, Germany) and a fine pattern was sprayed on the sample surface, as depicted in Figure 3a.

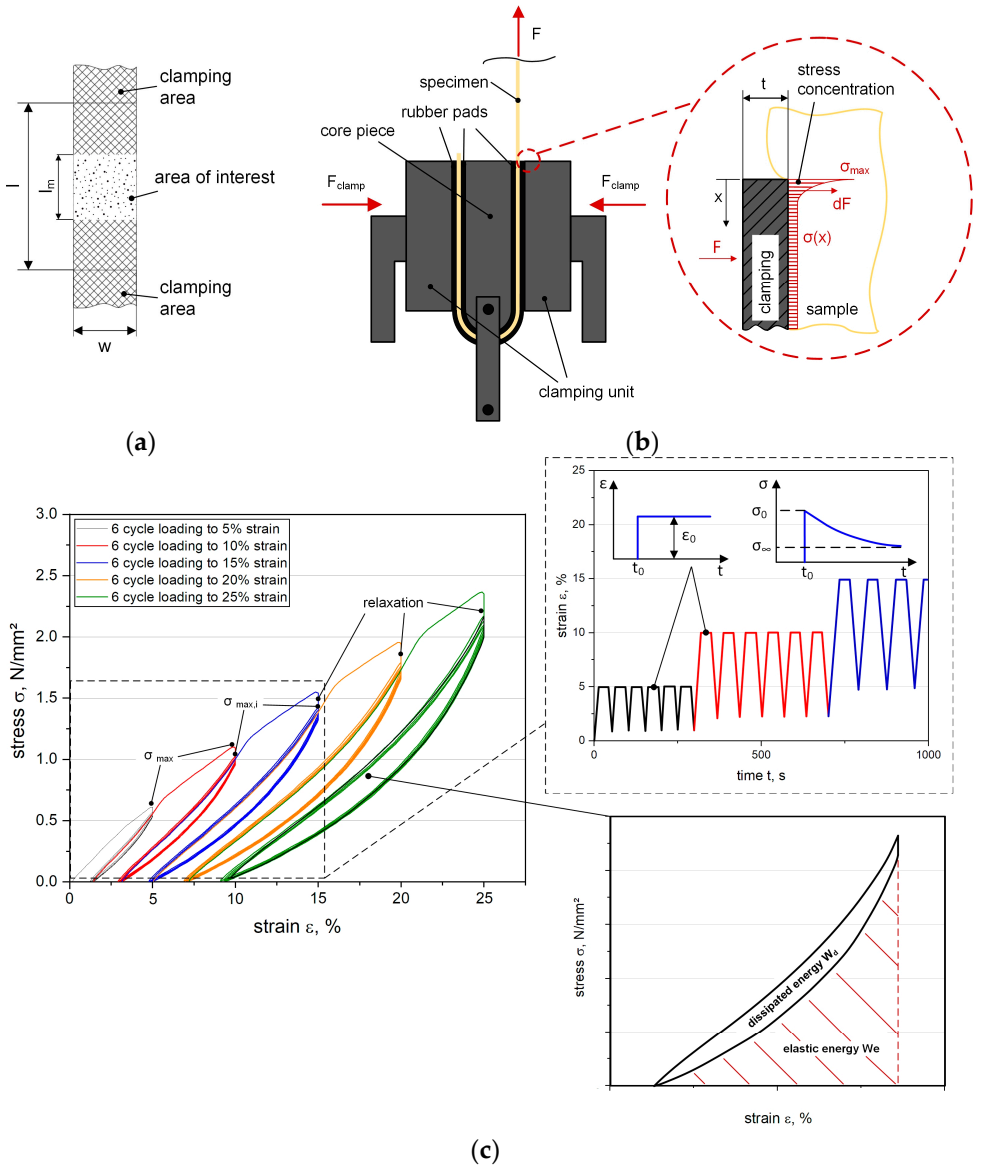

Figure 3. Specimen used in step cycle test (**a**) with the novel clamping device (**b**) [48], schematic build-up of the step cycle test ((**c**), left), and the relaxation and hysteresis diagram ((**c**), right) [59].

The experimental characterization of fiber-reinforced composites using soft matrix materials revealed several problems, since the load transfer into the fibers and the surrounding matrix had to be ensured simultaneously to ensure the complete cross-section area of the sample underwent a homogeneous deformation. Because the substitution of classical thermosets by elastomeric matrix

materials in fiber-reinforced polymers leads to highly flexible and almost textile-like material behavior, conventional grippers are not suitable. Thus, a novel clamping system was developed to avoid slippage or failure caused by the grippers, while maintaining sufficient adhesion. This can cause new challenges, such as clearly visible necking of the specimen, particularly in the transition area (clamping gauge region), which increases the risk of slippage and failure of the clamps. Hence, the clamping force F_{clamp} has to be increased, which induces local stress σ_{max} caused by the required minimum clamping force. Subsequently, this can lead to fiber damage or preliminary failure. The novel patented device [48] consists of a combination of flat surface clamping using a compression force with an implemented deflection, which is schematically illustrated in Figure 3b. Moreover, due to the sensitivity of the flexible composite, additional rubber pads need to be placed in the clamps. These pads enable prevent slippage and also reduce local compressive stresses, especially in the edges (near-clamping region) of the sample. This is mainly related to the multiaxial stresses caused by large necking and deformation due to the sharp transition in the material between clamping and testing areas. The effects of these local stress concentrations, including their prevention by rubber pads, were already analyzed in previous research studies [51].

Deformation-induced stress softening is an important phenomenon that can be observed during the deformation of reinforced elastomers when tested in cyclic loading. Typically, stress softening can be determined by stretching the elastomer to a certain strain level, followed by unloading and reloading to the same strain level for a second time—the force required to deform the elastomer in the second loading step is lower than that in the first one. Due to this, the specimens were periodically stretched up to a certain strain level and the stress–strain behavior during the loading and unloading steps was recorded. The dissipated energy W_d (hysteretic area between the loading and unloding curves of each cycle) can be calculated as the difference between the total absorbed energy W_t (integration of the stress–strain response during loading phase) and the stored (elastic) energy W_e (integration of the stress–strain response during unloading phase) [60], which is given in Equation (1) and graphically descripted in Figure 3c:

$$W_d = W_t - W_e \tag{1}$$

In this study, the basic concept of the test procedure is to combine the common step cycle method, which was established for quasistatic loading–unloading tests, with an additional relaxation sequence between the loading and unloading phases before the next loading cycle is initiated. This offers the possibility of determining the stress softening between the cycles and the relaxation decrease gradient per cycle, so that a correlation between the current maximum stress value and the corresponding level of relaxation can be observed. Each specimen was stretched and displacement-controlled up to five fixed strain values ε_n, ranging from 5% up to 25%: at each strain level, each specimen was looped six times. Based on the knowledge gained from previous tensile tests (see Section 2.1), the lower and upper limits were defined to ensure the viscoelastic material behavior was exclusively within the test range [51]. An intermediate holding step at each ε_n of 0 s, 10 s, and 30 s was implemented after each loading phase. The unloading step was carried out down to 0.1 N to avoid slackening. A graphic illustration of the measurement procedure is shown in Figure 3c using an exemplary hysteresis loop, where the elastic deformation and the additional relaxation phase are conducted and displacement-controlled. To calculate the stress softening, the decrease of the stress level $\Delta\sigma$ (see Equation (2)) was determined as the difference between the maximum stress $\sigma_{max\,n,i}$ (first cycle) and the following maximum stresses $\sigma_{max\,n,i+1}$ (subsequent cycle number i) for a defined strain value ε_n. Furthermore, the intermediate relaxation sequence $f_{\sigma,relax}$ was calculated as the stress decrease (vertical load drop) at a constant strain during the holding step of each cycle for a defined strain value ε_n, which was evaluated with Equation (3):

$$\Delta\sigma = \sigma_{maxn,i} - \sigma_{maxn,i+1} \tag{2}$$

$$f_{\sigma,relax} = 100\frac{\sigma_{maxn,i} - \sigma_{relax\ n,i}}{\sigma_{maxn,i}} \tag{3}$$

For comparability and data reduction, the step cycle tests focused on fiber orientations of ±45° and 30°/60° to assess the impact on the shearing behavior. The main reason for choosing these orientations is reflected by the strong influence of shearing with different fiber orientations when the loading direction differs, especially during deformation of woven textiles. Constituted specimens with a definite length-to-width radio of 3:1 were chosen to guarantee a stress-free area of interest (see Figure 3a). This allowed the load coupling mechanism and the shearing behavior from the fiber–matrix adhesion to be investigated. Moreover, studies [45] revealed that the maximum in-plane deformation is limited by the fiber orientation until the displacement of the fibers relative to each other reaches the maximum shift angle (also known as "locking angle"), where wrinkling perpendicular to the textile plane (the so-called "trellis effect") emerges, leading to premature fiber breakage [44].

3. Results and Discussion

3.1. Dynamic Mechanical Analysis

Focusing on the study of the stiffness and damping behavior in the entropic elastic region, the influence of different fiber orientations, as well as the effect of the composite interface, the storage modulus was characterized as a function of the temperature, whereby the storage modulus E′ represents the elastic component of the material behavior and is, thus, associated with the material stiffness. Furthermore, the behavior of a fiber-reinforced elastomer (GF-PDMS) was compared with a non-reinforced elastomer (PDMS) to assess the reinforcing effect of the fibers. In Figure 4, the temperature dependence of the composite storage modulus E′ is compared with different fiber orientations in the application range between −80 °C and +100 °C. As is known from literature, the glass transition temperature (Tg) of PDMS is approximately −110 °C [59]. The transition step at about −50 °C is related to the melting of crystalline sequences, which are formed upon cooling due to the highly linear polymer structures [61].

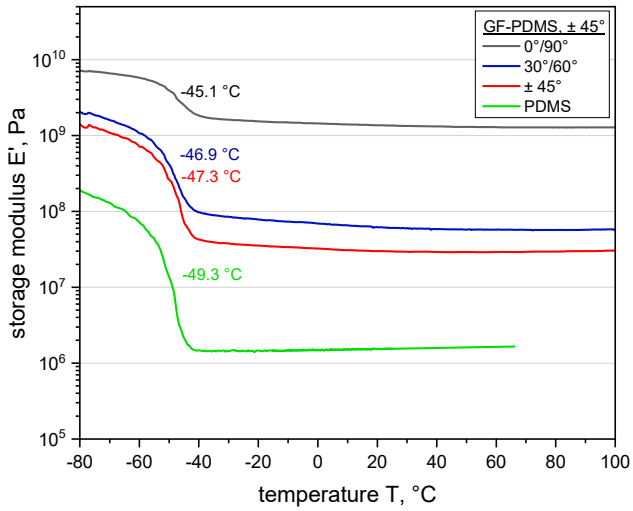

Figure 4. Comparison of storage moduli of glass fiber–polydimethylsiloxane (GF-PDMS) composites with different fiber orientations and polydimethylsiloxane obtained from dynamic mechanical analysis.

Overall, the results show that the storage modulus increases significantly when reinforcing PDMS with GF and that the reinforcing effect is more significant in the entropic elastic region, as expected. Further, it can be stated that the mechanical properties can be optimized properly, tailoring the fibers reinforcing effect. Nevertheless, the flexibility and characteristic soft regions dominated by the elastic matrix are retained [62]. Furthermore, the results reveal a significant dependence of the composite performance on the fiber orientation. As expected, the fiber-dominated 0°/90° orientation leads to the highest storage modulus compared with the other two orientations, however a small decrease in the

modulus can be seen in entropic elastic region. This could be explained by the fact that even with the fibers fully aligned in the loading direction, the fiber–matrix interface and the surrounding matrix have a considerable impact on the load coupling mechanism. The difference in the storage modulus between the 30°/60° and ±45° composites is related to the lay-up of the fiber orientation (asymmetric versus symmetric), causing a significant impact on the load transfer in the fabric. This could be explained by the fact that both composites are more strongly dominated (fiber orientation versus loading direction) by the matrix than the composite with the 0°/90° orientation, which results in the storage modulus being on a lower level. Accordingly, the load transfer between the weft and warp yarns in the fabric is primarily induced via shearing. Moreover, the influence of the fiber–matrix adhesion at the interface is affected by the elastomeric matrix. A detailed discussion of the shear induced load coupling mechanism by different fiber orientations can be found in [45].

3.2. Step Cycle Test

Since the viscoelastic properties of dynamically loaded elastomers have a decisive influence on their entropic elasticity, the hysteresis delivers information about the load coupling mechanism [62]. Apart from showing the reinforcing effect of fibers on the elastomeric matrix, the viscoelastic analysis conducted by means of step cycle testing could also indicate the dependence of the damage behavior on the stress level, deformation rate, and relaxation time. Related to this, the step cycle tests conducted on fiber-reinforced elastomers show the typical shape of a stress–strain curve with indicated stress softening, which is illustrated in Figure 5, where data relevant to the tests (performed at different displacement rates) are reported for comparison.

Generally speaking, it can be observed that: (i) no significant dependence of the maximum stress on the applied strain level can be seen in the first loading cycle; (ii) significant stress softening is observed with increasing cycle numbers, especially after the first cycle; (iii) since the unloading path is not affecting by cycling, the first cycle shows the largest hysteresis, and thus the highest amount of dissipated energy. For the study of the strain rate effect (see Figure 5a), a relaxation time of 30 s was adopted in the stress relaxation step, since conventional relaxation tests that had been previously conducted on flexible composites revealed an almost total stress release of more than 95% in this time frame. The slight differences observed between the stress–strain curves measured at different displacement rates could be related to experimental deviations caused by statistical influences (see Figure 5a). The non-reinforced elastomer tested at 10 mm/min showed no hysteretic behavior, which reflects its entropic elasticity, and thus its high rebound resilience [61,62]. This could be explained due to the hyperelasticity of unfilled silicone elastomers [10]. In contrast, the GF-PDMS composites have a distinctly retarded strain recovery ability that was observable under cyclic loading, indicating the occurrence of some dissipative phenomena (e.g., reduction in mechanical properties) during material deformation [63]. This can be explained by several factors, such as (i) the dissipation of energy in the fabric due to fiber–fiber friction, (ii) a weakened fiber–matrix interface due to local adhesion defects, or (iii) deformation and reorientation of fibers (strongly affected by induced shearing during loading, when the extent of fiber angle changes and in-plane deformation increases). In Figure 5d, the weaker fiber–matrix interaction caused by the emergence of several slight local detachments from the surrounding matrix in the interface area is indicated due to the different refractions of the light, whereby the corresponding fiber orientation can be predicted. This favors the formation of wrinkling as a typical behavior of textile-like composites with high flexibility, which further affects the local debonding between the fiber–matrix interaction and tends to augment viscoelastic behavior [23,64]. The results regarding the fiber–matrix interaction, pull-out behavior, and microscopy pictures of the impregnation quality of a fiber bundle with the surrounding matrix were investigated, while the effects of different fiber orientations induced by shearing and their consequences on the load coupling mechanism in flexible composites were analyzed in previous investigations [45]. With respect to the influence of the relaxation time, the experiments with 30 s relaxation time demonstrated slightly lower maximum stress values (at 25% strain) compared to those with 0 s or 10 s relaxation times, as depicted

in Figure 5b. This response could be related to the viscoelastic behavior of the elastomeric composite or to damaged induced by the local stress concentration of the fiber–matrix interface, so that recognizable stress softening is only visible above a certain relaxation time (see Figure 5b). Generally, it is evident that no significant difference related to the applied strain rate or relaxation time can be seen in the maximum stress values or for the significant stress softening in the first loading phase, which is clearly observable between the first and second cycles (see Figure 5). Accordingly, the hysteresis area W_d and corresponding dissipated energy reveal are highest in the first cycle for all strain levels. This beneficial finding can be adapted to influence either the displacement rate or the different relaxation sequences.

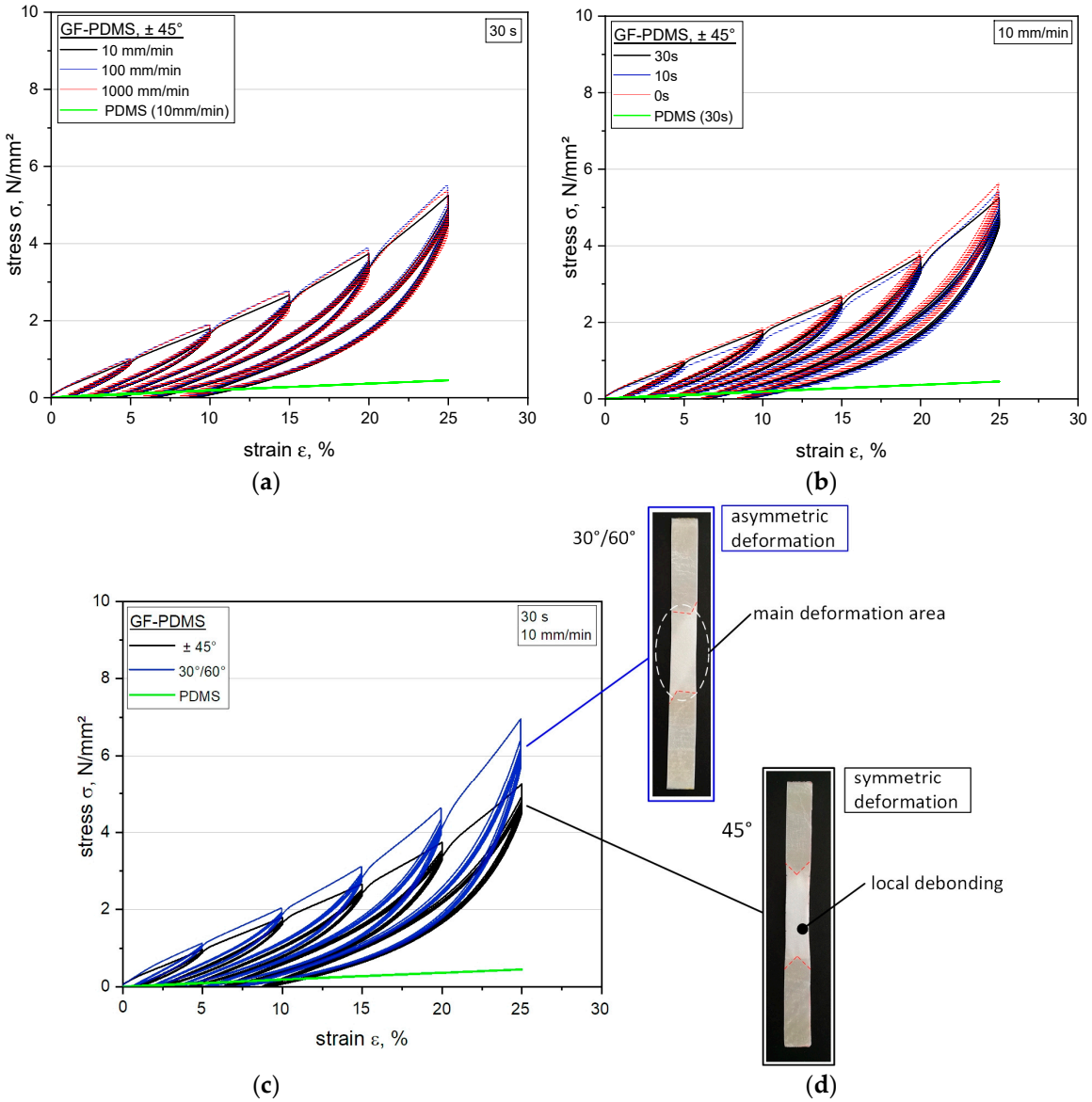

Figure 5. Comparison of stress–strain curves obtained from step cycle tests of glass fiber–silicone composites and silicone at different displacement rates (**a**), relaxation times (**b**), and the fiber orientations (**c**) with corresponding light microscope pictures after the tests (**d**).

Regarding the influence of the fiber orientation on shear stresses, as displayed in Figure 5c, the results clearly show that a decreasing fiber angle from ±45° to 30°/60° leads to an increased stiffness, and thus to a higher bearable load at equal strain levels. A comparison between both fiber orientations demonstrates that the maximum stress up to a strain of 10% differs only by about 0.3 N/mm^2 (approximately 17.5%), whereas at a higher strain level of 25%, a significantly increased stress level can

be reached with the 30°/60° orientation of about 7.1 N/mm^2, leading to a 1.9 N/mm^2 (approximately 36.5%) higher stress value than that obtained with the ±45° orientation. These findings show that despite an improved stiffness, the flexibility (given by the matrix) is maintained at a fiber orientation of 30°/60°, which has a positive effect on the fiber–matrix interface and further on the load-coupling mechanism. In this context, the material performance from step cycle tests reflects the behavior investigated with the performed DMA. In contrast, the ±45° orientation shows more matrix-dominated properties, which can be explained by the large difference between the fiber orientation and the loading direction. Thus, a larger locking angle and increased in-plane deformation inside the composite can be achieved, however this leads to more limitations regarding the maximum bearable stress level.

As an overview, the results of the step cycle tests on GF-PDMS composites are reported in Table 1, investigating decreases in the stress levels $\Delta\sigma$ and intermediate relaxation sequences $f_{\sigma,relax}$ for different values of the applied displacement rate, selected cycle loops, and maximum strain levels. The results show that a direct correlation between the stress level decrease $\Delta\sigma$ and the corresponding strain level ε is given, so that with a higher strain the $\Delta\sigma$ also increases. Moreover, the stress difference between the first and the second cycles reveals a higher stress decrease $\Delta\sigma$, showing more significant stress softening than between the fifth and sixth cycles until a new equilibrium (stable) state with a repeatable hysteresis loop is achieved. These findings can additionally be related to the relaxation sequence $f_{\sigma,relax}$ following the same trend.

Table 1. Decreases of the stress levels ($\Delta\sigma$) and the intermediate relaxation sequences ($f_{\sigma,relax}$) for different displacement rates and for selected maximum strain values and cycle numbers in step cycle tests of glass fiber–silicone composites with ±45° orientation.

V, mm/min	ε, %	Δσ, N/mm^2			$f_{\sigma,relax}$, % (30 s Relaxation)		
		Cycles 1–2	Cycles 2–3	Cycles 5–6	Cycle 1	Cycle 2	Cycle 6
10	5	0.07 ± 0.01	0.03 ± 0.00 *	0.01 ± 0.00 *	6.31 ± 0.15	3.24 ± 0.22	1.51 ± 0.04
	15	0.10 ± 0.02	0.06 ± 0.01	0.03 ± 0.00 *	7.23 ± 0.08	3.43 ± 0.25	2.35 ± 0.04
	25	0.53 ± 0.10	0.31 ± 0.08	0.06 ± 0.01	8.91 ± 0.11	4.11 ± 0.19	2.12 ± 0.03
100	5	0.07 ± 0.01	0.05 ± 0.00 *	0.02 ± 0.00 *	9.35 ± 0.60	2.91 ± 0.10	2.23 ± 0.09
	15	0.11 ± 0.05	0.06 ± 0.01	0.01 ± 0.00 *	10.51 ± 0.31	3.85 ± 0.21	3.52 ± 0.10
	25	0.51 ± 0.11	0.18 ± 0.09	0.03 ± 0.00 *	13.42 ± 0.48	5.31 ± 0.33	3.51 ± 0.12
1000	5	0.05 ± 0.00 *	0.02 ± 0.00 *	0.01 ± 0.00 *	8.93 ± 0.43	4.31 ± 0.15	2.12 ± 0.06
	15	0.14 ± 0.03	0.09± 0.01	0.01 ± 0.00 *	11.8 ± 0.52	4.20 ± 0.31	2.80 ± 0.13
	25	0.68 ± 0.10	0.27 ± 0.08	0.03 ± 0.00*	16.26 ± 0.71	5.24 ± 0.19	3.31 ± 0.09

* A certain deviation occurs after the third decimal place, therefore the standard deviation is insignificant.

The dissipated specific energy values W_d measured for GF-PDMS composites for the sixth cycle of step cycle tests (new equilibrium state) are plotted in Figure 6 as a function of the strain. As depicted, the amounts of dissipated energy (hysteresis area W_d) and viscoelastic behavior change with higher strain levels.

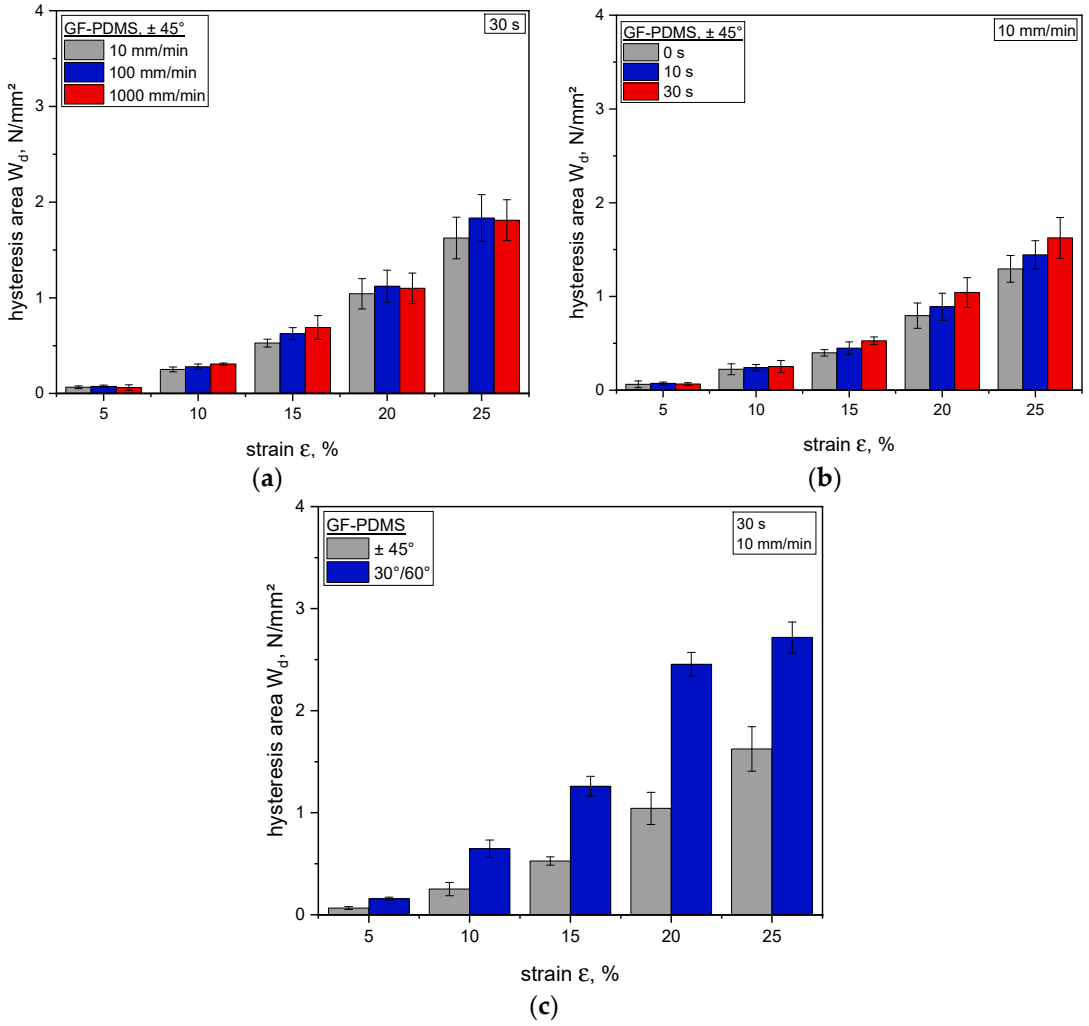

Figure 6. Comparison of hysteresis area (W_d) obtained from the sixth cycle (new equilibrium state) of the step cycle tests of glass fiber–silicone composites, dependent on the displacement rate (**a**), relaxation time (**b**), and fiber orientation (**c**).

As expected on the basis of the above reported results, different displacement rates considered at equal strain levels ε have a minor impact on the resulting hysteresis area, and thus on the dissipated energy. Based on this, a mean value of dissipated energy can be inferred, while the viscoelasticity and rebound resilience exhibit no appreciable strain rate dependency. Regarding the influence of different relaxation times on the viscoelastic performance (see Figures 5b and 6b), tests performed at 10 mm/min were considered. As seen before, the hysteresis area W_d increases with higher strain levels ε. Furthermore, it is observable that the duration of the stress relaxation step performed at the end of each loading ramp has a clear influence on the material dissipative behavior when it is then cyclically strained up to the same strain level as for the stress relaxation test. For example, at 25% strain, comparing between data relevant to relaxation times of 0 s and 30 s shows that the hysteresis area differs by more than 45 N/mm^2. Moreover, it is evident that the relaxation time has a significant effect on the hysteresis area—by increasing the relaxation time, the dissipated energy becomes larger, which leads to a decreasing rebound resilience. Further, this finding implies a reduced strain recovery, resulting in a pronounced residual strain. A reason for this behavior could be related to the viscoelastic nature of the elastomer matrix, meaning that the composite has more time to realign under tension loading, which leads to a new state due to the decreased stress, while the residual strain and dissipated energy increase (also reflected by the hysteresis area). Another possible explanation for this could be the energy dissipation due to fiber friction, as well as the presence of a locally affected interface within

the fiber–matrix adhesion favored by small defects or by already existing local detachments. Due to the contrary mechanical properties of the individual components, another factor could be the elevated inherent stiffness of the reinforcement structure, which is difficult to overcome or control compared to the hyperelastic matrix. A possible approach could be the use of special surface-treated fibers that offer optimized fiber–matrix adhesion, thus minimizing these effects. However, positive effects on the viscoelastic behavior and permanent irreversible deformation could also be possible.

In Figure 6c, the strong influence of the fiber orientation on the mechanical properties and structure–property interactions is demonstrated. The results reveal that the influence of fibers (e.g., fiber friction or fiber–matrix adhesion) is especially amplified due to the orientation, which exerts a significant effect on the viscoelastic behavior, reflecting the findings obtained from DMA (see Figure 4). In this context, the 30°/60° fiber orientation enhances the stiffness, while the corresponding amount of dissipated energy (at higher strains) also increases (in comparison with the ±45° fiber orientation). The results show that the mechanical and viscoelastic properties of fiber-reinforced elastomers are strongly influenced by the relaxation time and the fiber orientation, which strongly contribute to the final load coupling mechanism in flexible composites.

4. Conclusions

The aim of this research was to investigate the mechanical and viscoelastic properties of tailored fiber-reinforced elastomers subjected to cyclic loading. The presence of endless fibers imparts additional complexity in terms of the characterization and interpretation of the properties of flexible composites. Since the research interest in "smart materials" is constantly growing, endless-fiber-reinforced elastomers with high flexibility, in particular with silicone as the matrix material, were studied exclusively in this work. Dynamic mechanical analysis and modified step cycle tests were conducted. To investigate strain-induced stress softening and the stress relaxation behavior of the composites, step cycle tests were implemented. Additionally, a novel testing device was developed to enable the testing of highly flexible elastomer composites. A methodical test plan was elaborated to study the impacts of various relaxation times, displacement rates, strain levels, and different fiber orientations on the composite properties. Furthermore, the impacts of these parameters on the viscoelastic behavior and the effects on the reversible energy and irreversible dissipated energy were assessed.

The results of the dynamic mechanical tests demonstrate that the mechanical properties can be optimized in a specific manner depending on the fiber orientation. In this context, the stiffness can be controlled and improved without significantly impairing the properties of the matrix material (such as flexibility or structure–property interaction for the glass transition and melting temperature range). In general, all step cycle tests showed that although fibers reinforce the elastomer matrix and increases the stiffness, they also contribute to the viscoelastic behavior, which is not evident in the neat matrix, when strained in similar loading conditions. It was found that a higher strain level and relaxation time lead to an increase of the dissipated energy. In contrast, the variation of the displacement rate revealed no impact on the dissipated energy. Tests on flexible composites with different fiber angles revealed an increase of the stiffness (36.5% higher stress at 25% strain) when going from composites with a ±45° to composites with a 30°/60° fiber orientation, while barely reducing the flexibility of the composite. Finally, this reveals adequate correlations between different composite structures and various loading conditions in terms of the cyclic performance. Hence, this study contributes to better understanding the performance of elastomers reinforced with endless fibers, and therefore will help in developing tailored flexible composite materials. It also assesses the structure–property interactions of endless-fiber-reinforced elastomers and emphasizes the importance the effects of tailored load coupling mechanisms of fiber-reinforced elastomer composites on material properties.

Further research is currently ongoing, focusing on the fracture mechanics behavior of flexible composites and investigating significant parameters such as the toughness and dissipated energy due to breakage or fiber–matrix-interaction-related failure, including the effects of tailored surface-treated fibers.

Further studies are in progress to develop an accurate simulation model for cyclic-loaded fiber-reinforced elastomers, considering their viscoelastic behavior using data obtained from this study. This material model will help to simulate the material behavior and failure mechanisms of flexible composites more precisely, enabling optimization and upscaling with regard to component-like applications. Further research is already ongoing to investigate the dependence of the fiber surface on the load coupling mechanism. Therefore, different chemical surface modifications will be applied and their impacts on the cyclic performance and structure–property interactions will be studied.

Author Contributions: Literature research, investigation, formal analysis, writing—original draft preparation, J.B.; conceptualization, methodology, J.B., B.S., and C.M.; visualization J.B., B.S., and B.L.; testing, J.B. and B.L.; validation, writing—review and editing, J.B., B.S., C.M., M.R.M., and P.F.F.; supervision, project administration, C.M., B.S., P.F.F., and G.P. All authors have read and agreed to the published version of the manuscript.

Funding: This research was funded by the Federal Ministry for Climate Action, Environment, Energy, Mobility, Innovation, and Technology and the Federal Ministry for Digital and Economic Affairs, grant number 854178.

Acknowledgments: This research work was performed at the Polymer Competence Center Leoben GmbH (PCCL, Austria) and within the COMET module "Polymers4Hydrogen", within the framework of the COMET program of the Federal Ministry for Climate Action, Environment, Energy, Mobility, Innovation, and Technology and the Federal Ministry for Digital and Economic Affairs, with contributions by the Department of Polymer Engineering and Science (Montanuniversitaet Leoben, Austria). The PCCL is funded by Austrian Government and the State Government of Styria.

Conflicts of Interest: The authors declare no conflict of interest. The funders had no role in the design of the study; in the collection, analyses, or interpretation of data; in the writing of the manuscript, or in the decision to publish the results.

References

1. Neitzel, M.; Mitschang, P.; Breuer, U. Handbuch Verbundwerkstoffe. In *Werkstoffe, Verarbeitung, Anwendung*, 2nd ed.; Carl Hanser Verlag: Munich, Germany, 2014; ISBN 978-3-446-43696-1.
2. Smitthipong, W.; Suethao, S.; Shah, D.U.; Vollrath, F. Interesting green elastomeric composites: Silk textile reinforced natural rubber. *Polym. Test.* **2016**, *55*, 17–24. [CrossRef]
3. Chou, T.-W. Flexible composites. *J. Mater. Sci.* **1989**, *24*, 761–783. [CrossRef]
4. Kang, G.J.; Kang, B.-S. Dynamic analysis of fiber-reinforced elastomeric isolation structures. *J. Mech. Sci. Technol.* **2009**, *23*, 1132–1141. [CrossRef]
5. Kishi, H.; Kuwata, M.; Matsuda, S.; Asami, T.; Murakami, A. Damping properties of thermoplastic-elastomer interleaved carbon fiber-reinforced epoxy composites. *Compos. Sci. Technol.* **2004**, *64*, 2517–2523. [CrossRef]
6. Drenkelford, S. Energy-Saving Potential of Aramid-Based Conveyor Belts. Master's Thesis, Delft University of Technology, Delft, The Netherlands, 2015.
7. Moon, B.-Y.; Kang, G.-J.; Kang, B.-S.; Kelly, J.M. Design and manufacturing of fiber reinforced elastomeric isolator for seismic isolation. *J. Mater. Process. Technol.* **2002**, *130–131*, 145–150. [CrossRef]
8. Geethamma, V.; Kalaprasad, G.; Groeninckx, G.; Thomas, S. Dynamic mechanical behavior of short coir fiber reinforced natural rubber composites. *Compos. Part A Appl. Sci. Manuf.* **2005**, *36*, 1499–1506. [CrossRef]
9. Gerhaher, U. Faserverstärkte Elastomerlager—Konzeption und Bemessung. Ph.D. Thesis, Universität für Bodenkultur, Wien, Austria, 2010.
10. Peel, L. Fabrication and Mechanics of Fiber-Reinforced Elastomers. Ph.D. Thesis, Brigham Young University, Brigham, MA, USA, 1998.
11. Jin, H.; Dong, E.; Xu, M.; Liu, C.; Alici, G.; Jie, Y. Soft and smart modular structures actuated by shape memory alloy (SMA) wires as tentacles of soft robots. *Smart Mater. Struct.* **2016**, *25*, 85026. [CrossRef]
12. Kim, S.; Laschi, C.; Trimmer, B. Soft robotics: A bioinspired evolution in robotics. *Trends Biotechnol.* **2013**, *31*, 287–294. [CrossRef]
13. Chillara, V.S.C.; Dapino, M.J. Review of Morphing Laminated Composites. *Appl. Mech. Rev.* **2019**, *72*, 10801. [CrossRef]
14. Peel, L.D.; Mejia, J.; Narvaez, B.; Thompson, K.; Lingala, M. Development of a Simple Morphing Wing Using Elastomeric Composites as Skins and Actuators. *J. Mech. Des.* **2009**, *131*, 091003. [CrossRef]
15. Connolly, F.; Walsh, C.J.; Bertoldi, K. Automatic design of fiber-reinforced soft actuators for trajectory matching. *Proc. Natl. Acad. Sci. USA* **2017**, *114*, 51–56. [CrossRef]

16. Connolly, F.; Polygerinos, P.; Walsh, C.J.; Bertoldi, K. Mechanical Programming of Soft Actuators by Varying Fiber Angle. *Soft Robot.* **2015**, *2*, 26–32. [CrossRef]
17. Vocke, R.D.; Kothera, C.S.; Woods, B.K.; Wereley, N.M. Development and Testing of a Span-Extending Morphing Wing. *J. Intell. Mater. Syst. Struct.* **2011**, *22*, 879–890. [CrossRef]
18. Peel, L.D.; Baur, J.; Phillips, D.; McClung, A. The effect of scaling on the performance of elastomer composite actuators. *Proc. SPIE Int. Soc. Opt. Eng.* **2010**, *7644*, 76441W. [CrossRef]
19. Toopchi-Nezhad, H.; Tait, M.; Drysdale, R.G. Bonded versus unbonded strip fiber reinforced elastomeric isolators: Finite element analysis. *Compos. Struct.* **2011**, *93*, 850–859. [CrossRef]
20. Vassilopoulos, A.P. *Fatigue Life Prediction of Composites and Composite Structures*, 2nd ed.; Woodhead Publishing: Oxford, UK, 2019; ISBN 978-1845695255.
21. Hanif, A.; Usman, M.; Lu, Z.; Cheng, Y.; Li, Z. Flexural fatigue behavior of thin laminated cementitious composites incorporating cenosphere fillers. *Mater. Des.* **2018**, *140*, 267–277. [CrossRef]
22. Castillo, E.; Fernández-Canteli, A. *A Unified Statistical Methodology for Modeling Fatigue Damage*; Springer: Dordrecht, The Netherlands, 2009; ISBN 978-1-4020-9182-7.
23. Mansouri, M.; Fuchs, P.; Criscione, J.; Schrittesser, B.; Beter, J. The contribution of mechanical interactions to the constitutive modeling of fiber-reinforced elastomers. *Eur. J. Mech. A Solids* **2020**, *85*, 104081. [CrossRef]
24. Mansouri, M.; Fuchs, P.F.; Schuecker, C. Hyperelastic modeling of woven structures undergoing large deformations. In Proceedings of the 18th European Conference on Composite Materials (ECCM18), Athen, Greece, 25–28 June 2018.
25. Ehrenstein, G.W.; Riedel, G.; Trawiel, P. *Praxis der Thermischen Analyse Von Kunststoffen*, 2nd ed.; Carl Hanser Verlag: Munich, Germany, 2003; ISBN 978-3-446-22340-0.
26. Gent, A.N. Engineering with Rubber. In *How to Design Rubber Components*, 3rd ed.; Carl Hanser Verlag: Munich, Germany, 2012; ISBN 978-3-446-42871-3.
27. Fleischmann, D.D.; Arbeiter, F.; Schaller, R.; Holzner, A.; Kern, W.; Schlögl, S. Influence of crosslinker and water on cyclic properties of carboxylated nitrile butadiene rubber (XNBR). *Polym. Test.* **2018**, *67*, 309–321. [CrossRef]
28. Diani, J.; Fayolle, B.; Gilormini, P. A review on the Mullins effect. *Eur. Polym. J.* **2009**, *45*, 601–612. [CrossRef]
29. Almeida, J.H.S., Jr.; Ornaghi, H.L., Jr.; Amico, S.C.; Amado, F.D.R. Study of hybrid intralaminate curaua/glass composites. *Mater. Des.* **2012**, *42*, 111–117. [CrossRef]
30. Guo, C.; Song, Y.-M.; Wang, Q.-W.; Shen, C.-S. Dynamic-mechanical analysis and SEM morphology of wood flour/polypropylene composites. *J. For. Res.* **2006**, *17*, 315–318. [CrossRef]
31. Hassan, A.; Rahman, N.A.; Yahya, R. Extrusion and injection-molding of glass fiber/MAPP/polypropylene: Effect of coupling agent on DSC, DMA, and mechanical properties. *J. Reinf. Plast. Compos.* **2011**, *30*, 1223–1232. [CrossRef]
32. Liu, Y.; He, M.; Qin, S.-H.; Yu, J. Effect of fiber length and dispersion on properties of long glass fiber reinforced thermoplastic composites based on poly(butylene terephthalate). *RSC Adv.* **2017**, *7*, 15439–15454. [CrossRef]
33. Vleugels, N. Short Fibre-Reinforced Elastomeric Composites: Fundamental Routes towards Improvement of the Interfacial Interaction of Short-Cut Aramid Fibres in a SBR Compound, to Improve Friction and Wear Properties. Ph.D. Thesis, University of Twente, Enschede, The Netherlands, 2017.
34. Song, Y.S.; Lee, J.T.; Ji, D.S.; Kim, M.W.; Lee, S.H.; Youn, J.R. Viscoelastic and thermal behavior of woven hemp fiber reinforced poly(lactic acid) composites. *Compos. Part B Eng.* **2012**, *43*, 856–860. [CrossRef]
35. Liu, M.H.; Li, R.; Wang, G.; Hou, Z.Y.; Huang, B. Morphology and dynamic mechanical properties of long glass fiber-reinforced polyamide 6 composites. *J. Therm. Anal. Calorim.* **2016**, *126*, 1281–1288. [CrossRef]
36. Cordin, M.; Bechtold, T.; Pham, T. Effect of fibre orientation on the mechanical properties of polypropylene–lyocell composites. *Cellulose* **2018**, *25*, 7197–7210. [CrossRef]
37. Jawaid, M.; Khalil, H.A.; Hassan, A.; Dungani, R.; Hadiyane, A. Effect of jute fibre loading on tensile and dynamic mechanical properties of oil palm epoxy composites. *Compos. Part B Eng.* **2013**, *45*, 619–624. [CrossRef]
38. Saha, A.K.; Das, S.; Bhatta, D.; Mitra, B.C. Study of jute fiber reinforced polyester composites by dynamic mechanical analysis. *J. Appl. Polym. Sci.* **1999**, *71*, 1505–1513. [CrossRef]

39. Prioglio, G.; Agnelli, S.; Conzatti, L.; Balasooriya, W.; Schrittesser, B.; Galimberti, M. Graphene Layers Functionalized with a Janus Pyrrole-Based Compound in Natural Rubber Nanocomposites with Improved Ultimate and Fracture Properties. *Polymers* **2020**, *12*, 944. [CrossRef]
40. Göktepe, S. Micro-Macro Approaches to Rubbery and Glassy Polymers: Predictive Micromechanically-Based Models and Simulations. Ph.D. Thesis, Universität Stuttgart, Stuttgart, Germany, 2007.
41. Sedlan, K. Viskoelastisches Materialverhalten von Elastomerwerkstoffen: Experimentelle Untersuchung und Modellbildung. Ph.D. Thesis, Universität Gesamthochschule Kassel, Kassel, Germany, 2000.
42. Gao, J.; Yang, X.; Huang, L.; Suo, Y. Experimental study on mechanical properties of aramid fibres reinforced natural rubber/SBR composite for large deformation—Quasi-static mechanical properties. *Plast. Rubber Compos.* **2018**, *47*, 381–390. [CrossRef]
43. Jiménez, F.L.; Pellegrino, S. Folding of fiber composites with a hyperelastic matrix. *Int. J. Solids Struct.* **2012**, *49*, 395–407. [CrossRef]
44. Cherif, C. Textile Werkstoffe für den Leichtbau. In *Techniken—Verfahren—Materialien—Eigenschaften*, 1st ed.; Springer: Berlin, Germany, 2011; ISBN 978-3-642-17992-1.
45. Beter, J.; Schrittesser, B.; Meier, G.; Fuchs, P.F.; Pinter, G. Influence of Fiber Orientation and Adhesion Properties On Tailored Fiber-reinforced Elastomers. *Appl. Compos. Mater.* **2020**, *27*, 149–164. [CrossRef]
46. Liao, M.; Yang, Y.; Hamada, H. Mechanical performance of glass woven fabric composite: Effect of different surface treatment agents. *Compos. Part B Eng.* **2016**, *86*, 17–26. [CrossRef]
47. Beter, J.; Schrittesser, B.; Maroh, B.; Sarlin, E.; Fuchs, P.F.; Pinter, G. Comparison and Impact of Different Fiber Debond Techniques on Fiber Reinforced Flexible Composites. *Polymers* **2020**, *12*, 472. [CrossRef]
48. Beter, J.; Schrittesser, B.; Grassegger, F. *Klemmvorrichtung und Verfahren zur Prüfung Einer Zugfestigkeit Eines Objektes*; A50009/2020; Austrian Patent Office: Vienna, Austria, 20 January 2020.
49. Muliana, A.H.; Rajagopal, K.R.; Tscharnuter, D.; Schrittesser, B.; Saccomandi, G. Determining Material Properties of Natural Rubber Using Fewer Material Moduli in Virtue of a Novel Constitutive Approach for Elastic Bodies. *Rubber Chem. Technol.* **2018**, *91*, 375–389. [CrossRef]
50. Hanif, A.; Kim, Y.; Park, C. Numerical Validation of Two-Parameter Weibull Model for Assessing Failure Fatigue Lives of Laminated Cementitious Composites—Comparative Assessment of Modeling Approaches. *Materials* **2018**, *12*, 110. [CrossRef] [PubMed]
51. Beter, J.; Schrittesser, B.; Fuchs, P.F. Investigation of adhesion properties in load coupling applications for flexible composites. *Mater. Today Proc.* **2020**. [CrossRef]
52. American Society for Testing and Materials. *ASTM D2256-02:2015: Test Method for Tensile Properties of Yarns by the Single-Strand Method*; American Society for Testing and Materials: West Conshohocken, PA, USA, 2015.
53. International Organization for Standardization. *ISO 37:2011-12: Rubber, Vulcanized or Thermoplastic—Determination of Tensile Stress-Strain Properties*; International Organization for Standardization: Geneva, Switzerland, 2011.
54. International Organization for Standardization. *ISO 527-4:1997: Plastics. Determination of Tensile Properties*; International Organization for Standardization: London, UK, 1997.
55. Hoffmann, J. Characterization of Fibre Reinforced Elastomers for Shape Morphing Structural Surfaces. Ph.D. Thesis, Technical University of Munich, München, Germany, 2012.
56. International Organization for Standardization. *ISO 6721-1:2019-04: Plastics—Determination of Dynamic Mechanical Properties*; International Organization for Standardization: Berlin, Germany, 2019.
57. International Organization for Standardization. *ISO 4664:2011-11: Rubber, Vulcanized or Thermoplastic—Determination of Dynamic Properties*; International Organization for Standardization: Berlin, Germany, 2011.
58. International Organization for Standardization. *ISO 291:2008-08: Plastics—Standard Atmospheres for Conditioning and Testing*; International Organization for Standardization: Berlin, Germany, 2008.
59. Röthemeyer, F.; Sommer, F. *Kautschuk—Technologie. Werkstoffe—Verarbeitung—Produkte*, 3rd ed.; Carl Hanser Verlag: Munich, Germany, 2013; ISBN 978-3-446-43776-0.
60. Calabrò, R. Mechanical Characterization of Elastomers under Quasi-Static and Dynamic Biaxial Loading Conditions. Ph.D. Thesis, Politecnico di Milano, Milan, Italy, 2013.
61. Domininghaus, H.; Elsner, P.; Eyerer, P.; Hirth, T. *Kunststoffe. Eigenschaften und Anwendungen*, 8th ed.; Springer: Berlin, Germany, 2012; ISBN 978-3-642-16173-5.

62. Ehrenstein, G. *Polymer-Werkstoffe. Struktur; Eigenschaften; Anwendung*, 3rd ed.; Carl Hanser Verlag: Munich, Germany, 2011; ISBN 978-3-446-42283-4.
63. Abts, G. *Einführung in die Kautschuktechnologie*; Carl Hanser Fachbuchverlag: Munich, Germany, 2019; ISBN 978-3-446-45461-3.
64. Yang, Y.; Fu, C.; Xu, F. A finite strain model predicts oblique wrinkles in stretched anisotropic films. *Int. J. Eng. Sci.* **2020**, *155*, 103354. [CrossRef]

3.7 Paper 6: The tension-twist coupling mechanism in flexible composites: A systematic study based on tailored laminate structures using a novel test device

Julia Beter[1,*], Bernd Schrittesser[1], Gerald Meier[1], Bernhard Lechner[1], Mohammad Reza Mansouri[1], Peter Filipp Fuchs[1] and Gerald Pinter[2]

[1] Polymer Competence Center Leoben GmbH, Roseggerstrasse 12, 8700 Leoben, Austria.

[2] Department of Polymer Engineering and Science, Montanuniversitaet Leoben, Otto- Gloeckel- Strasse 2, 8700 Leoben, Austria.

Published in Polymers, 2020, 12(12), 2780.

DOI: 10.3390/polym12122780

polymers

MDPI

Article

The Tension-Twist Coupling Mechanism in Flexible Composites: A Systematic Study Based on Tailored Laminate Structures Using a Novel Test Device

Julia Beter [1,*], Bernd Schrittesser [1], Gerald Meier [1], Bernhard Lechner [1], Mohammad Mansouri [1], Peter Filipp Fuchs [1] and Gerald Pinter [2]

[1] Polymer Competence Center Leoben GmbH, Roseggerstrasse 12, 8700 Leoben, Austria; Bernd.Schrittesser@pccl.at (B.S.); Gerald.Meier@pccl.at (G.M.); Bernhard.Lechner@pccl.at (B.L.); Mohammad.Mansouri@pccl.at (M.M.); PeterFilipp.Fuchs@pccl.at (P.F.F.)

[2] Department of Polymer Engineering and Science, Montanuniversitaet Leoben, Otto Gloeckelstrasse 2, 8700 Leoben, Austria; Gerald.Pinter@unileoben.ac.at

* Correspondence: Julia.Beter@pccl.at; Tel.: +43-3842-42962-31

Received: 6 November 2020; Accepted: 22 November 2020; Published: 24 November 2020

Abstract: The focus of this research is to quantify the effect of load-coupling mechanisms in anisotropic composites with distinct flexibility. In this context, the study aims to realize a novel testing device to investigate tension-twist coupling effects. This test setup includes a modified gripping system to handle composites with stiff fibers but hyperelastic elastomeric matrices. The verification was done with a special test plan considering a glass textile as reinforcing with different lay-ups to analyze the number of layers and the influence of various fiber orientations onto the load-coupled properties. The results demonstrated that the tension-twist coupling effect strongly depends on both the fiber orientation and the considered reinforcing structure. This enables twisting angles up to 25° with corresponding torque of about 82.3 Nmm, which is even achievable for small lay-ups with 30°/60° oriented composites with distinct asymmetric deformation. For lay-ups with ±45° oriented composites revealing a symmetric deformation lead, as expected, no tension-twist coupling effect was seen. Overall, these findings reveal that the described novel test device provides the basis for an adequate and reliable determination of the load-coupled material properties between stiff fibers and hyperelastic matrices.

Keywords: flexible composite; fiber-reinforced elastomer; load-coupling mechanism; bending-extension coupled structures; extension-shear coupling effect

1. Introduction

The demand for customized products that are tailored to meet specific requirements is continually growing. Due to the increase in efficiency, weight reduction and performance, lightweight designs are receiving increased interest in numerous applications. Hence, conventional materials are reaching their application limits, which creates the need to focus on multi-material solutions [1,2]. Especially for elastomers, the additional integration of reinforcing structures has already led to promising concepts enabling higher bearable loads while good flexibility, damping and absorption performance are still retained [3]. This approach has been successfully applied in the industry such as automotive tires [4], conveyor belts [5] or fiber-reinforced elastomeric seismic isolators [6,7]. Advancing from traditional composite, the basic idea of "learning from nature", e.g., nacre mimetic nanostructures [8] or staggered model [9], is also pursued in the design of new composite structures. The implementation of methods, designs, and processes from nature with suitable transfer criteria into various fields of engineering is

described as biomimetics [10]. Recent scientific approaches have demonstrated interesting concepts by implementing fiber-reinforced elastomers with distinct hyper-elasticity as so-called smart materials. The concept of these soft matter applications can be found in the field of aerospace or automotive industries as aeroelastic wings [11,12] with the ability to serve multiple functions for optimized aerodynamic performances. Another aspect for the usage of morphing structures are in soft robotic applications such as exoskeletons [13] or artificial fingers [14], where sufficient strength combined with significant large deformations have to be ensured. The crucial challenge is to apply the right material, fiber-matrix material combination and resulting functionality in order to find the best solution. Especially for soft matter applications, the combination of elastomers with controlled oriented reinforcement can generate advanced composites with distinct direction-dependent properties. Whilst the acting energy can be merged or the resulting force redirected, no damage is initiated and the energy might even be used favorably [14–16]. The state of the art regarding current developments for stimuli-responsive materials with load-coupling effects enhanced by external triggers can be structured into four classes relying on: (i) pressure (pneumatically or hydraulic) [17,18], (ii) electrically [19,20], (iii) temperature [16,21] and (iv) mechanically [22,23] initiated deformation. Most of the work has been done on pressure or temperature triggered load-coupled effects, which are often hybridized with an electrical trigger [24–26], except if the electricity is not exclusively implemented as e.g., piezoelectric generated effect to enable shape-memory effects [27,28]. However, the focus is mainly put on the demonstration and feasibility of demonstrators [29,30], whilst the mechanical properties related to structure-property interactions, especially for microstructure analysis, are considered in a limited way [31,32]. Therefore, profound knowledge and an adequate quantitative investigation regarding the performance and mechanical behavior of fiber reinforced elastomers combined with an external trigger is necessary. Since the ability of load transfer between the fibers and the matrix is crucial to analyze load-coupling mechanisms, a tailored fiber orientation as well as an optimized interfacial fiber-matrix bonding is indispensable to ensure an adequate adhesion with an intended load-coupling [23,33].

The classical laminate theory (CLT) as a material law for the prediction of stiffness and stress in multilayer composites offers a well-established method to quantify stress-deformation couplings of composite materials numerically [34,35]. Since this material law is based on Kirchhoff's plate theory [35], simplifications and boundary conditions, such as linear elasticity and ideal composite conditions, are unavoidable [23,36]. Extensive studies including the CLT for thermoset-based composites have already been carried out. However, this material law cannot be transferred directly into flexible composite materials, which possess a significant textile-like behavior [22,37]. Compared to stiff matrices, fiber reinforced elastomers show further beneficial aspects regarding the damage performance by showing a significant broader motion range, especially when it comes to bending or twisting coupled behavior [34]. Due to the hyperelastic matrix, the distinct greater mobility of the embedded fibers can induce local stress concentrations by out-of-plane wrinkling, which results in folding or buckling. This behavior may lead to a local fiber-matrix debonding at micro scale without resulting into a complete failure or premature composite breakage induced by delamination like for thermoset-based composites [38–40]. Recent studies on soft morphing structures with anisotropic properties using bend-twist or bend-extension coupling described the need of a modified formulation of the CLT, as stiffness and strength of fibers and elastomers differ significantly [34,37,41]. Subsequently, the right choice of the test device with a corresponding setup is crucial to determine exact material properties of highly flexible composites. Most of the existing measurement devices for fiber reinforced composites are limited to thermoset-based matrices, which cannot fulfill the required test conductions due to local stress concentrations, slippage or pre-damages by inappropriate clamps [38,42]. These test methods related to thermoset-based composites and their load-coupled properties assume that clamping induced compressive stresses can be neglected [41,43]. In this context, additional tabs with a certain tab taper angle are typically considered for a better load transfer and uniform deformation distribution during the test. However, those are not applicable for fiber reinforced elastomers due to the high necking, which leads to an interface release between sample and the tab [44,45]. As the stiffness and strength

of fibers and the elastomer matrix differ significantly, the mechanical properties are much more complex to determine and crucial for evaluating the fiber-matrix adhesion [1,46]. Moreover, to trigger load-coupling mechanisms in flexible composites effectively, an in-depth knowledge of the fiber-matrix bonding and mechanical performance of single-fiber, fiber-bundle and simple composite structures within the principle of a test chain constituting the aspects from model- and component level are required [47]. Recent studies on fiber reinforced silicones were carried out focusing on the properties of the fiber-matrix interface and reported on the challenge of dealing with hyperelastic elastomers [48].

The aim of this research is to investigate the mechanical properties of tailored fiber-reinforced elastomers triggered by tension-twist coupling effects. A newly developed test setup is designed to avoid negative clamping or other influences e.g., local stress concentrations, slippage or premature failure, whilst providing a convenient, fast and reliable method. Since endless fibers encapsulated in elastomer increase the complexity for the material characterization, the main challenge is to overcome the hyperelasticity, which implies a limited inherent stiffness. One focus was on the verification of the new load-coupling test device to study the distortion stresses and twisting induced by an external force. Thus, several parameters and their influence on the load-coupling were analyzed by a test plan including fiber orientation, lay-up and stacking sequence. Based on this, the possibility to obtain the indicating parameters of maximum tension force and torque including the associated twisting was proven. The generated customized material parameters provide the basis for further numerical elastic body simulations based on well-established composite material laws, e.g., CLT, and to emphasize tailored performance predictions.

Theoretical Background for Load Coupled Structures and Design Principles

In general, flexible composites or so-called smart materials, are designed by combining the characteristics of anisotropic materials with soft morphing structures [37,41]. By exploiting these structure-properties, the interaction of different components is indispensable considering the rigid fibers as anisotropic reinforcement, the soft matrix and the mandatory trigger e.g., mechanical or pneumatical initiated as an external stimulus. The interaction of all individual elements in total generates and quantifies the intended load-coupling mechanism [34]. The stiffness towards twist as well as the in-plane shear strength of the flexible composite related to different directions is controlled by the force transmission of the anisotropic oriented fibers versus the viscoelastic behavior of the matrix [33,49]. Hence, the CLT represents a computational tool to describe overall deformations. These findings on load-coupled effects can be integrated featuring any combination of in-plane deformation, out-of-plane deformation, and twisting in the flexible composites. Following the purely formal derivation of the CLT, this can be written according to Equation (1), where the layer structure is basically described by the material law of the single layer. Thus, a correlation is established between the internal forces **n** and moments **m** of the laminated plies, the elasticity parameters constituting the layer built-up, and distortions ε as well as curvatures κ of the intermediate surfaces inside the composite [34,35].

$$\begin{bmatrix} \mathbf{n} \\ \mathbf{m} \end{bmatrix} = \begin{bmatrix} A & B \\ B & D \end{bmatrix} \begin{bmatrix} \varepsilon \\ \kappa \end{bmatrix} \quad (1)$$

The combination of matrices A, B and D is also known as the stiffness matrix K. For different occurring extents of symmetry of material properties depending on the stress-strain relationship and the corresponding anisotropic composite structure, the subsequent reduction in the number of elastic constants in the stiffness matrix needs to be considered [35]. In this context, the determination of the material data parameters with a new test device have to fulfill these requirements. Matrix A equals the strain stiffness (in-plane moduli) connecting the load transfer with the distortion of the intermediate surfaces and thus, contains the elasticity law that connects in-plane loads to in-plane strains. Furthermore, matrix D represents the bending stiffness matrix, which links the moments of elongation with the curvatures of the intermediate surfaces. Matrix B is consequentially combining the curvatures of the intermediate surfaces with the normal and shear force transition, whilst the distortions

of the mid-surfaces is linked to the intersection moments and is referred as the matrix of coupling stiffness [34,35]. Due to this, the load transmission leads to specific distortion of the intermediate surfaces as well as to associated curvatures (also in reverse conclusion). A graphic illustration of the deformation concept versus subsequent distortion possibilities is schematically shown in Figure 1. For composite materials with a pronounced flexibility, further challenges occur, which are unavoidable and inherent to the material characteristics and can lead to considerable influences, such as trellis effects and maximum locking angle induced wrinkling. These phenomena have been investigated in detail in previous studies based on quasi-static tensile tests [45,47]. The results reveal a correlation between the maximum bearable in-plane shearing until out-of-plane shearing (wrinkling or the trellis effect) occurs. The main reason for this is the deformation obstruction due to the conventional rigid clamping system of the used test setup, which suppresses a twist and inevitably leads to the trellis effect [50]. Using a movable or semi-movable test device, these generated deformation-induced stresses will be relieved within a twist or bending motion, which results in a load-coupling mechanism [35].

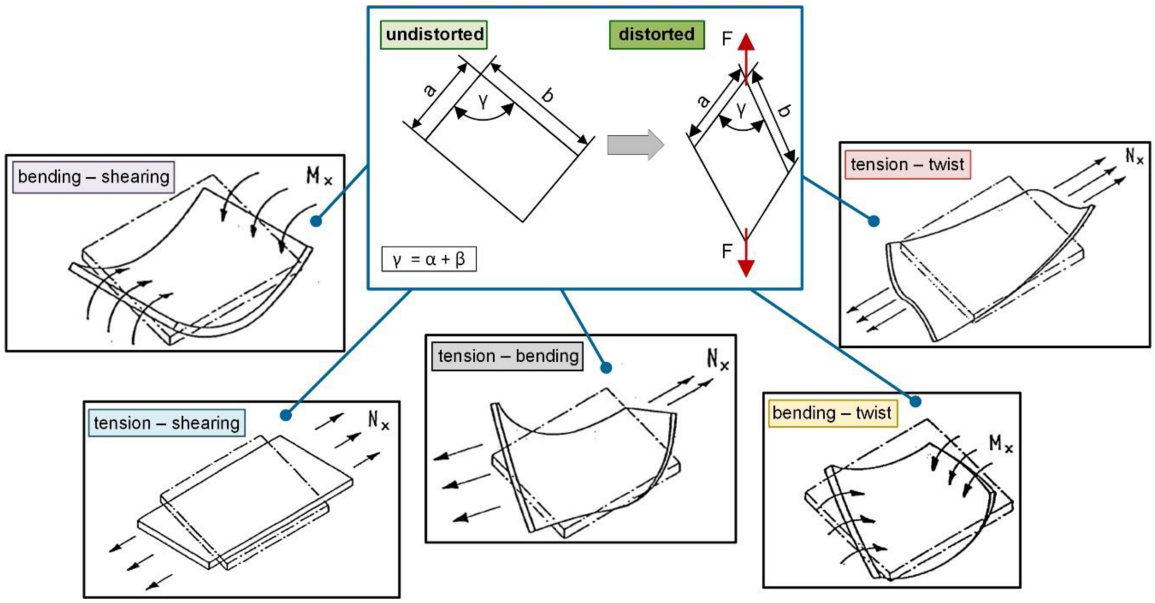

Figure 1. Schematic illustration of distortion processes (undistorted versus distorted) and corresponding deformation possibilities of bending, shearing, twist or tension depending on the load-coupling related to the material's law for fiber reinforced composites [35].

2. Materials and Methods

2.1. Reinforcement

Commercial E-type glass fibers used in this study were provided from CS Interglas AG (Erbach, Germany) with a twine thickness in warp and weft-direction of about 68 tex. A textile from a single batch and with a plain weave exhibits an area bundle distribution of 50/50 in the 0°/90° direction yielding an area weight of 220 g/m^2 ± 5%. The filaments comprised a mean diameter of 10 µm and were modified with a standard industrial silane-based surface sizing (FK144). Moreover, the mechanical properties of glass fibers were investigated by standardized tensile tests according to ASTM D2256 [51] using a universal testing machine (Series 5500, Instron GmbH, Darmstadt, Germany). The tests were performed with the settings of a 1 kN load cell, a free gauge length of 250 mm and a crosshead speed of 300 mm/min including a pneumatically controlled mandrel type clamping system for fixing the fibers. Additional rubber pads were required to protect the fibers from any pre-damage in the clamping area as well as a preload of 1 N to ensure identical initial test conditions.

2.2. Matrix Material

Elastosil RT601 A/B was used as matrix material and was obtained from Wacker Chemie AG (Munich, Germany). Elastosil RT601 A/B is a hyperelastic two-component polydimethylsiloxane (PDMS), (the prepolymer, part A and crosslinking system, part B comprising a platinum catalyst). Based on the characteristic inorganic structure and organic groups with siloxane units, PDMS represents a good intermediate position between inorganic and organic compounds. Due to the exploitation of these structural properties, the stronger bonding energy of PDMS in combination with glass fibers (GF) results in an enhanced interfacial adhesion, which consequently influences the flexible composite properties, particularly for the investigation of load-coupling effects. Thus, further effects caused by fillers or material morphology can be reduced. For the formation of the PDMS network, a mixing ration of 9:1 (part A: part B) was applied. According to the manufacturer's recommendations, the uncured elastomer formulation degassed under vacuum to avoid any air bubbles or inclusions. The curing and polymerization were carried out at 70 °C for 60 min in an air circulating drying oven. Furthermore, the mechanical properties of PDMS were evaluated in standardized uniaxial tensile tests according to ISO 37 [52] with the corresponding specimen geometry of type 2 by utilizing a universal testing machine (Z010, Zwick Roell GmbH & Co. KG, Ulm, Germany) equipped with a 500 N load cell. The gauge length was set to 50 mm with a measuring length of 20 mm and a test speed of 10 mm/min including a pneumatically controlled clamping unit.

2.3. Shear Stresses Coupled by Fiber Orientation

In particular, during the deformation process of fabrics, shearing is an important influencing factor, which is strongly affected by the fiber orientation and thus, emerges whenever the orientation differs from the loading direction of the external acting force. In this context, three main zones (A, B and C) occur in the textile through an applied load, which obtain significant different deformation modes and are schematically illustrated in Figure 2 [44,53].

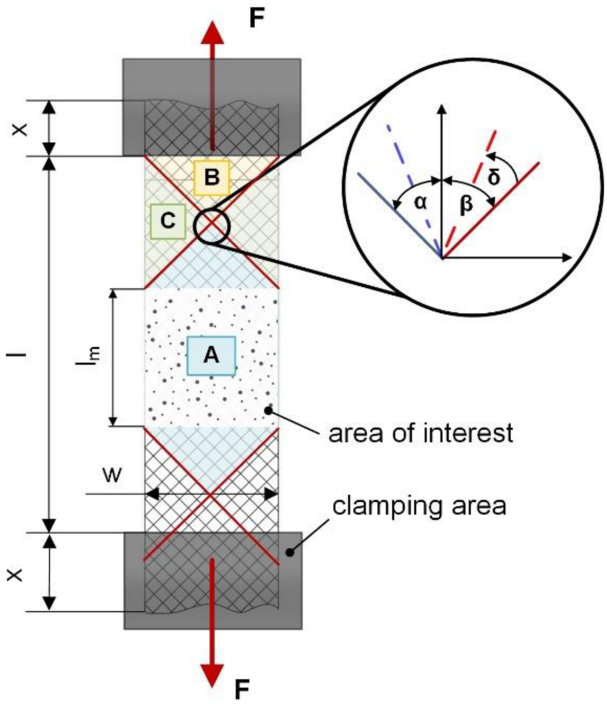

Figure 2. The three main shear zones (A, B and C) corresponding to the exemplary ±45° fiber orientation in a composite tensile test configuration [44] and the explanation of the in-plane shearing effect with the shear angel δ on undistorted (blue and red line) and distorted (dashed blue and red line) fibers [47].

The area of zone A comprises no impaired fibers, since all fibers are unaffected by grips and only connected via weave points (between warp- and weft yarns) by the surrounding elastomeric matrix whilst the necessary adhesion is achieved by the matrix and supported through e.g., friction or ondulation effects. Thus, this region is defined as clamping stress free and deformation is only constituted by the present shearing [53]. In contrast to this, zone B is not deformed due to the clamping, where fixed fibers are hindered in shearing. However, zone C contains partially constrained and unfixed fibers, which represents a sort of mixed type of shear and elongation [44]. Based on this, composites with strong textile behavior lead to pronounced out-of-plane deformation after exceeding a certain threshold value (locking angle) [44,54]. This causes wrinkling especially in rigid test, since bending or twisting motion is inhibited during progressive deformation. This effect is termed as the trellis effect which is related to the fiber orientation and the composite lay-up [54]. The in-plane and out-of-plane shearing versus the trellis effect in fiber reinforced elastomers was investigated in detail in previous studies [47].

2.4. Specimen Preparation and Test Method

For better comparability and to minimize any negative influences concerning the manufacturing of the composite test specimens, a vacuum resin infusion (VARI) process was chosen [33,47]. The maximum feasible pressure during the impregnation and consolidation phase was set with about 0.1 MPa (atmosphere pressure) [2,55]. The used mold release agent (Mono-Coat 1625W) was provided by Chem-Trend GmbH (Maisach, Germany). The cutting step of the reinforcement layers was carried out with a professional cutter (G3 M-1600, Zünd Systemtechnik AG, Altstaetten, Switzerland), which is additionally equipped with vacuum table to minimize fiber undulations or drape defects. Due to the high viscosity of the uncured PDMS besides the presence of vacuum, permeable lines, flow help and a perforated release film are mandatory to achieve a good laminate quality. After the curing step, the GF-PDMS composite plates were demolded and rectangular specimens were prepared with the cutter. All samples consist two layers of reinforcement regardless the implemented fiber orientation in the subsequent tests.

Based on previous studies [47] focusing on tailored fiber-reinforced elastomers with different fiber orientations and their influence on structure-property interactions and adhesion properties, composite tension tests with a specific width to length ratio were used to analyze the in-plane shearing. The results showed a significant effect caused by different fiber orientations and obtained that an out of plane deformation starts to occur sooner if the textile is unbalanced related to stresses. This leads to distortion inhibitions and further to load-coupling effects. In order to establish a definite comparability with the conducted tensile tests, the width to length ratio of 1:3 is implemented for these tests [47]. In this context, the gauge length is defined as the distance between the clamps in the testing machine and set to 45 and 90 mm. The measurement length corresponds to 20 mm and was recorded optically due to the textile-like behavior.

To determine load-coupling mechanisms in flexible composites, a new test setup was developed to accommodate the high flexibility as well as to be able to implement the test device in conventional testing machines (see Figure 3). Furthermore, this device has to prevent slippage or clamp-induced damage during the tests to avoid further stresses which leads to misleading results and premature material failure. Conventional pneumatic grips with one side closing function (Zwick Roell GmbH and Co. KG, Ulm, Germany) are not suitable and a modified clamping system had to be considered. Thus, another challenge is the accurate specimen position to avoid any negative effects related to tilting or asymmetrical stress distribution. Therefore, the modified clamping system is able to prevent this mechanism and ensures a loading situation self-aligned along the machine axis. The developed test setup is designed in order to measure a torsional moment in fixed mode and a twist angle in rotating mode. In this context, sensors are an essential tool for data recording to adequately describe these two states. Subsequently, corresponding measuring units are implemented using a torque sensor 9339A provided by Kistler Group (Winterthur, Switzerland) with a designated measuring range between

−10 Nm and 10 Nm and an angle sensor AEDB-9340 series from Avago Technologies (Broadcom Inc, San Jose, CA, USA). This novel test setup is replacing the lower clamping unit, whilst the upper clamping comprises the standard pneumatically driven grips from Zwick enhanced additionally with a special fixing unit [42] especially for fiber reinforced elastomers. Due legal reasons, any further information or visual illustration of the test setup cannot be provided regarding the current patenting process, since this presented assembly is a special concept that is designed to switch between fixed and rotating mode enabling measurements of torque and twist including a modified clamping system, which ensures sufficient clamping especially for such flexible composites.

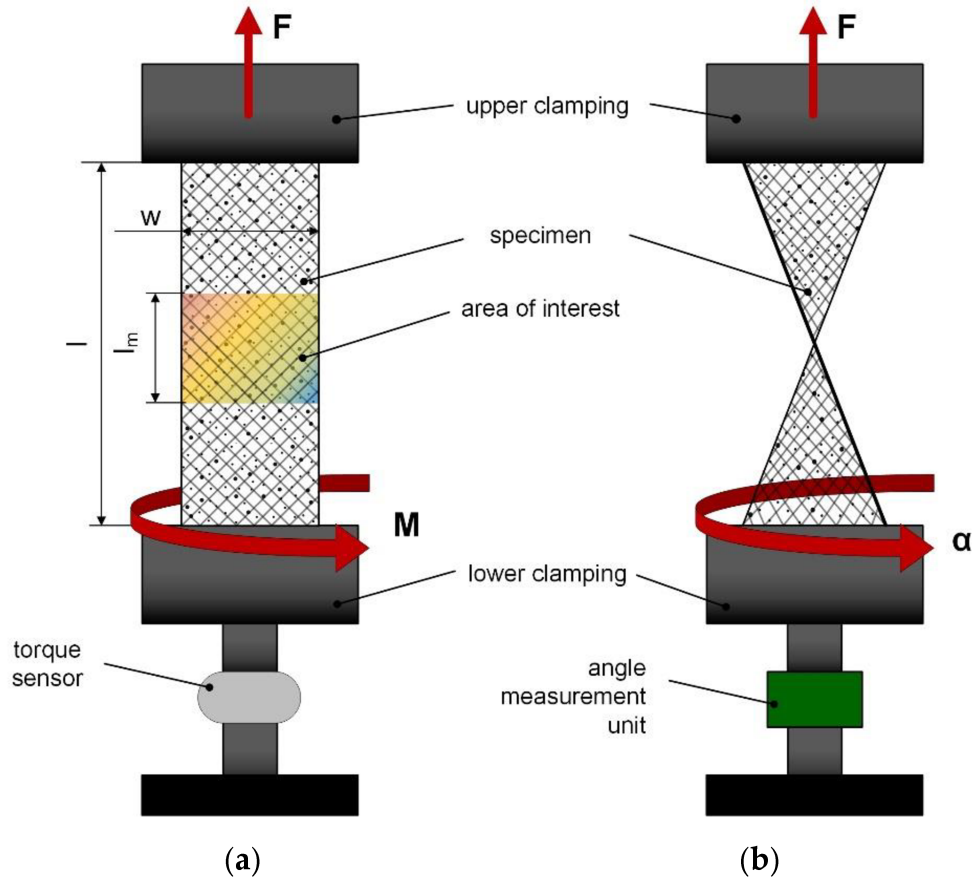

Figure 3. Schematic measurement procedure of tension-twist load coupling test principle on glass fiber-polydimethylsiloxane (GF-PDMS) composite specimens in fixed mode (**a**) for measuring the torque M and in movable mode (**b**) for measuring the twist angle α triggered by external tension force.

All tests were performed at standard atmosphere conditions according to ISO 291 (20 °C, 50% r.h.) [56] with a constant displacement rate of 10 mm/min. The tests were conducted with a universal testing machine (Zwick Roell GmbH and Co. KG, Ulm, Germany) equipped with a 10 kN load cell. The composite specimens were deformed to a maximum elongation of 20% in order to ensure an almost unaffected fiber-matrix bonding, since in zone A the load is transferred only by shearing [57] in the weave points of the textile and Elastosil RT601 A/B shows linear elasticity until approximately 40% deformation [55] and thus a reliable load-coupling is provided. For the subsequent data interpretation, the average value of three specimens for each setting was calculated. To ensure equal test and the same initial starting conditions during the experiments, a preload of 1 N was considered.

For the evaluation of the load-coupling, further effects of viscoelasticity in flexible composites [33,49] are reduced by the constant set test speed. Due to that, a methodically validated test plan was developed, where the fiber orientation was set depending on the considered reinforcing structure. Therefore, the orientations ±45°, 30°/60° and a combination of both 30°/60° and ±45° (henceforth written as

30°/60°//±45°) related to previous findings on numerical simulation models [58] were chosen for the composite lay-up with textile. In order to determine the maximum bearable twist angle and corresponding torque, both gauge lengths were considered in addition due to the high flexible behavior of these composites, since the form stability and the distinct textile-like character can be influenced significantly.

2.5. Optical Analysis

Supplementary optical analysis including light microscopy of the composite samples to support the comparability and interpretation of the performed tests was performed prior to (as reference purpose) and directly after the load-coupling test to prove the unaffected fiber-matrix interface and to avoid further environmental influences. Regarding the pronounced elasticity of the flexible composite as well as to record deformation behavior in three dimensions, the strain ratio and twist was measured together with a digital image correlation system (Prosilica GT 6600, Allied Vision Technologies GmbH, Stadtroda, Germany) along with the implemented sensors. Moreover, a sprayed pattern was used on the sample surface to achieve a higher accuracy in data.

3. Results and Discussion

In previous work, promising and reliable results were achieved using a modified test setup for tension tests on flexible composites to investigate the feasibility as well as the effect of different fiber orientations on wrinkling caused by trellis effects [47]. Based on these findings, the following study focuses on the realization and verification of a new test setup to determine tailored tension-twist coupling mechanisms in flexible composites. Therefore, a suitable step-by-step transferability based on the test chain concept and its transfer criteria (from model to component-like level) was developed whilst enabling a quantitative understanding and clear validation. With this approach, the influence of specific stiff reinforcing fibers on hyperelastic elastomers and their load-coupled behavior could be studied in detail, within the findings from the single component materials, the fiber-matrix material combination and shearing behavior due to analyzed tension tests already considering different reinforcing orientations. The applicability of the presented load-coupling test setup was assessed to determine the twist angle as well as torque and to get a deeper insight into the mechanical properties of flexile composites.

3.1. Reinforcement, Matrix and Composite

The mechanical properties of the constituents (fibers and matrix) are compared in Table 1. The results for PDMS revealed an elongation at break of about 108.6% with a determined stress at break of about 4.5 MPa. Thus, an elongation at break of approximately 1.4% with a corresponding force at break of about 119.8 N is given for the glass fibers of the textile.

Table 1. Results for single component tests on GF and PDMS.

	GF	PDMS
max. force F_{max}, N	119.8 ± 2.3	36.1 ± 1.1
max. strain ε_{max}, %	1.4 ± 0.1	108.6 ± 8.6

Former investigations based on quasi-static tensile tests were conducted to investigate the mechanical properties of tailored fiber-reinforced elastomers, which are added as supplemental information to complement the results (see Figure 4). In this context, the influence of different fiber orientations (±45°, 30°/60° and 0°/90°) versus the deformation behavior, the shear-induced in-plane distortion and maximum possible locking angle (resulting in the trellis effect) were analyzed [59]. The results reveal that shearing becomes increasingly dominant depending on how significantly the fiber orientation deviates from the loading direction. Therefore, the ±45° fiber oriented composite

material has a higher flexibility (matrix dominated performance) with an elongation at break of about 38.2% ± 0.5 with a stress at break of about 34.3 N/mm^2 ± 2.9 compared to the configuration of e.g., a composite configuration with 0°/90° fiber orientation (fiber dominated). As expected, the stiffness can be enhanced particularly at small strain rates between 0% to 10% but also with a clear reduction in flexibility, which is directly correlating with the maximum locking angle. Since the use of elastomers such as PDMS as alternative matrix for composites, the trellis effect is amplified compared to typical thermoset-based composites [44,57] due to the textile-like behavior [33].

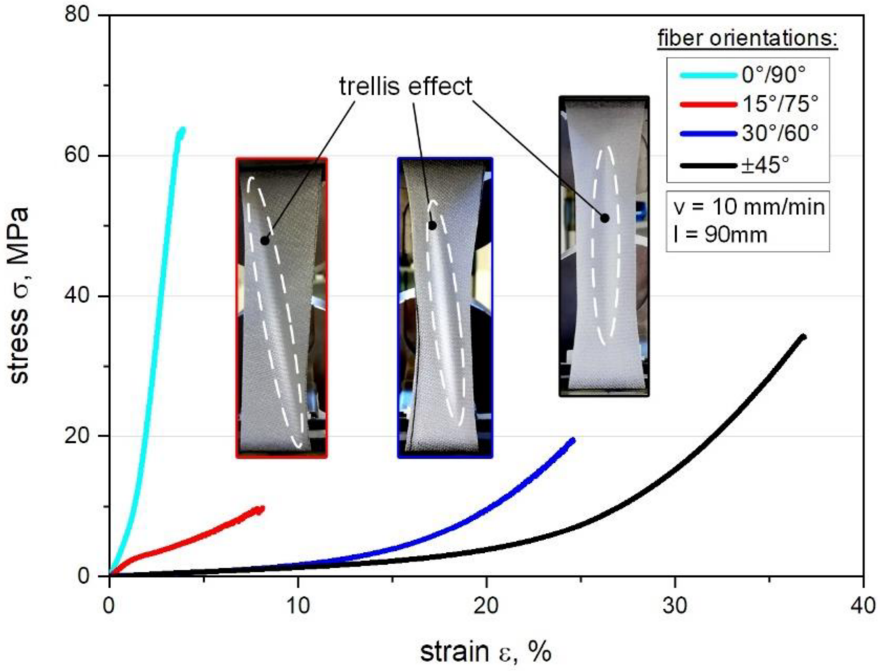

Figure 4. Comparison of stress-strain curves of the different fiber orientations (±45°, 30°/60°, 15°/75° and 0°/90°) for the GF-PDMS composite with textile reinforcement as obtained from composite tensile tests with the accompanying trellis effect related to the wrinkling and out-of plane shearing.

3.2. Tension-Twist Coupled Effect

Regarding the load-coupling test device, the stress-strain curves for tension-twist coupling measurements with 45 mm gauge length are illustrated in Figure 5a representing all three different fiber orientations. Due to the expected behavior, the results of the ±45° oriented composites reveal a significant matrix dominated performance, which can be compared with the tension tests given in Figure 4. This can be explained by the behavior of the warp and weft yarns, which starts to shift during deformation and the yarns are able to undergo larger displacements until the fibers converge with the loading direction [53]. Related to this, the 30°/60° composite shows a steeper slope, which can be attributed to the increased fiber dominated properties leading to a higher stress of about 10 N/mm^2 (approximately 40%) than for ±45° composites at the same strain level of 20%.

In contrast to that, the special configuration of 30°/60°//±45° composite as mixed type indicates a significant higher stress-strain slope at the beginning compared to the other settings. However, this trend tends to converge with increasing deformation, so that the material behavior approximates more closely to the 30°/60° composite, which is visible in Figure 5a. In this context and contributed to the conducted pre-simulations this mixed configuration has an intermediate position regarding the predicted twist versus torque load-coupling behavior [23,41]. Moreover, the results show that the stiffness differs, especially at small strain ratios from 0% up to about 10% deformation. In particular the highest stiffness is observed for the mixed configuration, which can be explained by the interaction of

the two differently oriented layers creating further locking effects in terms of several effect of shearing during the deformation [44,47].

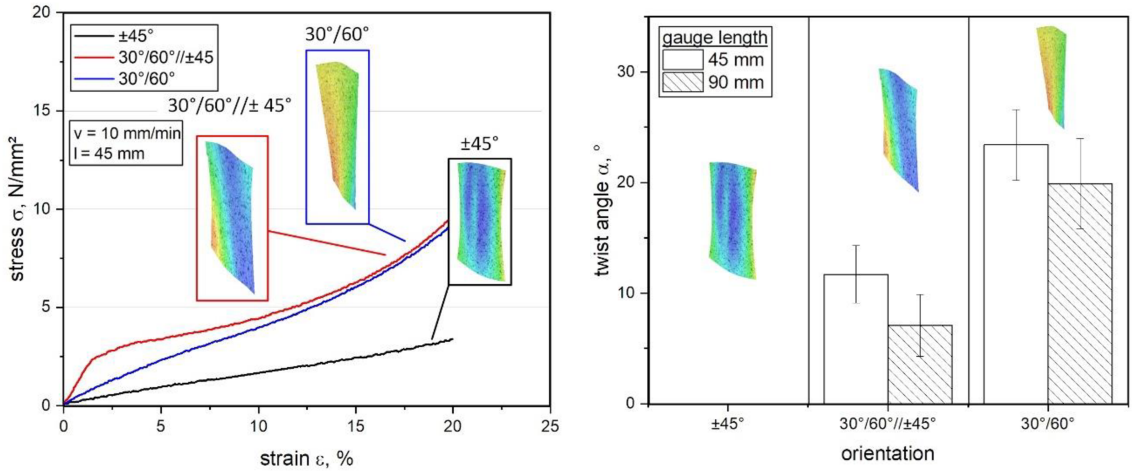

(**a**) (**b**)

Figure 5. Stress-strain curves obtained from tension-twist load-coupling tests for GF-PDMS composites with textile reinforcement (**a**) and comparison of different gauge lengths versus inherent stiffness on the twist angle α performed with different fiber orientations (**b**) including digital image correlation in false color display.

Thus, the results for twisting and corresponding torque versus different fiber orientations are reported in Table 2, investigating an increase of the twist angle as well as torque from ±45° composites up to 30°/60° composites, which shows the highest maximum twist angle of about 24.4° and torque of about 82.3 Nmm. As expected, the ±45° composite reveals no twist or torque, which can be explained by the symmetric lay-up whilst the wrinkling is occurring parallel to the loading direction (see Figure 5a) [60]. Generally, this behavior proves that shearing becomes increasingly dominant according to the degree of deviation between the loading direction and fiber orientation [44,61]. Therefore, the effect of in-plane shearing during deformation is mainly influenced by the fiber orientation, since the displacement of fibers relative to each other reaches a maximum deformation angle (in-plane) at some point and the flexible composite starts to wrinkle [47,59]. This locking angle appears sooner in terms of asymmetric composite lay-ups causing an unbalanced stress state so that out-of plane deformation leads to a twist based on load-coupling [45,54]. However, if this decisive rotating mechanism is inhibited, torque is inevitably generated. Besides, all reported measurements for torque and twist angle show generally higher standard deviations, which are currently under investigation and compared with accompanying simulations. In this context, those preliminary analysis cannot be attributed unambiguously to the test setup, since in accordance to the recent findings several different influences are included such as specimen production influences, specimen handling or inherent rigidity of the test setup. Due to that, the results of this study represent initial measurements within the focus on the principal realization and feasibility of a potential test device, so that those effects are investigated in detail in ongoing studies.

Table 2. Results for GF-PDMS composite with glass fiber textile and 45 mm gauge length for different fiber orientations.

	Max. Twist Angle α, °	Max. Torque T, Nmm
±45°	0.0	0.0
30°/60°//±45°	11.7 ± 2.6	56.3 ± 9.6
30°/60°	24.4 ± 3.2	82.3 ± 11.1

For determining the load-coupling behavior due to the influence of different parameters of gauge length and fiber orientation versus the maximum reachable twist angle α, the results of GF-PDMS composites are displayed in Figure 5b. To provide a better overview, the influence of various clamping lengths versus maximum twist angle α (descripted in Figure 3) is considered in a quantitative manner. As expected, the results demonstrate a significant increase of α when reducing the gauge length from 90 mm to 45 mm. A reason for this is the fact, that the inherent stiffness of such highly flexible composites can be clearly increased due to this adjustment, especially in combination with PDMS matrix [62,63]. Regarding the mixed configuration of 30°/60°//±45° composite, the results indicate no clear effect in the twist angle although a significant increase in stiffness can be observed in the stress strain curve especially at the beginning (see Figure 5a). This could be due to the fact, that the already achieved deformation was too small to reach a sufficient influence on twisting, which is probably also supported by the hyperelasticity of the matrix. However, the standard deviation tends to increase with higher gauge length, which could be due to the fact of the hyperelastic matrix as well as for the higher bearable elasticity by the fibers. Moreover, the quantitative comparison of the maximum twist angle versus the fiber orientation shows a good agreement with the stress-strain curve obtained from measurements with the presented load-coupling test device. Generally, it is evident, that a reduced fiber angle from ±45° to 30°/60° results to an enhanced stiffness and thereby to higher tension stresses at equal strain level e.g., at a strain of 20%. However, these findings demonstrate that despite an enhanced stiffness, the flexibility (imparted by the PDMS matrix) is still retained even with a more fiber dominated 30°/60° composite. This has a positive influence on the fiber-matrix interface and thus, for the load-coupling mechanism [33]. Based on this, further experiments need to be carried out to investigate and to verify the measurement sensitivity varying the fiber-matrix adhesion and thus, the load transfer by tailored fiber surface treatments which influences the interface and load-coupling effect. Furthermore, the influence of different reinforcing types is currently under investigation, how fiber-fiber friction, reorientation of fibers by extension towards fiber angle changes or undulation affects the load transfer in textiles compared to mats, clutches and prepregs. Subsequently, further experimental investigations are analyzed in ongoing studies and compared with simulations related to load-coupling predictions with the CLT.

3.3. Optical Damage Analysis

To ensure an unaffected fiber-matrix adhesion with no visible local debonding and thus an adequate load transfer, light microscopy images were taken from the GF-PDMS composite samples. Besides the results obtained from the tension-twist coupling and simple tension tests, the accompanying optical damage analysis show further information about the test performance providing a good comparability with the mechanical measurements [64]. As illustrated in Figure 6a,b, the results on pure tension tests according to the ISO 527-4 [65] reveal that a symmetric deformation is occurring for ±45° composite following the affiliated wrinkling shape during deformation [59,66].

Compared to this, the 30°/60° fiber-oriented composite clearly indicates an asymmetric deformation accompanying with the wrinkling performance. Both configurations display local debonding in the interface at the main deformation area, which can be recognized by the shift of the light refraction due to the separation process [64]. This finding can be further confirmed in more detail with a corresponding light microscopy image (see Figure 6e). Further, despite the debonding, a complete failure of the entire sample is not generated. In contrast to that, the optical damage analysis of the load-coupling tests (see Figure 6d) shows an undamaged and still good fiber-matrix adhesion compared to the original initial state (see Figure 6c), respectively. Therefore, it can be assumed that the adhesion is unchanged, which verifies a successful load transfer via the presented load-coupling test setup.

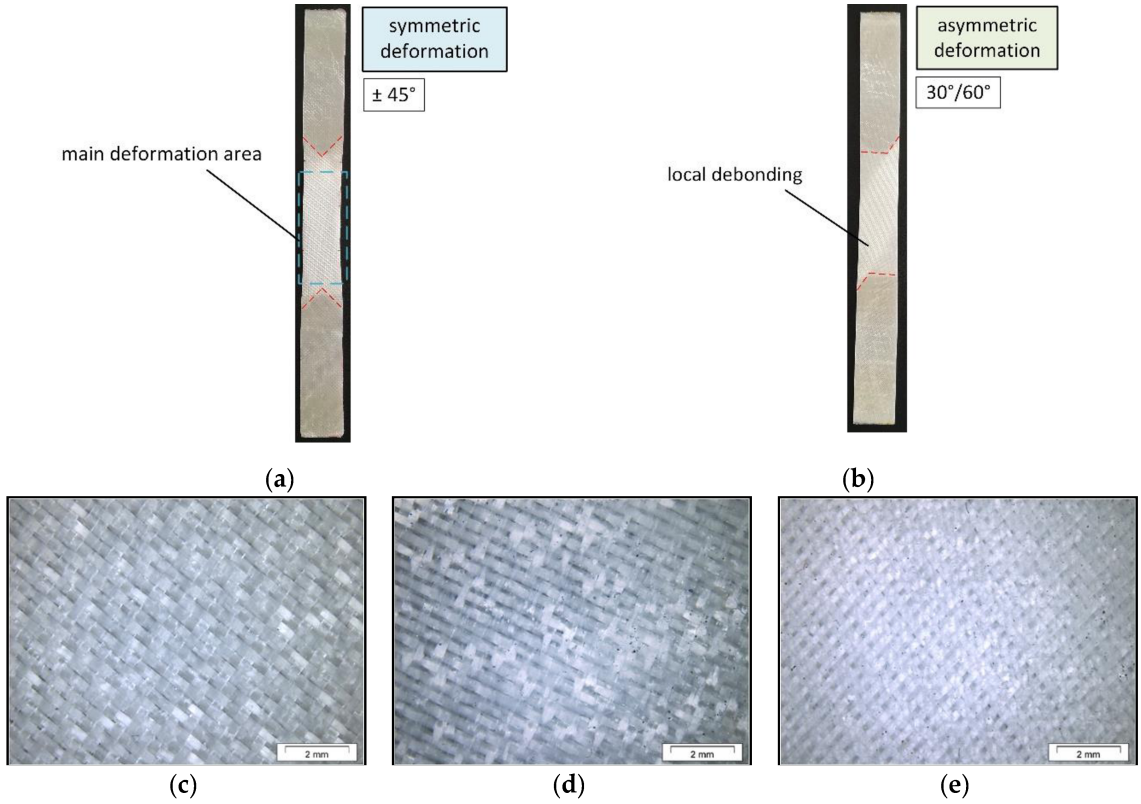

Figure 6. Optical damage analysis of GF-PDMS composites from tension tests with ±45° fiber orientation (**a**) and 30°/60° (**b**) oriented compared tension-twist load-coupling tests with ±45° composite: in initial state (**c**), after load-coupling test (**d**) and after tension tests (**e**).

4. Conclusions

Since research interest on so-called smart materials is continuously growing, this work mainly focuses on the demonstration and feasibility of a new test device intended to provide the basis for an adequate analysis of tension-twist mechanisms triggered by an external mechanical force in specific flexible composite with tailored fiber orientation. The aim of this research is to investigate structure-property interaction towards load-coupling effects to obtain material data including customized twist and torque properties especially for morphology analysis as well as to implement these findings in constitutive numerical approaches, in simulation models including well-established composite material laws. Due to the high flexibility, silicone in combination with glass fibers as the considered single components were chosen to demonstrate a selected fiber-matrix combination as well as the fiber orientation to achieve a reliable direction-dependent characterization accompanying anisotropic composite performance. Within the focus, a quantitative study including a methodical test plan was elaborated to study the impact of various influencing parameters and to assess their effects on the twist and torque.

The results of the tension-twist coupled tests reveal that the mechanical properties related to the structure-properties and thus the load-coupling effect can be optimized in a specific manner depending on the fiber orientation and the composite lay-up. Furthermore, the stiffness can be controlled and improved without impairing the flexible properties of the silicone significantly, whilst the fibers are reinforcing the composite. Additional studies are currently under investigation focusing on the impact and effect of different reinforcing types on the load-coupling properties. Moreover, further work on various treated fiber surfaces to influence the fiber-matrix adhesion and therefore the load transfer with tailored chemical surface modifications as well as different fiber-matrix material combination is already in progress. Related to this, more studies on the physical phenomena behind the developed load-coupling test device needs to be carried out. Overall, the results demonstrate that the presented test

method improved by specific sensor systems shows a good agreement in combination with the optical damage analysis. The results of the load coupling tests reveal that even for small lay-ups the 30°/60° oriented composite with an asymmetric deformation triggers the highest torque of about 82.3 Nmm with a twisting angle of almost 25°. The mixed configuration of 30°/60°//±45° composite has an intermediate performance with a maximum achievable twisting angle of about 12°, since the ±45° composite with the highest deviation between fiber orientation and loading direction, as expected, undergoes no tension-twist coupling related to the symmetric deformation. Knowing this, the verification of the test device is validated, which allows sufficient accuracy of the material pre-analysis on tension-twist coupling mechanisms in a fast and easy way, whilst also contributing to a better understanding of the performance of fiber reinforced elastomers. Hence, this study evaluates the structure-property interaction of smart materials and highlights the essential contribution on the composite properties due to tailored load-coupling mechanisms. Moreover, further research should be carried out in terms of the comparability to macro scale performance between microstructure and application-like performances. This test method was developed to provide a base model to study load-coupling mechanisms adequately as well as a suitable link in a possible test chain between laboratory and industry applications.

Author Contributions: Literature research, investigation, formal analysis, writing—original draft preparation, J.B.; conceptualization, methodology, J.B., B.S. and M.M.; visualization J.B., B.S. and B.L.; test conduction J.B., G.M. and B.L.; validation, writing—review and editing, J.B., B.S., M.M., P.F.F. and G.P.; supervision, project administration B.S., P.F.F. and G.P. All authors have read and agreed to the published version of the manuscript.

Funding: This research was funded by the Federal Ministry for Climate Action, Environment, Energy, Mobility, Innovation and Technology and the Federal Ministry for Digital and Economic Affairs with the grant number 854178 and the COMET-modul "Polymers4Hydrogen" under the grant number 21647053.

Acknowledgments: The assistance of Ivan Raguž for support during testing is gratefully acknowledged. This research work was performed at the Polymer Competence Center Leoben GmbH (PCCL, Austria) and within the COMET-modul "Polymers4Hydrogen" within the framework of the COMET-program of the Federal Ministry for Climate Action, Environment, Energy, Mobility, Innovation and Technology and the Federal Ministry for Digital and Economic Affairs, with contributions by the Department of Polymer Engineering and Science (Montanuniversitaet Leoben). The PCCL is funded by Austrian Government and the State Government of Styria.

Conflicts of Interest: The authors declare no conflict of interest. The funders had no role in the design of the study; in the collection, analysis, or interpretation of data; in the writing of the manuscript, or in the decision to publish the results.

References

1. Peel, L. Fabrication and Mechanics of Fiber-Reinforced Elastomers. Ph.D. Thesis, Brigham Young University, Brigham, UT, USA, 1998.
2. Neitzel, M.; Mitschang, P.; Breuer, U. *Handbuch Verbundwerkstoffe. Werkstoffe, Verarbeitung, Anwendung*, 2nd ed.; Carl Hanser Verlag: Munich, Germany, 2014; ISBN 978-3-446-43696-1.
3. Chillara, V.S.C.; Dapino, M.J. Review of Morphing Laminated Composites. *Appl. Mech. Rev.* **2020**, *72*, 10801. [CrossRef]
4. Chou, T.-W. Flexible composites. *J. Mater. Sci.* **1989**, *24*, 761–783. [CrossRef]
5. Drenkelford, S. Energy-Saving Potential of Aramid-Based Conveyor Belts. Master's Thesis, Delft University of Technology, Delft, The Netherlands, 2015.
6. Toopchi-Nezhad, H.; Tait, M.J.; Drysdale, R.G. Bonded versus unbonded strip fiber reinforced elastomeric isolators: Finite element analysis. *Compos. Struct.* **2011**, *93*, 850–859. [CrossRef]
7. Kang, G.J.; Kang, B.S. Dynamic analysis of fiber-reinforced elastomeric isolation structures. *J. Mech. Sci. Technol.* **2009**, *23*, 1132–1141. [CrossRef]
8. Katti, K.S.; Katti, D.R.; Mohanty, B. Biomimetic Lessons Learnt from Nacre. In *Biomimetics Learning from Nature*; Mukherjee, A., Raichur, A.M., Mathew, L., Chandrasekaran, N., Eds.; INTECH Open Access Publisher: London, UK, 2010; ISBN 978-953-307-025-4.
9. Gupta, H.S.; Seto, J.; Wagermaier, W.; Zaslansky, P.; Boesecke, P.; Fratzl, P. Cooperative deformation of mineral and collagen in bone at the nanoscale. *Proc. Natl. Acad. Sci. USA* **2006**, *103*, 17741–17746. [CrossRef]

10. Cianchetti, M.; Laschi, C.; Menciassi, A.; Dario, P. Biomedical applications of soft robotics. *Nat. Rev. Mater.* **2018**, *3*, 143–153. [CrossRef]
11. Vocke, R.D.; Kothera, C.S.; Woods, B.K.S.; Wereley, N.M. Development and Testing of a Span-Extending Morphing Wing. *J. Intell. Mater. Syst. Struct.* **2011**, *22*, 879–890. [CrossRef]
12. Peel, L.D.; Baur, J.; Phillips, D.; McClung, A. The effect of scaling on the performance of elastomer composite actuators. *Proc. SPIE- Int. Soc. Opt. Eng.* **2010**. [CrossRef]
13. Chen, Y.; Tan, X.; Yan, D.; Zhang, Z.; Gong, Y. A Composite Fabric-Based Soft Rehabilitation Glove with Soft Joint for Dementia in Parkinson's Disease. *IEEE J. Transl. Eng. Health Med.* **2020**, *8*, 1400110. [CrossRef]
14. Connolly, F.; Walsh, C.J.; Bertoldi, K. Automatic design of fiber-reinforced soft actuators for trajectory matching. *Proc. Natl. Acad. Sci. USA* **2017**, *114*, 51–56. [CrossRef]
15. Shan, S.; Kang, S.H.; Raney, J.R.; Wang, P.; Fang, L.; Candido, F.; Lewis, J.A.; Bertoldi, K. Multistable Architected Materials for Trapping Elastic Strain Energy. *Adv. Mater.* **2015**, *27*, 4296–4301. [CrossRef] [PubMed]
16. Jin, H.; Dong, E.; Xu, M.; Liu, C.; Alici, G.; Jie, Y. Soft and smart modular structures actuated by shape memory alloy (SMA) wires as tentacles of soft robots. *Smart Mater. Struct.* **2016**, *25*, 85026. [CrossRef]
17. Kim, S.; Laschi, C.; Trimmer, B. Soft robotics: A bioinspired evolution in robotics. *Trends Biotechnol.* **2013**, *31*, 287–294. [CrossRef] [PubMed]
18. Bishop-Moser, J.; Krishnan, G.; Kim, C.; Kota, S. Design of soft robotic actuators using fluid-filled fiber-reinforced elastomeric enclosures in parallel combinations. In Proceedings of the 2012 IEEE/RSJ International Conference on Intelligent Robots and Systems, Vilamoura, Portugal, 7–12 October 2012; pp. 4264–4269. [CrossRef]
19. Li, Z.; Wang, Z.L. Air/Liquid-Pressure and Heartbeat-Driven Flexible Fiber Nanogenerators as a Micro/Nano-Power Source or Diagnostic Sensor. *Adv. Mater.* **2011**, *23*, 84–89. [CrossRef]
20. Patrick, L.; Gabor, K.; Silvain, M. Characterization of dielectric elastomer actuators based on a hyperelastic film model. *Sens. Actuat. A-Phys.* **2007**, *135*, 748–757. [CrossRef]
21. Wang, Q.; Tian, X.; Huang, L.; Li, D.; Malakhov, A.V.; Polilov, A.N. Programmable morphing composites with embedded continuous fibers by 4D printing. *Mater. Des.* **2018**, *155*, 404–413. [CrossRef]
22. Tasdemir, B.; Coker, D. Comparison of damage mechanisms in curved composite laminates under static and fatigue loading. *Compos. Struct.* **2019**, *213*, 190–203. [CrossRef]
23. Haynes, R.; Armanios, E. Overview of hygrothermally stable laminates with improved extension-twist coupling. In Proceedings of the 17th International Conference on Composite Materials, Edinburgh, UK, 27–31 July 2009.
24. Yamashita, T.; Takamatsu, S.; Miyake, K.; Itoh, T. Fabrication and evaluation of a conductive polymer coated elastomer contact structure for woven electronic textile. *Sens. Actuat. A Phys.* **2013**, *195*, 213–218. [CrossRef]
25. Tawfik, S.A.; Stefan Dancila, D.; Armanios, E. Unsymmetric composite laminates morphing via piezoelectric actuators. *Compos. Part A* **2011**, *42*, 748–756. [CrossRef]
26. Bowen, C.R.; Butler, R.; Jervis, R.; Kim, H.A.; Salo, A.I.T. Morphing and Shape Control using Unsymmetrical Composites. *J. Intell. Mater. Syst. Struct.* **2006**, *18*, 89–98. [CrossRef]
27. Shian, S.; Bertoldi, K.; Clarke, D.R. Dielectric Elastomer Based "Grippers" for Soft Robotics. *Adv. Mater. Weinh.* **2015**, *27*, 6814–6819. [CrossRef]
28. Subramani, K.B.; Cakmak, E.; Spontak, R.J.; Ghosh, T.K. Enhanced electroactive response of unidirectional elastomeric composites with high-dielectric-constant fibers. *Adv. Mater. Weinh.* **2014**, *26*, 2949–2953. [CrossRef]
29. Kim, H.-S.; Lee, J.-Y.; Chu, W.-S.; Ahn, S.-H. Design and Fabrication of Soft Morphing Ray Propulsor: Undulator and Oscillator. *Soft Robot.* **2017**, *4*, 49–60. [CrossRef]
30. Capuzzi, M.; Pirrera, A.; Weaver, P.M. Structural design of a novel aeroelastically tailored wind turbine blade. *Thin-Walled Struct.* **2015**, *95*, 7–15. [CrossRef]
31. Cui, D.; Li, D. Bending-twisting coupled structures based on composite laminates with extension-shear coupling effect. *Compos. Struct.* **2019**, *209*, 434–442. [CrossRef]
32. Carlsson, L.A.; Adams, D.F.; Pipes, R.B. Basic Experimental Characterization of Polymer Matrix Composite Materials. *Polym. Rev.* **2013**, *53*, 277–302. [CrossRef]
33. Beter, J.; Schrittesser, B.; Lechner, B.; Mansouri, M.R.; Marano, C.; Fuchs, P.F.; Pinter, G. Viscoelastic Behavior of Glass-Fiber-Reinforced Silicone Composites Exposed to Cyclic Loading. *Polymers* **2020**, *12*, 1862. [CrossRef]

34. Ahn, S.-H.; Lee, K.-T.; Kim, H.-J.; Wu, R.; Kim, J.-S.; Song, S.H. Smart soft composite: An integrated 3D soft morphing structure using bend-twist coupling of anisotropic materials. *Int. J. Precis. Eng. Manuf.* **2012**, *13*, 631–634. [CrossRef]
35. Vannucci, P. *Anisotropic Elasticity*; Springer: Singapore, 2018; ISBN 978-981-10-5438-9.
36. Brunetti, M.; Vincenti, A.; Vidoli, S. A class of morphing shell structures satisfying clamped boundary conditions. *Int. J. Sol. Struct.* **2016**, *82*, 47–55. [CrossRef]
37. Chillara, V.S.C.; Headings, L.M.; Dapino, M.J. Multifunctional composites with intrinsic pressure actuation and prestress for morphing structures. *Compos. Struct.* **2016**, *157*, 265–274. [CrossRef]
38. Selden, P.H. *Glasfaserverstärkte Kunststoffe*; Springer: Berlin/Heidelberg, Germany, 1967; ISBN 978-3-642-48456-8.
39. Koschmieder, M. Verarbeitung und Eigenschaften von Faserverbundkunststoffen mit Elastomermatrix. Ph.D. Thesis, Rheinisch-Westfälischen Technischen Hochschule Aachen, Aachen, Germany, 2000.
40. Modi, V.; Singh, K.K.; Shrivastava, R. Effect of Stacking Sequence on Interlaminar Shear Strength of Multidirectional GFRP Laminates. *Mater. Today-Proc.* **2020**, *22*, 2207–2214. [CrossRef]
41. Rohde, S.E.; Ifju, P.G.; Sankar, B.V.; Jenkins, D.A. Experimental Testing of Bend-Twist Coupled Composite Shafts. *Exp. Mech.* **2015**, *55*, 1613–1625. [CrossRef]
42. Beter, J.; Schrittesser, B.; Grassegger, F. Klemmvorrichtung und Verfahren zur Prüfung Einer Zugfestigkeit Eines Objektes. Austrian Patent A50009/2020, 20 January 2020.
43. Gude, M.; Hufenbach, W.; Andrich, M.; Mertel, A.; Schirner, R. Modified V-notched rail shear test fixture for shear characterisation of textile-reinforced composite materials. *Polym. Test.* **2015**, *43*, 147–153. [CrossRef]
44. Cherif, C. *Textile Werkstoffe für den Leichtbau. Techniken—Verfahren—Materialien—Eigenschaften*; Springer: Berlin/Heidelberg, Germany, 2011; ISBN 978-3-642-17992-1.
45. Selezneva, M.; Naouar, N.; Denis, Y.; Gorbatikh, L.; Hine, P.; Lomov, S.V.; Swolfs, Y.; Verpoest, I.; Boisse, P. Identification and validation of a hyperelastic model for self-reinforced polypropylene draping. *Int. J. Mater. Form.* **2020**, *39*, 1455. [CrossRef]
46. Palola, S.; Sarlin, E.; Kolahgar Azari, S.; Koutsos, V.; Vuorinen, J. Microwave induced hierarchical nanostructures on aramid fibers and their influence on adhesion properties in a rubber matrix. *Appl. Surf. Sci.* **2017**, *410*, 145–153. [CrossRef]
47. Beter, J.; Schrittesser, B.; Meier, G.; Fuchs, P.F.; Pinter, G. Influence of Fiber Orientation and Adhesion Properties On Tailored Fiber-reinforced Elastomers. *Appl. Compos. Mater.* **2020**, 149–164. [CrossRef]
48. Beter, J.; Schrittesser, B.; Maroh, B.; Sarlin, E.; Fuchs, P.F.; Pinter, G. Comparison and Impact of Different Fiber Debond Techniques on Fiber Reinforced Flexible Composites. *Polymers* **2020**, *12*, 472. [CrossRef]
49. Sedlan, K. Viskoelastisches Materialverhalten von Elastomerwerkstoffen: Experimentelle Untersuchung und Modellbildung. Ph.D. Thesis, Universität Gesamthochschule Kassel, Kassel, Germany, 2000.
50. Gereke, T.; Döbrich, O.; Hübner, M.; Cherif, C. Experimental and computational composite textile reinforcement forming: A review. *Compos. Part A* **2013**, *46*, 1–10. [CrossRef]
51. American Society for Testing and Materials. *ASTM D2256-02: 2015: Test Method for Tensile Properties of Yarns by the Single-Strand Method*; American Society for Testing and Materials: West Conshohocken, PA, USA, 2015.
52. International Organization for Standardization. *ISO 37: 2011-12: Rubber, Vulcanized or Thermoplastic—Determination of Tensile Stress-Strain Properties*; International Organization for Standardization: Geneva, Switzerland, 2011.
53. Nosrat-Nezami, F.; Gereke, T.; Eberdt, C.; Cherif, C. Characterisation of the shear–tension coupling of carbon-fibre fabric under controlled membrane tensions for precise simulative predictions of industrial preforming processes. *Compos. Part A* **2014**, *67*, 131–139. [CrossRef]
54. Potter, K. Bias extension measurements on cross-plied unidirectional prepreg. *Compos. Part A* **2002**, *33*, 63–73. [CrossRef]
55. Hoffmann, J. Characterization of Fibre Reinforced Elastomers for Shape Morphing Structural Surfaces. Ph.D. Thesis, Technical University of Munich, Munich, Germany, 2012.
56. International Organization for Standardization. *ISO 291:2008-08: Plastics—Standard Atmospheres for Conditioning and Testing*; International Organization for Standardization: Berlin, Germany, 2008.
57. Beter, J.; Schrittesser, B.; Fuchs, P.F. Investigation of adhesion properties in load coupling applications for flexible composites. *Mater. Today-Proc.* **2020**. [CrossRef]

58. Mansouri, M.; Fuchs, P.F.; Schuecker, C. Hyperelastic modeling of woven structures undergoing large deformations. In Proceedings of the 18th European Conference on Composite Materials ECCM18, Athen, Greece, 24–18 June 2018.
59. Harrison, P.; Abdiwi, F.; Guo, Z.; Potluri, P.; Yu, W.R. Characterising the shear–tension coupling and wrinkling behaviour of woven engineering fabrics. *Compos. Part A* **2012**, *43*, 903–914. [CrossRef]
60. Peng, X.; Guo, Z.; Du, T.; Yu, W.-R. A simple anisotropic hyperelastic constitutive model for textile fabrics with application to forming simulation. *Compos. Part B* **2013**, *52*, 275–281. [CrossRef]
61. Berthold, U. Beitrag zur Thermoformung Gewebeverstärkter Thermoplaste Mittels Elastischer Stempel. Ph.D. Thesis, Technische Universität Chemnitz, Chemnitz, Germany, 2001.
62. Röthemeyer, F.; Sommer, F. *Kautschuk—Technologie. Werkstoffe—Verarbeitung—Produkte*, 3rd ed.; Carl Hanser Verlag: Munich, Germany, 2013; ISBN 978-3-446-43776-0.
63. Ehrenstein, G. *Polymer-Werkstoffe. Struktur; Eigenschaften; Anwendung*, 3rd ed.; Carl Hanser Verlag: Munich, Germany, 2011; ISBN 978-3-446-42283-4.
64. Bergmann, T.; Heimbs, S.; Maier, M. Mechanical properties and energy absorption capability of woven fabric composites under ±45° off-axis tension. *Compos. Struct.* **2015**, *125*, 362–373. [CrossRef]
65. International Organization for Standardization. *ISO 527-4: 1997: Plastics. Determination of Tensile Properties*; International Organization for Standardization: London, UK, 1997.
66. Fu, C.; Wang, T.; Xu, F.; Huo, Y.; Potier-Ferry, M. A modeling and resolution framework for wrinkling in hyperelastic sheets at finite membrane strain. *J. Mech. Phys. Solids* **2019**, *124*, 446–470. [CrossRef]

3.8 Patent B: Prüfvorrichtung zur Messung von Zug-Torsion-Lastkopplungen

Julia Beter[1,*], Bernd Schrittesser[1] and Gerald Meier[1]

[1] Polymer Competence Center Leoben GmbH, Roseggerstrasse 12, 8700 Leoben, Austria.

Under Review in Österreichisches Patentamt, 2020

This invention entitled “Test device for measuring tension-torsion load couplings” is the realization of a novel developed test fixture to measure load coupling mechanisms in flexible, single or multi-component continuous fiber reinforced elastomers. Additionally, sensors are implemented to determine the torsion angle due to the deflection as well as the corresponding torsion force due to the acting torque. Furthermore, a multi-axis hinged load bearing element is implemented to ensure a bending moment-free test so that the test specimen is aligned parallel to the test axis.

PCCL
Polymer Competence Center Leoben

An
Frau DI Julia Beter
Schlachthofgasse 6
8700 Leoben

Leoben, am 25. Jänner 2021

Bestätigung der Mitwirkung an einer Diensterfindung

Es ist uns eine Freude zu bestätigen, dass Frau DI Julia Beter, geboren am 19. Mai 1992, während ihrer Forschungstätigkeit als Mitarbeiterin der Polymer Competence Center Leoben GmbH im Rahmen eines Projektes des COMET-K1-Zentrums PCCL maßgeblich als Erfinderin an folgender Diensterfindung bzw. folgendem Patent beteiligt war:

(Vorläufiger) Titel des Patents: *„Prüfvorrichtung zur Messung von Zug-Torsion-Lastkoppelungen“*

Die Prüfung der zugrundeliegenden Diensterfindung durch die Patentanwaltskanzlei Puchberger & Partner Patentanwälte hat ergeben, dass eine Patentanmeldung jedenfalls als aussichtsreich anzusehen wäre. Die Entscheidung hierüber ist allerdings aufgrund des Umstandes, dass das Ergebnis der Prüfung durch den Patentanwalt erst vor einer Woche bei uns eingelangt ist, noch nicht erfolgt. Wir ziehen eine Anmeldung zum Patent jedoch definitiv in Betracht.

Mit freundlichen Grüßen

DI Dr. Elisabeth Ladstätter
(Geschäftsführerin)

Polymer Competence Center Leoben GmbH
Roseggerstraße 12, A-8700 Leoben
www.pccl.at

Tel: +43 3842 42962-0
Fax: +43 3842 42962-6
office@pccl.at

Firmenbuch: LG Leoben
FN 223698v
UID-Nr. ATU 54829208

Steiermärkische Sparkasse
IBAN AT41 2081 5000 4032 7439
BIC STSPAT2GXXX

REFERENCES

1. Kalpana S., K.; Dinesh R., K.; Bedabibhas, M. Biomimetic Lessons Learnt from Nacre. Biomimetic Synthesis of Nanoparticles: Science, Technology & Applicability; INTECH Open Access Publisher, 2010, ISBN 978-953-307-025-4.
2. Gupta, H.S.; Seto, J.; Wagermaier, W.; Zaslansky, P.; Boesecke, P.; et al. Cooperative deformation of mineral and collagen in bone at the nanoscale. Proc. Natl. Acad. Sci. U.S.A. 2006, 103, 17741–17746, DOI:10.1073/pnas.0604237103.
3. Addington, M. Smart Materials - Design dictionary. Perspectives on design terminology; Birkhäuser Verlag: Basel, 2008, ISBN 978-3-7643-7739-7.
4. Kim, S.; Laschi, C.; Trimmer, B. Soft robotics: A bioinspired evolution in robotics. Trends Biotechnol. 2013, 31, 287–294, DOI:10.1016/j.tibtech.2013.03.002.
5. Bishop-Moser, J.; Krishnan, G.; Kim, C.; Kota, S. Design of soft robotic actuators using fluid-filled fiber-reinforced elastomeric enclosures in parallel combinations. In . IEEE/RSJ International Conference on Intelligent Robots and Systems, Vilamoura, Portugal, 07-12. October 2012, DOI:10.1109/IROS.2012.6385966.
6. Li, Z.; Wang, Z.L. Air/Liquid-Pressure and Heartbeat-Driven Flexible Fiber Nanogenerators as a Micro/Nano-Power Source or Diagnostic Sensor. Adv. Mater. 2011, 23, 84–89, DOI:10.1002/adma.201003161.
7. Patrick, L.; Gabor, K.; Silvain, M. Characterization of dielectric elastomer actuators based on a hyperelastic film model. Sensor. Actuat. A- Phys. 2007, 135, 748–757, DOI:10.1016/j.sna.2006.08.006.
8. Jin, H.; Dong, E.; Xu, M.; Liu, C.; Alici, G.; et al. Soft and smart modular structures actuated by shape memory alloy (SMA) wires as tentacles of soft robots. Smart Mater. Struct. 2016, 25, 85026, DOI:10.1088/0964-1726/25/8/085026.
9. Wang, Q.; Tian, X.; Huang, L.; Li, D.; Malakhov, A.V.; et al. Programmable morphing composites with embedded continuous fibers by 4D printing. Mater. Des. 2018, 155, 404–413, DOI:10.1016/j.matdes.2018.06.027.
10. Tasdemir, B.; Coker, D. Comparison of damage mechanisms in curved composite laminates under static and fatigue loading. Compos. Struct. 2019, 213, 190–203, DOI:10.1016/j.compstruct.2019.01.072.
11. Haynes, R.; Armanios, E. Overview of hygrothermally stable laminates with improved extension-twist coupling. In . Proceedings of the 17th International Conference on Composite Materials, Edinburgh, UK, 27-31 July 2009.
12. Shian, S.; Bertoldi, K.; Clarke, D.R. Dielectric Elastomer Based "Grippers" for Soft Robotics. Adv. Mater. Weinheim 2015, 27, 6814–6819, DOI:10.1002/adma.201503078.

13. Subramani, K.B.; Cakmak, E.; Spontak, R.J.; Ghosh, T.K. Enhanced electroactive response of unidirectional elastomeric composites with high-dielectric-constant fibers. Adv. Mater. Weinheim 2014, 26, 2949–2953, DOI:10.1002/adma.201305821.

14. Martinez, R.V.; Fish, C.R.; Chen, X.; Whitesides, G.M. Elastomeric Origami: Programmable Paper-Elastomer Composites as Pneumatic Actuators. Adv. Funct. Mater. 2012, 22, 1376–1384, DOI:10.1002/adfm.201102978.

15. Zhang, Q.; Wommer, J.; O'Rourke, C.; Teitelman, J.; Tang, Y.; et al. Origami and kirigami inspired self-folding for programming three-dimensional shape shifting of polymer sheets with light. Extreme Mech. Lett. 2017, 11, 111–120, DOI:10.1016/j.eml.2016.08.004.

16. López Jiménez, F.; Pellegrino, S. Folding of fiber composites with a hyperelastic matrix. Int. J. Solids Struct. 2012, 49, 395–407, DOI:10.1016/j.ijsolstr.2011.09.010.

17. Fejős, M.; Romhány, G.; Karger-Kocsis, J. Shape memory characteristics of woven glass fibre fabric reinforced epoxy composite in flexure. J. Reinf. Plast. Compos. 2012, 31, 1532–1537, DOI:10.1177/0731684412461541.

18. Chillara, V.S.C.; Dapino, M.J. Review of Morphing Laminated Composites. Appl. Mech. Rev. 2020, 72, 10801, DOI:10.1115/1.4044269.

19. Chillara, V.S.C.; Headings, L.M.; Dapino, M.J. Multifunctional composites with intrinsic pressure actuation and prestress for morphing structures. Compos. Struct. 2016, 157, 265–274, DOI:10.1016/j.compstruct.2016.08.044.

20. Kim, S.; Laschi, C.; Trimmer, B. Soft robotics: A bioinspired evolution in robotics. Trends Biotechnol. 2013, 31, 287–294, DOI:10.1016/j.tibtech.2013.03.002.

21. Cianchetti, M.; Laschi, C.; Menciassi, A.; Dario, P. Biomedical applications of soft robotics. Nat. Rev. Mater. 2018, 3, 143–153, DOI:10.1038/s41578-018-0022-y.

22. Henning, F.; Moeller, E. Handbuch Leichtbau. Methoden, Werkstoffe, Fertigung, 2nd ed; Carl Hanser Verlag: Munich, Germany, 2020, ISBN 978-3-446-45638-9.

23. Menges, G.; Haberstroh, E.; Michaeli, W.; Schmachtenberg, E. Menges Werkstoffkunde Kunststoffe, 6th ed.; Carl Hanser Verlag: Munich, Germany, 2014, ISBN 978-3-446-42762-4.

24. Haspel, B. Werkstoffanalytische Betrachtung der Eigenschaften mittels neuartiger RTM-Fertigungsprozesse hergestellten glasfaserverstärkten Polymerverbunden. Doctoral thesis, Karlsruher Institut für Technologie, Karlsruhe, 2014.

25. Neitzel, M.; Mitschang, P.; Breuer, U. Handbuch Verbundwerkstoffe. Werkstoffe, Verarbeitung, Anwendung, 2nd ed.; Carl Hanser Verlag: Munich, Germany, 2014, ISBN 978-3-446-43696-1.

26. Ehrenstein, G. Polymer-Werkstoffe. Struktur; Eigenschaften; Anwendung, 3rd ed.; Carl Hanser Verlag: Munich, Germany, 2011, ISBN 978-3-446-42283-4.

27. Schoßig, M. Schädigungsmechanismen in faserverstärkten Kunststoffen. Quasistatische und dynamische Untersuchungen, 1st ed.; Vieweg+Teubner (GWV): Wiesbaden, Germany, 2011, ISBN 978-3-8348-1483-8.

28. Cherif, C. Textile Werkstoffe für den Leichtbau. Techniken - Verfahren - Materialien - Eigenschaften, 1st ed.; Springer Verlag: Berlin, Germany, 2011, ISBN 978-3-642-17992-1.

29. AVK - Industrievereinigung. Handbuch Faserverbundkunststoffe, 3rd ed.; Springer Fachmedien: Wiesbaden, Germany, 2010, ISBN 978-3-8348-0881-3.

30. Schürmann, H. Konstruieren mit Faser-Kunststoff-Verbunden, 2nd ed.; Springer Verlag: Berlin, Germany, 2007, ISBN 978-3-540-72189-5.

31. Moser, K. Faser-Kunststoff-Verbund. Entwurfs- und Berechnungsgrundlagen, 1st ed.; Springer Verlag: Berlin, Germany, 2013, ISBN 978-3-642-63469-7.

32. Vannucci, P. Anisotropic Elasticity, 1st ed.; Springer Singapore: Singapore, 2018, ISBN 978-981-10-5438-9.

33. Peel, L.D.; Mejia, J.; Narvaez, B.; Thompson, K.; Lingala, M. Development of a Simple Morphing Wing Using Elastomeric Composites as Skins and Actuators. J. Mech. Des. 2009, 131, 91003, DOI:10.1115/1.3159043.

34. Vocke, R.D.; Kothera, C.S.; Woods, B.K.S.; Wereley, N.M. Development and Testing of a Span-Extending Morphing Wing. J. Intell. Mater. Syst. Struct. 2011, 22, 879–890, DOI:10.1177/1045389X11411121.

35. Debiasi, M.; Leong, C.W.; Bouremel, Y. Application of Macro-Fiber-Composite Materials on UAV Wings. In . Conference: Aerospace Technology Seminar, Signapore, March 2013.

36. Koschmieder, M. Verarbeitung und Eigenschaften von Faserverbundkunststoffen mit Elastomermatrix. Doctoral thesis, Rheinisch-Westfälischen Technischen Hochschule Aachen, Aachen, 2000.

37. Hassan, A.; Rahman, N.A.; Yahya, R. Extrusion and injection-molding of glass fiber/MAPP/polypropylene: Effect of coupling agent on DSC, DMA, and mechanical properties. J. Reinf. Plast. Compos. 2011, 30, 1223–1232, DOI:10.1177/0731684411417916.

38. Zhang, D.; He, M.; Qin, S.; Yu, J. Effect of fiber length and dispersion on properties of long glass fiber reinforced thermoplastic composites based on poly(butylene terephthalate). RSC Adv. 2017, 7, 15439–15454, DOI:10.1039/c7ra00686a.

39. Vleugels, N. Short Fibre-Reinforced Elastomeric Composites: fundamental routes towards improvement of the interfacial interaction of short-cut aramid fibres in a SBR compound, to improve friction and wear properties. Doctoral thesis, University of Twente, Enschede, 2017.

40. Abts, G. Einführung in die Kautschuktechnologie; Carl Hanser Fachbuchverlag: Munich, Germany, 2019, ISBN 978-3-446-45461-3.

41. Hoffmann, J. Characterization of fibre reinforced elastomers for shape morphing structural surfaces. Doctoral thesis, Technical University of Munich, Munich, 2012.

42. Peel, L. Fabrication and Mechanics of Fiber-Reinforced Elastomers. Doctoral thesis, Brigham Young University, Brigham, 1998.

43. Lang, R.W.; Stutz, H.; Heym, M.; Nissen, D. Polymere Hochleistungsfaserverbundwerkstoffe. Angew. Makromol. Chemie 1986, 145, 267–321, DOI:10.1002/apmc.1986.051450115.

44. Wiedemann, J. Leichtbau. Elemente und Konstruktion, 3rd ed.; Springer Verlag: Berlin, Germany, 2007, ISBN 10 3-540-33656-7.

45. Campbell, F.C. Structural composite materials, 1st ed.; ASM International: Ohio, U.S.A., 2010, ISBN 978-1-61503-037-8.

46. Reumann, R.-D. Prüfverfahren in der Textil- und Bekleidungstechnik, 1st ed.; Springer Verlag: Berlin, Germany, 2013, ISBN 978-3-642-63033-0.

47. Cheng, S.Z.D.; Wunderlich, B. Thermal analysis of thermoplastic polymers. Thermochim. Acta 1988, 161–166, DOI:10.1016/0040-6031(88)85232-8.

48. George, J.; Bhagawan, S.S.; Thomas, S. Thermogravimetric and dynamic mechanical thermal analysis of pineapple fibre reinforced polyethylene composites. J. Therm. Anal. 1996, 47, 1121–1140, DOI:10.1007/BF01979452.

49. Karpf, R. Mechanische Eigenschaften von Epoxidharz-Faserverbundwerkstoffen in Abhängigkeit vom Aushärtungsgrad. Master thesis, Montanuniversität Leoben, Leoben, 2012.

50. Röthemeyer, F.; Sommer, F. Kautschuk - Technologie. Werkstoffe - Verarbeitung - Produkte, 3rd ed.; Carl Hanser Verlag: Munich, Germany, 2013, ISBN 978-3-446-43776-0.

51. Ehrenstein, G.W.; Riedel, G.; Trawiel, P. Praxis der thermischen Analyse von Kunststoffen, 2nd ed.; Carl Hanser Verlag: Munich, Germany, 2003, ISBN 978-3-446-22340-0.

52. Bonnet, M. Polymere Verbundwerkstoffe, 1st ed.; Vieweg+Teubner Verlag: Wiesbaden, Germany, 2009, ISBN 978-3-8348-9303-1.

53. Schönleitner, F. Faserverbundwerkstoffe in Wickelköpfen. Master thesis, Technische Universität Graz, Graz, 2012.

54. Njuhovic, E. Einfluss der Grenzflächenstruktur auf die mikro-mechanischen Versagensmechanismen metallisierter Faserverbundkunststoffe. Doctoral thesis, Universität Bayreuth, Bayreuth, 2018.

55. Kanerva, M.; Korkiakoski, S.; Lahtonen, K.; Jokinen, J.; Sarlin, E.; et al. DLC-treated aramid-fibre composites: Tailoring nanoscale-coating for macroscale performance. Compos. Sci. Technol. 2019, 171, 62–69, DOI:10.1016/j.compscitech.2018.11.043.

56. Plueddemann, E.P. Silane Coupling Agents, 2nd ed.; Springer US: Boston, U.S.A., 1991, ISBN 978-1-4899-2070-6.

57. Sahin, M.; Schlögl, S.; Kalinka, G.; Wang, J.; Kaynak, B.; et al. Tailoring the interfaces in glass fiber-reinforced photopolymer composites. Polym. 2018, 141, 221–231, DOI:10.1016/j.polymer.2018.03.020.

58. Zhandarov, S. Characterization of fiber/matrix interface strength: Applicability of different tests, approaches and parameters. Compos. Sci. Technol. 2005, 65, 149–160, DOI:10.1016/j.compscitech.2004.07.003.

59. Zhou, J.; Li, Y.; Li, N.; Hao, X.; Liu, C. Interfacial shear strength of microwave processed carbon fiber/epoxy composites characterized by an improved fiber-bundle pull-out test. Compos. Sci. Technol. 2016, 133, 173–183, DOI:10.1016/j.compscitech.2016.07.033.

60. Kinloch, A.J. Adhesion and Adhesives. Science and Technology, 1st ed.; Chapman & Hall; Springer Netherlands: London, UK, 2010, ISBN 978-94-015-7764-9.

61. Michler, G.H. Kunststoff-Mikromechanik. Morphologie, Deformations- und Bruchmechanismen; Carl Hanser Verlag: Munich, Germany, 1992, ISBN 978-3446170681.

62. Cao, Y.; Cao, Z.; Zhao, Y.; Zuo, D.; Tay, T.E. Damage progression and failure of single-lap thin-ply laminated composite bolted joints under quasi-static loading. Int. J. Mech. Sci. 2020, 170, 105360, DOI:10.1016/j.ijmecsci.2019.105360.

63. Friedrich, K. Application of fracture mechanics to composite materials; Elsevier: New York, U.S.A., 1989, ISBN 9780444597212.

64. Piggott, M.R. Why interface testing by single-fibre methods can be misleading. Compos. Sci. Technol. 1997, 57, 965–974, DOI:10.1016/S0266-3538(97)00036-5.

65. Beter, J.; Schrittesser, B.; Maroh, B.; Sarlin, E.; Fuchs, P.F.; et al. Comparison and Impact of Different Fiber Debond Techniques on Fiber Reinforced Flexible Composites. Polym. 2020, 12, 32085523, DOI:10.3390/polym12020472.

66. Kim, B.W.; Nairn, J.A. Observations of Fiber Fracture and Interfacial Debonding Phenomena Using the Fragmentation Test in Single Fiber Composites. J. Compos. Mater. 2016, 36, 1825–1858, DOI:10.1177/0021998302036015243.

67. Sørensen, B.F.; Lilholt, H. Fiber pull-out test and single fiber fragmentation test - analysis and modelling. IOP Conf. Ser.: Mater. Sci. Eng. 2016, 139, DOI:10.1088/1757-899X/139/1/012009.

68. Essen M, Sarlin E, Tanhuanpää O, Kakkonen M, Laurikainen P, et al. Automated high-throughput microbond tester for interfacial shear strength studies. In . The SAMPE Europe Conference, Stuttgart, November 2017; 14–16, ISBN 978-90-821727-7-5.

69. Zarges, J.-C.; Kaufhold, C.; Feldmann, M.; Heim, H.-P. Single fiber pull-out test of regenerated cellulose fibers in polypropylene: An energetic evaluation. Compos. Part A 2018, 105, 19–27, DOI:10.1016/j.compositesa.2017.10.030.

70. Schulz, E.; Kalinka, G.; Auersch, W. Effect of transcrystallization in carbon fiber reinforced poly(p -phenylene sulfide) composites on the interfacial shear

strength investigated with the single fiber pull-out test. J. Macromol. Sci. Part B 2006, 35, 527–546, DOI:10.1080/00222349608220393.

71. DiFrancia, C.; Ward, T.C.; Claus, R.O. The single-fibre pull-out test: Review and Interpretation. Compos. Part A 1996, 27, 597–612, DOI:10.1016/1359-835X(95)00069-E.

72. Kalinka, G.; Leistner, A.; Hampe, A. Characterisation of the fibre/matrix interface in reinforced polymers by the push-in technique. Compos. Sci. Technol. 1997, 57, 845–851, DOI:10.1016/S0266-3538(96)00159-5.

73. Kerans, R.J.; Parthasarathy, T.A. Theoretical Analysis of the Fiber Pullout and Pushout Tests. J. Am. Ceram. Soc. 1991, 74, 1585–1596, DOI:10.1111/j.1151-2916.1991.tb07144.x.

74. Hampe, A.; Kalinka, G.; Meretz, S.; Schulz, E. An advanced equipment for single-fibre pull-out test designed to monitor the fracture process. Compos. 1995, 26, 40–46, DOI:10.1016/0010-4361(94)P3628-E.

75. Kalinka, G.; Neumann, B. Bestimmung von Interface-Festigkeit oder Trennarbeit mit dem Pull-out-Versuch: Kassel, Germany, 2005. Available online: https://opus4.kobv.de/opus4-bam/frontdoor/index/index/docId/6085 (accessed on 6 February 2021).

76. Brandstetter, J.; Peterlik, H.; Kromp, K.; Weiss, R. A new fibre-bundle pull-out test to determine interface properties of a 2D-woven carbon/carbon composite. Compos. Sci. Technol. 2003, 63, 653–660, DOI:10.1016/S0266-3538(02)00250-6.

77. Domnanovich, A.; Peterlik, H.; Kromp, K. Determination of interface parameters for carbon/carbon composites by the fibre-bundle pull-out test. Compos. Sci. Technol. 1996, 56, 1017–1029, DOI:10.1016/0266-3538(96)00060-7.

78. Zhamu, A.; Zhong, W.H.; Stone, J.J. Experimental study on adhesion property of UHMWPE fiber/nano-epoxy by fiber bundle pull-out tests. Compos. Sci. Technol. 2006, 66, 2736–2742, DOI:10.1016/j.compscitech.2006.03.005.

79. Zhang, X.; Fan, X.; Yan, C.; Li, H.; Zhu, Y.; et al. Interfacial microstructure and properties of carbon fiber composites modified with graphene oxide. ACS Appl. Mater. Interfaces 2012, 4, 1543–1552, DOI:10.1021/am201757v.

80. Beter, J.; Schrittesser, B.; Fuchs, P.F. Investigation of adhesion properties in load coupling applications for flexible composites. Mater. Today-Proc. 2020, DOI:10.1016/j.matpr.2020.01.181.

81. Jones, R.M. Mechanics of composite materials, 1st ed.; Taylor & Francis: Bristol, UK, 1975, ISBN 978-0891164906.

82. Denonville, J. Eine neue materialgerechte Fügetechnologie für uni-direktionale Faser-Kunststoff-Verbundwerkstoffe mit Glas- und Carbonfasern. Doctoral thesis, Universität Stuttgart, Stuttgart, 2015.

83. Ahn, S.-H.; Lee, K.-T.; Kim, H.-J.; Wu, R.; Kim, J.-S.; et al. Smart soft composite: An integrated 3D soft morphing structure using bend-twist coupling of anisotropic materials. Int. J. Precis. Eng. Manuf. 2012, 13, 631–634, DOI:10.1007/s12541-012-0081-8.

84. Brunetti, M.; Vincenti, A.; Vidoli, S. A class of morphing shell structures satisfying clamped boundary conditions. Int. J. Sol. Struct. 2016, 82, 47–55, DOI:10.1016/j.ijsolstr.2015.12.017.

85. Selden, P.H. Glasfaserverstärkte Kunststoffe; Springer Berlin: Berlin, Germany, 1967, ISBN 978-3-642-48456-8.

86. Hayat, K.; Ha, S.K. Load mitigation of wind turbine blade by aeroelastic tailoring via unbalanced laminates composites. Compos. Struct. 2015, 128, 122–133, DOI:10.1016/j.compstruct.2015.03.042.

87. Debiasi, M.T.; Chan, W.L.; Jadhav, S. Measurements of a Symmetric Wing Morphed by Macro Fiber Composite Actuators. In . 54th AIAA Aerospace Sciences Meeting, San Diego, U.S.A., 04-08. January 2016, DOI:10.2514/6.2016-1565.

88. Thor, M.; Sause, M.G.R.; Hinterhölzl, R.M. Mechanisms of Origin and Classification of Out-of-Plane Fiber Waviness in Composite Materials - A Review. J. Compos. Sci. 2020, 4, 130, DOI:10.3390/jcs4030130.

89. Song, Y.S.; Lee, J.T.; Ji, D.S.; Kim, M.W.; Lee, S.H.; et al. Viscoelastic and thermal behavior of woven hemp fiber reinforced poly(lactic acid) composites. Compos. Part B 2012, 43, 856–860, DOI:10.1016/j.compositesb.2011.10.021.

90. Beter, J.; Schrittesser, B.; Lechner, B.; Mansouri, M.R.; Marano, C.; et al. Viscoelastic Behavior of Glass-Fiber-Reinforced Silicone Composites Exposed to Cyclic Loading. Polym. 2020, 12, 1862, DOI:10.3390/polym12091862.

91. Diani, J.; Fayolle, B.; Gilormini, P. A review on the Mullins effect. Eur. Polym. J. 2009, 45, 601–612, DOI:10.1016/j.eurpolymj.2008.11.017.

92. Peng, X.; Guo, Z.; Du, T.; Yu, W.-R. A simple anisotropic hyperelastic constitutive model for textile fabrics with application to forming simulation. Compos. Part B 2013, 52, 275–281, DOI:10.1016/j.compositesb.2013.04.014.

93. Gude, M.; Hufenbach, W.; Andrich, M.; Mertel, A.; Schirner, R. Modified V-notched rail shear test fixture for shear characterisation of textile-reinforced composite materials. Polym. Test. 2015, 43, 147–153, DOI:10.1016/j.polymertesting.2015.03.007.

94. Gereke, T.; Döbrich, O.; Hübner, M.; Cherif, C. Experimental and computational composite textile reinforcement forming: A review. Compos. Part A 2013, 46, 1–10, DOI:10.1016/j.compositesa.2012.10.004.

95. Hallander, P.; Sjölander, J.; Åkermo, M. Forming induced wrinkling of composite laminates with mixed ply material properties; an experimental study. Compos. Part A 2015, 78, 234–245, DOI:10.1016/j.compositesa.2015.08.025.

96. Hassan, M.H.; Othman, A.R.; Kamaruddin, S. A review on the manufacturing defects of complex-shaped laminate in aircraft composite structures. Int. J. Adv. Manuf. Technol. 2017, 91, 4081–4094, DOI:10.1007/s00170-017-0096-5.

97. Mansouri, M.R.; Fuchs, P.F.; Criscione, J.C.; Schrittesser, B.; Beter, J. The contribution of mechanical interactions to the constitutive modeling of fiber-

reinforced elastomers. Eur. J. Mech. A-Solid 2020, 104081, DOI:10.1016/j.euromechsol.2020.104081.

98. Lindberg, J.; Behre, B.; Dahlberg, B. Part III: Shearing and Buckling of Various Commercial Fabrics. Text. Res. J. 2016, 31, 99–122, DOI:10.1177/004051756103100203.
99. Grosberg, P.; Park, B.J. The Mechanical Properties of Woven Fabrics. Text. Res. J. 2016, 36, 420–431, DOI:10.1177/004051756603600505.
100. Gutowski, T.; Hoult, D.; Dillon, G.; Gonzalez-Zugasti, J. Differential geometry and the forming of aligned fibre composites. Composites Manufacturing 1991, 2, 147–152, DOI:10.1016/0956-7143(91)90133-2.
101. Prodromou, A.G.; Chen, J. On the relationship between shear angle and wrinkling of textile composite preforms. Compos. Part A 1997, 28, 491–503, DOI:10.1016/S1359-835X(96)00150-9.
102. Luo, S.-Y.; Chou, T.-W. Finite Deformation and Nonlinear Elastic Behavior of Flexible Composites. J. Appl. Mech. 1988, 55, 149–155, DOI:10.1115/1.3173621.
103. Peel, L.D.; Jensen, D.W. The Response of Fiber-Reinforced Elastomers under Simple Tension. J. Compos. Mater. 2016, 35, 96–137, DOI:10.1106/V3YU-JR4G-MKJG-3VMF.
104. Bergmann, T.; Heimbs, S.; Maier, M. Mechanical properties and energy absorption capability of woven fabric composites under ±45° off-axis tension. Compos. Struct. 2015, 125, 362–373, DOI:10.1016/j.compstruct.2015.01.040.
105. Rohde, S.E.; Ifju, P.G.; Sankar, B.V.; Jenkins, D.A. Experimental Testing of Bend-Twist Coupled Composite Shafts. Exp. Mech. 2015, 55, 1613–1625, DOI:10.1007/s11340-015-0050-0.
106. Potter, K. Bias extension measurements on cross-plied unidirectional prepreg. Compos. Part A 2002, 33, 63–73, DOI:10.1016/S1359-835X(01)00057-4.
107. Modi, V.; Singh, K.K.; Shrivastava, R. Effect of Stacking Sequence on Interlaminar Shear Strength of Multidirectional GFRP Laminates. Mater. Today: Proc. 2020, 22, 2207–2214, DOI:10.1016/j.matpr.2020.03.301.
108. Kim, J.-K.; Mai, Y.-W. Engineered interfaces in fiber reinforced composites, 1st ed.; Elsevier Science: Oxford, UK, 1998, ISBN 0-08-042695-6.
109. Bheemreddy, V.; Chandrashekhara, K.; Dharani, L.R.; Hilmas, G.E. Modeling of fiber pull-out in continuous fiber reinforced ceramic composites using finite element method and artificial neural networks. Comput. Mater. Sci. 2013, 79, 663–673, DOI:10.1016/j.commatsci.2013.07.026.
110. Marotzke, C.; Qiao, L. Interfacial crack propagation arising in single-fiber pull-out tests. Compos. Sci. Technol. 1997, 57, 887–897, DOI:10.1016/S0266-3538(96)00179-0.
111. Zhandarov, S.; Mäder, E. Analysis of a pull-out test with real specimen geometry. Part I: Matrix droplet in the shape of a spherical segment. J. Adhes. Sci. Technol. 2013, 27, 430–465, DOI:10.1080/01694243.2012.715730.

112. Ehrenstein, G.W. Faserverbund-Kunststoffe. Werkstoffe - Verarbeitung - Eigenschaften, 2nd ed.; Carl Hanser Verlag: Munich, Germany, 2006, ISBN 978-3-446-22716-3.

113. Yu A. Gorbatkina. Adhesive strength in fibre-polymer systems, 1st ed.; Ellis Horwood: New York, U.S.A., 1992, ISBN 978-0130054555.

TABLE OF FIGURES